36TH

NATIONAL SYMPOSIUM ON PLASMA SCIENCE AND TECHNOLOGY

PLASMA-2021

13th-15th Dec. 2021

PLASMA 2021

Book of Abstracts

Organized by:

Department of Physics
Birla Institute of Technology Mesra, Jaipur Campus
&
Plasma Science Society of India

आज़ादी का अमृत महोत्सव

TECHNOLOGIES FOR NEW INDIA@75
आज़ादी का अमृत महोत्सव

Azadi Ka Amrit Mahotsav

36th National Symposium on Plasma Science and Technology

PLASMA-2021

(through Online mode)

13-15 December, 2021

Book of Abstracts

Edited by:

Dr. Anand Kumar Srivastava
Dr. Ravindra Kumar
Mr. Sanjay Tambi

Organised by

Department of Physics
Birla Institute of Technology, Mesra, Jaipur Campus

in association with

Plasma Science Society of India

First Impression: 2021

36th National Symposium on Plasma Science & Technology (PLASMA-2021)

Disclaimer

The authors are solely responsible for the contents of the papers compiled in this volume. The publishers or editors do not take any responsibility for the same in any manner. Errors, if any, are purely unintentional and readers are requested to communicate such errors to the editors or publishers to avoid discrepancies in future.

Published by
Department of Physics
Birla Institute of Technology, Mesra
Jaipur Campus
27, Malviya Industrial Area, Jaipur
Jaipur, Rajasthan -302017
INDIA

BIRLA INSTITUTE OF TECHNOLOGY, MESRA
(A Deemed to be University u/s 3 of the UGC Act, 1956)
JAIPUR CAMPUS

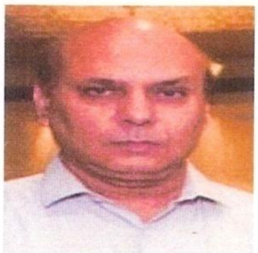

Message

It is an important and pride moment for Birla Institute of Technology and Plasma Science Society of India to jointly organize the 36 th National Symposium on Plasma Science and Technology during 13-15 December 2021 at BIT Jaipur Campus . The broader theme of the symposium "Plasma for Benefit of Mankind" is well addressing the concern of common people through technology intervention at the time of Covid 19 pandemic when the humanity has been facing serious challenge to its survival which includes threats related to economic and social perturbation. It is quite appropriate here to say that this symposium is going to make a significant contribution to address some of the serious concerns the mankind is presently facing with discussions and deliberations on the application of plasma technology . The validity of this hope and assurance to the society is based on the broader platform of plasma applications which have positive impact on well being of people , the notable plasma applications of interest here are- Plasma medicines, fusion energy , application to agriculture and food processing , environment friendly material processing , waste management , air and water purification , etc . The applications of plasma in space and defence sectors are also playing vital role in shaping the better future of the society .

It is quite encouraging to learn that the symposium has got a good participative response from about 300 scientists and researchers from reputed institutions and universities . Definitely , discussions and deliberations at such intellectual level would result in fruitful outcome in terms of industrial application or realization of research ideas in a real time processes or products.

On behalf of the host institution , I welcome all guests and participants and wish the symposium a great success.

Abhinav Dinesh

(Dr. Abhinav Dinesh)
Director
Birla Institute of Technology , Mesra
Jaipur Campus

प्लाज़्मा अनुसंधान संस्थान
Institute for **Plasma Research**

MESSAGE

I am happy to know that the Plasma Science Society of India (PSSI) is organizing its 36th National Symposium on Plasma Science and Technology (PLASMA-2021) as an online event in association with the Birla Institute of Technology, Mesra, Jaipur Campus during 13-15 December, 2021. This meeting holds special importance as the last Plasma conference could not be held due to the Covid-19 pandemic.

With so many societal applications of plasmas, it is slowly but surely becoming part and parcel of our daily life! I am happy to know that the theme of this edition of the Plasma conference is "Plasma for Benefit of Mankind", which truly reflects how plasma will play an important role in our lives. Plasma science & technology has also made major advances over the past few decades, with the ITER project on track to establish the usefulness of Controlled Thermonuclear Fusion. In parallel with the mega-projects related to fusion, the ever-growing list of plasma applications in industry, medicine/healthcare, agriculture, textile processing, waste disposal, aerospace technologies, communications and so on only adds to the wide adaptability of plasma science & technology. A promising new area of particular importance for India, is the application of plasmas for the eco-friendly and low-carbon production of hydrogen.

In the 75th year of India's independence, I really hope that participation in this Symposium would motivate young researchers from different branches of science and engineering to enter the challenging fields of plasma science & technology. Lastly, on behalf of IPR, I would like to thank PSSI and the organizers for their sincere efforts for organizing this symposium. I extend my best wishes to all the participants and hope that the Symposium will achieve its desired objectives.

(Dr. Shashank Chaturvedi)
Director, Institute for Plasma Research

आज़ादी का अमृत महोत्सव
TECHNOLOGIES FOR NEW INDIA@75
आज़ादी का अमृत महोत्सव
Azadi Ka Amrit Mahotsav

पी एस एस आई अध्यक्ष का संदेश

मुझे यह जानकर बहुत खुशी है कि प्लाज़्मा साइंस सोसाइटी आफ इंडिया "PSSI", बिरला इंस्टिट्यूट आफ टेक्नॉलजी, मेसरा, जयपुर केम्पस के साथ मिलकर प्लाज़्मा विज्ञान तथा तकनीकि पर 36वी राष्ट्रीय संगोष्टी (प्लाज़्मा-2021) जयपुर में 13-15 दिसम्बर के अंतराल मे आयोजित कर रहे है। इस संगोष्ठी में नए खोजकर्ता प्लाज़्मा विज्ञान तथा तकनीकि के क्षेत्र में विद्वान वैज्ञानिकों के साथ चर्चा में भाग लेते है तथा अपनी खोज का प्रदर्शन करते हैं। PSSI इस तरह की संगोष्ठी भारत में भिन्न-भिन्न विश्वविद्यालयों तथा अनुसंधान संस्थाओ के साथ मिलकर हर वर्ष आयोजित करती हैं। PSSI हर वर्ष रिसर्च स्कोलर का वर्तालाप भी आयोजित करती है। मुझे उम्मीद है कि सभी वैज्ञानिक तथा छात्र मिलकर अपने ज्ञान का आदान प्रदान करेंगे तथा इस संगोष्ठी को सफल बनाएंगे।

शुभ कामनाओं सहित

डॉ पी के आत्रेय

अध्यक्ष, प्लाज़्मा सोसाइटी आफ इन्डिया (PSSI)

DEPARTMENT OF PHYSICS
BIRLA INSTITUTE OF TECHNOLOGY, MESRA, JAIPUR CAMPUS, JAIPUR, RAJASTHAN-302017

Preface

The 36th National Symposium on Plasma Science and Technology (PLASMA-2021)is jointly organized by Department of Physics, Birla Institute of Technology, Mesra, Jaipur Campus and Plasma Science Society of India (PSSI) during 13-15 December 2021. Due to COVID-19 pandemic related limitations, this year the symposium is organized in online mode. The symposium on Plasma Science and Technology was started in 1990s and successfully organized in various national institutes all over the country. The symposium aims to promote plasma science and technology within the country and also to encourage & involve a large number of Indian researches to participate & exchange their ideas in the symposium.

It is well known that achieving the controlled Nuclear Fusion is prime objective of Plasma Physics research. Simultaneously, a lot more industrial and societal applications of Plasma are also explored in various sectors like healthcare, aerospace, semiconductor, agriculture, automobiles, displays etc. Surprisingly, many of them have given promising results at laboratory level. So exploring societal plasma applications are now another focus of plasma research, Hence we have taken the theme of this symposium as “Plasma for Benefit of mankind”.

For this PLASMA-2021 symposium, we have received around 300 participant registration. As per schedule, there will be 9 Invited talks, 1 keynote address, 18 Oral presentations, approx. 210 poster presentations, 6 Buti Award presentations and few other special award presentations as well. The good response received from participants in this difficult time of COVID pandemic is really remarkable. The symposium ran for three-days (13-15 December) and have various technical & non-technical sessions. There are 6 Technical sessions, Buti Award presentations, A K Sundaram Memorial lecture, Sodha Award lecture, Parvez Guzdar Award lecture, M S Sodha Award lecture, Sholapurwala award lecture etc. The students of BIT Jaipur campus had also prepared a cultural program as a part of the symposium. The keynote address was delivered by Prof. Prabhat Ranjan, Vice Chancellor, D Y Patil International University, Pune. First time in this symposium, a special lecture was introduced in the memory of Prof. A K Sundaram, that was delivered by Prof. Gurudas Ganguli from Naval Research Laboratory, USA.

On behalf of organizing committee, I would like to express our thanks to Plasma Science Society ofIndia (PSSI) for providing us the opportunity to organize PLASMA-2021 at BIT Mesra, Jaipur Campus. We would also like to express our sincere thanks to Vice Chancellor, BIT Mesra, Ranchi and Director, BIT Jaipur Campus for all possible support to organize this symposium. We are thankful to members of National Advisory Committee, Scientific Program Committee and Local Organizing Committee for their support and encouragement. We are thankful to invited speakers, all award committee members and session chairs. We would like to express our thanks to the sponsors of the symposium, Aditya High Vacuum Pvt. Ltd. and Plasma & Vacuum Technologies of their financial support. We express our thanks to proceeding editors and all members of BIT and PSSI who are directly and indirectly involved in organizing the symposium.

At the end we would like to announce that the NAC has initiating the selection process for finalizing the host institute for next PSSI symposium, PLASMA-2022, it is under process. We look forward to see you again at PLASMA-2022.Wishing all of you for attending this conference online and having very productive scientific sessions.

Dr. Anand Kumar Srivastava
Convener
PLASMA-2021

Sponsors

Aditya High Vacuum Pvt. Ltd.

Plasma And Vacuum Technologies

Committees of the Symposium

National Advisory Committee (NAC)

Indranil Manna	Vice Chancellor, BIT Mesra, Ranchi	Patron
Shashank Chaturvedi	Director, IPR, Ahmedabad	Chairman
B. S. Murti	Director, IIT, Hyderabad	Member
Abhijit Sen	IPR, Ahmedabad	Member
Arun Kumar Bhaduri	IGCAR, Kalpakkam	Member
Arnab Roy Chowdhury	IISc, Bangalore	Member
Ashok K. Das	OSHEC, Bhubaneshwar	Member
AvinashKhare	VC, SCU, Sikkim	Member
Ganesh Prasad	IAR, Gandhinagar	Member
Harish K. Dwivedi	MUIT, Lucknow	Member
HerembaBailung	IASST, Guwahati	Member
Nareshpal Singh Saini	GNDU, Amritsar	Member
Rajesh Srivastava	IIT, Roorkee	Member
M. Krishnamurthy	TIFR, Hyderabad	Member
SrikumarGhorui	BARC, Mumbai	Member
SwapanKonar	BIT Mesra, Ranchi	Member
Ujjwal Baruah	ITER India, Ahmedabad	Member

Scientific Program Committee (SPC)

Praveen K. Atrey	IPR, Ahmedabad	Chairman
Anand Kumar Srivastava	BIT Jaipur Campus	Co-chairman
Amit Srivastava	IPR, Ahmedabad	Member
Anand Moorti	RRCAT, Indore	Member
Bhuvan Joshi	PRL, Ahmedabad	Member
Devki Nandan Gupta	Delhi University	Member
Devendra Sharma	IPR, Ahmedabad	Member
Mainak Bandyopadhyay	IPR, Ahmedabad	Member
Manoj Gupta	IPR, Ahmedabad	Member
Mrityunjay Kundu	IPR, Ahmedabad	Member
Paritosh Chaudhuri	IPR, Ahmedabad	Member
Ramesh Narayan	IIT, Delhi	Member
Ram Prakash Lavania	IIT, Jodhpur	Member
Ranjana Manchanda	IPR, Ahmedabad	Member
Shishir Deshpande	IPR, Ahmedabad	Member
Sudip Bhattacharya	IIT, Kanpur	Member
Supriya Nair	IPR, Ahmedabad	Member

Local Organizing Committee (LOC)

Indranil Manna	Vice Chancellor, BIT Mesra, Ranchi	Patron
Abhinav Dinesh	Director, BIT Jaipur Campus	Chairman
Sanjay Kumar Sinha	BIT Mesra, Ranchi	Co-chairman
Anand Kumar Srivastava	BIT Jaipur Campus	Convener
Ravindra Kumar	BIT Jaipur Campus	Coordinator
Dheeraj Bhardwaj	BIT Jaipur Campus	Co-coordinator
Sanjay Kumar Sinha	BIT Patna Campus	Member
Madhavi Sinha	BIT Jaipur Campus	Member
Alok Pandey	BIT Jaipur Campus	Member
Abhijeet Mustafi	BIT Mesra, Ranchi	Member
Madan Mohan Agarwal	BIT Jaipur Campus	Member
Vibhuti Pandya	BIT Jaipur Campus	Member
Ritu Pareek	BIT Jaipur Campus	Member
Rishika Sharma	BIT Jaipur Campus	Member
Abinash Pankaj	BIT Jaipur Campus	Member
Rajni Agarwal	BIT Jaipur Campus	Member
Sanjay Tambi	BIT Jaipur Campus	Member

PPOGRAM SCHEDULE
PLASMA-2021, 13-15 DECEMBER, 2021

Day-1 (13th December 2021, Monday)

09:30 to 10:30	10:30 to 11:15	11:15 to 13:00		13:00 to 14:15	14:15 to 15:45		15:45 to 18:00	18:00 to 19:00
Inaugural Function	**Keynote Address**	**Session-1 (Basic Plasma)**		**Lunch Break**	**Session-2 (Nuclear Fusion)**		**Buti Award Presentations**	**Special Session:** Dr. Sundaram Memorial Lecture
		Invited-1	30 min		Invited-3	30 min		
		Invited-2	30 min		Oral-NF-1	15 min		
		Oral-BP-1	15 min		Oral-NF-2	15 min		
		Oral-BP-2	15 min		Oral-NF-3	15 min		
		Oral-BP-3	15 min		Oral-NF-4	15 min		

Keynote: Dr. Prabhat Ranjan, DYPIU, Pune
Special Lecture: Dr. Gurudas Ganguly, NRL, USA
Invited-1: Devendra Sharma, IPR;
Invited-2: Sudeep Bhattacharjee, IIT-K
Invited-3: Arun Chakraborty, ITER-India

Day-2 (14th December 2021, Tuesday)

9:30 to 11:15		11:15 to 12:30		12:30 to 13:45	13:45 to 15:30	15:30 to 18:30
Session-3 (Plasma Application)		**Session-4 (Plasma Diagnostics)**		**Lunch Break**	**Award Presentations** **1) Parvez Guzdar Award** **2) Sodha-PSSI Award** **3) Sholapurwala Award**	**PSSI GBM & Cultural Program** (Pre -Recorded)
Invited-4	30 min	Invited-6	30 min			
Invited-5	30 min					
Oral-PA-1	15 min	Oral-PD-1	15 min			
Oral-PA-2	15 min	Oral-PD-2	15 min			
Oral-PA-3	15 min	Oral-PD-3	15 min			

Invited-4: Ganesh Prasad, IAR, Gandhinagar
Invited-5: Rajneesh Kumar, BHU
Invited-6: Jinto Thomas, IPR

Day-3 (15th December 2021, Wednesday)

9:30 to 11:15		11:15 to 12:30		12:30 to 13:45	13:45 to 15:00	15:00 to 16:00
Session-5 (Space & Astrophysical Plasma)		**Session-6 (Laser Plasma, Pulsed Power & Others)**		**Lunch Break**	**Poster Awards**	**Concluding Session**
Invited-7	30 min	Invited-9	30 min			
Invited-8	30 min					
Oral-SP-1	15 min	Oral-LP-1	15 min			
Oral-SP-2	15 min	Oral-LP-2	15 min			
Oral-SP-3	15 min	Oral-LP-3	15 min			

Invited-7: Bhuwan Joshi, PRL
Invited-8: Anand Moorti, RRCAT
Invited-9: K. Ramachandran, Bharathiar University, Coimbatore

Note: The Invited-5 and Invited-9 were interchanged as per the availability of speakers.

SESSION CHAIR-PERSON FOR PLASMA-2021

Session	Chair-Person
Basic Plasma	Prof. S. P. Deshpande, IPR Gandhinagar
Nuclear Fusion	Dr. Amit Sircar, IPR Gandhinagar
Plasma Application	Dr. Ram Prakash, IIT Jodhpur
Plasma Diagnostics	Dr. P. K. Atrey, IPR Gandhinagar
Space and Astrophysical Plasma	Dr. Ramesh Chandra, Kumaun University, Nainital
Laser Plasma, Pulsed Power and Others	Dr. Rishi Verma, BARC, Vizac
Buti Young Scientist Award	Dr. H. K. Dwivedi, MUIT, Lucknow

SPEAKERS for PLASMA-2021

Keynote Speaker:

Prof. Prabhat Ranjan Vice-Chancellor, D Y Patil International University, Pune

Dr. A. K. Sundaram Memorial Lecture:

Dr. Gurudas Ganguli Naval Research Laboratory, USA

Invited Speakers

Basic Plasma

Invited1: Dr. Devendra Sharma Institute for Plasma Research, Gandhinagar
Invited 2: Dr. Sudeep Bhattacharya Indian Institute of Technology, Kanpur

Nuclear Fusion

Invited 3: Dr. Arun Chakraborty ITER-India

Plasma Application

Invited 4: Dr. Ganesh Prasad Institute of Advanced Research (IAR), Gandhinagar
Invited 5: Dr. K. Ramachandran Bharathiar University, Coimbatore

Plasma Diagnostics

Invited 6: Dr. JintoThomos Institute for Plasma Research, Gandhinagar

Space and Astrophysical Plasma

Invited 7: Dr. Bhuwan Joshi Physical Research Laboratory (PRL), Ahmedabad
Invited 8: Dr. Anand Moorti Raja Ramanna Centre for Advanced Technology (RRCAT), Indore

Laser Plasma, Pulsed Power and Others

Invited 9: Dr. Rajneesh Kumar Banaras Hindu University, Varanasi

ORAL PRESENTATIONS

ID	Date	Time	Abstract -Id	Title	Presenting Author	Affiliation
Session -1 Basic Plasma						
ORAL-BP-1	13-Dec-21	12:15 - 12:30	87	An experimental investigation of oscillating plasma bubbles and its non linear structure in a magnetized plasma system	Mariammal Megalingam	IPR, Gandhinagar
ORAL-BP-2	13-Dec-21	12:30 - 12:45	25	Study of Two Stream Instability in Inhomogeneous Dusty Plasmas with Uniform Magnetic Field	Shachi Pachauri	Manipal University, Jaipur
ORAL-BP-3	13-Dec-21	12:45 - 13:00	188	Strong magnetic field effects in the strongly coupled rotating dusty plasma	Prince Kumar	IPR, Gandhinagar
Session -2 Nuclear Fusion						
ORAL-NF-1	13-Dec-21	14:45 - 15:00	196	Study of MHD activity and Runaway Electrons in the ADITYA and ADITYA-U Tokamak	Sharvil Patel	IPR, Gandhinagar
ORAL-NF-2	13-Dec-21	15:00 - 15:15	79	Heat Transfer Analysis of PINI Ion Source Back Plate Using ANSYS	Tejendra Patel	IPR, Gandhinagar
ORAL-NF-3	13-Dec-21	15:15 - 15:30	131	Design Updates and Current Status of Installation works of Experimental Helium Cooling Loop (EHCL)	Ankit Gandhi	IPR, Gandhinagar
ORAL-NF-4	13-Dec-21	15:30 - 15:45	152	Towards a 3D Quiescent nonneutral plasma state in small aspect ratio torus - a particle-in-cell simulation study	Swapnali Khamaru	IPR, Gandhinagar
Session -3 Plasma Applications						
ORAL-PA-1	14-Dec-21	10:30 - 10:45	138	Microplasma synthesis of Ce-doped hausmannite Mn_3O_4 Nanoparticles for supercapacitor application	Kavitha E R	Bharathiar University, Coimbatore
ORAL-PA-2	14-Dec-21	10:45 - 11:00	205	Rapid Crystallization of Amorphous TiO_2 using Atmospheric Pressure Plasma	Parismita Kalita	IASST, Guwahati
ORAL-PA-3	14-Dec-21	11:00 - 11:15	238	Cold plasma treatment of raw milk and its physical properties analysis	Kiran Ahlawat	IIT, Jodhpur

ID	Date	Time	Abstract -Id	Title	Presenting Author	Affiliation
Session -4 Plasma Diagnostics						
ORAL-PD-1	14-Dec-21	11:45 - 12:00	206	Argon impurity transport in Aditya-U tokamak using spectroscopy	Kajal shah	PDEU, Gandhinagar
ORAL-PD-2	14-Dec-21	12:00 - 12:15	112	Collisional Radiative (CR) Model for the Diagnostics of Ne-Ar Mixture Plasma	Shubham Singh Baghel	IIT, Rourkee
ORAL-PD-3	14-Dec-21	12:15 - 12:30	132	Aditya tokamak plasma disruption characterization	Shishir Purohit	IPR, Gandhinagar
Session -5 Space & Astrophysical Plasma						
ORAL-SL-1	15-Dec-21	10:30 - 10:45	178	Shear flow effects on Magnetic Island Coalescence	Jagannath Mahapatra	IPR, Gandhinagar
ORAL-SL-2	15-Dec-21	10:45 - 11:00	222	Cosmic Rays Diffusion and Gravitational Collapse in Radiative Molecular Clouds including ion Larmor radius corrections	Ram Prasad Prajapati	JNU, Newdelhi
ORAL-SL-3	15-Dec-21	11:00 - 11:15	91	Generation of kinetic Alfvén waves by multiple free energy sources	Krushna Chandra Barik	IIG, Mumbai
Session -6 Laser Plasma, Pulsed Power & Others						
ORAL-PO-1	15-Dec-21	11:45 - 12:00	171	Indigenous High Power Pseudospark Switches for Fast Pulse Power Applications	Ram Prakash Lamba	CSIR-CEERI Campus, Pilani
ORAL-PO-2	15-Dec-21	12:00 - 12:15	48	Pulsed laser deposition of CuO/Cu_2O films and their application in photocatalytic dye degradation	Rudrashish Panda	IPR, Gandhinagar
ORAL-PO-3	15-Dec-21	12:15 - 12:30	218	Excitation of Lower Hybrid and Magneto-sonic Perturbations by Laser in X-mode Configuration of Magnetized Plasma	Ayushi Vashistha	IPR, Gandhinagar

Papers Selected for BUTI YOUNG SCIENTIST PRESENTATION

13th December, 2021

ID	Date	Time	Abstract - Id	Title	Presenting Author	Affiliation
Buti -01	13-Dec-21	16:00 - 16:15	5	*Fluid simulation of ion acoustic solitary waves in a relativistic pulsar wind*	**Kuldeep Singh**	GNDU, Amritsar
Buti -02	13-Dec-21	16:15 - 16:30	29	*Dynamics of electrostatic waves in a dense relativistic pair plasma*	**Ridip Sarma**	Assam Don Bosco University, Guwahati
Buti -03	13-Dec-21	16:30 - 16:45	100	*First Order Phase Transition and Crystal-Fluid Coexistence in a Complex Plasma System*	**Hariprasad MG**	IPR, Gandhinagar
Buti -04	13-Dec-21	16:45 - 17:00	61	*Storage of Excessive Magnetic Free Energy and Evolution of Photospheric Current in Solar Active Regions Leading to Extreme Solar Eruptive Phenomena*	**Prabir Kumar Mitra**	Udaipur Solar Observatory, PRL, Ahmedabad
Buti -05	13-Dec-21	17:00 - 17:15	117	*2D-3V PIC-MCC based Simulations of Plasma Transport across Magnetic Filter : Instabilities and Double Layer formation*	**Miral Shah**	DAIICT, Gandhinagar
Buti -06	13-Dec-21	17:15 - 17:30	195	*Experimental verification of cavity modes in a microwave ion source and its influence on the plasma dynamics and the extracted ion beam*	**Chinmoy Mallick**	IPR, Gandhinagar

Keynote Address

Date: 13 December 2021 10.30 am; Link:

Nuclear Fusion in India: Past, Present and Future

by

Prof. Prabhat Ranjan

Vice Chancellor, D Y Patil International University, Akurdi, Pune, India

Abstract

Activity in Indian Nuclear Fusion program started in early 1980s with two programs: (1) Institute for Plasma Research, Gandhinagar funded by DST and (2) Hot Plasma Project in Saha Institute of Nuclear Physics, Kolkata funded by DAE. Both these projects followed Magnetic Confinement route to confine very high temperature plasma using "Tokamak" device. In mid 90s, Govt of India gave a go ahead to an ambitious project of developing Superconducting Tokamak, SST-1 with very long plasma discharge of 1000 sec.

In mid 2000s, India also joined hands with other countries to participate in an International project called ITER that is being built in south of France with the goal to produce 500 MW net power. This is of a huge dimension and after starting the design in 2007, it would be ready in 2025 at huge cost. Commercialization based on this path was expected sometime in 2060.

In the meantime, many technological advancements such as high temperature high magnetic field superconducting magnets are proving to be game changer and suddenly nuclear fusion as energy source has started to look much closer. It is expected that we would be able to produce net energy in a device of much smaller dimension than ITER in 2020s and we would be ready to feed power to grid in early 2030s and then it would keep on scaling up till 2045 or so to replace fossil fuel across the globe as a clean energy source.

These developments have resulted in many private initiative with good level of funding and with focused objective across the globe in last few years. Are we ready for such an initiative in India? Or India would miss this bus also like many others and be dependent on other countries to supply us this technology.

Fortunately for the first time in India, a private initiative "Project Sanlayan" has been initiated with Prof Ranjan as Chief Mentor and with funding from Albot Technologies Pvt Ltd (Set up by Dr Akash Singh, Innovator and Investor based in Silicon Valley). Initial work is being done at D Y Patil International Univ. Akurdi, Pune and a number of Scientists and Engineers have joined the project. Talk would provide brief details of what this project is trying to achieve.

About the Speaker:

Prof. Prabhat Ranjan is currently Vice Chancellor of D Y Patil International University (DYPIU), Akurdi, Pune. He is a Nuclear Fusion Scientist, a Futurist, an Educator, an Innovator and a Science Communicator.

Prof.. Ranjan has worked on Nuclear Fusion in National and International Labs in India and USA and made major contributions to this field for nearly two decades. He was Project Leader of ADITYA Tokamak and SST-1 Tokamak Operation and Control Group at IPR till 2002. He is a life member of PSSI and was PSSI newsletter editor from 1992-96.

From 2002, he served as Professor at Dhirubhai Ambani Institute of ICT in Gandhinagar for 11 years. His remarkable innovative contributions include India's Moon Mission, Wildlife and Agriculture sector. He is particularly known for his innovations in the field of assistive technology that has helped to put smiles on the faces of persons with severe disability.

From 2013-18, he was heading India's Technology Think Tank, TIFAC(Technology Information, Forecasting and Assessment Council) in Delhi as its Executive Director. During his tenure, TIFAC developed Technology Vision 2035, which was released by Hon'ble PM in Jan 2016.

He obtained his PhD from University of California, Berkeley and did college education from IIT Kharagpur and University of Delhi after schooling from Netarhat School. He has received many awards and accolades for his contribution to Science, Technology and Society.

As a founder Vice Chancellor of DYPIU, he has created a flexible and futuristic multitrack B Tech (Comp Sci and Engg.) program in 2019, which won appreciation from AICTE and has resulted in modernization of Comp Science curriculum across the country this year. He is also Chairing AICTE IDEA Lab National Steering Committee to setup digital fabrication facility across country. Recently he has also been nominated to represent India in ISO for Brain Computer Interface standardization effort.

1st A K SUNDARAM MEMORIAL LECTURE

By

Dr. Gurudas Ganguli

"Behavior of Solar Wind Compressed Plasma in the Earth's Magnetotail"

Date: 13 December 2021 Time: 18:30 hrs [IST]

Meeting link: http://tiny.cc/3e3muz

Meeting ID: 841 6133 3104 Password: BITPLAS21

Prof A. K. Sundaram

Professor A.K. Sundaram, former Dean and a past distinguished faculty member of IPR, was an internationally known plasma physicist who had played a major role in the establishment and early development of the Institute. He belonged to the ange of topics spanning space plasma physics, fusion physics and fundamental aspects of fluid dynamics. Known for his detailed and rigorous calculations – all carried out in neat long hand- he tackled frontline problems related to magnetic reconnection in the magnetospheoriginal team of seven scientists who had been handpicked by Dr. Vikram Sarabhai in 1971 to initiate a fusion program at the Physical Research Laboratory (PRL), Ahmedabad. His active contributions in the research program planning and in the training of young `would be plasma scientists' at PRL were of considerable help in the formation of a core group for the fusion program that was launched in 1982. Subsequently as the first Dean of IPR he set up the administrative structure of the Institute and successfully oversaw its operation for a number of years. An accomplished theoretical physicist with a strong background in Applied Mathematics his research interests encompassed a wide rre, tearing and ballooning mode instabilities in tokamaks and fundamental aspects of basic fluid instabilities. His scientific accomplishments attracted international attention and led to invitations for collaborations and visits to a number of leading research centres in the world. After taking retirement from IPR in 1993, Dr. Sundaram immigrated to the USA and worked for several years at the Goddard Space Flight Center, Greenbelt, Maryland where he continued to actively research magnetospheric and ionospheric phenomena. However his heart always remained at IPR – as he was fond of saying – the organization that he had known from its infancy and had helped to grow and in which he had invested so much of his love and care. To honour his memory his family has contributed funds to establish this annual memorial lecture to be organized by PSSI. The lecture is to be delivered by an eminent scientist preferably on a topic of research interest of Dr.Sundaram.

About the Speaker

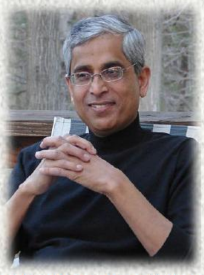

Dr. Gurudas Ganguli is the Senior Scientist for Intense Particle Beams and Plasma Processes in the Plasma Physics Division at the Naval Research Laboratory (NRL). Prior to this appointment in June 2012, he was the Head of the Space Analysis and Applications Section, Plasma Physics Division, NRL. He has a broad range of experience in plasma processes including beam-plasma interactions, plasma turbulence, dusty plasma dynamics, laser-produced plasma expansion, and high energy density physics in hypervelocity impact of projectiles in space. His work has addressed both natural plasmas as well as induced disturbances in the near-earth space environment. His research has motivated a number of laboratory and space experiments. He has led several ONR/NRL, DTRA, DARPA, Air Force and NASA sponsored research programs in ionospheric and magnetospheric plasmas as well as negative ion and dusty plasmas. He has authored/co-authored more than 170 publications.

He is the recipient of 2014 E. O. Hulburt Award for science, several NRL Berman awards for excellence in research publications, 2014 Edison Award for patent on a novel technique to de-orbit the lethal small orbital debris, and 2010 Technology Transfer Award. He was a member of the NRL Invention Evaluation Board and ONR panel member to upgrade the Navy S&T strategy plan in 2011 - 2012. He obtained his B.Sc. degree, from St. Xavier's College, Ahmedabad, India, in 1974 and Ph.D degree from Boston College, Boston, Massachuttes, in 1980. He was the Chairman of the International Union of Radio Science, Commission H (US National Chapter), during 2002 – 2005. He is a Fellow of the American Physical Society, Adjunct Professor of Physics at West Virginia and Auburn Universities, and a member of the American Geophysical Union. He has given over 100 invited talks at various national and international institutions and was appointed by the American Physical Society as a Distinguished Lecturer in Plasma Physics for 2001 –2002.

Abstract of the Talk

Plasma in the earth's magnetosphere is subjected to compression by solar wind during geomagnetically active periods and relaxation in subsequent quiet periods. Repeated compression and relaxation is the origin of much of the plasma dynamics and intermittency in the near-earth environment. An observable manifestation of compression is the thinning of the plasma sheet resulting in magnetic reconnection when the solar wind mass, energy, and momentum floods into the magnetosphere affecting the "space weather" and culminating in the spectacular auroral display. In situ measurements show compression of the magnetotail can create a thin current sheet of width comparable to the ion gyro-radius (pi), occasionally with single or double peaked substructures in the current density. These unusual multi scale substructures, as well as the origin of non gyrotropic plasma distribution with strongly sheared plasma flows cannot be explained by the standard Harris model. Intense lower hybrid wave activity and subsequent magnetic reconnection and substorm onset are also observed, which result in a plasma dipolarization front accelerating towards earth, driving space weather and injecting energetic particles into the radiation belts. We discuss a kinetic theory that can explain these seemingly disparate phenomena comprehensively and explain their causal connections. This elucidates the origin of the kinetic scale structures and the associated dynamics including anomalous dissipation processes necessary to initiate magnetic reconnection.

Invited Talks

Basic Plasma **Invited-1**

Why quasi-longitudinality is the order of the day in electromagnetic turbulence?

Devendra Sharma

Institute for Plasma Research, Bhat, Gandhinagar, 382428, India

Abstract

Turbulence is characteristics of fluctuations in continuum systems driven at macroscopic scales that are largely dissipationless. The electromagnetically coupled continua often possess too strong anisotropies for readily applying the universal zero dimensional scale-free description of the turbulence. Finite dimensional analysis and simulations are therefore essential for exploring operation of turbulence in such systems, e.g., in a magnetized plasma. Recent simulations highlight that ideally transverse electromagnetic fluctuations acquire strong longitudinal character in order to couple with electrostatic modes in order for turbulence to operate in a magnetized plasma. Computer simulations show that the visible nonlinear effects exclusively appear in quasi-longitudinal regime of electromagnetic modes in the form of small scale fluctuations excited perpendicular to the magnetic field that are associated with large scale structures parallel to the field. This corresponds to the situations in the nature [1,2] as well as in recent observations in laboratory [3] where a predominantly parallel drive is observed to excite strongly quasi-longitudinal small-scale electromagnetic fluctuations. Since even strongly nonlinear electrostatic fluctuations do not couple with small scale fluctuations for nearly transverse propagation, the strong anisotropy (quasi-longitudinality) is noted as the most plausible means for the observed turbulence to operate efficiently in the magnetized plasmas.

References:

[1] D. A. Gurnett *et al.,* J. Geophys. Res. 77, 172 (1972)

[2] D. A. Gurnett *et al.,* Geophys. Res. Lett. 13, 225 (1986)

[3] Sanyasi A. K. *et al.,* Phys. Plasmas 24, 102118 (2017)

Basic Plasma **Invited-2**

Understanding plasma adaptation for biomedical application : strong magnetic field effects and potential fluctuation dynamics

Sudeep Bhattacharjee[1], Deepika Behmani[1], Kalyani Barman[1] and Ramkrishna Rane[2]

[1]*Department of Physics, Indian Institute of Technology – Kanpur, Kanpur 208016, UP, India*
[2]*FCIPT, Institute for Plasma Research, Gandhinagar 382016, Gujarat, India*

Email: sudeepb@iitk.ac.in

Abstract

Cold atmospheric pressure micro-plasmas, are non-equilibrium plasmas with widely different electron (~6000 K) and ion temperatures (~300 K) [1]. These plasmas can be produced rather inexpensively in the atmosphere, and possess high electron densities ~10^{19} m^{-3} [2]. The typical plasma frequency lies in the GHz range and the Debye length is in ~ μm. The lower gas temperatures provide a conducive environment for application of these plasmas toward biological cells and tissues. Besides, the interaction of the charged particles with the ambient air, gives rise to a rich gaseous chemistry leading to the formation of reactive oxygen and nitrogen species (RONS) such as OH, HO_2, H_2O_2, including NO and N_2O_5 and radiation such as UV photons, which are critical for many biomedical applications such as sterilization, blood coagulation, healing of wounds, and in cancer therapy [3]. However, understanding plasma adaptation for these applications, and controlling the inherent physical processes that can influence them is a major challenge.

In this work, we report results of investigation of plasma potential fluctuations and the effect of a transverse magnetic field in an atmospheric pressure micro-plasma jet. Fluctuations can lead to particle and energy transport and modify the electron energy distribution function, thereby affecting plasma process rates and generation of RONS and radiation. It is found that the fluctuations grow and attain enhanced levels at certain magnitudes of the experimental parameters, such as applied voltage, gas flow rate and gas mixing ratio, before decreasing. Strong magnetic fields ($\geq$ 0.4 T) can significantly affect the dynamics of the plasma jet and reaction mechanisms. It is found to give rise to Zeeman splitting of the emission lines which lead to further broadening, and influences the plasma density. Additionally, finite ion Larmor radius effects at strong magnetic field, reduces the collisional drag considerably, and collisionally broadened ion cyclotron resonance condition can be realized, which alter the emission intensities of the RONS. More details will be presented in the conference.

References:

[1] K. Barman, D. Behmani, M. Mudgal, S. Bhattacharjee, R. Rane and S. K Nema, Plasma Res. Express **2**, 025007 (2020)
[2] T. Abuzairi, M. Okada, S Bhattacharjee and M. Nagatsu, Appl. Surf. Sci. **390**, 480–96 (2016)
[3] Li Lin and M. Keidar, Appl. Phys. Rev. **8**, 011306 (2021)
[4] K. Barman, M. Mudgal, R. Rane, and S. Bhattacharjee, Physics of Plasmas (**in press**)

Nuclear Fusion **Invited-3**

Technology for Fusion Reactors – A Weave, Through the Interdisciplinary Spectrum

A. K. Chakraborty

ITER-India, Institute for Plasma Research, Bhat, Gandhinagar – 382428

Abstract

Production of energy from fusion is the dream of a plasma physicist and fusion technologist. Harnessing the energy from fusion reaction and its sustained production involves challenges that appeal to the scientists and engineers, from different perspectives.

The scientist's objective is to explore a configuration space where the plasma, formed primarily inside the magnetically confined device – predominantly in form of a Tokamak, is experimented in several configurations to arrive at a stable operational mode which maintains the confinement for long enough durations. The engineer, on the other hand, has his focus on ensuring the necessary attributes in the device and its subsystems to enable these experimental explorations.

In meeting the requirements, Fusion Technology demands development of technologies where many of them are of a first of a kind. Few examples are i) The development of large size Super Conducting magnets; ii) Special cryogenic pumps for pumping capacity exceeding 10^6 l/s; iii) Ultra High Vacuum (UHV) compatible > 10 MW/m^2 class, High Heat Flux (HHF) facing components; iv) Specialized joining for similar and dissimilar material by processes that induce least impact on the heat affected zones; v) Engineering joint designs that can be subject to volumetric inspection; vii) Shaping and forming precision machined large structures; vii) precision machining of components to tolerances in the order of microns; viii) Hundred kW class Liquid Helium (LHe) refrigerator systems for cryogenic supplies; ix) Development of insulators that provide Mega Volt class isolation; x) High Voltage Power systems (HVPS) capable of switching multi-megawatts of power in the order of micro seconds; xi) Multi Megawatt Radio Frequency (RF) and microwave systems; xii) Large area multi-ampere and Megavolt class ion beam generators that provide the ion beams for the Neutral Beam Injection (NBI) system; xiii) Fast acquisition high throughput data acquisition system; xiv) High speed and high throughput pellet injectors; xv) Advanced imaging systems using a wide band of spectrograph systems; xvi) Advanced computer simulations for the generation of advanced configurations.

A blend of interdisciplinary areas of R&D leading to development of the specialized technologies, listed above is therefore a necessity for the realization of the objectives of Fusion Technology. Participation in ITER has enabled the creation of such an expertise pool, not only at the Institutional level, in ITER-India, Institute for Plasma Research (IPR), but also at the industrial level, where, several industries have collaborated in the effort to deliver systems to ITER, meeting all stipulated requirements. While ITER is a collaboration of 7 nations, the path to the next step, of building of a demonstration reactor, shall primarily be an indigenous effort, as the race towards realizing a carbon free energy source intensifies in the coming decades.

The talk proposes to share the Indian experience the development of Fusion Technology, its present status and possible paths forward, involving the nation's industry, technology institutes and centers of excellence.

Plasma Application **Invited-4**

Plasma Technology: Skill development support

Dr. K. S. Ganesh Prasad

Institute of Advanced Research
Institutional Area, Coba, Gandhinagar 382426.

Abstract

Plasma Physics started few decades ago in India. Development of tokamak work perused by IPR initiated plasma technology development. There are several plasma machines working in the country. Absorption of plasma technology by the industry requires technically trained manpower at different levels. Technically trained manpower should be aware of associated fields like vacuum technology, analog, digital circuits, power electronics etc. Universities in India have developed course to support bio-technology, computer science, information technology etc. University has realized the potential development and scope for the society and accommodated the courses. However, other fields like vacuum technology, material science etc. have come up with short term courses or workshops to train technical manpower for their fields in addition to conducting seminars and conferences. The simplest and most widely used application of plasma is welding. Technical training institutes run by both government and private agencies provide one-year certificate courses. It has given substantial support to mechanical fabrication industry. Some of the universities have come up with advanced courses in welding in India. A short term courses in plasma engineering with work shop training is required to progress of technology into industry. This will also increase the scope of absorption of plasma device in the society. This presentation focus on different initiatives that can be followed by academic institutes or universities.

Plasma Application **Invited-5**

Transferred arc plasma processing of waste aluminium dross

K.Ramachandran
Department of Physics, Bharathiar University, Coimbatore – 641 046
rams@buc.edu.in

Abstract

Waste aluminium dross is a byproduct of aluminium melting process and it contains aluminium metal, aluminium oxide, aluminium oxy-nitride and impurities such as sodium chloride and potassium chloride. Several million tons of dross have been generated annually from domestic aluminium smelting process alone in many countries and more than 90 % of these waste dross have been land filled without any treatment and recovery of value added products. Recently recycling of aluminium attracts more attention since the production of aluminium from its ore is costly process. Conventional methods for the metal recovery from the recycling of aluminium dross involve large amount of chemicals and are time consuming.

In this presentation, a transferred arc plasma process for producing value added products from the waste aluminium dross is discussed. The aluminium dross was melted and evaporated by the plasma arc established between a crucible anode and a rod type hollow cathode made of graphite. Raw dross and products of plasma treated dross such as slag and fine powder were characterized. The generation of ultrafine alumina powder and slag are explained using simulation of the plasma arc inside the crucible and free energy minimization calculations. High temperature and air entrainment into the plasma inside the crucible converted the dross into alumina slag and fine powder. The amount of fine alumina powder produced increased substantially with plasma power initially as seen from the results of alumina obtained at 5 kW and 10 kW. However, further increase in plasma power resulted only in marginal increase in the conversion of Al dross to alumina. Results of this study indicate that arc plasma technology can be effectively applied to convert Al dross into value added fine alumina powder. Rapid processing and eco-friendly nature are the merits of the plasma process reported in this presentation.

Plasma Diagnostics **Invited-6**

Overview of SST-1 Thomson system: Installation calibration and operation

Jinto Thomas

Institute for Plasma Research, Bhat, Gandhinagar – 382428

Abstract

A multipulse, Nd:YAG (yttrium aluminum garnet) Thomson scattering (TS) system has been designed and developed for measuring electron temperature (Te) and density (ne) profiles of SST-1 tokamak. The developed TS system has been installed on SST-1 for measuring the temperature and density profile along the vertical chord at R=1.1 meter. Six Nd:YAG lasers synchronized with external control are used for versatile of measurement. The scattered light is collected using multiple lenses imaging system and a 2mm core optical fiber is used to transport the scattered light into the lab for spectral dispersion and detection. A low cost and compact five-channel interference filter polychromator is designed and indegenously fabricated for the spectral dispersion.. High gain avalanche photodiodes are used as the detection system. Complete electronics for detection and control has been implemented indegenously. Using the detectors with enhanced quantum efficiency in the IR region, improves the detection efficiency and the measurement limits of the diagnostics. A charge integrator based data acquisition system operating on PXI bus is developed for data acquisition. The entire system is calibrated using a pulsed whilte light source to correctly ascertain the spectral shape of the scattered spectrum. Rotational Raman and Rayleigh scatterings are used for the absolute calibration of the TS system installed in SST-1. In the recent SST-1 campaign, the system recorded the temperature and desnity profiles of SST-1 plasma. An overview of different subsystems of TS diagnsotics will be discussed along with the results from the recent campaign. Future plans and up gradation of this diagnostics will also be pointed out.

References:

1. Design of multipulse Thomson scattering diagnostic for SST-1 tokamak, Ajai Kumar etal, Review of scientific instruments 78(4):043507, 2007
2. Design and development of detector signal conditioning electronics for SST-1 Thomson scattering system, Aruna etal Review of scientific instruments 79(9):093505, 2008
3. Design and development of five-channel interference filter polychromator for SST-1 Thomson scattering system, Jinto Thomas etal, Fusion Engineering and Design 87(2):134–140, 2012
4. Enhancing detection sensitivity of SST-1 Thomson scattering experiment, V choudhary etal. Fusion Engineering and Design 108:67-76, 2016

Space and Astrophysical Plasma **Invited-7**

Application of 2D and 3D magnetic reconnection in solar flares: A perspective

Bhuwan Joshi

Udaipur Solar Observatory, Physical Research Laboratory, Udaipur 313001, India

Abstract

Solar flares are characterized by the sudden release of excess energy stored in the magnetic fields of solar corona. The modern multi-wavelength observations have immensely improved our understanding of the various physical processes occurring in different atmospheric layers of the Sun during a solar flare. The standard flare model, a two-dimension (2D) model, has been successful in broadly recognizing the impulsive energy release and eruption of magnetic flux role (MFR) as the consequence of large-scale magnetic reconnection in the corona. Despite general success of the standard model, it cannot fail to explain several observed features of solar flares which have been identified in high-resolution data, mostly gathered in the last decade, from space-borne telescopes in extreme ultraviolet (EUV), ultraviolet (UV) and X-ray bands. In order to understand the complex observations, contemporary works have probed into the nature and the characteristics of magnetic reconnection in three dimensions (3D). In this talk, I will review the efforts made on different fronts to approach the problem of magnetic reconnection in solar flares. In particular, I will highlight our recent works on the magnetic topology in 3D, formation of flux ropes and plasmoids, and evolution of flaring loops.

Space and Astrophysical Plasma **Invited-8**

Extreme Laser Fields Driven Electron Acceleration in Plasmas

A. Moorti[1,2]

[1]*Advanced Plasma Acceleration Section, Laser Plasma Division, RRCAT, Indore 452013*
[2]*Faculty of Physics, HBNI, Training School Complex, Anushaktinagar, Mumbai 400 094*

E-mail : moorti@rrcat.gov.in

Abstract

With applications in almost every aspect of life, LASER has turned out to be one of the greatest inventions of the modern time. At the same time, it has also been recognized as a ubiquitous tool for the advancement of science and technology. Successive development of the mode-locking techniques has brought down the laser pulse duration in the femtosecond (ultra-short) regime, and using Chirped Pulse Amplification (CPA) technique (for which G. Mourou and D. Strickland, were jointly awarded Nobel Prize in Physics, 2018), laser systems providing peak powers of several Terawatt (TW) to few Petawatt (PW) level now has become a reality. When focused to a tiny spot of few microns to few tens of microns diameter, such high-power, ultra-short duration laser systems could provide extreme intensities of ~10^{18} Wcm^{-2} to greater than 10^{20} Wcm^{-2}, which has led to fascinating physics and applications of high-intensity laser matter interaction[1]. Due to associated extreme electric field with ultra-high focused intensities and also with generated collective fields in the plasma, this has facilitated research and development of laser-driven plasma based advanced particle (electron/proton/ion) accelerators[2]. Compact electron accelerators of energy in the range of 100s of MeV to more than GeV have been demonstrated, which could also facilitate development of laser driven synchrotron (x-rays and γ-rays) sources. In this talk, advanced acceleration techniques based on ultra-short, ultra-intense laser plasma interaction with an emphasis on role of extreme laser fields, along with recent experimental investigations performed in this area using both solid and gaseous targets at RRCAT, Indore would be presented.

REFERENCES:

1. A. Moorti, *Kiran: A Bulletin of the Indian Laser Association,* **2015,** 26(2), 19.
2. A. Moorti, *Physics News, Bulletin of the Indian Physics Association,* **2018**, 48(3), 19.

Laser Plasma, Pulsed power and Others **Invited-9**

Plasma Applications in Electronic Devices

Rajneesh Kumar

Department of Physics, Institute of Science, Banaras Hindu University, Varanasi, India
Phone: +91 9179702674, Email: rajneeshipr@gmail.com, rajneesh.physics@bhu.ac.in

Abstract

Recently, number of spin-off plasma based technologies have spawned in the area of tunable electronic devices because material properties (electric permittivity and magnetic permeability) of plasma can be tuned by changing the plasma parameters as per the requirement of the electronic device. Hence, in this presentation, industrial applications of plasmas in the size of centimeters to nanometers for radio frequency to terahertz electronic devices will be discussed. It is known that use of high-tech devices in aerospace technology, communication and optical systems, and micro-machines is showing a strong growth. Wireless data communication is playing an important role in our daily life because it offers flexibility and mobility. To transmit and receive the data among devices in various communication environments, a reconfigurable antenna that can fit various environments is needed. In an overcrowded radio spectrum environment, a frequency reconfigurable antenna is an attractive solution to avoid interference among signals. Therefore, the development of such an antenna has become a focus of research. With the above mentioned concerns, antenna properties and communication capability of commercially available fluorescent lamps and compact florescent lamps (CFL) are investigated. Experiments are conducted to examine the transmission capability of the fluorescent tube plasma and antenna parameters such as gain, directivity, resonance frequencies and radiation patterns are obtained. In addition, simulation of the model is also studied to optimize the experimental results. Findings of the present study invoke the interesting feature of a commercially available fluorescent tube which can be employed for wireless communication of microwave of 2.40 GHz. In addition, simulation study indicates that CFLs can be used for 5G communication. Moreover, it is also demonstrated that array of fluorescent tubes can be used for microwave attenuation and plasma windowing effect.

Findings of analytical, experimental and simulation study reveal that microwave absorption is maximum when neutral-electron collision frequency is nearly equal to the microwave frequency. Moreover, if we want to use plasma for millimeter and THz technology, we have to scale down the size of plasma. I have an opportunity to mention that plasmas where at least one plasma dimension is in the sub-millimeter range is called microplasmas. During the last decade a number of microcavity plasma devices have been developed. Examples are microhollow cathode (MHC) discharges and cathode boundary layer (CBL) discharges. The advantage of this technology is that large numbers of miniature atmospheric-pressure non-equilibrium discharges can be operated in parallel. Applications include emitters for visible and UV radiation, photodetectors, sensors, decontamination, surface modification, etching, film deposition, implementation of semiconductor and microelectronics and MEMs microfabrication techniques, micromaching tools, micrchemical analysis, biomaterial processing, photonic devices etc. In our study, three electrodes are made by molybdenum foil and

alumina used as a dielectric to make sandwich of electrodes with the hole of diameter 0.5 to 1 mm. High temperature glue is used to pack the electrodes and alumina. Two DC power supplies are used to produce voltage differences between electrodes. Typical cathode voltage is 800 V and anode voltage varies from 1 to 2 kV maintaining current up to 15 mA. Argon and helium gases are used as background gases in the glass chamber. Further, in our present simulation study, microplasma has also been used in the photonic crystal for study the positive and negative refraction of x-band microwave (18 GHz). It is interesting to mention that CFL can also be used as a plasma source in the plasma photonic crystal. Findings of this study show that flat and forbidden bands can be controlled in such a way that the negative and positive refractions can be achieved at particular angles. Hence, it reveals importance of plasma to enhance the controllability of microwave propagation in photonic crystals. Microplasmas can be scaled down up to nanoplasmas. Nanoscale plasma switch goes from zero to Kilowatts in Picoseconds to 100 femtoseconds, therefore such plasmas can be used for ultrafast electronics and can be used in 6G terahertz transmitters.

CONTENTS

	Page No.
Preface	**7**
Sponsors	**9**
Committees of the Symposium	**10**
Program Schedule	**12**
Session Chairperson for Plasma 2021	**12**
Speakers for Plasma 2021	**13**
Schedule of Oral Presentations	**14**
Schedule of BUTI young scientist award presentation	**15**
Keynote Address	**16**
A.K. Sundaram Memorial Lecture	**17**
Invited Talks	**18**

ORAL PRESENTATIONS

ORAL-BP-1	**AN EXPERIMENTAL INVESTIGATION OF OSCILLATING PLASMA BUBBLES AND ITS NON LINEAR STRUCTURE IN A MAGNETIZED PLASMA SYSTEM** Mariammal Megalingam and Bornali Sarma	**47**
ORAL-BP-2	**STUDY OF TWO STREAM INSTABILITY IN INHOMOGENEOUS DUSTY PLASMAS WITH UNIFORM MAGNETIC FIELD** Shachi Pachauri, Jyoti, Kamakhya Prakash Misra	**48**
ORAL-BP-3	**STRONG MAGNETIC FIELD EFFECTS IN THE STRONGLY COUPLED ROTATING DUSTY PLASMA** Prince Kumar* and Devendra Sharma	**49**
ORAL-NF-1	**STUDY OF MHD ACTIVITY AND RUNAWAY ELECTRONS IN THE ADITYA AND ADITYA-U TOKAMAK** S. Patel, J. Ghosh, M. B. Chowdhuri, K. B. K. Mayya, S. Purohit, T. Macwan, S. Aich, S. Dolui, K. Singh, R. L. Tanna, K. A. Jadeja, K. M. Patel, R. Kumar, N. Yadava, R. Manchanda, N. Ramaiya,K. Shah, A. Kumar, Y. S. Joisa, S. K. Jha, D. Raju, U. Nagora, P. K. Atrey, S. B. Bhatt, D. Chenna Reddy, Y. C. Saxena, ADITYA Team and ADITYA-U Team	**50**
ORAL-NF-2	**HEAT TRANSFER ANALYSIS OF PINI ION SOURCE BACK PLATE USING ANSYS** Tejendra Pateland M. R. Jana	**51**
ORAL-NF-3	**DESIGN UPDATES AND CURRENT STATUS OF INSTALLATION WORKS OF EXPERIMENTAL HELIUM COOLING LOOP (EHCL)** B. K. Yadav, A. Gandhi, A. Saraswat, S. Verma, P. Chaudhuri	**52**
ORAL-NF-4	**TOWARDS A 3D QUIESCENT NONNEUTRAL PLASMA STATE IN SMALL ASPECT RATIO TORUS - A PARTICLE-IN-CELL SIMULATION STUDY** Swapnali Khamaru, Rajaraman Ganesh,Meghraj Sengupta	**53**

ORAL-PA-1	**MICROPLASMA SYNTHESIS OF CE-DOPED HAUSMANNITE MN_3O_4NANOPARTICLES FOR SUPERCAPACITOR APPLICATION** E.R. Kavitha, K. Suresh, and S. Yugeswaran	**54**
ORAL-PA-2	**RAPID CRYSTALLIZATION OF AMORPHOUS TIO_2 USING ATMOSPHERIC PRESSURE PLASMA** Parismita Kalita, Palash Jyoti Boruah and Heremba Bailung	**55**
ORAL-PA-3	**COLD PLASMA TREATMENT OF RAW MILK AND ITS PHYSICAL PROPERTIES ANALYSIS** Kiran, Ramavtar,Vigyan Gadodia, Shikha Panday, Ritesh Mishra and Ram Prakash	**56**
ORAL-PD-1	**ARGON IMPURITY TRANSPORT IN ADITYA-U TOKAMAK USING SPECTROSOCPY** K. Shah, M. B. Chowdhuri,J. Ghosh, K. A. Jadeja, R. Manchanda, G. Shukla, S. Patel, N. Yadava, N. Ramaiya, R. Dey, T. Macwan, R. L. Tanna,R. Kumar, S. Aich, K. M. Patel, S. Purohit, M. K. Gupta, U. C. Nagora, S. K. Pathak, K. B. K. Mayya and Aditya-U Team	**57**
ORAL-PD-2	**COLLISIONAL RADIATIVE (CR) MODEL FOR THE DIAGNOSTICS OF NE-AR MIXTURE PLASMA** S. S. Baghel, R. K. Gangwar and R.Srivastava	**58**
ORAL-PD-3	**ADITYA TOKAMAK PLASMA DISRUPTION CHARACTERIZATION** S. Purohit, M. B. Chowdhuri, J. Ghosh, C. N. Gupta, S. K. Jha, D. Raju, K. A. Jadeja, M. K. Gupta, P. K. Atrey, S. K. Pathak, Y. S. Joisa, R. L. Tanna, P. K. Chattopadhyay, and ADITYA Team	**59**
ORAL-SP-1	**SHEAR FLOW EFECTS ON MAGNETIC ISLAND COALESCENCE** Jagannath Mahapatra, Rajaraman Ganesh, Arkaprava Bokshi, and Abhijit Sen	**60**
ORAL-SP-2	**COSMIC RAYS DIFFUSION AND GRAVITATIONAL COLLAPSE IN RADIATIVE MOLECULAR CLOUDS INCLUDING ION LARMOR RADIUS CORRECTIONS** Ram Prasad Prajapati	**61**
ORAL-SP-3	**GENERATION OF KINETIC ALFVÉN WAVES BY MULTIPLE FREE ENERGY SOURCES** Krushna Chandra Barik, Satyavir Singh, and G.S. Lakhina	**62**
ORAL-PO-1	**INDIGENOUS HIGH POWER PSEUDOSPARK SWITCHES FOR FAST PULSE POWER APPLICATIONS** Ram Prakash Lamba, Udit Narayan Pal and Ram Prakash	**63**
ORAL-PO-2	**PULSED LASER DEPOSITION OF CUO/CU_2O FILMS AND THEIR APPLICATION IN PHOTOCATALYTIC DYE DEGRADATION** RudrashishPanda, Milaan Patel, JintoThomas and Hem Chandra Joshi	**65**
ORAL-PO-3	**EXCITATION OF LOWER HYBRID AND MAGNETO-SONIC PERTURBATIONS BY LASER INX-MODE CONFIGURATION OF MAGNETIZED PLASMA** Ayushi Vashistha, Devshree Mandal andAmita Das	**66**

POSTER PRESENTATIONS

CATEGORY: BASIC PLASMA THEORY (BPT)

BPT-P-1	**DATA COMPRESSION BY AZADBINRAJIB (ABR) QUANTUM GATE** A.B.Rajib Hazarika	**67**
BPT-P-2	**EFFECT OF ELECTRON- POSITRON- ION ON MODULATION OF NONLINEAR WAVES IN WARM PLASMA: A NONLINEAR SCHRÖDINGER EQUATION** Latika Kalita and Ranjit Kumar Kalita	**67**
BPT-P-3	**NONLINEAR DYNAMIC MODELLING OF HIGH FREQUENCY ELECTROSTATIC DRIFT WAVES IN FLUID THEORETICAL APPROACH**S.P. Acharya and M.S. Janaki	**68**
BPT-P-4	**CRYPTOCURRENCY: THE FUTURE OF MONEY ON PATTERN OF QUANTUM CRYPTOGRAPHY** A.B.Rajib Hazarika	**69**
BPT-P-5	**TWO STREAM INSTABILITY IN UNMAGNETIZED INHOMOGENEOUS NONRELATIVISTIC QUANTUM PLASMAS** Shiva ShaktiSingh, Jyoti, Kamakhya Prakash Misra	**69**
BPT-P-6	**EFFECT OF K-DEFORMED KANIADAKIS DISTRIBUTION ON MODULATIONAL INSTABILITY OF ION-ACOUSTIC WAVES**Gurleen Kaur and Parveen Bala	**70**
BPT-P-7	**MODIFIED BURGER'S EQUATION USING SCHAMEL KAPPA DISTRIBUTION** Parveen Bala and Gurleen Kaur	**70**
BPT-P-8	**EFFECT OF DAMPING ON TERAHERTZ RADIATION GENERATION FROM LASER INTERACTION WITH NANO-PARTICLES** *P. Varshney, A. P Singh, M. Kundu1 and K. Gopal	**71**
BPT-P-9	**EFFECT OF DENSITY RIPPLE ON THZ GENERATION BY Q-GAUSSIAN LASER IN PLASMA** Dipender Singha, NitiKanta, Shivani Vij	**71**
BPT-P-10	**MODELLING AND SIMULATION STUDY OF MAGNETIC ENHANCEMENT IN PLASMA DENSITY FOR RF BASED H^- ION SOURCE** Rajnish Kumar, Dharmraj V. Ghodke, Vijendra Prasad and Purushottam Shrivastava	**72**
BPT-P-11	**ROLE OF QUANTUM PLASMA IN SOCIETY AND ITS APPLICATION** Manisha Raghuvanshi, Sanjay Dixit	**73**
BPT-P-12	**EFFECT OF OBSTACLE AND GEOMETRIC ASPECT RATIO ON LANE DYNAMICS IN PAIR ION PLASMAS** Vishal K. Prajapati, Swati Baruah and R. Ganesh	**73**
BPT-P-13	**SECOND HARMONIC GENERATION BY A COSH-GAUSSIAN LASER BEAM DRIVEN ELECTRON PLASMA WAVE: HIGHER-ORDER PARAXIAL THEORY** Gunjan Purohit, Pradeep Kothiyal and Ramesh Kumar Sharma	**74**

BPT-P-14	**EXISTENCE AND STABILITY OF ALTERNATIVE DUST ION ACOUSTIC SOLITARY WAVES IN ADUSTY PLASMA CONSISTING OF NONTHERMAL ELECTRONS HAVING VORTEX-LIKE VELOCITY DISTRIBUTION** Sankirtan Sardar, Anup Bandyopadhyay, K.P Das	**75**
BPT-P-15	**THZ SURFACE PLASMON PROPAGATION ON AN ULTRATHIN SEMICONDUCTOR LAYER DEPOSITED OVER GLASS SLAB** Roopkiranpreet Kaur and Sukhdeep Kaur	**76**
BPT-P-16	**OBSERVATION OF E x B ELECTRON DRIFT INSTABILITY IN HALLTHRUSTERSIMULATION** Sneha Gupta, Debraj Mandal, Devendra Sharma	**77**
BPT-P-17	**BEAM–PLASMA INSTABILITY IN SPIN POLARIZED HIGH DENSITY DEGENERATE PLASMA** Punit Kumar and Shiv Singh	**77**
BPT-P-18	**NONLINEAR MIXING IN A DUSTY PLASMA GOVERNED BY A PERIODICALLY DRIVEN KORTEWEG-DE VRIES MODEL** Ajaz Mir, Sanat Tiwari, and Abhijit Sen	**78**
BPT-P-19	**NUMERICAL STUDY OF MAGNETIZED DUSTY PLASMA SHEATH WITH TWO ION SPECIES AND OBLIQUE MAGNETIC FIELD** A.K. Shaw and A. K. Sanyasi	**79**
BPT-P-20	**CHARGING KINETICS OF SPUTTERED PARTICLES IN PSEUDOSPARK DISCHARGE PLASMA** Shikha Misra, Akhilesh Mishra, Ram Prakash Lamba and Udit Narayan Pal	**80**
BPT-P-21	**QUASI-LONGITUDINAL PROPAGATION OF NONLINEAR ELECTROMAGNETIC EXCITATIONS IN MAGNETIZED PLASMA** Gayatri Barsagade, Devendra Sharma	**81**
BPT-P-22	**WAVELET ANALYSIS OF FLOATING POTENTIAL OSCILLATIONS OF ANODIC DOUBLE LAYERS PRODUCED IN DC GLOW DISCHARGE PLASMA** *ThangjamRishikanta Singh and Suraj Kumar Sinha*	**81**
BPT-P-23	**HYDRODYNAMIC MATRIX AND DENSITY AUTOCORRELATION FUNCTION FOR STRONGLY COUPLED CHARGED FLUIDS IN GENERALIZED HYDRODYNAMIC FRAMEWORK** Ankit Dhaka, PV Subhash, Pintu Bandyopadhyay	**82**
BPT-P-24	**RATCHET DYNAMICS OF ACTIVE YUKAWA PARTICLES** Anshika Chugh, Rajaraman Ganesh, Soumen De Karmakar	**83**
BPT-P-25	**ROTATIONAL KELVIN-HELMHOLTZ INSTABILITY AND ANOMALOUS TRANSPORT IN A 2D STRONGLY COUPLED YUKAWA LIQUID** SurujKalita, Rajaraman Ganesh	**84**
BPT-P-26	**ION-ACOUSTIC COMPRESSIVE AND RAREFACTIVE WAVES IN MAGNETOPLASMA WITH NEGATIVE IONS AND NONTHERMAL ELECTRONS** J. K. Chawla	**85**

BPT-P-27	**TEMPERATURE GUIDED CONFINING EFFECTS OF REALISTIC WALLS ON HELIUM GAS DYNAMICS AT LOW TEMPERATURES: UNRAVELING MOLECULAR MYSTERIES OF CRYOPLASMAS** Swati Swagatika Mishra, Sudeep Bhattacharjee	85
BPT-P-28	**ELECTROMAGNETIC WAVE TRANSPARENCY INDUCED IN A STRONGLY MAGNETIZED PLASMA** Devshree Mandal, Ayushi Vashistha and Amita Das	86
BPT-P-29	**ULTRA-LOW EMITTANCE ELECTRON-BUNCH GENERATION IN PLASMA WAKEFIELD ACCELERATION** Sandeep Kumar	87
BPT-P-30	**ARBITRARY AMPLITUDE ION-ACOUSTIC SOLITARY WAVES IN NEGATIVE ION PLASMA WITH RELATIVISTIC DEGENERATE ELECTRONS** Kishan Kumar and M. K. Mishra	88
BPT-P-31	**TUNABLE DIFFUSIVE PROPERTY OF COMPLEX PLASMA DRIVEN BY MAGNETIZED WAKE** Biswajit Dutta, Nilakshi Das	88
BPT-P-32	**SIMULATING PLASMA DYNAMICS IN A MAGNETIC NOZZLE** Subhasish Bag and Vikrant Saxena	89
BPT-P-33	**NONLINEAR ELECTRON-ACOUSTIC WAVES WITH SCHAMEL-KAPPA DISTRIBUTED HOT ELECTRONS** Gurmant Kaur, Praveen Bala	90
BPT-P-34	**ROTATIONAL PROPERTIES OF ANNULUS DUSTY PLASMA IN A STRONG MAGNETIC FIELD** Mangilal Choudhary, Markus H Thoma Markus	91
BPT-P-35	**A HEURISTIC STUDY OF NONLINEAR WAVE-PARTICLE INTERACTION IN AN UNMAGNETISED PLASMA** Priyangana Chatterjee, Arghya Mukherjee	91
BPT-P-36	**NONLINEAR EVOULTION AND PHASE MIXING OF LOWER HYBRID MODES IN COLD PLASMA** MithunKarmakar, Chandan Maity, Sourav Pramanik	92
BPT-P-37	**EFFECT OF TWO-TEMPERATURE ELECTRONS ON ION-ACOUSTIC SOLITARY WAVES IN A MAGNETIZED PLASMA** Jintu Ozah	92
BPT-P-38	**EFFECTS OF NEUTRAL COLLISIONS AND RADIATIVE HEAT-LOSS FUNCTIONS ON THERMAL INSTABILITY OF TWO-COMPONENT PLASMA WITH HALL CURRENT AND FINITE ELECTRON INERTIA IN HI REGION** Sachin Kaothekar, S. Mishra, and S. Phadke	93

CATEGORY: BASIC PLASMA EXPERIMENTS (BPE)

BPE-P-1	**MULTI-FILAMENTARY W-BASED PLASMA SOURCE FOR LARGE VOLUME PLASMA DEVICE - UPGRADE** A.K. Sanyasi, P. K. Srivastava, Ayan Adhikari, Pinakin Leuva, Prosenjit Santra, Ritesh Sugandhi, L. M. Awasthi, Bharat Doshi and M. K. Gupta	**94**
BPE-P-2	**ROLE OF WHISTLERS IN MITIGATION OF ENERGETIC (RUNAWAY) ELECTRONS** A.K. Sanyasi, L. M. Awasthi,P. K. Srivastava, Ritesh Sugandhi, and D. Sharma	**95**
BPE-P-3	**CONTINUOUS TEMPERATURE MONITORING SYSTEM FOR LARGE VOLUME PLASMA DEVICE - UPGRADE** D. Khanduri, R. Sugandhi, P. K. Srivastava, A. Balaji, U. Pallapothu, A. Adhikari, A. K. Sanyasi, and L. M. Awasthi	**96**
BPE-P-4	**DESIGN OF PROCESS AUTOMATION SYSTEM FOR LARGE VOLUME PLASMA DEVICE UPGRADE** R. Sugandhi, P. K. Srivastava, A. K. Sanyasi,A.Adhikari D.Khanduri, and L. M. Awasthi1,	**97**
BPE-P-5	**WEB EDITOR FOR CONFIGURATION MANAGEMENT OF LABORATORY PLASMA EXPERIMENTS** V.Soumya, R. Sugandhi, M. Jha, D. Khanduri, Ayan Adhikari, P.K. Srivastava, A. K. Sanyasi, L. M. Awasthiand S. D. Panchal	**98**
BPE-P-6	**BROADBAND UV AND TEMPERATURE SENSOR PROBE FOR PLASMA STERILIZATION APPLICATION** Kushagra Nigam, G. Ravi and S.K. Nema	**99**
BPE-P-7	**OBSERVATION OF DUST IN PLASMA TO DUSTY PLASMA TRANSITION IN HOLLOW ANODE DISCHARGE** Nidhi Pateland G.Prasad	**99**
BPE-P-8	**EVOLUTION OF SPONTANEOUS DUST DENSITY WAVES IN NANODUSTY PLASMAS UNDER STRONG HAVNES EFFECT** Bidyut Chutia	**100**
BPE-P-9	**NANODUPLEX: A NEW DUSTY PLASMA EXPERIMENTAL SETUP TO PRODUCE EXTENDED DUST CLOUDS USING REACTIVE ARGON ACETYLENE PLASMAS** BidyutChutia, T. Deka, Y. Bailung, S. K. Sharma and H. Bailung	**101**
BPE-P-10	**HIGH CURRENT PULSED POWER SUPPLY SYSTEM FOR LARGE VOLUME PLASMA DEVICE-UPGRADE** P. K. Srivastava, R. Sugandhi, A. K. Sanyasi, A.Adhikari, and L. M. Awasthi1,	**102**
BPE-P-11	**UTILIZATION OF AN INERTIAL ELECTROSTATIC CONFINEMENT FUSION DEVICE AS A NEUTRON AND X-RAY SOURCE** D. Bhattacharjee, L. Saikia and S. R. Mohanty	**103**
BPE-P-12	**EFFECT OF MULTIPLE GRID CONFIGURATION ON PLASMA PARAMETERS OF AN INERTIAL ELECTROSTATIC CONFINEMENT FUSION DEVICE** L. Saikia, D. Bhattacharjee, A. Maurya and S. R. Mohanty	**104**

BPE-P-13	**PROTOTYPE AUTOMATED LINEAR AND ROTATIONAL PROBE DRIVE FOR LARGE VOLUME PLASMA DEVICE-UPGRADE** P. Chauhan, R. Sugandhi, A. K. Sanyasi, P. K. Srivastava, D. Khanduri, A. Adhikari, P. K. Leuva, M. K. Gupta, B. R. Doshi and L. M. Awasthi	105
BPE-P-14	**INTERACTION OF A PRECURSOR SOLITON WITH A WAKE-FIELD IN A FLOWING DUSTY PLASMA** Krishan Kumar, Pintu Bandyopadhyay, Swarnima Singh, Abhijit Sen	106
BPE-P-15	**TRANSITION OF A MONOLAYER CRYSTAL TO A LIQUID-SOLID COEXISTENCE STATE IN A COMPLEX PLASMA** Swarnima Singh, Krishan Kumar, M.G. Hariprasad, A. Saravanan, P. Bandyopadhyayand A. Sen	107
BPE-P-16	**DESIGN CONSIDERATION FOR A LINEAR MAGNETIZED PLASMA DEVICE** Dibyajyoti Bora and Subir Biswas	107
BPE-P-17	**NOVEL EXPLANATION OF THE COLD PULSE PROPAGATION PHENOMENON INDUCED BY GAS PUFF IN ADITYA-U TOKAMAK** Tanmay Macwan, Harshita Raj, Kaushlender Singh, Suman Dolui, Sharvil Patel, Ankit Kumar , P Gautam, J Ghosh, R L Tanna, K A Jadeja, K M Patel, Rohit Kumar, Suman Aich, Umesh Nagora, M B Chowdhuri, R Manchanda, Nandini Yadava, Ritu Dey, Kiran Patel, S. K. Pathak, M. K. Gupta, K. Tahiliani, P. K. Chattopadhyay, A Sen, Y C Saxena, R Pal	108
BPE-P-18	**INITIAL PLASMA EXPERIMENTS IN SIMPLE TIGHT ASPECT RATIO MACHINE ASSEMBLY** T. Ram, Jagbandhu kumar, P. K. Sharma, Raju Daniel	109
BPE-P-19	**EXPLORING POSSIBILITY OF ETG SUITABLE PROFILES IN VARYING RATIO OF TRANSVERSE TO LONGITUDINAL MAGNETIC FIELD IN LVPD-U** Ayan Adhikari, A. K. Sanyasi, L.M. Awasthi , P. K. Srivastava, Ritesh Sugandhi and Mainak Bandyopadhyay	110
BPE-P-20	**UNDERSTANDING DENSITY DEPLETION IN CROSS-FIELD DIFFUSED PLASMA OF LVPD-U** Ayan Adhikari, A. K. Sanyasi, L. M. Awasthi, P. K. Srivastava , Ritesh Sugandhiand Mainak Bandopadhyay	111
BPE-P-21	**THREE DIMENSIONAL DUST CLOUD IN DC GLOW DISCHARGE PLASMA** Sachin Sharma, G Veda Prakash, Meenakshee Sharma, Sayak Bose, Sanat Kumar Tiwari	112
BPE-P-22	**TEMPERATURE ANISOTROPY DIRECTED PARTICLE TRANSPORT IN A PLASMA CONFINED IN A DIPOLE MAGNETIC FIELD** Ayesha Nanda and Sudeep Bhattacharjee	112
BPE-P-23	**DESIGN AND DEVELOPMENT OF MULTI-GAP PSEUDOSPARK DISCHARGE BASED PLASMA CATHODE ELECTRON SOURCE FOR EUV/SOFT X-RAY RADIATION GENERATION** Varun, Navin Kumar Sharma, Akhilesh Mishra, Ram Prakash Lamba and Udit Narayan Pal	113

BPE-P-24	**REALIZATION OF NONLINEAR DEMAGNIFICATION IN PLASMA-BASED ION BEAM OPTICS** Sushanta Barman, Sanjeev K. Maurya, and Sudeep Bhattacharjee	**115**
BPE-P-25	**COLD ATMOSPHERIC PRESSURE PLASMA JETS: RONS DYNAMICS AND ELECTRIC FIELD ASYMMETRY** Deepika Behmani and Sudeep Bhattacharjee	**116**
BPE-P-26	**A DBD PLASMA BASED PACKED BED DISCHARGE SYSTEM USEFUL FOR EFFECTIVE VOCS REDUCTION** Ramavtar*, Kiran, and Ram Prakash	**117**

CATEGORY: NUCLEAR FUSION TECHNOLOGY (NFT)

NFT-P-1	**TWEAKING FOR LOOP VOLTAGE PROFILE OF OHMIC TRANSFORMER POWER SUPPLY IN ADITYA-U TOKAMAK** Shivam Kumar Gupta, Kunal S Shah, M N Makwana, B V Nair, S Nair, Rohit Kumar, R L Tanna, Joydeep Ghosh and Aditya-U Team	**118**
NFT-P-2	**DESIGNOF SUPPORT STRUCTURE FOR THE WAVEGUIDE SYSTEM FOR MICHELSON INTERFEROMETER SYSTEM FOR SST-1** Pratibha Gupta, Manoj Kumar Gupta, Bharat Doshi, Abhishek Sinha, S.K.Pathak	**119**
NFT-P-3	**UPGRADE IN SOFTWARE BASED INTERLOCK FOR ICRH DAC FOR EXPERIMENTS** Ramesh Joshi, H. M. Jadav, Manoj Singh, Kishore Misra, Sunil kumar& High Power *ICRH Systems Division*	**119**
NFT-P-4	**SOFTWARE MODIFICATIONS IN ICRH DAC FOR 45.6MHZ SYSTEM** Ramesh Joshi, H. M. Jadav, Sunil kumar& High Power ICRH Systems Division	**120**
NFT-P-5	**CONCEPTUAL DESIGN OF SIGNAL CONDITIONING AND INTERLOCK OF 82.6GHZ GYROTON BASED ECRH SYSTEM** Harshida Patel ,J Patel, D Purohit, K G Parmar, Hardik Mistry, B K shukla and ECRH Group	**121**
NFT-P-6	**INTERFACE OF ANODE POWER SUPPLY WITH 42GHZ GYROTRON FOR DUAL PULSE OPERATION IN SST TOKAMAK** Harshida Patel,DPurohit,J Patel, N Rajan Babu, K G Parmar, Hardik Mistry, B K shukla and ECRH Group	**121**
NFT-P-7	**OVERHAULING OF POWER TRANSFORMER 132KV / 11KV, 15000KVA AT 132KV IPR SUBSTATION** Prakash Parmar, Chandra Kishor Gupta, Supriya Nair, Chirag Bhavsar	**122**
NFT-P-8	**FOCUSING OF HIGH CURRENT ION BEAM BY APERTURE DISPLACEMENT TECHNIQUE** Mukti Ranjan Jana	**123**
NFT-P-9	**QUANTUM COMPUTER USING PROTEIN SYNTHESIS AS BLOCKCHAIN TECHNOLOGY** A.B. Rajib Hazarika	**124**
NFT-P-10	**OVERVIEW OF THE RECENT INVESTIGATIONS ON THE SURROGATE-PARTICLE-IRRADIATION IN TUNGSTEN PLASMA-FACING-MATERIALS** P.N. Mayaand S.P. Deshpande	**124**

NFT-P-11	**MECHANICAL DESIGN OF PROTOTYPE CENTER STACK (PCS) FOR SPHERICAL TOKAMAK BASED TECHNOLOGIES DEVELOPMENT** A.K. Verma, S. Ranjithkumar, Prasada Rao P, Shiju Sam, Y.S.S. Srinivas, E.Rajendra Kumar	**125**
NFT-P-12	**DESIGN OPTIMIZATION OF PROTOTYPE CENTER STACK (PCS) TOROIDAL FIELD COILS** S. Ranjithkumar, A.K. Verma, Prasada Rao P., Shiju Sam, Y.S.S. Srinivas, E.Rajendra Kumar	**126**
NFT-P-13	**R&D IN FABRICATION OF CENTER STACK FOR SPHERICAL TOKAMAK TECHNOLOGIES DEVELOPMENT** Shiju Sam, A.K. Verma, S. Ranjithkumar, Prasada Rao P., Y.S.S. Srinivas, E. Rajendra Kumar	**127**
NFT-P-14	**ELECTRICAL DESIGN OF CENTER STACK FOR SPHERICAL TOKAMAK BASED TECHNOLOGIES DEVELOPMENT** Prasada Rao P, Y.S.S. Srinivas, A.K. Verma, S. Ranjithkumar, Shiju Sam, E.Rajendra Kumar	**129**
NFT-P-15	**ERECTION, INSTALLATION, TESTING AND COMMISSIONING OF 1600KVAR, 11KVAPFC SYSTEM** *Chirag B. Bhavsar, Prakash Parmar, C.K Gupta, Supriya Nair*	**129**
NFT-P-16	**STRUCTURAL DESIGN OF WINCH SYSTEMFOR REMOTE HANDLING APPLICATION** Manoah Stephen M1, Ravi Ranjan Kumar1, Naveen Rastogi1, Krishan Kumar Gotewal1, Jignesh Chauhan1	**130**
NFT-P-17	**SST-1 CRYOGENICS PLANT MONITORING SYSTEM USING EPICS OPC** V.B. Patel, A.L. Sharma, H.H. Chudasma, H. Masand, I.A Mansuri, J.J. Patel, M.K. Bhandarkar, P. GaddamP.N. Panchal,R.J. Patel, T.S. Rao, V.L.Tanna, K. Mahajan and SST1 Cryogenics Team	**131**
NFT-P-18	**COMPARATIVE STUDY ON THERMAL PROPERTIES OF DIFFERENT GRADES OF HIGH DENSITY GRAPHITE** ArunPrakash Arumugam*, K.P. Singh, P. Patel, S. Khirwadkar, D.C. Raval and Z. Khan	**131**
NFT-P-19	**DESIGN AND SIMULATION OF TWO-WAY RF COAXIAL SWITCH FOR ICRH EXPERIMENTS** Uttam Kumar Goswami, Nikhil Vispara, Raj Singh and P. K. Atrey	**132**
NFT-P-20	**STUDIES OF EDGE PLASMA PARAMETER IN ADITYA-U TOKAMAK USING UEDGE CODE** Ritu Dey, Tanmay M. Macwan, Harshita Raj, M. B. Chowdhuri, Joydeep Ghosh1, R. L.Tanna, R.Manchanda, Deepti Sharma, T. D. Rognlien	**133**
NFT-P-21	**INSTALLATION AND COMMISSIONING OF THE ARC DETECTION SYSTEM FOR PF BUS BARS IN SST-1 CRYOGENICS INTERFACE** H. Nimavat, H. Dalicha, N. Ramaiya, D. Sonara, R. G. Trivedi, R. Manchanda, V. L. Tannaand D. Raju	**134**
NFT-P-22	**PIPING LAYOUT OF CRYOGENIC EXPERIMENTAL SET-UP FOR 3-STREAM PLATE-FIN HEAT EXCHANGER** O Chandratre, Vivek sharma, A K Sahu, H Kavad	**134**
NFT-P-23	**PARAMETRIZATION OF OHMIC TRANSFORMER POWER SUPPLY FOR ADITYA-U TOKAMAK** K S Shah, M N Makwana, Shivam Kumar Gupta, B V Nair, S Nair, R L Tanna, Joydeep Ghosh, and Aditya-U Team	**135**

NFT-P-24	**SIMULATION OF UNIAXIAL COMPRESSION TESTS ON CERAMIC PEBBLE BEDS FOR ITS MECHANICAL CHARACTERIZATION** Maulik Panchal, Harsh Patel, Paritosh Chaudhuri	136
NFT-P-25	**AN ARTIFICIAL INTELLIGENCE BASED SOLUTION FOR SST1TOKAMAK BUILDING MONITORING** Agraj Abhishek, Abhishek Sharma, Gaurav A. Garg, Hitesh H. Chudasama, DanielRaju, Manika Sharma	137
NFT-P-26	**UHV TESTING OF PROTOTYPE STEERABLE ECRH LAUNCHER** Hardik Mistry, Dharmesh Purohit, Siju George, Harshida Patel, Jatin Patel, K G Parmar, Dilip Raval, Manoj Kumar Gupta, B K Shukla	137
NFT-P-27	**DEVELOPMENT OF CALIBRATION UNIT FOR CALORIMETRIC PULSED POWER MEASUREMENT OF HIGH POWER MICROWAVE SOURCE** Hardik Mistry, Harshida Patel, Jatin Patel, DharmeshPurohit, K G Parmar,B K Shukla	138
NFT-P-28	**IMPLEMENTATION OF THREE-DIMENSIONAL SIMULATIONS FOR SCRAPE-OFF LAYER TRANSPORT IN INBOARD LIMITED ADITYA-UPGRADE PLASMA CONFIGURATION** Arzoo Malwal, Devendra Sharma	139
NFT-P-29	**PERFORMANCE STUDY OF METAL HYDRIDE REACTOR EQUIPPED WITH SPIRAL HEAT EXCHANGER** Sudhir Rai, Amit Sircar	140
NFT-P-30	**CONCEPTUAL DESIGN OF GLOW DISCHARGE CLEANING SYSTEM FOR SMALL SCALE-SPHERICAL TOKAMAK** M. S. Khan, Ranjith Kumar, Shiju Sam, Y S SSrinivas,Ziauddin Khan, E. Rajendra Kumar	140
NFT-P-31	**LAYOUT OF CRITICAL PERIPHERAL EQUIPMENT'S FOR INDIGENOUS HELIUM REFRIGERATOR/ LIQUEFIER PLANT** Hitesh R Kavad, A K Sahu, R Bhatasana, H Dave, O Chandratre, N Kumar, Prashant Singh, Priyanka Brahmbhatt	141
NFT-P-32	**STATUS OF AUXILIARY POWER SUPPLIES FOR ITER PROTOTYPE RF SOURCE** Hrushikesh Dalicha, Gajendra Suthar, Kartik Mohan, Rohit Agarwal, Rajesh Trivedi, Kumar Rajnish, Raghuraj Singh, Aparajita Mukherjee	142
NFT-P-33	**AMPLITUDE ANDPHASE CONTROL USING I-Q MODULATOR: APROTOTYPE DEVELOPMENT** DipalSoni, Kumar Rajnish, Sriprakash Verma, Raghuraj Singh,R.G. Trivedi and Aparajita Mukherjee	143
NFT-P-34	**TESTING OF HIGH-POWER AMPLIFIER AT 1.5MW FOR CONTINUOUS WAVE (CW) OPERATION** Raghuraj Singh, Aparajita Mukherjee, R.G. Trivedi, Kumar Rajnish, Akhil Jha, Manoj Patel, Gajendra Suthar, DipalSoni, Sriprakash Verma, Kartik Mohan, Rohit Agrawal, Rohit Anand, HrushikeshDalicha and Paresh Vasava	144
NFT-P-35	**DEVELOPMENT OF WATER-COOLED BLEEDER HEATSINK FOR PROTOTYPE AUXILIARY POWER SUPPLIES** Paresh Vasava, HrushikeshDalicha, Rohit Anand, Rajesh Trivedi, Kumar Rajnish, Raghuraj Singh, Aparajita Mukherjee	145
NFT-P-36	**RAMI ANALYSIS FOR UPPER PORT 09 AND PERFORMING FMECA TO FIND OUT THE EXPECTED CRITICALITY MATRIX** Suraj Pillai, Siddharth Kumar, Sandip Roy, Hitesh Pandya	146

NFT-P-37	**INVESTIGATION OF STRUCTURAL INTEGRITY OF SWIFT HEAVY ION IRRADIATED AL2O3** Paramita Patra1, Sejal Shah, M. J. Singh, I. Sulania, S. Kedia, F. Singh	147
NFT-P-38	**DEVELOPMENT OF 16 CHANNEL CURRENT MEASUREMENT MODULE FOR SSPA** Manoj Kumar Patel, Hrushikesh Dalicha, Gajendra Suthar, Akhil Jha, Kumar Rajnish, Raghuraj Singh, R.G. Trivedi and Aparajita Mukherjee	148
NFT-P-39	**DEVELOPMENT OF PLC BASED CONTROL SYSTEM FOR REMOTE OPERATION OF 200KV HIGH VOLTAGE POWER SUPPLY** Kumar Saurabh, Amal S, Aritra Chakraborty, Paul Christian and Ashok Mankani	149
NFT-P-40	**DEVELOPMENT OF ARCHITECTURE FOR CONTROLLING ELECTRICAL MOTORS OF ITERSECONDARY COOLING WATER SYSTEM** Jinendra Dangi, A.G. Ajith Kumar, D. K. Gupta, Nirav Patel	150
NFT-P-41	**RF DESIGN OF POWER LEVEL 2.5 MW COMPATIBLE TRANSMISSION LINE COMPONENTS**Akhil Jha, Rohit Anand, P. Ajesh, Paresh Vasava, Ulhas K. Dethe, Sunil Dani, R.G. Trivedi, and Aparajita Mukherjee	151
NFT-P-42	**DEVELOPMENT AND INTEGRATION OF MODULAR CONTROL AND ACQUISITION SYSTEM FOR LASER ABSORPTION SPECTROSCOPY IN ROBIN** Kartik Patel, Himanshu Tyagi, Manas Bhuyan, Hiren Mistri, Ratnakar Yadav, Kaushal Pandya, MJ Singh, Mainak Bandyopadhyay, Arun Chakraborty	152
NFT-P-43	**DESIGN & DEVELOPMENT OF OPERATIONAL PROTECTION AND INTERLOCK CIRCUIT FOR VACUUM PUMPING SYSTEM OF TWIN SOURCE (TS)** Hardik Shishangiya, Deepak Parmar, R. Yadav, R Pandey, J. Bhagora, K Joshi, M Bhuyan,A. Gahlaut, M. Singh, M. Bandyopadhyay and A. Chakraborty	153
NFT-P-44	**TWIN SOURCE PLASMA OPERATION USING 40 KW, 1 MHZ SOLID STATE HIGH FREQUENCY POWER SUPPLY** Manas Bhuyan, Ravi Pandey, Jignesh Bhagora, Mahesh. Vuppugalla, Ratnakar Yadav, Himanshu. Tyagi, S. Gajjar, D. Upadhyay, Hardik. Shishangiya, Bhavesh Prajapati, M. N. Vishnudev, Deepak Parmar, Agrajit Gahlaut, Hiren Mistri, Kaushal Joshi, Kaushal Pandya, Mainak Bandyopadhyay, N P Singh, Mahendrajit Singh and Arun Chakraborty	154
NFT-P-45	**REMOTE TUNING SYSTEM FOR RF MATCHING NETWORK OF TWIN SOURCE USING STEPPER MOTOR** V. Mahesh, A. Gahlaut, D. Parmar, B. Prajapati, H. Shishangiya, M. Bandyopadhyay, M. J. Singh and A. Chakraborty	155
NFT-P-46	**EXPERIENCE OF MANUFACTURING BEAM LINE COMPONENTS FOR ITER DNB** H Patel, J Joshi, M J Singh, M. V. Nagaraju , A Chakraborty, J Chareyre, B Schunke , C Rotti, E Pfaff , J Schäfer, M Krohll, C Eckardt	156
NFT-P-47	**DESIGN DEVELOPMENT OF DNB VACUUM VESSEL FOR ITER** Ashish Yadav, Jaydeep Joshi, Mahendrajit Singh, Arun Chakraborty	157
NFT-P-48	**COMPARISON OF TOPOLOGIES FORTWIN SOURCEHVDC TRANSMISSION LINE** Vishnudev M N, Deepak Parmar, Hardik Shishangiya, Santosh C. Vora, Agrajit Gahlaut, Mainak Bandyopadhyay, Arun Chakraborty	158

NFT-P-49	**MODIFICATION IN PERIOD OF SAWTOOTH OSCILLATION AFTER GAS PULSE INJECTION IN ADITYA-U TOKAMAK** Suman Dolui,Tanmay Macwan, Kaushlender Singh, Ankit Kumar, Sharvil Patel, Suman Aich, Rohit Kumar, Laxmikant Pradhan, Ankit Patel, Kalpesh Gadoliya, K. A. Jadeja, K. M. Patel, R.L. Tanna, Joydeep Ghosh and ADITYA-U Team	**159**
NFT-P-50	**DESIGN OF A BALL PEN PROBE FOR THE MEASUREMENT OF EDGE ION TEMPERATURE IN ADITYA-U TOKAMAK** Ankit Kumar, Kaushlender Singh, Suman Dolui, Tanmay Macwan, Pramila Gautam, Rohit Kumar, Suman Aich, Laxmikant Pradhan, Ankit Patel, Kalpesh Gadoliya, K. M. Patel, K. A. Jadeja, R.L. Tanna, Joydeep Ghosh and ADITYA-U Team	**160**
NFT-P-51	**DESIGN AND INSTALLATION OF TRIPLE LANGMUIR PROBE FOR DIRECT MEASUREMENT OFEDGE DENSITY AND TEMPERATURE IN ADITYA-U TOKAMAK** Kaushlender Singh, Suman Dolui, Ankit Kumar, Tanmay Macwan, Pramila Gautam, Rohit Kumar, Suman Aich, Laxmikant Pradhan, Ankit Patel, Kalpesh Gadoliya, K. M. Patel, K. A.Jadeja, R.L. Tanna, Joydeep Ghosh and ADITYA-U Team	**161**
NFT-P-52	**DESIGN OF LASER INDUCED BREAKDOWN SPECTROSCOPY (LIBS) BASED WALL MONITORINGDIAGNOSTICS FOR ADITYA-U TOKAMAK** Bharat Hegde, Ashok Kumar, Ankit Kumar, Kaushlender Singh, Suman Dolui, Tanmay Macwan, Rohit Kumar, Suman Aich, Laxmikant Pradhan, Ankit Patel, Kalpesh Gadoliya, K.M. Patel, K. A. Jadeja, R.L. Tanna, Joydeep Ghosh and ADITYA-U Team	**162**
NFT-P-53	**FEASIBILITY STUDY AND DEVELOPMENT OF A DIAGNOSTIC FOR MEASUREMENT OF TOROIDAL ASYMMETRY IN THE RADIATION DURING DISRUPTIONS IN ADITYA-U TOKAMAK** Ashok Kumar, Bharat Hegde, Ankit Kumar, Kaushlender Singh, Suman Dolui, Tanmay Macwan, Pramila Gautam, Rohit Kumar, Suman Aich, Laxmikant Pradhan, Ankit Patel, Kalpesh Gadoliya, K. M. Patel, K. A. Jadeja, R.L. Tanna, Joydeep Ghosh and ADITYA-U Team	**163**
NFT-P-54	**DEVELOPMENT ANDMEASUREMENT OF 2.45 GHZ, UHV COMPATIBLE RF WINDOW FOR ECR SYSTEM** K. K. Ambulkar, P. R. Parmar, A. L. Thakur,P. K .Sharma	**164**
NFT-P-55	**SMALL ASPECT-RATIO NUCLEAR TOKAMAK AS FUSION FISSION HYBRID** Pranjal Singh, Prabhat Ranjan, Nirav Bhaliya, Gaurav Singh, Jay Joshi, Kamya Chandrasekhar, Chandresh Shah, Manoj Srivastava, Akash Singh	**165**
NFT-P-56	**COMPENSATION OF FAST FEEDBACK CORRECTION MAGNETIC FIELD ON MAGNETIC DIAGNOSTIC IN ADITYA-U TOKAMAK** Rohit Kumar, Shivam Gupta, R.L Tanna, S.K Jha, Suman Aich, Tanmay Macwan, Kunal Shah, M.N Makwana, Supriya Nair, Kaushlender Singh, Suman Dolui, Kaushal Patel, Kumarpal Jadeja and J Ghosh	**165**
NFT-P-57	**A METHOD FOR PREPARATION OF ELECTRICAL CONTACT ON CARBON MATERIAL** K.P Singh, Priyanka Patel, Tushar Patel, Samir S Khirwadkar, Amardas Alli	**166**

CATEGORY: INDUSTRIAL PLASMA APPLICATION, PLASMA PROCESSING AND SOCIETAL BENEFIT OF PLASMA (IPS)

IPS-P-1	**EMERGENCE OF NANOSCALE FEATURES USING LOW-ENERGY IONS PRODUCED BY PLASMA SOURCE** Sukriti Hans, Mukesh Ranjan	167
IPS-P-2	**THE ANTIMICROBIAL EFFICACY OF ARGON COLD ATMOSPHERIC PLASMA JET ON MULTIDRUG-RESISTANT BACTERIA ISOLATED FROM HUMAN BLOOD** Sarthak Dasa, Veda Prakash Gajulab, Sarita Mohapatrac, Satyananda Karb	168
IPS-P-3	**EFFICACY AND BIOSAFETY EVALUATION OF COLD ATMOSPHERIC PLASMA FOR HAND STERLIZATION** Abu Sufiyan Chhipa, Vikas Rathore, Snehal Patel, Priti Mehta, AkshayVaid, Shital Butani	169
IPS-P-4	**SURFACE PROPERTIES OF PULSED PLASMA ION NITRIDED INCONEL 601 ALLOY** Ravindra Kumar	170
IPS-P-5	**EFFECT OF GAS ENVIRONMENT DURING SULFURIZATION PROCESS OF CZTS THIN FILM ON SOLAR CELL PERFORMANCE** Sagar Agrawal, Rinkal Kanani,	170
IPS-P-6	**AN ACTIVE ARC SENSING AND CONTROLLING TECHNIQUE FOR PLASMA NITRIDING PROCESS** Keena Kalaria, Naresh Vaghela and Suryakant B. Gupta	171
IPS-P-7	**STUDIES ON THE ROLE OF AXIAL MAGNETIC FIELD FOR LINE AND RING CUSP MAGNETIC CONFIGURATIONS IN A LOW ENERGY ION SOURCE** Bharat Singh Rawat, S. K. Sharma , B. Choksi, P. Bharathi, B. Sridhar, L.N. Gupta, D. Thakkar, S.L. Parmar, V. Prahlad and U.K. Baruah	172
IPS-P-8	**LOW TEMPERATURE PLASMA CARBURIZING OF AUSTENITIC STAINLESS STEEL 316L** Ghanshyam Jhala, Vijay Chauhan, Pravin Dwivedi and Alphonsa Joseph	173
IPS-P-9	**STUDY ON SYNTHESIS OF TITANIUM NITRIDE NANOPARTICLES FROM WASTE TITANIUM SCRAPS BY THERMAL PLASMA ARC DISCHARGE METHODAND ITS MAGNETIC PROPERTIES** L. Kumaresan and G. Shanmugavelayutham	174
IPS-P-10	**INVESTIGATION OF GAS DIFFUSION BARRIER AND ANTIFOULING PROPERTIES OF PLASMA TREATED LOW DENSITY POLYETHYLENE FOR PACKAGING APPLICATIONS** Purvi Dave, Balasubramanian C, Sukriti Hans and S. K. Nema	175
IPS-P-11	**STUDY OF CHARACTERISTICS OF PLASMA ANTENNA** Manisha Jha1, Nisha Panghal, Unnati Patel, Rajesh Kumar	176
IPS-P-12	**BULK RATE SYNTHESIS OF METAL-OXIDE NANO MATERIALS FOR TREATMENT OF WASTEWATER AND OTHER BIOMEDICAL APPLICATIONS** Mizanur Rahman, Deepak B. Pemmaraju& M. Kakati	176
IPS-P-13	**SPHEROIDIZATION OF METAL POWDERINMETHANE-CARBON DIOXIDE PLASMA JETAT ATMOSPHERIC PRESSURE** Yugesh.V, Amarnath. P, Yugeswaran. S, Ananthapadmnabhan. PV	177

IPS-P-14	**EFFECT OF CHARGE EXCHANGE COLLISIONS ON VELOCITY DISTRIBUTION OF N_2 AND N_2 FOR SELECTIVE EXTRACTION OF ENERGETIC SPECIES FOR COLD PLASMA FOOD PROCESSING** M. Perumal and Suraj Kumar Sinha,	178
IPS-P-15	**NITROGEN FIXATION THROUGH SUBMERGED THERMAL PLASMA PROCESS** Nanditta Nandy, Indumathy B, Amarnath. P, Yugeswaran. S	179
IPS-P-16	**STABILITY OF AL AND AG METALLIC THIN FILM MIRRORS IN SPACE ENVIRONMENT UNDER IMPLANTATION OF LOW ENERGY HYDROGEN AND HELIUM IONS FROM MICROWAVE PLASMAS** Krishn Pal Singh and Sudeep Bhattacharjee	180
IPS-P-17	**DESIGN AND CHARACTERIZATION OF COLD ATMOSPHERIC PRESSURE PLASMA SOURCES SUITABLE FOR FOOD AND AGRICULTURE APPLICATIONS** PritiPal, VishaliSingh, ShubhanshuNema Bhatiyara,Navin Kumar Sharma, Shikha Misra, Ravindra Kumar, Alok Mishra,Rajendra Kumar Verma,Udit Narayan PalShivendra Mauryaand Ram Prakash Lamba	181
IPS-P-18	**DESIGN AND DEVELOPMENT OF COLD ATMOSPHERIC PRESSURE PLASMA JETS SUITABLE FOR BIOMEDICAL APPLICATIONS** Navin Kumar Sharma, Shikha Misra, Priti Pal, Ravindra Kumar, Alok Misra, Mahendra Singh, Ram Prakash Lamba, Murali M Pandey, Yaduvendra Choyal and Udit Narayan Pal	182
IPS-P-19	**DESIGN AND DEVELOPMENT OF DIELECTRIC BARRIER DISCHARGE BASED EFFICIENT VACUUM ULTRAVIOLET (VUV), FAR UV-C, AND UV EXCIMER RADIATION SOURCES** Navin Kumar Sharma, Surbhi Bidawat, Shikha Misra Shyam Sundar Jaiswal, Varun, Niraj Kumar, Ram Prakash Lamba, and Udit Narayan Pal	183
IPS-P-20	**HIGH VOLTAGE AND HIGH FREQUENCY PULSE POWER SUPPLY FOR PLASMA APPLICATIONS** A K Dhakar, S K Rai, M Mishraand U N Pal	184
IPS-P-21	**PLASMA JET INTERACTION WITH GB-SCC (ITOC-03) CELL LINE** A.Vaid1, K. Pansare, S. Singh, R. Rane, A. Visani, M. Ranjan, C. Krishna, R. Sarin, A. Joseph	185
IPS-P-22	**GERMINATION ENHANCEMENT OF TOMATO AND CAPSICUM SEEDS USING DIELECTRIC BARRIER DISCHARGE (DBD) PLASMA TREATMENT** R.Rane, A. Vaid, R.Parihar, P. Maila, A. Visani, A. Vikram, A. Joseph, M. Kumar	185
IPS-P-23	**ON UTILIZATION OF DIELECTRIC BARRIER DISCHARGE PLASMA FOR BENEFIT OF MANKIND** Anand Kumar Srivastava	186
IPS-P-24	**PURE AND SAMARIUM INCORPORATED LITHIUM TITANATE AS LOW ACTIVATION CERAMICS FOR BREEDER BLANKET APPLICATION** S.K.Sinha	187
IPS-P-25	**TISSUE THICKNESS PLAYS AN IMPORTANT ROLE IN PENETRATION OF COLD ATMOSPHERIC PLASMA IN TUMOR TISSUES RESECTED FROM GLIOMA PATIENTS** Yogesh Aggarwal, Akshay Vaid, Jyotirmoy Banerjee, P.S. Chandra, Alphonsa Joseph, Ramakrishna Rane, Anand Visani, Manjari Tripathi, Ramesh Doddamani, Aparna Dixit	188

CATEGORY: PLASMA DIAGNOSICS (PDG)

PDG-P-1	**STUDY AND CHARACTERIZATION OF HYDROGEN / ARGON / NITROGEN PLASMA PRODUCED BY ELECTRON CYCLOTRON RESONANCE USING DOUBLE LANGMUIR PROBE** S. K. Jain,,, Rekhya Naika, Manish Pathak, Rajnish Kumar, Dharmraj V. Ghodke, Vijendra Prasad, Purushottam Shrivastava	**189**
PDG-P-2	**ELIMINATING FLUX CONTRIBUTED BY EXTERNAL CURRENTS AND EDDY CURRENT FROM MAGNETIC PROBE MEASUREMENT IN SST-1 DISCHARGES** Sameer Kumar, Kumudni Tahiliani, Surya Kumar Pathak, Daniel Raju, Praveena Kumari, Vismaysinh D Raulji, Praveenlal Edappala, Ashish Ranjan, Jasraj Dongde and SST -1 Team	**190**
PDG-P-3	**DENOISING THE NOISY PLASMA IMAGES CAPTURED THROUGH WOUND OPTICAL FIBER BUNDLE** Abhishek Sharma, Agraj Abhishek, Gaurav A. Garg, Surajkumar Gupta, Manoj Kumar , Manika Sharma	**190**
PDG-P-4	**IMAGING DIAGNOSTICS IN SST-1** Suraj Kumar Gupta, Vishnu Chaudhari, Manoj Kumar	**191**
PDG-P-5	**STUDY OF A PROTOTYPE METAL FOIL BOLOMETER** Devilal Kumawat, Kumudni Tahiliani, Praveen Lal E.V, Prabal Biswas, Suresh I, Santosh P Pandya, Manoj K Gupta, S.K. Pathak	**192**
PDG-P-6	**DYNAMICS OF SLOW AND FAST COMPONENTS IN LASER PRODUCED PLASMA OF CARBON AND RUBY** Archana Kushwaha, Satchi Kumari and Alika Khare	**192**
PDG-P-7	**INITIAL RESULTS OBTAINED FROM NEAR-INFRARED SPECTROSCOPIC SYSTEM ON ADITYA-U TOKAMAK** N. Ramaiya, R. Manchanda, M. B. Chowdhuri, N. Yadava, S. K. Pathak, R. L. Tanna, K. A. Jadeja, K. M. Patel, R. Kumar, S. Aich, and J. Ghosh	**194**
PDG-P-8	**FABRICATION, INSTALLATION, DATA ACQUISITION OF DIAMAGNETIC LOOP IN ADITYA-U TOKAMAK** S. Aich, K. Singh, S. Dolui, J. Ghosh, K. Galodiya, T. M. Macwan, R. L. Tanna, R. Kumar, H. Mandliya, A. Kumar, Praveenlal E. V., Ankit Kumar, K. A. Jadeja, K. Patel, and ADITYA-U team	**195**
PDG-P-9	**IMPURITY TRANSPORT IN ADITYA-U TOKAMAK WITH INDIGENOUSLY DEVELOPED SEMI-IMPLICIT IMPURITY TRANSPORT CODE** Nandini Yadava, J. Ghosh, M. B. Chowdhuri, Ashoke De, R. Manchanda, N. Ramaiya, K. Shah, S. Patel, S. Purohit, M. K. Gupta, U. C. Nagora, S. K. Pathak, K. A. Jadeja, K. M. Patel, Ankur Pandya, R. Kumar, Tanmay Macwan, S. Aich, Suman Dolui, Kaushlender Singh R. L. Tanna and Aditya-U Team	**196**
PDG-P-10	**OPTICAL DIAGNOSTICS OF PLASMA DISCHARGE INSIDE LIQUID DURING THE SYNTHESIS OF AU/CUO NANOCOMPOSITES** Palash Jyoti Boruah, Parismita Kalita, Rakesh Ruchel Khanikar, H. Bailung	**197**
PDG-P-11	**STUDY OF TEMPORAL PROFILES OF ELECTRIC FIELDAND PLASMA TEMPERATURE IN SOL REGION OF ADITYA-U TOKAMAK** Abha Kanik, Arun Sarma, Joydeep Ghosh, Tanmay Macwan, Sharvil Patel, R. L. Tanna, Minsha Shah, Kalpesh Galodiya, Kumarpal Jadeja, Kaushalendra Singh, Suman Duloi, Ankit Kumar, Suman Aich, Rohit Kumar, Kaushal Pateland ADITYA-U Team	**198**

PDG-P-12	**OBSERVATION OF ANOMALOUS DOPPLER RESONANCE EFFECT IN ADITYA-UPGRADE** Varsha.S., Santosh Pandya, S.K. Pathak, Umesh Nagora, Jayesh Raval, M.K. Gupta, K. Tahiliani, R.L.Tanna, Rohit Kumar , Suman Aich, J.Ghosh and Aditya-U Team.	199
PDG-P-13	**PLASMA POSITION MEASUREMENTS FOR SST1 DISCHARGES USING FUNCTION PARAMETERIZATION (FP) METHOD** Sameer Kumar, Kumudni Tahiliani, Daniel Raju, Surya Kumar Pathak, Jayesh Raval, Praveenlal Edappala, Suresh I, Devilal Kumavat, Ashish Ranjan, Jasraj Dongde and SST -1 Team	199

CATEGORY: LASER PLASMA, PULSED POWER AND OTHERS (LPP)

LPP-P-1	**THZ GENERATION VIA GAUSSIAN LASER INTERACTION WITH VA-CNTS** Sandeep Kumar, Shivani Vij, Niti Kant and Vishal Thakur	200
LPP-P-2	**ELECTRONBERNSTEIN WAVE EXCITATION BY NONLINEAR INTERACTIONS OF TWO LASER BEAMS IN A COLLISIONAL NANOCLUSTER PLASMA** Ashish Varma and Asheel Kumar	200
LPP-P-3	**EXCITATION OF ELECTRON BERNSTEIN WAVE BY BEATINGOF TWO HIGH POWER LASER BEAMS IN A COLLISIONAL PLASMA** Arvind Kumar and Asheel Kumar	201
LPP-P-4	**ELECTRON ACCELERATION BY TIGHTLY FOCUSED RADIALLY POLARIZED LASER PULSE IN AN ION CHANNEL** Ram Jeet and Asheel Kumar	202
LPP-P-5	**SECOND HARMONIC GENERATION BY OBLIQUE INCIDENT GAUSSIAN LASER BEAM IN PLASMA** Vinay Sharma, Vishal Thakur, Arvinder Singh and Niti Kant	203
LPP-P-6	**PROPAGATION DYNAMICS OF SINGLE AND LATERALLY COLLIDING LASER PRODUCED PLASMAS** Shilpa S.and Pramod Gopinath	203
LPP-P-7	**ELLIPTICALLY POLARIZED THZ RADIATION GENERATION IN OBLIQUELY MAGNETISED PLASMA** Dinkar Mishra and Bhupesh Kumar	204
LPP-P-8	**HEATING OF ELECTRONS BY INTERACTION OF HIGH INTENSE ULTRA-SHORT LASER PULSES IN NANOPARTICLES** S P Mishra and Ashish Varma	205
LPP-P-9	**HIGH-ORDER HARMONIC GENERATION FROM STRONGLY OVERDENSE PLASMAS IRRADIATED BY ASYMMETRIC LASER PULSES** Deep Kumar Kuri	205
LPP-P-10	**COMPARATIVE STUDY OF WAKEFIELD GENERATION IN HOMOGENEOUS AND INHOMOGENEOUS PLASMA** Saumya Singh and Bhupesh Kumar	206
LPP-P-11	**3D SIMULATION STUDIES OF A DOUBLE-SIDED LINEAR INDUCTION MOTOR FOR ELECTROMAGNETIC LAUNCH APPLICATIONS** Ananya Kundu, Arvind Kumar, Ankur Jaiswal, Prasad Rao P, Vilas C Chaudhari, Rambabu Sidibomma, Y.S.S. Srinivas, E. Rajendra Kumar	206

LPP-P-12	**AN ALTERNATIVE APPROACH FOR BIOSCOURING AND BLEACHING OF KNITTED COTTON FABRIC IN SINGLE PROCESS USING AIR PLASMA** T. Anupriyanka and G. Shanmugavelayutham	207
LPP-P-13	**INFLUENCE OF AN AXIAL MAGNETIC FIELD ON PULSED PLASMA STREAM** Ahmed, S. Singha, S. Borthakur, N. K. Neog and T. K. Borthakur	208
LPP-P-14	**INVESTIGATIONS OF COMPLEX FAST ELECTRON TRANSPORT PHENOMENA IN INTENSE ULTRASHORT LASER FOIL INTERACTION** T. Mandal, V. Arora, A. Moorti and J. A Chakera	209
LPP-P-15	**UNDERSTANDING GRAZING INCIDENCE INTERACTION THROUGH FAST ELECTRON GENERATION IN THIN FOIL AT EXTREME INTENSITIES** T. Mandal, V. Arora, A. Moorti and J. A Chakera	210
LPP-P-16	**SELF-FOCUSING OF AN AMPLITUDE MODULATED LASER FILAMENT IN A MAGNETIZED PLASMA** Raju Ram Meena	211
LPP-P-17	**SELF-FOCUSING OF LOWER MODES OF BESSEL BEAMS: MOMENT THEORY APPROACH** Proxy Kad, Arvinder Singh	212
LPP-P-18	**LASER-CLUSTER INTERACTION IN A STATIC MAGNETIC FIELD WITHOUT DIPOLE APPROXIMATION** Kalyani Swain and Mrityunjay Kundu	213
LPP-P-19	**SELF-FOCUSING OF BESSEL-GAUSSIAN LASER BEAM IN COLLISIONLESS PLASMA** Aman Bhatia, Arvinder Singh	214
LPP-P-20	**PARAMETER OPTIMIZATION FOR TERAHERTZ RADIATION GENERATION FROM LASER-PULSE INTERACTION WITH ELECTRON-HOLE PLASMAS** M. C. Gurjar and D. N. Gupta	214
LPP-P-21	**A STUDY AND SIMULATIONS OF PLASMA OPENING SWITCH FOR HIGH VOLTAGE AND HIGH CURRENT APPLICATIONS** Kanchi Sunil, Rohit Shukla, Archana Sharma	215
LPP-P-22	**ENHANCED ELECTRON ACCELERATION IN A SUBCRITICAL DENSITY ION CHANNEL USING CHIRPED LASER PULSE** Harjit Singh Ghotra	216
LPP-P-23	**ROLE OF SATURABLE INDUCTOR FOR IMPROVING THE COMMUTATION LOSSES IN HIGH POWER PSEUDOSPARK SWITCH** Akhilesh Mishra, Shikha Misra, B. L. Meena, Ram Prakash Lamba and Udit Narayan Pal	217
LPP-P-24	**ENERGETIC PROTONS FROM A LASER EXPLODED MICROSPHERE WITH DENSITY GRADIENTS** Ankita Bhagawati, Nilakshi Das	218
LPP-P-25	**GOLD ASSISTED HOLE-BORING SCHEME FOR ION ACCELERATION IN PARABOLICALLY DECREASING BACKGROUND DENSITY PLASMA PROFILE** Nivedya Krishnan	219

LPP-P-26	**MODELING OF ULTRASHORT TWO COLOUR PUMP-INDUCED THERMAL STRAIN PROPAGATION IN GE [111]** R. Rathore, H. Singhaland J. A. Chakera	219
LPP-P-27	**ELECTRON ACCELERATION BY HERMITE COSH GAUSSIAN LASER BEAM IN VACUUM WITH GEV ENERGY GAIN** Ashok Kumar Pramanik, Niti Kant, Harjit Singh Ghotraand Jyoti Rajput	221
LPP-P-28	**EXPERIMENTAL STUDY OF POWER FREQUENCY BREAKDOWN CHARACTERISTICS OF VARIOUS SF_6 ADMIX IN NON-UNIFORM FIELDS** Vinod Kumar Gandi, Rishi Verma, Manoj Kumar Warrier, Gursharn Singh and Archana Sharma	221
LPP-P-29	**HEATING OF ELECTRONS BY INTERACTION OF HIGH INTENSE ULTRA-SHORT LASER PULSES IN NANOPARTICLES** Shri Prakash Mishra, Ashish Varma	222

CATEGORY: SPACE, ASTROPHYSICAL AND IONOSPHERIC PLASMA (AIP)

AIP-P-1	**EQUATORIAL PLASMA BUBBLES OVER INDIA DURING 2017 - A QUALITATIVE ANALYSIS** Sunil Kumar Chaurasiya, Kalpana Patel, Abhay Kumar Singh	223
AIP-P-2	**KINETIC SCALE DENSITY FLUCTUATIONS TO STUDY SOLAR CORONAL HEATING** Bheem Singh Jatav	224
AIP-P-3	**A STUDY ON THE VERTICAL COUPLING OF THE MESOSPHERE-THERMOSPHERE SYSTEM USINGTIMED-SABER SATELLITE DATA** Sandhya K Nair, Tarun Kumar Pant, Kishore Kumar K. and Vineeth C.	224
AIP-P-4	**STUDY OF CHARACTERISTICS OF IONOSPHERIC IRREGULARITIES USING GNSS TECHNIQUES OVER EQUATORIAL ANOMALY REGIONVARANASI** Sanjay Kumar, Mukulika Mondal and A. K. Singh	225
AIP-P-5	**STUDY THE EFFECT ON THE IONOSPSHERE DURING SOLAR ECLIPSE OF 21 JUNE 2020 USING VLF WAVE** S. B. Singh and A. K. Singh	226
AIP-P-6	**THE SELF-GRAVITATIONAL JEANS INSTABILITY IN MAGNETIZED DUSTY PLASMA WITHCHARGE GRADIENT AND POLARIZATION FORCES AND NONTHERMAL EFFECTS** Shweta Jain and Prerana Sharma	227
AIP-P-7	**HIGH FREQUENCY ELECTRON ACOUSTIC SHOCK WAVES IN NON-MAXWELLIAN PLASMA** Rajneet Kaurand N. S. Saini	227
AIP-P-8	**SOLAR WIND PLASMA CATEGORIZATION BASED ON THE SW PARAMETERS AT 1AU** Priyank Srivastava, A.K. Singh	228
AIP-P-9	**EFFECT OF POLARIZATION FORCE ONDUST ACOUSTIC ALFVÉNDRESSED SOLITONS** Sunidhi Singla and N. S. Saini,	229
AIP-P-10	**INTERACTION BETWEEN ION ACOUSTIC SOLITONS IN A QUANTUM PLASMA WITH TWO SPIN DEGENERATE ELECTRONS** Manveet Kaur and N. S. Saini	230

AIP-P-11	**LARGE SCALE MAGNETIC FIELD GENERATION IN A 3D MHD PLASMA VIA INDUCTION DYNAMO ACTION: A NUMERICAL STUDY** Shishir Biswas, Rajaraman Ganesh	231
AIP-P-12	**EVOLUTION OF EMIC WAVE SUBPACKETS WITHIN ONE WAVELENGTH: A MULTIPOINT THEMIS OBSERVATIONS** Biswajit Ojha, Yoshiharu Omura, Satyavir Singh, and Gurbax Lakhina	232
AIP-P-13	**STUDY OF ION ACOUSTIC WAVE WITH KAPPA DISTRIBUTION FUNCTION FOR BOTH ION AND ELECTRON AND ITS RELEVANCE TO MAGNETOSPHERE** N.Tandon, G. Ahirvaar, R. K. Chhajalani	233
AIP-P-14	**EXOTIC PLASMAS OF THE NEUTRON STAR ATMOSPHERE: WHY ARE THEY INTERESTING** Anoop Singh, Shishir P. Deshpande, Mrityunjay Kundu	234
AIP-P-15	**QUASIPERIODIC INERTIAL ALFVÉN SOLITARY WAVES IN MULTICOMPONENT PLASMA** Geetika Slathia, N. S. Saini	235
AIP-P-16	**ROLE GRAVITY WAVE INDUCED SEED PERTURBATIONS ON EQUATORIAL SPREAD F DAY TO DAY VARIABILITY UNDER THE INFLUENCE OF POST SUNSET ELECTRODYNAMICAL AND NEUTRAL WIND FORCINGS: A QUANTITATIVE ASSESSMENT** Sruthi T V, Manju G	236

PAPERS FOR BUTI YOUNG SCIENTIST AWARD

BUTI-01	**FLUID SIMULATION OF ION ACOUSTIC SOLITARY WAVES IN A RELATIVISTIC PULSAR WIND** Kuldeep Singh, Amar Kakad, Bharati Kakad, and N.S. Saini	237
BUTI-02	**DYNAMICS OF ELECTROSTATIC WAVES IN A DENSE RELATIVISTIC PAIR PLASMA** Ridip Sarma	249
BUTI-03	**FIRST ORDER PHASE TRANSITION AND CRYSTAL-FLUID COEXISTENCE IN A COMPLEX PLASMA SYSTEM** M.G. Hariprasad, P. Bandyopadhyay, G. Arora, A Saravanan, Swarnima Singh and A. Sen	276
BUTI-04	**STORAGE OF EXCESSIVE MAGNETIC FREE ENERGY AND PHOTOSPHERIC CURRENT LEADING TO EXTREME ERUPTIVE ACTIVITY FROM SOLAR ACTIVE REGIONS** Prabir Kumar Mitra and Bhuwan Joshi	283
BUTI-05	**2D-3V PIC-MCC BASED SIMULATIONS OF PLASMA TRANSPORT ACROSS MAGNETIC FILTER: INSTABILITIES AND DOUBLE LAYER FORMATION** Miral Shah and Bhaskar Chaudhury	288
BUTI-06	**EXPERIMENTAL VERIFICATION OF CAVITY MODES IN A MICROWAVE ION SOURCE AND ITS INFLUENCE ON THE PLASMA DYNAMICS AND THE EXTRACTED ION BEAM** C. Mallick, M. Bandyopadhyay, and R. Kumar	293

ORAL PRESENTATIONS

Session: Basic Plasma **ORAL-BP-1**

AN EXPERIMENTAL INVESTIGATION OF OSCILLATING PLASMA BUBBLES AND ITS NON LINEAR STRUCTURE IN A MAGNETIZED PLASMA SYSTEM

Mariammal Megalingam[1,2] and Bornali Sarma[3]
[1]*Institute for Plasma Research, Bhat, Gandhinagar*
[2]*Vellore Institute of Science and Technology, Chennai.*
[3]*University of Delhi, New Delhi*
Email: mariammal@ipr.res.in

Plasma bubbles are large scale structures of depleted plasma density in our earth's ionosphere that affect communication signals propagating through atmosphere, to include global navigation satellite systems. Plasma bubbles have been studied for decades using different techniques such as incoherent backscatter radar, ionogram analysis, insitu satellite measurements etc. An attempt has been made through experiments to understand the occurrence of plasma bubbles along with its instabilities and its complete nonlinear structure in a filamentary discharge magnetized plasma system. A spherical mesh grid of 80% optical transparency was negatively biased and introduced into the plasma for creating a plasma bubble. Diagnostics are electrical Langmuir probe and a hot emissive probe were extensively used for scanning the plasma bubble. Plasma floating potential fluctuations were measured at three different positions of the plasma bubble. The instability in the pattern showed the dynamic transition from periodic to chaotic for increasing magnetic fields. Time scale analysis using continuous wavelet transform was carried out to identify the presence of non-linearity from the contour plots. The mechanisms of the low-frequency instabilities along with the transition to chaos could be qualitatively explained. Non-linear techniques such as fast Fourier transform, phase space plot, and recurrence plot were used to explore the dynamics of the system appearing during plasma fluctuations. In order to demonstrate the observed chaotic phenomena in this study, characteristics of chaos such as the Lyapunov exponent were obtained from experimental time series data. The experimentally observed potential structure is confirmed with numerical analysis based on fluid hydrodynamics.

Session: Basic Plasma **ORAL-BP-2**

STUDY OF TWO STREAM INSTABILITY IN INHOMOGENEOUS DUSTY PLASMAS WITH UNIFORM MAGNETIC FIELD

Shachi Pachauri[1], Jyoti[2], Kamakhya Prakash Misra[1]
[1]*Department of Physics, School of Basic Sciences, Manipal University Jaipur, Dehmi Kalan, Jaipur, Rajasthan 303007, India*
[2] *Department of Physics, Govt College for Women, Gurawara, Haryana-123035, India*
Email: shachipachauri@gmail.com

Inhomogeneous magnetised collisional dusty plasma is selected for study of two stream instability. Static magnetic field (B_0) is applied in z-direction and having obliqueness (θ) with the direction of propagation of plasma wave. Fundamental fluid equations are formed for equally dense electrons and ions, where ions are considered cold and singly charged along with stationary dust particles having unperturbed density. Normal mode analysis method with linear approximation is used to get perturbed densities (n_{i1}, n_{e1}) and perturbed potential (ϕ_1) to get dispersion relation.Using typical plasma parameters, profiles of growth rates for both the instabilities are observed with oblique angle, electrostatic potential, static magnetic field and dust density/charge.

Session: Basic Plasma **ORAL-BP-3**

STRONG MAGNETIC FIELD EFFECTS IN THE STRONGLY COUPLED ROTATING DUSTY PLASMA

Prince Kumar* and Devendra Sharma,
Institute for Plasma Research, HBNI, Gandhinager-382428, Gujarat- India
**E-mail: prince.kumar@ipr.res.in*

We have constructed a full QLCA (Quasi-localized charged approximation) theory [1] for the strongly coupled rotating dusty plasma [2,3] and analysed their collective modes dispersion characteristic which are strongly depended on the strength of the Coriolis force acting exactly as Lorentz force. The obtained longitudinal dispersion relations show a finite jump of a frequency (2Ω) at $k\rightarrow 0$ which corresponds to the cyclotron frequency (ω_c) in the presence of magnetic field. The close correspondence between strong coupling and weakly coupling limit of the theory have been emphasized in their dispersion relation at higher rotational frequency (Ω) concludes that rotation tend to reduce the coupling among the dust particles as observed in recent rotating dusty plasma experiments [3,4]. These results from theory predict that strong coupling effects compete with the strong magnetic effects in the rotating dusty plasma viz strong coupling effects are limited by the rotational frequency.

References:

[1] Kumar, Prince, and Devendra Sharma. "Collective excitations of rotating dusty plasma under quasi-localized charge approximation of strongly coupled systems." Physics of Plasmas 28.8 (2021): 083704

[2] Kumar, Prince, and Devendra Sharma. "Dust vortex flow analysis in weakly magnetized plasma." Physics of Plasmas 27.6 (2020): 063703

[3] Kählert, H., et al. "Magnetizing a complex plasma without a magnetic field." *Physical review letters* 109.15 (2012): 155003.

[4] Hartmann, Peter, et al. "Magnetoplasmons in rotating dusty plasmas." *Physical review letters* 111.15 (2013): 155002.

Session: Nuclear Fusion **ORAL-NF-1**

STUDY OF MHD ACTIVITY AND RUNAWAY ELECTRONS IN THE ADITYA AND ADITYA-U TOKAMAK

S. Patel[1], J. Ghosh[2,3], M. B. Chowdhuri[2], K. B. K. Mayya[1], S. Purohit[2], T. Macwan[2,3], S. Aich[2], S. Dolui[2,3], K. Singh[2,3], R. L. Tanna[2,4], K. A. Jadeja[2], K. M. Patel[2], R. Kumar[2], N. Yadava[4], R. Manchanda[2], N. Ramaiya[2],K. Shah[1], A. Kumar[2,3], Y. S. Joisa[2], S. K. Jha[2], D. Raju[2], U. Nagora[2], P. K. Atrey[2], S. B. Bhatt[2], D. Chenna Reddy[2], Y. C. Saxena[2], ADITYA Team[2] and ADITYA-U Team[2]

[1]Pandit Deendayal Energy University, Gandhinagar 382007, India
[2]Institute for Plasma Research, Gandhinagar 382428, India
[3]HBNI, Anushaktinagar, Mumbai 400094, India
[4]Institute of Science, Nirma University, Ahmedabad 382481, India
E-mail :sharvil.pphd19@sot.pdpu.ac.in

Study of runaway electrons (RE’s) with energies in the several keV to tens of MeV is important considering its interaction with plasma facing components (PFC’s) results in large heat loads, sputtering and melting of the vacuum chamber, especially for reactor-scale devices such as ITER and DEMO. In order to provide methods to minimize the harmful effects of RE’s on PFC’s, a good understanding of the mechanism responsible for RE generation and transport is required.In ADITYA and ADITYA-U tokamak, extensive experimental studies related to runaway electrons, like, sawtooth induced runaway electron generation and transport, runaway mitigation using local vertical magnetic field perturbation and supersonic molecular beam injection (SMBI) fuel injection has been carried out [1-3]. These studies indicated the influence of magnetic field configuration and its various properties, like the presence of islands in rational flux surfaces, overlapping islands and interaction of island with plasma facing components, on RE confinement and transport. Moreover, amongst various RE mitigation schemes, magnetic field turbulence has long been realized to strongly influence the RE transport. The present work explains the mechanism of the confinement degradation for runaway electrons in presence of magnetic island and stochastic magnetic field configurations. To study relationship of MHD activity and RE deconfinement, events like, plasma disruption, impurity and fast fuel injection are analyzed. Based on these learnings, runaway mitigation technique via control of magnetic field turbulence is proposed for ADITYA-U tokamak.

References:

[1] Generation and transport of runaway electrons during sawteeth crash in the ADITYA tokamak, Nucl. Fusion, **58**, 076004, (2018)

[2] Novel approaches for mitigating runaway electrons and plasma disruptions in ADITYA tokamak, Nucl. Fusion, **55**, 063010, (2015)

[3] Runaway electron mitigation with supersonic molecular beam injection (SMBI) in ADITYA-U tokamak, Nucl. Fusion, **61**, 016027, (2020)

Session: Nuclear Fusion **ORAL-NF-2**

HEAT TRANSFER ANALYSIS OF PINI ION SOURCE BACK PLATE USING ANSYS

Tejendra Pateland M. R. Jana
Institute for Plasma Research, Bhat, Gandhinagar 382428, Gujarat, India
E-mail: tejendra.patel@ipr.res.in

Injection of energetic neutral beam (H^o/D^o) into tokamak plasma is successful method for plasma heating and current drive. The system which produced energetic neutral beam is called Neutral Beam Injection (NBI) system. Steady-state Superconducting Tokamak (SST-1) has a provision of Positive hydrogen ion-based Neutral Beam Injection (NBI) system to inject 0.5 MW neutral hydrogen power at 30 keV. The important component of NBI system is PINI (Positive Ion Neutral Injector) ion source which consists of plasma box, back plate, ion extractor system and neutralizer. The functions of the back plate are to provide the vacuum integrity to the plasma box, to accommodate magnet filament holders and to remove the heat load. In order to satisfy all these functions, back plate consists of (i) Oxygen Free Electronic (OFE) copper cooling plate of size 588 mm (L) × 318 mm (B) × 4 mm (T) machined of 35 inner and 8 outer cooling grooves each of size $4^{+0.1}$mm (W) ×$1.8^{+0.2}$ mm(H)(ii) SS304L magnet positioning plate of size 667 mm (L) × 397 mm (B) × 27 mm(T) (iii) SS304L Magnet cover plate of size 590 mm (L) ×293mm (B) ×2mm (T). The copper cooling plate is vacuum brazed with magnet positioning plate using BINI-7 brazing material. Thermal analysis of back plate is very important in the view of thermos-structural stability. This paper described the 2D steady-state thermal analysis of back plate using the Finite Element (FE) numerical model with the help of ANSYS computer program considering cross-section of 31 mm (W) × 17 mm (H) for back plate. The model includes OFE copper cooling plate with five cooling channel each of size 4 mm (W) ×1.8mm (H), one magnet positioning plate with groove of 10mm (W) ×9mm (H) and magnet cover plate of 2 mm thickness. The heat flux boundary condition has been given to the outer top surface of the OFE copper cooling plate. The peak heat flux of 8 MW/m^2 is given to the top surface near the magnet position whereas average heat flux of 2 MW/$m^2$is given to the remaining top surface area of the OFE copper cooling plate. The convection heat transfer coefficient of 52 kW/ (m^2K) is used as a boundary condition at the internal surface of a cooling channel near the magnet position while 44 kW/ (m^2 K)at the internal surface of remaining cooling channels. The other surfaces of the model has been consider as adiabatic surface. The results of analysis shows the temperature distribution of OFE copper cooling plate and the maximum surface temperature is ~ 155 ^{0}C at the middle surface of OFE copper cooling plate near the magnet position. The maximum temperature around the magnet is observed to be 82 ^{0}C.

Session: Nuclear Fusion **ORAL-NF-3**

DESIGN UPDATES AND CURRENT STATUS OF INSTALLATION WORKS OF EXPERIMENTAL HELIUM COOLING LOOP (EHCL)

B. K. Yadav*[1], A. Gandhi[1], A. Saraswat[1], S. Verma[1], P. Chaudhuri[1, 2]
[1]Institute for Plasma Research, Bhat, Gandhinagar, India
[2]Homi Bhabha National Institute, Mumbai, India
Email: byadav@ipr.res.in

Institute for Plasma Research is developing an Experimental Helium Cooling Loop (EHCL) as a part of R&D activities in fusion blanket technologies. This helium cooling system is designed for testing various fusion components such as tritium breeding blanket and helium-cooled divertor. The cooling channels of breeding blanket and divertor comprise of complex channel geometry having several parallel channels carrying helium gas for efficient heat extraction. Several mock-ups of these systems need to be tested before finalizing the design and fabrication. In addition to the individual testing of mock-ups of breeding blanket and divertor, integrated operation of the loop as well as understanding the behaviour of the EHCL sub-systems [1] are very essential for the development of high-pressure, high-temperature (8.0 MPa, 300-500 ⁰C) Helium Cooling System for Indian Test Blanket Module [2 & 3]. This paper briefly discusses the process design, process & instrumentation details, and operating & design parameters of the EHCL system. It briefly discusses about the architecture of major subsystems and components of the loop. Performance of the lab scale circulator test loop with its associated loop are also presented in this paper. It also presents the progress on the ongoing installation works at IPR premises.

References:

[1] B. K. Yadav, A. Gandhi, et al., Conceptual design of experimental helium cooling loop for Indian TBM R&D experiments, world academy of science, engineering and technology Int. J. Phys. Nucl. Sci. Eng., 8 (2) (2014).

[2] B.K. Yadav, A. Gandhi, et al., Helium Cooling Systems for Indian LLCB TBM, Fusion Engineering and Design, 124 (2017) 710–718.

[3] B.K. Yadav, K.T. Sandeep, et al., Design updates for Helium cooling system of Indian LLCB BLANKET,Fusion Engineering and Design, 167 (2021) 112342.

Session: Nuclear Fusion **ORAL-NF-4**

TOWARDS A 3D QUIESCENT NONNEUTRAL PLASMA STATE IN SMALL ASPECT RATIO TORUS - A PARTICLE-IN-CELL SIMULATION STUDY

Swapnali Khamaru[1], Rajaraman Ganesh[1], Meghraj Sengupta[2]
[1]*Institute for Plasma Research, HBNI, Bhat, Gandhinagar 382428, India*
[2]*Department of Physics and Engineering Physics, University of Saskatchewan, Saskatoon, Canada*
E-mail: swapnali.khamaru@ipr.res.in

Effective absolute or near-absolute equilibria are much sought after in every plasma trapping device. One of the most successful device configurations where near absolute thermal equilibrium condition has been achieved, is a straight cylindrical trap with electrons/ions, called Penning-Malmberg traps. This non-neutral plasma device has been studied theoretically/computationally and experimentally, to explore the fundamental ideas (as for example: isomorphism between 2D inviscid Euler fluids, ion resonance instability).

Finding a quiescent quasi-steady inhomogeneous, equilibrium state of a toroidal electron plasma, with excellent confinement properties of the plasma has been a long-standing, open problem. One of the reasons is that, toroidal magnetic fields come with natural radial inhomogeneity, due to Maxwell's equations, which has been a deterrent in achieving an absolute equilibrium. In experiments a small fraction of ion population is inevitable, which leads to ion resonance instability resulting in destabilization of the electron cloud. In first part of this presentation, existence of a quiescent quasi-steady solution**[1]** (QQS) is demonstrated in an axi-symmetric tight aspect ratio toroidal magnetic field configuration with pure electrons, using combination of a mean field theoretic extremum entropy solution and high fidelity 3D3V Particle-in-Cell**[2]**simulations. Effect of controlled ion population on this state is also addressed**[3]**. In the second part, it is shown that this QQS solution is generalizable to 3D partial toroidal traps**[4]**, which due to confining end-plugs do not enjoy device axisymmetry. Conditions for this latter study are akin to experimental devices**[5]**. We report on several new findings related to the small aspect ratio toroidal electron plasma in the present numerical study.

References:

[1] S. Khamaru, R. Ganesh, and M. Sengupta, “A novel quiescent quasi-steady state of a toroidal electron plasma," Phys. Plasmas 28, 042101 (2021)

[2] S. Khamaru, M. Sengupta, and R. Ganesh, “Dynamics of a toroidal pure electron plasma using 3d pic simulations," Physics of Plasmas 26, 112106 (2019)

[3] S. Khamaru, R. Ganesh and M. Sengupta, “3D3V PIC Simulation of ions-driven destabilization of a toroidal electron cloud ", Manuscript Under Preparation

[4] M.Sengupta, S.Khamaru, R.Ganesh, “Self organization of pure electron plasma in a partially toroidal magnetic-electrostatic trap: A 3D Particle-in-Cell simulation,” J. Appl. Phys. 130, 133305 (2021)

[5] L. Lachhvani et al. Phys. Plasmas 24, 102132 (2017)

Session: Plasma Application **ORAL-PA-1**

MICROPLASMA SYNTHESIS OF CE-DOPED HAUSMANNITE MN_3O_4NANOPARTICLES FOR SUPERCAPACITOR APPLICATION

E.R. Kavitha[1], K. Suresh[1*], and S. Yugeswaran[2]
[1]*Surface & Environmental Control Plasma Lab, Department of Physics, Bharathiar University, Coimbatore–641046, Tamilnadu, India.*
[2]*Department of Physics, Pondicherry University, Puducherry–605014, India*
** Email: ksureshphy@buc.edu.in*

The electrochemical performance of hausmanniteMn_3O_4nanoparticles (NPs) was enhanced by dopingwith one of the rare earth material cerium. The Ce-doped Mn_3O_4 NPs was synthesizedby microplasma array discharge method. High electron density, continuous flow, small dimension and non-thermal plasma characteristics make microplasmasuitable method for nanomaterial synthesis.The precursor solution containing(cerium nitrate hexahydrate and potassium permanganate) was subjected to microplasma treatment for 30 minutes by air plasma. The cerium was successfully doped at various concentrations ranging from 3%, 5%, and 7% in the presence of radicals during microplasma discharge. After post treatment, the collected precipitates were subjected to different characterization techniques. XRD analysis revealed phase and crystallinity of the synthesized material. The Ce doped Mn_3O_4 NPs maintained tetragonal structure. Raman spectra analysis also confirmed the formation of Ce doped Mn_3O_4 NPs. FE-SEM analysis depicted that the produced NPs are in narrow range with spherical morphology,and mapping revealed the uniform distribution of Mn, O and Ce elements. The electrochemical studies involved cyclic voltammetry (CV), galvanostatic charge-discharge (GCD) and electrochemical impedance spectroscopy (EIS), and all the measured capacitive characteristics deliver the excellent capacitive performance of Ce doped Mn_3O_4 NPs at various concentrations. Hence the present work enlighten for the promotion of Ce doped Mn_3O_4 NPs as pseudocapacitive electrode material for supercapacitor application.

Keywords: Microplasma discharge, Ce doped Mn_3O_4 NPs, Electrochemical performances

Acknowledgements: This work was supported byUGC-BSR Start-up grant(No.F.30-354/2017 BSR) from University GrantsCommission,New Delhi. ERK acknowledges the University Research Fellowship (No. C2/18369/2021) received from Bharathiar University, Coimbatore

Session: Plasma Application **ORAL-PA-2**

RAPID CRYSTALLIZATION OF AMORPHOUS TIO_2 USING ATMOSPHERIC PRESSURE PLASMA

Parismita Kalita[1,2*], Palash Jyoti Boruah[1] and Heremba Bailung[1]

[1]Plasma Application Laboratory, Physical Sciences Division, Institute of Advanced Study in Science and Technology (IASST), Paschim Boragaon, Guwahati – 781035, Assam, India

[2]Academy of Scientific and Innovative Research (AcSIR), Ghaziabad – 201002, India

E-mail: 2015parismitakalita@gmail.com

Atmospheric pressure plasma (APP) assisted material fabrication, as well as surface modification of materials, is a recently growing interdisciplinary research field in the interface between plasma and material science. Presence of a wide range of reactive species in the plasma zone which plays the role of reducing agent results in an intrinsic high chemical reactivity compared to ordinary chemical reaction media that offers several advantages in material processing. The high chemical reactivity leads this process to be quite rapid [1]. Despite this well-known process of plasma-assisted material preparation, one aspect of plasma synthesis technique that is still poorly understood is plasma-induced crystallization of materials. It is believed that heating of the particles due to collision between energetic short-lived as well as long-lived reactive species with the particles is responsible for the crystalline phase of the material[2].

Herein, we have developed a plasma-liquid reactor in such a way that the APP is produced above the liquid surface which is then transferred to the liquid medium. This work demonstrates rapid phase transition of amorphous to phase pure anatase TiO_2 using titanium butoxide (TTB) as the raw material. Upon hydrolysis of TTB white color precipitation is observed which results in amorphous TiO_2. XRD spectra reveal that the crystallization process of TiO_2 is very fast compared to the conventional annealing process for crystallization. 10 minutes of plasma treatment is sufficient for the phase transformation of TiO_2. It is also observed that the crystallinity index decreases with the plasma treatment time. As in the conventional annealing process that is used for crystallization of material particles, the formation of phase pure anatase TiO_2 is difficult to achieve, therefore, this plasma-induced crystallization can be regarded as an efficient alternative tool for crystallization of material. In addition, to investigate the plasma properties such as gas temperature and to confirm the formation of various reactive species in the plasma zone, OES spectra have been recorded.

References:

[1] Plasma-Assisted Approaches in InorganicNanostructure Fabrication, Adv. Mater., **22**, p 1451-1473, (2010)

[2] Plasma-Induced Crystallization of Silicon Nanoparticles, J. Phys. D: Appl. Phys., **47**, p 075202-075209, (2014)

Session: Plasma Application **ORAL-PA-3**

COLD PLASMA TREATMENT OF RAW MILK AND ITS PHYSICAL PROPERTIES ANALYSIS

Kiran*, Ramavtar,Vigyan Gadodia, Shikha Panday, Ritesh Mishra and Ram Prakash
Department of Physics,
Indian Institute of Technology Jodhpur,
N.H. 62, Nagaur Road, Karwar, Jodhpur, Rajasthan, 342037
**Email: ahlawat.1@iitj.ac.in*

In the dairy sector, thermal techniques such as high-temperature-short-time (HTST) are used to ensure milk safety and shelf life. While thermal treatments ensure milk safety, they can harm milk quality, such as protein denaturation, non-enzymatic browning, vitamin loss, and flavour alterations[1]. Dielectric Barrier Discharge (DBD) based cold plasma treatment [2] is an emergent and non-thermal method that can be used for milk decontaminationso as to ensure food safety while keeping milk quality. In this work an effort has been made to study the changes in the physical parameters of the milk like pH, conductivity, temperature, and colour after direct treatment of milk using a BDB based large volume surface plasma discharge system. The developed system is optimized for operational parameters and raw milk has been treated at different time intervals. The pH and colour characteristics of raw milk samples have not been affected by the proposed cold plasma treatment. Nevertheless, the conductivity of the milk has significantly increased which may help in reducing the harmful bacterial growth in the milk. After the continuous operation of the system even for more than 30 mins, there is no significant change in the raw milk temperature, which is a key success for milk decontamination using a cold plasma treatment in the developed DBD geometry. The results of these efforts will be presented.

References:

[1] N. Nikmaram and K. M. Keener, "The effects of cold plasma technology on physical, nutritional, and sensory properties of milk and milk products," *Lwt*, vol. 154, p. 112729, 2022, doi: 10.1016/j.lwt.2021.112729.

[2] N. M. Coutinho *et al.*, "Cold plasma processing of milk and dairy products," *Trends Food Sci. Technol.*, vol. 74, no. October 2017, pp. 56–68, 2018, doi: 10.1016/j.tifs.2018.02.008.

Session: Plasma Diagnostics **ORAL-PD-1**

ARGON IMPURITY TRANSPORT IN ADITYA-U TOKAMAK USING SPECTROSOCPY

K. Shah[1], M. B. Chowdhuri[2],J. Ghosh[2], K. A. Jadeja[2], R. Manchanda[2], G. Shukla[1], S. Patel[1], N. Yadava[3], N. Ramaiya[2], R. Dey[2], T. Macwan[2], R. L. Tanna[2],R. Kumar[2], S. Aich[2], K. M. Patel[2], S. Purohit[2], M. K. Gupta[2], U. C. Nagora[2], S. K. Pathak[2], K. B. K. Mayya[1] and Aditya-U Team

[1]*Deptt. of Physics, Pt. Deendayal Energy University, Raisan, Gandhinagar 382007, India*

[2]*Institute for Plasma Research, Bhat, Gandhinagar 382428, India*

[3]*Institute of Science, Nirma University, Ahmedabad 382481, India*

E-mail: kajal.sphd16@sot.pdpu.ac.in

In case of future generation reactors such as ITER, a controlled injection of impurities into the plasma, so called impurity seeding, is inevitable for radiative power dissipation and thus reducing the tungsten divertor plate temperatures and power load [1]. Argon is envisaged to be a good candidate in such scenario which can provide high radiated power, fine controllability and compatibility withplasma confinements. However, impurity injection often leads to modification of the main ion background plasma through fuel dilution and thereby causing confinement degradation. Consequently, for the operation of a future fusion reactor, it will be crucial to find an optimum seeding recipe which provides sufficient power dissipation and at the same time ensures a minimal detrimental impact on the confined plasma and the burn conditions. Hence it is of utmost importance to understand transport and behavior of such impurities inside the plasma.

In case of Aditya-U tokamak, argon impurity transport study has been recently performed through high resolution spectroscopic diagnostics by measuring various line emissions in the visible and VUV region [1]. Using a recently upgraded high resolution multi-track visible spectroscopic diagnostic, spatial profile of Ar^{1+} line emissions has been observed for the first time in Aditya-U plasma. The system consists of a 1.0 m f/8.7 Czerny – Turner spectrometer with a grating of 1800 grooves coupled with a CCD detector. All the observed line emissions of Ar^{1+} ions have been identified using NIST database. Moreover, Ar^{13+} and Ar^{14+} line emissions at 18.796 nm and 22.115 nm respectively have also been observed using VUV spectrometer coupled with a CCD detector. From these measurements, argon transport through the estimation of the diffusion coefficient and convective velocity has been investigated by comparing the radial profile of Ar^{1+}emission obtained by inverting the line-integrated Ar^{1+}data, with those simulated using 1D impurity transport code. Together with this, line ratio Ar^{13+} and Ar^{14+} emissions have also been used to estimate the transport parameters. Detailed experimental investigation of Argon transport in the edge plasma region of ADITYA-U tokamak will be discussed in the paper.

References:

[1] I. Ivanova-Stanik et al., Fusion Eng. Des. 109-111, 342 (2016).

[2] K. Shah et al., Rev. Sci. Instrum. 92, 053548 (2021).

Session: Plasma Diagnostics **ORAL-PD-2**

COLLISIONAL RADIATIVE (CR) MODEL FOR THE DIAGNOSTICS OF NE-AR MIXTURE PLASMA

S. S. Baghel[1], R. K. Gangwar[2] and R.Srivastava[1]
[1]*Department of Physics, Indian Institute of Technology (IIT) Roorkee, Roorkee-247667, India*
[2]*Department of Physics &Center for Atomic, Molecular and Optical Sciences & Technologies, Indian Institute of Technology (IIT) Tirupati, Yerpedu-517619, Andhra Pradesh, India*
E-mail: sbaghel@ph.iitr.ac.in

Optical emission spectroscopy (OES) based diagnostics of any plasma is a very popular technique due to its non-invasive nature. However, it requires a suitable population-kinetic model to be coupled for the extraction of the plasma parameters viz. electron temperature and electron density. Particularly, for a low temperature plasma which deviates significantly from the equilibrium nature, one needs to utilize a consistent collisional radiative (CR) model to perform the diagnostics [1].

In the present work, we have developed a fine-structure resolved CR model for the diagnostics of Ne-Ar mixture plasma which has several important industrial applications. We consider, the 40 fine structure resolved energy levels of neon corresponding $2p^53s$, $2p^53p$, $2p^53d$, $2p^54s$ and $2p^54p$ along with its ground state ($2p^6$) and ionic state ($2p^5$). All the essential population and de-population channels *viz.* electron impact excitation-deexcitation, ionization, two/three-body recombination, radiative decay, self-absorption correction, diffusion, etc. have been considered in the model. The quenching of relatively higher lifetime states $2p^53s$ due to interaction with Ar atoms through associative and Penning ionizations is also included in the model. The applicability of our CR model is demonstrated by coupling it with the emission and absorption measurements of the Ne-Ar mixture plasma from a rf ICP discharge [2]. The plasma parameters *viz.* electron temperature, electron density and population distribution of levels at various mixture conditions are extracted. The obtained results are compared with the Langmuir probe measurements [2] and the associated emission model estimates [2]. The self-absorption correction (escape) factors and electron impact excitation rates at various Ne-Ar mixture concentrations are also presented. The details of the CR model along with the obtained various results will be presented in the conference.

References:

[1] S S Baghel*et al.*, Diagnostics of low-temperature neon plasma through a fine-structure resolved collisional – radiative model,Plasma Sources Sci. Technol.**28** 115010 (2019)

[2] J B Boffard*et al.*, Evidence of weak plasma series resonance heating in the H-mode of neon and neon/argon inductively coupled plasmasJ. Phys. D: Appl. Phys., **45**, 382001 (2012).

Session: Plasma Diagnostics **ORAL-PD-3**

ADITYA TOKAMAK PLASMA DISRUPTION CHARACTERIZATION

S. Purohit[1*], M. B. Chowdhuri[1], J. Ghosh[1],C. N. Gupta[1], S. K. Jha[1], D. Raju[1], K. A. Jadeja[1], M. K. Gupta[1], P. K. Atrey[1], S. K. Pathak[1], Y. S. Joisa[1], R. L. Tanna[1], P. K. Chattopadhyay[1], and ADITYA Team

[1]*Institute for Plasma Research, Gandhinagar, Gujarat 382428, India*

*E-mail: *pshishir@ipr.res.in*

The Tokamak plasma disruptions possess a significant threat to the device and limit the performance of any current or future tokamak operations. Under disruption, the vacuum vessel and the plasma-facing components (PFC) are subjected to a generous amount of heat, particles, and energy, which results in the degradation of the vessel's inner walls and PFC. A substantial amount of change of flux is also experienced, this introduces sizable electromotive force (EMF) in the vacuum vessel, PFC, and the peripheral subsystems. Such characterization advocates a detailed study of disruption, their triggering mechanism, and possible disruption mitigation strategies for any tokamak. Disruption characterization for the ADITYA tokamak has been studied for a range of plasma discharges and it has been found that different types of disruptions are taking place. Disruptions are seen at low and high edge safety factors which are associated with equilibrium and stability of the plasma. Disruptions leading to the density limit are also observed, where the line integrated electron density (n_e) reaches up to the Greenwald density limit. However, it is also observed that with a higher Greenwald density limit the disruption is relatively slower. The current quench phase of disruptions are parameterized via the current quench time, quenching rates (average and instantaneous), current density, etc. tokamak plasma exhibits area-normalized plasma current quench time to be ~ 0.05 $s\ m^{-2}$, and the current density at the disruption resides within ~1.1kAm^{-2}. Disruptions are higher current densities are relatively slow. The ratio of the instantaneous to average current quench rate creeps up to 6, for a very few discharges, which indicates an extremely non-linear current pattern. The area-normalized plasma current quench time displays an inverse proportionality with the edge safety factor which suggests the faster current quench with island growth and possible coupling.

Session: Space and Astrophysical Plasma **ORAL-SP-1**

SHEAR FLOW EFECTS ON MAGNETIC ISLAND COALESCENCE

Jagannath Mahapatra[1,2], Rajaraman Ganesh[1,2], Arkaprava Bokshi[1], and Abhijit Sen[1,2]
[1]*Institute for Plasma research, HBNI, Bhat, Gadhinagar, Gujarat, India 382428*
[2]*Homi Bhabha National Institute, BARC Training School Complex, Mumbai, Maharashtra 400094*
E-mail :jagannath.mahapatra@ipr.res.in/jaga.physics94@gmail.com

Magnetic reconnection is a fundamental process observed in both astrophysical as well as fusion device plasmas. Although the sites of magnetic reconnection in the plasma are the local magnetic X-type null points, it is responsible for the change in the global magnetic field topology and converts a large fraction of magnetic field energy in the form of kinetic energy and bulk plasma heating. Hence, any change in the profile of plasma parameters around the reconnection site can potentially change the reconnection process and affects the system globally. Shear flow in the plasma is one of such parameters and its role in the reconnection process (see Ref. 1 and references therein) has been studied extensively in recent years. In the previous studies, the effect of shear flows on the magnetic reconnection has been explored along with tearing mode instability [2] and plasmoid instability [3] in the Harris-type current sheet only.

In the present work, we study the role of shear flow on the magnetic island coalescence using Fadeev's equilibrium [4] using a 2D viscoresistive Reduced-MHD (2D VR-RMHD) model [1]. We calculate the new scaling laws of various parameters like reconnection rate, reconnecting current sheet width, upstream magnetic field with respect to shear flow amplitude and shear length scale. We find the suppression of Kelvin-Helmholtz instability in the super-Alfvenic shear flows. Detail of this work will be presented.

References:

[1] J. Mahapatra et. al., Phys. Plasmas **28,** 072103 (2021).
[2] P. A. Cassak, Phys. Plasmas **18**, 072106 (2011).
[3] M. Hosseinpour et. al., Phys. Plasmas **25,** 102117 (2018).
[4] V. M. Fadeev et. al., Nucl. Fusion **5**,202 (1965).

Session: Space and Astrophysical Plasma ORAL-SP-2

Cosmic Rays Diffusion and Gravitational Collapse in Radiative Molecular Clouds including ion Larmor radius corrections

Ram Prasad Prajapati

School of Physical Sciences, Jawaharlal Nehru University, New Delhi-110067, India

ABSTRACT

Cosmic rays (CRs) are believed to play a significant role in the ionization of interstellar gas and its dynamics in the interstellar medium (ISM), supernova remnants associated with molecular clouds, diffuse molecular clouds solar atmosphere, formation of protostellar discs, galaxy clusters, etc. In this work the effects of cosmic rays (CRs) diffusion and finite Larmor radius (FLR) corrections have been studied on the gravitational collapse in H II region of molecular clouds. The hydrodynamic fluid-fluid approach is considered to interact CRs with gravitating, magnetized, and thermally conducting gas in molecular clouds. The MHD fluid model is formulated considering gradients of the CR pressure, CRs diffusion, radiative and FLR effects in terms of particles Larmor radius. The dispersion properties of thermal and gravitational instabilities have been analyzed with combined effects of CRs and FLR corrections in longitudinal and transverse modes.

It is found that coupling of FLR corrections in terms of magnetic viscosity with CR effects significantly decreases the growth rate of the instability. The CR pressure stabilizes the growth rates of the gravitational and thermal instabilities while parallel CR diffusion destabilizes the growth rate of the gravitational instability. The Jeans length of the system gets increased due to an increase in the CR to gas pressure ratio. The gravitational collapse is supported by the system with high energy (above knee) CR particles with Larmor radius comparable to the cloud size. The results have been applied in H II region of molecular clouds to understand the interplay between CR parameters and FLR corrections on the gravitational collapse of the medium.

Key words: ISM: Cosmic rays; Plasmas; Instability; Diffusion; Magnetic fields; ISM; HII region

Session: Space and Astrophysical Plasma **ORAL-SP-3**

GENERATION OF KINETIC ALFVÉN WAVES BY MULTIPLE FREE ENERGY SOURCES

Krushna Chandra Barik[1]*, Satyavir Singh[2], and G.S. Lakhina[3]
[1,2,3] *Indian Institute of Geomagnetism, New Panvel-410218, India*
E-mail: krushna.b@iigm.res.in, satyavir.s@iigm.res.in, gslakhina@gmail.com

The generation mechanism of ultra-low frequency (ULF) waves observed in different regions of Earth's magnetosphere is not understood completely, albeit various mechanisms, for instance, Kelvin-Helmholtz (K-H) instability, cavity modes, field line resonances etc. have been proposed so far. Further, the magnetospheric transition regions, such as, magnetopause, polar cusp, plasma sheet boundary layer (PSBL), magnetotail etc. are thick boundaries that support gradients in velocity, magnetic field and plasma density. These gradients along with ion beams which are observed in magnetospheric regions act as free energy sources and can excite plasma waves. A theoretical model is presented to investigate the generation of kinetic Alfvén waves (KAWs) by the combined energy sources of ion beam and velocity shear. The resonant instability of KAWs is discussed through a three component theoretical model comprising of background Maxwellian ions, non-Maxwellian kappa electrons and drifting Maxwellian beam ions. It is found that in velocity shear driven resonant instability of KAWs, the presence of parallel streaming (along the ambient magnetic field) beam ions has stabilizing effect, whereas, the counter streaming (opposite to ambient magnetic field) beam ions leads to larger growth of KAWs. On the other hand, in the ion beam driven resonant instability of KAWs, presence of negative velocity shear enhances the growth rate of KAWs, while the positive velocity shear has stabilizing effect. Further, it is found that presence of kappa electrons hinders the growth rate of KAWs. The effect of other plasma parameters, such as, temperature, plasma beta, propagation angle, ion beam number density etc. in the resonant instability of KAWs are also discussed. The generation of KAWs is attributed to explain few of characteristics of observed ULF waves. The model is able to excite KAWs with frequency up to $\approx (6.2 - 93.4)$ mHz which falls in the range of ULF waves.

Session: Laser Plasma, Pulsed Power and Others **ORAL-PO-1**

INDIGENOUS HIGH POWER PSEUDOSPARK SWITCHES FOR FAST PULSE POWER APPLICATIONS

Ram Prakash Lamba[1,2], Udit Narayan Pal[1,2] and Ram Prakash[3]
[1]*CSIR-Central Electronics Engineering Research Institute (CSIR-CEERI), Pilani, Rajasthan-333031.*
[2]*Academy of Scientific & Innovative Research, CSIR-CEERI Campus, Pilani*
[3]*Indian Institute of Technology, Jodhpur, Rajasthan*
E-mail: rplamba@ceeri.res.in

In India there is a specific requirement of high power pseudospark switches (particularly very high current ≥ 20 kA and very high voltage ≥ 20 kV) for many high energy research application areas of strategic and industrial needs, such as, pulse modulators, crowbar, shock wave generation, capacitor discharge in coil gun experiments, dense plasma focus, electromagnetic forming, kicker magnet, etc.[1-2] Such pseudospark switches (PSS) are being imported and have been subject to import restrictions from time to time.In this work, efforts have been made to indigenously develop PSS with enhanced voltage and current handling capabilities for fast pulsed power applications by optimizing the geometrical configurations and operating parameters. A coaxial multi-gap multi-channel and a radial multi-channel configuration of the PSS have been developed at CSIR-CEERI and analyzedwith respect to their underlying physics for high voltage and high current switching capabilities.

The synergistic cascading of two gaps in coaxial multi-channel configuration has facilitated the development of double gap pseudospark switch (DG-PSS)for high voltage switching [3]. Accordingly, its breakdown behaviorhas been studied for optimal dependency of switching parameters on working pressure and charge transfer. The optimum performance of the DG-PSS has beenachieved in the pressure range of 30-45 Pa. The time delay and voltage fall time are found minimum at the optimum gas pressure of 45 Pa and anode voltage 40 kV. The minimum delay time to breakdown and voltage fall time are recorded as ~100 ns and ~30 ns, respectively, which indicate faster switching. Continuous switching up to arate of 50 Hz in a burst of 50 shots has beendemonstrated successfully without any undesired breakdown events. The developed voltage divider circuit has helped in better coupling of plasma through thedrift region for coherent breakdown of both the gaps with lesser delay and jitter. During the repetitive operation, jitter of ~ 20 ns isachieved in thecurrent pulse at its optimum operating conditions. The switching characterization of the DG-PSS confirmed its suitability for high voltage,however at low to moderate current switching. During thehigh current switching, the axial discharge channels in coaxial PSS pinch due to strong Lorentz forces which limits its operation.

In order to mitigate the critical issue of discharge pinching, a novel geometry radial multi-channel pseudospark switch (RM- PSS) with linear apertures has also been designed and developed [4-6].The temporal and spatial evolution of the discharge through radial multi-channels is simulated using COMSOL software and field penetrationis analysed for simultaneous multichannel discharge. In this geometry of RM-PSS, the larger interaction distance among the discharge channels enabled itto commute high current without pinching. A peak current of ~135 kA atacharging voltage of 13 kV using a 14 μF capacitorhas been achieved successfully. A good correlation has been obtained between simulation and experimental results which further confirms that RM-PSS is appropriate for high current switching while DG-PSS is suitable for high voltage switching. The efforts made paves the way for indigenous development of high-power 40kV/5kA DG-PSS and 20kV/100 kA RM-PSS for the first time in the country. The results of these efforts will be presented.

References:

[1] K. Frank, I. Petzenhauser, “Do Gas-Filled Switches Still Have a Future?” *IEEE 34th International Conference on Plasma Science (ICOPS),* (2007).

[2] UN Pal, RP Lamba, BL Meena, Klaus Frank, “A multi-gap multi-aperture pseudospark switch and its performance analysis for high-voltage applications”, *IEEE Transactions on Electron Devices*, **67**(12), P 5600-5604, (2020).

[3] R P Lamba,U N Pal, B L Meena, R Prakash, A sealed-off double-gap pseudospark switch and its performance analysis, *Plasma Sources Science and Technology*. **27** (3), p 035003, (2018).

[4] R. P. Lamba, B.L. Meena, H. Rahaman, Niraj Kumar, U. N. Pal, and Ram Prakash, an Indian patent titled "A 20kV/20kA Linear Aperture Radial Multichannel Pseudospark Switch (LARM-PSS) for High Current Applications" Indian Patent, *Application No., 1220/DEL/2015* filed on 01/05/2015, published on 11/04/2016.

[5] R P Lamba, BL Meena, UN Pal, N Kumar, R Prakash “Design and development of a high current pseudospark switch for pulse power applications”*19th IEEE Pulsed Power Conference (PPC)*, p 1-4, (2013)

[6] R. P. Lamba, V. Pathania, B. L. Meena, H. Rahaman, U. N. Pal, and Ram Prakash, Investigations of a High Current Linear Aperture Radial Multichannel Pseudospark Switch, *Review of Scientific Instruments,* **86** (10), p 103508, (2015).

Session: Laser Plasma, Pulsed Power and Others **ORAL-PO-2**

PULSED LASER DEPOSITION OF CUO/CU_2O FILMS AND THEIR APPLICATION IN PHOTOCATALYTIC DYE DEGRADATION

RudrashishPanda[a*], MilaanPatel[a,b]JintoThomas[a] and Hem Chandra Joshi[a,b]
[a]*Institute For Plasma Research, Bhat, Gandhinagar, Gujarat, India, 382428*
[b]*Homi Bhabha National Institute, Maharashtra, India, 400094*
**Email address: r.panda550@gmail.com*

Pulsed laser deposition (PLD) is one of the physical deposition techniques for thin film growth with a better stoichiometry, tunability, reproducibility and simplicity. It is a well adopted method of thin film deposition since decades and has proven its efficiency in producing industrial level films for various kind of applications. Keeping this in mind, a PLD system is assembled with the available instruments and a pulsed Nd:YAG laser. The CuO and Cu_2O oxide thin films are synthesized using this system by tuning the ambient gas and pressure conditions. The crystallinity, surface morphology and the optical properties of the films were characterized by X-ray Diffraction (XRD), RAMAN spectroscopy, field emission scanning electron microscopy (FESEM) and UV-Vis spectroscopy respectively. The effect of ambient conditions on pure phase thin films synthesis has been demonstrated. The XRD and RAMAN spectroscopy show a transition of composite nanomaterial synthesis to pure phase Cu_2O and CuO formation by tuning the ambient gas and chamber pressure. FESEM show the effect of chamber pressure on crystallite size. The optical absorption of the samples are studied using an in-house developed absorption setup using HR4000 spectrometer. From the absorption spectra, the bandgap energies are measured to be 1.53 eV and 2.45 eV for CuO and Cu_2O samples respectively. A clear relationship between the band gap of the materials and the dye degradation efficiency was observed for both the samples. Photo induced dye degradation study of the samples is carried out under direct sunlight irradiation. Remarkable efficiency having the reaction rate constant of 0.020 min^{-1} with good recycling ability is shown by the samples.

Session: Laser Plasma, Pulsed Power and Others ORAL-PO-3

EXCITATION OF LOWER HYBRID AND MAGNETO-SONIC PERTURBATIONS BY LASER INX-MODE CONFIGURATION OF MAGNETIZED PLASMA

Ayushi Vashistha*[1], Devshree Mandal[1] andAmita Das[2]
[1]*Institute for Plasma Research, HBNI, Bhat, Gandhinagar – 382428*
[2]*Indian Institute of Technology, Delhi,India*
Email: ayushi.vashistha@ipr.res.in

We focus on interaction of laser with magnetized plasma in a particular configuration where laser is incident normally on a sharp plasma boundary and the applied magnetic field orientation conforms to the X-mode propagation of electromagnetic wave. This study has been carried out with the help of Particle-In-Cell (PIC) simulations using OSIRIS4.0. The magnetic field is considered so as to magnetize the lighter electron species at the laser frequency. It is shown that when the laser frequency is less than but close to the lower hybrid (LH) frequency, (and hence is in the pass band of X-mode) it is able to propagate inside the plasma[1,2]. It then excites electrostatic lower hybrid perturbations and thus gets absorbed in the plasma, preferentially heating the ions. Furthermore, our simulations show the formation of magnetosonic excitations. These excitations essentially occur as a result of the ponderomotive pressure of laser on the sharp plasma boundary. Thus, arising even when the laser frequency is chosen to lie in the stop band of X-mode. The LH excitation and ion heating is totally absent for this case. Our study has relevance to laboratory as well as space plasmas where ion heating via lower hybrid wave occur and the formation of magnetosonic structures are observed.

References:

[1] A. Vashistha, D. Mandal, A. Kumar, C. Shukla, and A. Das, “A new mechanism of direct coupling of laser energy to ions,” New Journal of Physics, vol. 22, p. 063023, jun 2020.

[2] A. Vashistha, D. Mandal and A. Das, “Excitation of lower hybrid and magneto-sonic perturbations in laser plasma interaction. Nuclear Fusion, 61(2), 026016.

POSTER PRESENTATIONS

CATEGORY: BASIC PLASMA THEORY (BPT)

BPT-P-1

DATA COMPRESSION BY AZADBINRAJIB (ABR) QUANTUM GATE

A.B.Rajib Hazarika
Department of Mathematics,Diphu Government College,Diphu Assam,India-782462
E.mail: drabrh_dgc5163@rediffmail.com , drabrh02@gmail.com

AzadBinRajib (ABR) Quantum Gate is studied for data compression and loose compression with Quantum Shannon theory, von-Neumann theory and with Schur - Weyl transform. The study is done for n length string or word by finding the density matrix as well for nth qubits state with fidelity. Application as Quantum communications.

Keywords: *Quantum gate, data compression,spectral density, fidelity*

BPT-P-2

EFFECT OF ELECTRON- POSITRON- ION ON MODULATION OF NONLINEAR WAVES IN WARM PLASMA: A NONLINEAR SCHRÖDINGER EQUATION

Latika Kalita[1] and Ranjit Kumar Kalita[2]
[1]Department of Mathematics, Kamrup Polytechnic, BaihataChariali, Assam, India
[2]Department of Mathematics, Morigoan College, Assam, India
E-mail:latika84k@rediffmail.com, kalitaranjit@yahoo.com

The modulation of nonlinear ion acoustic waves and stability conditions are studied in presence of electron-positron-ion (EPI) in warm plasmas by deriving a Nonlinear Schrödinger Equation (NLSE) with the help of modified reductive perturbation technique[1] (MRPT). The progressive waves as well as steady state solutions are obtained. A duffing like equation is also obtained from NLSE and corresponding solution shows some different stability effect for wave number k. Depending upon the value of k the stability condition may be stabilized or destabilized. Analytical expression for the bright (drak) solitons are obtained and their effect on plasma medium are studied in details and presented graphically for different set of plasma parameter values. (**Keywords:** NLSE, stability, soliton)

Reference:

[1] H. Demiray, *J. Phys. Soc. Jpn.*, **71,** 1921, (2002)

BPT-P-3

NONLINEAR DYNAMIC MODELLING OF HIGH FREQUENCY ELECTROSTATIC DRIFT WAVES IN FLUID THEORETICAL APPROACH

S.P. Acharya[a] and M.S. Janaki[b]
Saha Institute of Nuclear Physics, Block AF, Sector 1, Bidhannagar, Kolkata-700064, India
E-mail: (a) siba.acharya@saha.ac.in, (b) ms.janaki@saha.ac.in

A novel nonlinear evolution equation governing the dynamics of high frequency electrostatic drift waves has been derived in an inhomogeneous magnetized plasma in the framework of a plasma fluid model. The corresponding linear dispersion relation arising out of the fluid equations has been studied in detail for conventional low frequency as well as recently observed high frequency electrostatic drift waves. The detailed analyses of fixed points as well as bifurcations of phase portraits have been performed using the qualitative theory of differential equations and bifurcation theory of planar dynamical systems through the first integral or equivalent Hamiltonian function of the system. Then some exact as well as approximate travelling wave solutions of the derived nonlinear evolution equation for high frequency electrostatic drift waves are obtained using the Hamiltonian function in case of all the fixed points. The possible applications of our novel results on the dynamics of high frequency electrostatic drift waves are discussed along with future directions for research in this field.

References:

[1] A. Hasegawa, and K. Mima*The Physics of Fluids* ***21****, 87 (1978).*
[2] W. Horton, and A. Hasegawa Chaos **4**, 227 (1994).
[3] O. Pokhotelov, L. Steno, and P. K. Shukla *Journal of Plasma Physics* ***56****(1), 187-191.*
[4] J. Li and Y. Zhou *Discrete and continuous dynamical systems series S* ***13****, 11, 3083-3097 (2020).*
[5] A. Ghosh, S. K. Saha, S. Chowdhury, and M. S. Janaki *Physics of Plasmas* ***22****, 122111 (2015).*
[6] A. Ghosh, S. K. Saha, S. Chowdhury, and M. S. Janaki *Physics of Plasmas* ***24****, 012104 (2017).*

BPT-P-4

CRYPTOCURRENCY: THE FUTURE OF MONEY ON PATTERN OF QUANTUM CRYPTOGRAPHY

A.B.Rajib Hazarika
Department of Mathematics, Diphu Government College, Diphu Assam, India-782462
drabrh_dgc5163@rediffmail.com , drabrh02@gmail.com

DRABRHtoken (ABRH) a decentralized cryptocurrency for future trading having application in buying different assets,tickets for flights, railways, buses, tourism such as holiday travels and hotels booking etc. Quantum cryptography is used to understand the technology behind the cryptocurrency in providing liquidity pools i.e 50-50 approach for assets, token sale market study, pricing and providing the knowledge on market capitalization using prime factorization and quantum cryptography.
Keywords: Quantum cryptography, cryptocurrency ,liquidity,future of money

BPT-P-5

TWO STREAM INSTABILITY IN UNMAGNETIZED INHOMOGENEOUS NONRELATIVISTIC QUANTUM PLASMAS

Shiva ShaktiSingh[1], Jyoti[2], Kamakhya Prakash Misra[1]
[1]*Department of Physics, School of Basic Sciences, Manipal University Jaipur, Dehmi Kalan, Jaipur, Rajasthan 303007, India*
[2] *Department of Physics, Govt College for Women, Gurawara, Haryana-123035, India*
Email: shaktiphysics@gmail.com

In unmagnetized quantum plasma nonrelativistic highly dense degenerate electrons at low temperature and nonrelativistic nondegenerate ions are coupled with two-dimensional electrostatic field. To investigate two stream instability in nonrelativistic degenerate inhomogeneous quantum plasma Normal Mode Analysis method is used. First order perturbation in densities and velocities of plasma species is calculated afterLinearization. The propagation vector of plasma wave makes an oblique angle with z-direction. The basic QHD equations are formulated for electrons and ions. The perturbed electrostatics potential is calculated using Poisson's equation with quasi-neutrality condition. Using appropriate quantum plasma parameters, outlines of growth rates for instabilities are observed with oblique angle and electrostatic potential.

BPT-P-6

EFFECT OF K-DEFORMED KANIADAKIS DISTRIBUTION ON MODULATIONAL INSTABILITY OF ION-ACOUSTIC WAVES

Gurleen Kaur and Parveen Bala
Department of Mathematics, Statistics & Physics, Punjab Agricultural University, Ludhiana-141004, India.
E-mail: gurleenkaur76255@gmail.com, pravi2506@pau.edu

In the present study, we analyzed the growth rate for Modulational instability (MI) for both slow and fast modes in multicomponent unmagnetized plasma viz. H^+H^-, Ar^+F^-, and $H^+O_2^-$ plasma systems at different temperatures of positive and negative ions. The non-Maxwellian distribution known as κ-deformed kaniadakis distribution has been applied to the electrons in the range of deformation parameter κ, $-0.4 \leq \kappa \leq 0.4$. The Nonlinear Schrodinger equation has been derived by using the standard technique called Reductive Perturbation Method. It is observed that deformation parameter κ influences the MI criteria in both slow and fast modes. The obtained results are examined by deviating the different parameters such as deformation parameter κ, the temperature of positive and negative ions (σ_1, σ_2), mass ratio η, density ratio α, and modulational wave number K_{MI}. The present research may be usefulinunderstanding the study of astronomical physics, non-linear waves of plasma.

***Keywords*:** Non-linear Schrodinger equation, κ-deformed Kaniadakis distribution, reductive perturbation method, modulational instability, multicomponent plasma

BPT-P-7

MODIFIED BURGER'S EQUATION USING SCHAMEL KAPPA DISTRIBUTION

Parveen Bala and Gurleen Kaur
Department of Mathematics, Statistics & Physics, Punjab Agricultural University, Ludhiana-141004, India.
E-mail: pravi2506@pau.edu

Electron Acoustic Waves (EAWs) are the low frequency branch of electrostatic plasma waves exist in neutralized plasmas, pure electron plasmas and pure ion plasmas.The present problem deals with the investigation of electron acoustic shock waves comprising cold electron fluid and hot electrons using modified burger's equation. The hot electrons are assumed to be featuring non-Maxwellian electron distribution which is modelled by a kappa distribution function followed by Schamel distribution. A shock wave is a strong pressure wave that propagates at a speed greater than the speed of

sound in that medium. In the present model, we analyzed the physical properties of shock waves i.e. width (δ) and amplitude (θ) by varying the parameters kappa (κ) and trapping parameter (β) of dispersion and non-linear terms.

Keywords: Modified Burger's equation, Schamel kappa distribution, Shock waves, Electron-acoustic waves.

BPT-P-8

EFFECT OF DAMPING ON TERAHERTZ RADIATION GENERATION FROM LASER INTERACTION WITH NANO-PARTICLES

*P. Varshney[1], A. P Singh[2], M. Kundu1[3] and K. Gopal[2]
1Institute for Plasma Research, Bhat Gandhinagar-382428, Gujarat -India
2Department of Physics and Electronics, Rajdhani College (University of Delhi), Delhi-110015, India
3Homi Bhabha National Institute, Training School Complex, Anushaktinagar, Mumbai 400094, India
**Email: varshneyprateek28@gmail.com*

Terahertz radiation generation has been reported in the presence and absence of damping mechanism when laser beat wave interact with spherical graphite nanoparticles (NPs). A cloud of electron and ions forms during interaction of laser beat wave with a spherical NPs. Strong nonlinear current at the laser beat-wave frequency allows emission of radiations in THz regime. Damping factor has been introduced in dynamics of electrons to include the electron-electron scattering. Beam decentred (BDC) parameter is introduced in the laser field profile that redistribute the laser intensity spatially. THz amplitude enhances significantly with BDC parameter when damping is considered in electron dynamics. Effects of damping can be controlled or tuned using the BDC parameter, laser intensity and with the enhancement of density modulation.

BPT-P-9

EFFECT OF DENSITY RIPPLE ON THZ GENERATION BY Q-GAUSSIAN LASER IN PLASMA

Dipender Singha, NitiKanta, Shivani Vij
Lovely Professional University, Phagwara, Punjab
DAV Institute of Engineering & Technology, Jalandhar, Punjab
Email: niti.kant@lpu.co.in

A theoretical model for THz generation by non-linear mixing of two q-Gaussian laser beams in a rippled density plasma is proposed. Beating of lasers of the same mode incident on plasma surface gives non-linear ponderomotive force which induces electron drift. This electron drift couples with the density ripple to produce a nonlinear

current. The nonlinear current drives the resonant THz radiation at the beat frequency. Density ripple provides the proper phase matching and enhances the THz generation efficiency.

BPT-P-10

MODELLING AND SIMULATION STUDY OF MAGNETIC ENHANCEMENT IN PLASMA DENSITY FOR RF BASED H^- ION SOURCE

Rajnish Kumar[1,2,a], Dharmraj V. Ghodke[1], Vijendra Prasad and Purushottam Shrivastava
[1]*Ion Source Development & Diagnostic Section, Proton Linac Development Division*
Raja Ramanna Centre for Advanced Technology, Indore - 452 013, India.
[2]*Homi Bhabha National Institute, Training School Complex, Anushakti Nagar,*
Mumbai 400 094, India.
[a]*E-mail: rajnishk@rrcat.gov.in*

A multi-cusp free, RF based H^- ion source is designed and developed at RRCAT, with external main RF antenna operating at 2 MHz, and a low power RF based ignitor system working at 13.56 MHz frequency. This source is expected to have high operating life and has been developed to serve as an injector for the high current negative hydrogen linac for long term pulsed proton accelerator program. Hydrogen plasma is produced through inductive coupling inside the plasma chamber using a high power (20-100 kW) RF source. To reliably start the plasma discharge in the plasma chamber, it requires sufficient background ionization inside the chamber which is created using 13.56 MHz ignitor [2]. To enhance the power coupling and localized RF heating, antenna has been covered by ferrites. In this paper, a finite element method (FEM) based multi-physics software COMSOL [3], has been used to simulate the process of inductively coupled RF plasma discharge at 2 MHz. The effect of ferrites, particularly an enhancement in power coupling, leading to electron plasma density enhancement is discussed. Electron plasma density as well as mean electron energy for inductively coupled plasma (ICP) are evaluated by solving the drift and diffusion matrix equations using COMSOL. RF magnetic field produced by antenna RF current is also calculated. The reaction rates averaged for important collisional reactions responsible for ions recombination and production [4], RF power and gas pressure are main input parameters for simulation. This simulation produces surface and 1-D -plots for plasma parameters, viz. plasma potential, temperature, resistance, density etc. in the plasma chamber as well as the field distribution due to RF antenna. Initial simulation results show an enhancement of up to 100 % in the plasma density with the ferrite cover in RF heating using RF peak current of 100 A. This paper will present detailed results with and without the ferrite cover around the 2 MHz RF Antenna.

References:

[1] DharmrajV. Ghodke, R. K. Khare, Rajnish Kumar, Manish Pathak, S. K. Jain, Ajith Amban, K. Murali Krishnan, Kuldeep Kumar Singh, Purushottam Shrivastava and Vijendra Prasad "Development of External RF Antenna based Cusp Free High Duty Factor Pulsed Negative Hydrogen Ion Source," *AIP Conference Proceedings* **2373**, 030002 (2021).

[2] Rajnish Kumar, Manish Pathak, D. V. Ghodke, V. K. Senecha "Modelling and Simulation of 13.56 MHz, RF-Ignition System for RF Based Negative Hydrogen Ion Source" **PLASMA2017**, 07-10 Nov. 2017 Institute for Plasma Research (IPR), Gandhinagar, Gujrat, India.

[3] http://www.comsol.co.in

[4] www.lxcat.laplace.univtlse.fr/cross_sec_download.php

BPT-P-11

ROLE OF QUANTUM PLASMA IN SOCIETY AND ITS APPLICATION

Manisha Raghuvanshi[1], Sanjay Dixit[2]
Department of physics, Govt. M.V.M College Shivaji Nagar,
Barkatullah University, Bhopal, (M.P) India
*Email: * manishaphd85@gmail.com; ** sanjay_007dixit@rocketmail.com*

The plasma physics has mainly gave all attention on systems represented by high temperature and low densities, for which quantummechanical effects have almost no force of meeting importantly has an effect on its macroscopic properties . quantumplasma can be made up of electrons, positrons, ions, and charged nano particles particle is a new coming-to-be-important and rapidly growing subfield of plasma physics . The high relation between mass and size, low-temperaturequantum Fermi plasma is importantly different from the low-density, high-heat Greek and Latin plasma doing as ordered Maxwell-Boltzmann distribution.

Keywords: quantum plasma,electrons, positrons, ions, Maxwell-Boltzmann distribution, low temperature.

BPT-P-12

EFFECT OF OBSTACLE AND GEOMETRIC ASPECT RATIO ON LANE DYNAMICS IN PAIR ION PLASMAS

[1]Vishal K. Prajapati[*], [1]Swati Baruah and [2]R. Ganesh
[1]The Assam Kaziranga University, Jorhat-785006, Assam, India
[2] Institute for Plasma Research, Bhat, Gandhinagar-382428, Gujarat, India
E-mail :[*]vishalprjapati2335474@gmail.com

When driven out of equilibrium, many physical systems may spontaneously exhibit various different kinds of pattern formation which are much richer than traditional phase transitions in equilibrium systems and may be extremely challenging to predict, as such is a very interesting field of research.

Lane formation [1,2] is an important representative of non-equilibrium phase transition. We focus on a 2-D Pair ion (PI) plasma system and explore the lane formation dynamics using Langevin Dynamics (LD) simulation [1], specifically, both in presence and absence of the external magnetic field the influence of the obstacle and geometric aspect ratio is studied [3]. Lanes are found to form when like particles move along or opposite to the applied field direction. Lane order parameter, cumulative order parameter and the distribution of the order parameter have been evaluated to detect phase transition. Here, specular reflective boundary condition is implemented to mimic an obstacle. We demonstrate that obstacle promotes the merging of lanes for small aspect ratio values and the system transits into a partially mixed state for higher aspect ratio values. Furthermore, an appearance of void is observed on either side of the obstacle. The study in presence of the external magnetic field promotes acceleration of the phase transition process towards lane mixing phase, it also reveals the existence of the electric field drift in the system. This work provides a fundamental understandingof non-equilibrium lane formation phenomena in the naturally occurring PI plasma [1] systems and have important implications in technology, for example, from determining the uniformity of plasma surface treatments [4], particle separation in microfluidic devices [5] and many more. In this work, the details of the above study will be presented.

References:

[1] U. Sarma, Swati Baruah and R. Ganesh. Phys. Plasmas **27**, 012106 (2020).
[2] Swati Baruah, U. Sarma and R. Ganesh, J. Plasma Phys. **87**, 905870202 (2021).
[3] Swati Baruah, Vishal K. Prajapati, R. Ganesh, J. Plasma Phys. (2021) (Accepted).
[4] J. P. Trelles, J. Phys. D: Appl. Phys. **49**, 393002 (2016).
[5] G. H. Gelinck, H. E. A. Huitema, E. Van Veenendaal*et al.* Nat Matter **3**, 106 (2004).

BPT-P-13

SECOND HARMONIC GENERATION BY A COSH-GAUSSIAN LASER BEAM DRIVEN ELECTRON PLASMA WAVE: HIGHER-ORDER PARAXIAL THEORY

Gunjan Purohit[a], Pradeep Kothiyal[b] and Ramesh Kumar Sharma[a]
[a]*Department of Physics, DAV Post Graduate College, Dehradun, Uttarakhand-248001, India*
[b]*Department of Mathematics, DAV Post Graduate College, Dehradun, Uttarakhand-248001, India*
E-mail :gunjan75@gmail.com

This work presents the study of second harmonic generation (SHG) in a collisionless plasma by an intense self-focused cosh-Gaussian laser beam. The second harmonics of

a cosh-Gaussian laser beam is generated by the excitation of an electron plasma wave at the pump frequency. The excited electron plasma wave is coupled with the pump laser beam and produce radiation of double frequency. This work has been done under a higher-order paraxial ray approximation in the presence of a combined effect of relativistic and ponderomotive non-linearity. Nonlinear differential equations have been established for the self-focusing of the cosh-Gaussian laser beam in the plasma, the generation of electron plasma wave at the pump frequency, and the second harmonic generation. Numerical simulations have been carried out to investigate the effects of laser and plasma parameters such as incident laser intensity (a), decentred parameter(b) and relative plasma density (ω_{p0}/ω_0) on the self-focusing of the laser beam and the electric field associated with electron plasma wave and second harmonic wave. Numerical analysis shows that these parameters play an important role in the process of second harmonic generation in laser plasma interactions. The results show that the focusing of cosh-Gaussian laser beam, electric field of electron plasma wave and second harmonic wave increases with increasing the values of (a), (b) and (ω_{p0}/ω_0). The results are also compared with paraxial-ray approximation.It is observed that the focusing of the laser beam, electric field associated with electron plasma wave and second harmonic wave become enhance in the higher-order paraxial region.

BPT-P-14

EXISTENCE AND STABILITY OF ALTERNATIVE DUST ION ACOUSTIC SOLITARY WAVES IN ADUSTY PLASMA CONSISTING OF NONTHERMAL ELECTRONS HAVING VORTEX-LIKE VELOCITY DISTRIBUTION

Sankirtan Sardar[1], Anup Bandyopadhyay[2], K.P Das[3]

[1]*Guru Ghasidas Vishwavidyalaya, Bilaspur, (C.G), 495009,*

[2] *Department of Mathematics, Jadavpur University, Kolkata 700032, India,*

[3]*Department of Applied Mathematics, University of Calcutta, 92 Acharya Prafulla Chandra Road, Kolkata 700009, India*

E-mail : sankirtansardar@gmail.com

The recent work of Sardar et al. [1] on the existence and stability of the small amplitude dust ion acoustic solitary waves in a collisionless unmagnetized plasma consisting of warm adiabatic ions, static negatively charged dust grains, isothermal positrons, and nonthermal electrons due to Cairns et al. [2] has been extended by considering nonthermal electrons having a vortex-like velocity distribution due to Schamel [3,4] instead of taking nonthermal electrons. This distribution takes care of both free and trapped electrons. A Schamel's modified KadomtsevPetviashvili (SKP) equation describes the nonlinear behaviour of dust ion acoustic waves in this plasma system. The nonlinear behaviour of the dust ion acoustic wave is described by the same

KadomtsevPetviashvili (KP) equation of Sardar et al. [1] when B = 0, where B is the coefficient of nonlinear term of the SKP equation. A combined SKP-KP equation more efficiently describes the nonlinear behaviour of dust ion acoustic waves when B → 0. The solitary wave solution of the SKP equation and the alternative solitary wave solution of the combined SKP-KP equation having profile different from both sech^4 and sech^2 are stable at the lowest order of the wave number. It is found that this alternative solitary wave solution of the combined SKP-KP equation and its lowest order stability analysis are exactly the same as those of the solitary wave solution of the KP equation when B→0.

References:

[1] S. Sardar, A. Bandyopadhyay, and K. P. Das, Phys. Plasmas 23, 073703 (2016).
[2] R. A. Cairns, A. A. Mamum, R. Bingham, R. Boström, R. O. Dendy, C.M. C. Nairn, and P. K. Shukla, Geophys. Res. Lett. 22, 2709, (1995).
[3] H. Schamel, Plasma Phys. 13, 491 (1971).
[4] H. Schamel, Plasma Phys. 14, 905 (1972)

BPT-P-15

THZ SURFACE PLASMON PROPAGATION ON AN ULTRATHIN SEMICONDUCTOR LAYER DEPOSITED OVER GLASS SLAB

Roopkiranpreet Kaur[1] and Sukhdeep Kaur[2]
[1]S. L. Bawa DAV College, Batala, Gurdaspur, Punjab, India-143505
[2]Guru Nanak Dev University, Amritsar, Punjab, India-143005
E-mail : sukhdeep.iitd@gmail.com

We have analytically demonstrated a structure supporting the excitation of terahertz surface plasmon wave. Special properties of semiconductor leads them to support terahertz surface plasmon wave.. An ultrathin semiconducting film (InSb) is deposited on a dielectric slab made up of Glass. The dispersion relation for the structure consisting of a glass slab and a semiconductor is calculated assuming the Drude model for permittivity of semiconductor. The pot shows linear variation of frequency with wave vector at low frequency but as the frequency increases there is a gradual variation of frequency and wave vector leads to terahertz surface plasmon wave generation. This type of structure can be use full in THz spectroscopy, sensing and other potential applications.

BPT-P-16

OBSERVATION OF E x B ELECTRON DRIFT INSTABILITY IN HALL THRUSTERSIMULATION

Sneha Gupta1, Debraj Mandal2, Devendra Sharma1
1Institute for Plasma Research, Gandhinagar – 382428, India
1Université de Lorraine, Institut Jean Lamour, Nancy - 54011, France
E-mail: sneha.gupta@ipr.res.in

Hall thrusters are electrostatic ion accelerators which have application in satellite propulsion. Theyemploy a combination of an externally applied crossed electric and magnetic field in order togenerate and accelerate ions. In this configuration, E x B drift instability is frequently observed in allthe Hall thruster experiments as well as simulations. This instability has a dominant role in thegeneration of cross-field particle transport also known as anomalous transport.In the present study, we intend to characterize the E x B drift instability in the Hall-Thrusterconfiguration and also analyse their effect on the cross-field particle transport. For this, a 2D Particle-In-Cell simulations (PIC) are performed by means of an open source code XOOPIC to get an insightinto the physics of anomalous cross-field transport in Hall thruster devices. E x B drift instability isgenerated for a fully ionized Xenon plasma in the presence of an externally applied axial electricand radial magnetic field configuration akin to real Hall thrusters. Depending on the strength ofelectron current taken, different unstable modes of the E x B electron drift waves are generated andeventually saturated by the ion trapping. These modes seem to follow a linear dispersion relation of amodified ion acoustic instability. Finally, in the presence of different modes of the E x B drift waves,the cross-field electron transport also changes significantly.

BPT-P-17

BEAM–PLASMA INSTABILITY IN SPIN POLARIZED HIGH DENSITY DEGENERATE PLASMA

Punit Kumar and Shiv Singh
Department of Physics, University of Lucknow, Lucknow - 226007
E-mail: drpunitlko@gmail.com

In plasmas, where the de-Broglie wavelength of the charge carriers is comparable to the dimension of the plasma system, quantum mechanical effects are expected to play a major role in thebehavior of charged plasma particles. In recent years, quantum effects have proved to play a crucialrole in ultrasmall electronic devices, laser plasmas and dense astrophysical plasmas. The one and twostream instabilities in quantum plasma have been studied by various authors but all the previousstudies considered electrons as

a single fluid of macroscopically averaged spin-1/2 plasma. Theearlier papers did not show a full picture and didn't took spin-up and spin-down interaction force intoaccount. Very recently, a modified separate spin evolution (SSE) treatment of electrons inaccordance with Pauli equation has been developed.

In the present paper, using the modified SSE-QHD model the two-stream instability for a circularly polarized electromagnetic wave propagating through a high-density magnetized quantumplasma has been presented. Spin-up and spin-down electrons have been taken to be separate speciesof particles and spin-spin interaction picture has been developed. The effects of quantum Bohmpotential, electron Fermi pressure and spin have also been taken into account. The dielectric constanttensor using which the dispersion relation of two-stream as well as the beam-plasma instability hasbeen obtained. The results indicate that quantum effects and thermal effects play important rolesalongwith the spin polarization produced by the spin interaction of spin-up and down species of theelectron. The critical wave number for beam-plasma instability in magnetized quantum plasmas hasalso been described in the paper and effect of spin polarization has been analyzed.

BPT-P-18

NONLINEAR MIXING IN A DUSTY PLASMA GOVERNED BY A PERIODICALLY DRIVEN KORTEWEG-DE VRIES MODEL

Ajaz Mir[1], Sanat Tiwari[1], and Abhijit Sen[2]

[1]*Indian Institute of Technology Jammu, Jammu, India, 181221*

[2]*Institute for Plasma Research, Gandhinagar, India, 382428*

E.mail: 2018rph0028@iitjammu.ac.in

Nonlinear mixing (NLM) of waves generates the cascade of frequency by coherent nonlinear interaction between the two or more system modes. The NLM is found in physical systems that can sustain large amplitude waves [1]. Typically in optical mediums, three and four-wave mixing are observed due to the second-order and third-order nonlinearity in their susceptibility, respectively. In this paper, we demonstrate the nonlinear mixing phenomena in dusty plasmas that have fluid-like spatial-temporal nonlinearity. We have used the Korteweg-de Vries (KdV) model representing the weakly nonlinear regime of dusty plasma dynamics [2] along with periodic forcing. The nonlinear mixing phenomenon has been explained using a semi-analytic solution of the forced-KdV (fKdV) model driven with a time-dependent forcing. While for the travelling wave forcing form, the fKdV has been solved numerically. The coherent nature of modes is predominantly due to the three-wave mixing mechanism as confirmed via bispectralanalysis [3]. The theoretical model of wave mixing also shows promising similarities with mixing results obtained in earlier conducted dusty plasma laboratory experiments [4].

References:

[1] Antonio Picozzi and Marc Haelterman: Parametric Three-Wave Soliton Generated from Incoherent Light

[2] Bin Liu, J. Goree, and T. M. Flanagan, Abhijit Sen, Sanat Kumar Tiwari, Gurudas Ganguli and Chris Crabtree: Experimental observation of cnoidal waveform of nonlinear dust acoustic waves

[3] V. Nosenko, J. Goree, and F. Skiff: Bispectral analysis of nonlinear compressional waves in a two-dimensional dusty plasma crystal

[4] V. Nosenko, K. Avinash, J. Goree, and B. Liu: Nonlinear Interaction of Compressional Waves in a 2D Dusty Plasma Crystal

BPT-P-19

NUMERICAL STUDY OF MAGNETIZED DUSTY PLASMA SHEATH WITH TWO ION SPECIES AND OBLIQUE MAGNETIC FIELD

A.K. Shaw[1] and A. K. Sanyasi

Institute for Plasma Research, Bhat, Gandhinagar-382 428, Gujarat, India

E-mail: akshayak@ipr.res.in

The dynamics of low temperature magnetized multi-component dusty plasma sheath structure is explored with finite ion temperature in the presence of an oblique magnetic field. Using three-fluid hydrodynamic model [1], dimensionless equations are obtained and solved numerically using RK4 numerical method. Impacts of magnetic field strength, dust and plasma number densities, velocities, and the electron temperature on the sheath structure are investigated. In presence of a magnetic field and charged dust grains, the ion bunching at the sheath edge is observed and a qualitative explanation to the phenomenon is presented. It is also observed that the dynamics of sheath potential substantially change in presence of charged dust species. In addition, we investigated the influence of applied magnetic field strength at different incidence angles on the plasma parameters inside the sheath.

The output of our work has technological importance for many applications of low-temperature plasma where dust particles are omnipresent. For example, plasma surface modification of the polymers, fusion applications, and many more.

References:

[1] G. Foroutan, Phys. Plasmas **17**, 123711 (2010).

BPT-P-20

CHARGING KINETICS OF SPUTTERED PARTICLES IN PSEUDOSPARK DISCHARGE PLASMA

Shikha Misra[1], Akhilesh Mishra[1], Ram Prakash Lamba[1] and Udit Narayan Pal[1]
Vacuum Electron Devices Development Group, CSIR- Central Electronics Engineering Research Institute Pilani, Rajasthan-333031
Email: shikhamish@gmail.com

A charging kinetic model has been developed to analyse the characteristics of sputtered metal particles in pseudospark (PS) discharge plasma at low pressure. The sputtered metal particles probably arise because of the heating of the cathode surface due ion bombardment and distributed into the discharge plasma [1-5], which is responsible for the stability and confinement of the generated plasma in PS discharge configuration. The present investigation has been carried out for the charging, heating and evaporation phenomenon on the surface of the sputtered particles under the influence of high energetic electron beam and background electron-ion plasma. This theoretical and analytical model has explained the time scale of critical temperature (time of sublimation) and evaporation time of the sputtered particles on the basis of charging phenomenon. The obtained evaporation time of the sputtered particles are around 10 nano second (*ns*) to 10 micro second (μs), which is in correlation with the time of experimentally observed metal vapor density in various literatures [6-7]. It is also observed that bigger particles have taken longer time for evaporation than smaller one. The obtained value of critical temperature is 1500K, which also comes in the range of experimentally observed temperature of metal vapor density [7]. The obtained results have motivated for further investigations for better understanding of the formation of discharge plasma with metal vapor in pseudo spark discharge configurations, which are difficult to analyse experimentally.

References:

[1] Y D Korolev and N NKoval J. Phys. D: Appl. Phys. **51** 323001 (2018).
[2] Simone Anders and Andre Anders, IEEE Transactions on plasma science**19** 1 (1991).
[3] Werner Hartmann and Gunter Lins IEEE transactions on Plasma Science **21** 506 (1993).
[4] A Anders, S Anders, B J Uttner, and H Pursch, W Bijtticher and H Luck, Journal of Applied Physics **71** 4763 (1992).
[5] A J Lichtenberg and M A Lieberman Journal of Applied Physics **87** 7191 (2000).
[6] P. Felsner, J. Christiansen, K. Frank and M. Stetter IEEE transactions on Plasma Science **23** 305 (1995).
[7] Gunter Lins and Werner Hartmann, IEEE transactions on Plasma Science **21** 511 (1993).

BPT-P-21

QUASI-LONGITUDINAL PROPAGATION OF NONLINEAR ELECTROMAGNETIC EXCITATIONS IN MAGNETIZED PLASMA

Gayatri Barsagade[*,1,2], Devendra Sharma[1,2]
[1] *Institute for Plasma Research, Bhat, Gandhinagar – 382 428, India*
[2] *Homi Bhabha National Institute, Mumbai - 400 085, India*
E-mail[*]: gayatri.barsagade@ipr.res.in

Excitation of electromagnetic fluctuations in magnetized plasma in laboratory experiments, e.g., the Large Volume Plasma Device (LVPD), with a dominant low-frequency component ($\omega ci<\omega<\omega ce$) is recently observed to be accompanied with several characteristic features, including their dependence on beam electron energy and strongly oblique propagation [1]. The present study investigates the strong quasi-longitudinal character of these excitations in the parameter range nearly of the laboratory experiments [1]. The findings include that the waves propagating at sufficiently oblique angles exclusively undergo a nonlinear steepening while their propagation remains regular at smaller angles irrespective of the amplitude and the time of evolution of the initial perturbation. It is additionally concluded that for such excitations, the longitudinal electrostatic waves and obliquely propagating electromagnetic components are not independent of each other due to the presence of a large longitudinal electric field parallel to the ambient magnetic field B_0. These inferences are relevant to resolving the energy dissipation issue of the observed chorus in experiments and the associated spectral scaling of the electromagnetic wave turbulence in weakly magnetized space and laboratory plasma.

References:

[1] Observation of reflected electrons driven quasi- longitudinal (QL) whistlers in large laboratory plasma, Physics of Plasma **24**, 102118 (2017).

BPT-P-22

WAVELET ANALYSIS OF FLOATING POTENTIAL OSCILLATIONS OF ANODIC DOUBLE LAYERS PRODUCED IN DC GLOW DISCHARGE PLASMA

ThangjamRishikanta Singh and Suraj Kumar Sinha
Department of Physics, Pondicherry University, Pondicherry-605014
E-mail: *th.rishikanta@gmail.com*

Wavelet transform is a powerful mathematical tool that decomposes and cuts the data into various coefficients giving a time-scale representation of the signal. It is, indeed useful for analyzing of non-stationary signals because it could capture transient events and provide spectral features over time and frequency. In the present work, we investigate the formation of anodic Double Layers (DLs) in DC glow discharge plasma from two separate voltage power supplies under different conditions like change in voltage, pressure etc. The power supply V1 is used to initiate the discharge and produced plasmas, which is then is maintained stable throughout the chamber by keeping at constant voltage = 750V. The other power supply V2 (used in range of 0-200V) is used to create the DLs when the current is passed through plasmas. The floating potential oscillations corresponding to various changes in voltage V2 are observed and recorded in a digital oscilloscope. While observing and analyzing the oscillations, it is found that the system undergoes periodic nature to chaotic nature i,e, turbulent flows in plasma . The current research will be highly useful in understanding the basic mechanism of oscillations, studying space plasma physics and its near environment like auroral dynamics and the complex non-linear entity of plasma.

References:

[1] Lars. P. Block, Astrophysics and space science 55, 59-83, 1978.
[2] C Charles, Plasma Sources Sci. Technol. 16 (2007) R1–R25
[3] Prince Alex, Saravanan Arumugham and Suraj Kumar Sinha, “Triggering of Buneman Instability and Existence of Multiple Double Layers in Laboratory plasma”, Physics Letters A 381 (2017) 3652-3658
[4] Prince Alex, Benjamin Andres Carreras, Saravanan Arumugham and Suraj Kumar Sinha, “Self-Organized criticality: An interplay between stable and turbulent regimes of multiple anodic double layers in glow discharge plasma” Physics of Plasmas 25, 053514 (2018)
[5] P. Alex, S. Arumugam, K. Jayaprakash, K.S. Suraj, “Order–chaos–order–chaos transition and evolution of multiple anodic double layers in glow discharge plasma”, Results in Physics 5, 235–240(2015).
[6] Christopher Torrence and Gilbert P. Compo, “A Practical Guide to Wavelet Analysis”, 1998 American Meteorological Society
[7] Paul Addison,” The Illustrated Wavelet transform Handbook”.

BPT-P-23

HYDRODYNAMIC MATRIX AND DENSITY AUTOCORRELATION FUNCTION FOR STRONGLY COUPLED CHARGED FLUIDS IN GENERALIZED HYDRODYNAMIC FRAMEWORK

Ankit Dhaka[1,2], PV Subhash[2,3], Pintu Bandyopadhyay [1,2]
[1]*Institute for Plasma Research, Bhat, Gandhinagar, Gujarat 382428, India*
[2]*Homi Bhabha National Institute, Anushaktinagar, Mumbai 400094, India*
[3]*ITER-India, Institute for Plasma Research, Gandhinagar, Gujarat 382428, India*
E-mail: ankit.dhaka@ipr.res.in

A hydrodynamic matrix for a fluid is derived from fluid momentum equation supplemented with energy and continuity equations [1]. It relates the variations of microscopic density, current and temperature with their respective initial values in terms of various transport coefficients such as thermal diffusivity, viscosity and acoustic speeds. Thus, an autocorrelation function can be obtained analytically from the hydrodynamic matrix in terms of these transport coefficients providing a framework to use in molecular dynamics (MD) simulations. In this framework, the particle trajectories obtained from MD simulations are used to generate density autocorrelation function (DAF) and best fitted through transport coefficients using nonlinear least square routines. The transport coefficients obtained from this method across the coupling regimes are compared with existing models and results. It has been observed, counter-intuitively, that even when the analytic treatment involved in obtaining DAF assumes a simple fluid description i.e. uncharged fluid with no memory effects, yet the model seems to be working for strongly correlated charged systems such as dusty plasma with coulomb coupling parameter $\Gamma > 1$. To address this, we discuss a new approach to treat this problem using the Generalized Hydrodynamic model [3]. A method to obtain the hydrodynamic matrix for coupled charged liquids will be discussed and an attempt to address the application of this model on MD simulations of Dusty Plasma will be presented.

References:

[1] J. P. Hansen and I. R. MaDonald, Theory of Simple Liquids, Elsevier , 2013.

[2] H. Kahlert, "Thermodynamics and transport coefficient from the dynamic structure factor of Yukawa Liquids," *Physical Review Research* , vol. 2, no. 3, 2020.

[3] P. K. Kaw and A. Sen, "Low Frequency modes in strongy coupled dusty plasmas," *Physics of Plasma* , pp. 3552-3559, 1998.

BPT-P-24

RATCHET DYNAMICS OF ACTIVE YUKAWA PARTICLES

Anshika Chugh[1,2], Rajaraman Ganesh[1,2], Soumen De Karmakar[1,2]
1 Institute for Plasma Research, Bhat, Gandhinagar-382428
2 Homi Bhabha National Institute, Anushakti Nagar, Mumbai-400085
E-mail: anshika.chugh@ipr.res.in

In non-equilibrium systems, transport in general is achieved with the help of gradients in the system. When system becomes small, fluctuations become dominant and transport becomes complex. In such noise dominated systems, asymmetric potential profile called Ratchet is used to have directed motion in the system. Ratchet systems[1] are an important class of study as it helps achieve control over the transport properties of the system. Protein motors is one such example which work in complex environments dominated by fluctuations and help achieve inter-cellular transport in a controlled manner. There is another class of particles called active particles whose motion is self-directed for example, the motion of bacteria.

Active Yukawa systems [2] or Complex plasmas with 'Janus' particles act as an interesting testing ground to perform such studies. In our study, we show that for a range of parameters transport can be achieved in passive Yukawa systems [3] having "zero-average forces" with the help of asymmetric potential profile called Ratchet. We show that how relative strength of particle-particle interaction with respect to particle-ratchet interaction can affect the dynamics of the system. We further investigate through active Yukawa particles whether activity assists or suppresses the directed motion in Ratchet systems. The study might prove useful for controlled drug delivery.

References:

[1] P. Reimann, Brownian motors: noisy transport far from equilibrium, Physics reports 361 (2-4) (2002) 57–265.

[2] S. De Karmakar and R. Ganesh, Phase transition and emergence of active temperature in an active Brownian system in underdamped background, Phys. Rev. E 101, 032121 (2020).

[3] A. Chugh and R. Ganesh, Emergence of directed motion in a 2D system of Yukawa particles on 1D Ratchet, Under Review (2021).

BPT-P-25

ROTATIONAL KELVIN-HELMHOLTZ INSTABILITY AND ANOMALOUS TRANSPORT IN A 2D STRONGLY COUPLED YUKAWA LIQUID

Suruj Kalita, Rajaraman Ganesh
Institute For Plasma Research, HBNI, Bhat, Gandhinagar, Gujarat, 382428
E-mail: suruj.kalita@ipr.res.in

Kelvin-Helmholtz (KH) instability is a well known example of instability in Hydrodynamics, whichmay be regarded as "supercritical" in nature, meaning, KH has a linear stability threshold, in contrast to plane Couette flows [1] which are known to be ``subcritical". Planar KH instability has been studied in 2D Yukawa liquids using "first principles" molecular dynamics simulation [2]. In the present work, we investigatethe KH instability in 2D Yukawa liquid and the ensuing anomalous transport in an annularrotating flow. A strongly correlated Yukawa liquid is thermalized between annular regionsin 2D using an inner and outer wall. A vortex strip when appropriately initialized, is shown to get destabilized linearly when perturbed with appropriate mode number. For certain ``wall conditions", it is shown that the transport in the angular direction can become super-diffusive. This and related details will be presented.

References:

[1] S Kalita, R Ganesh, Phys. Fluids 33, 095118 (2021).
[2] Ashwin et al, PRL 104, 215003 (2010).

BPT-P-26

ION-ACOUSTIC COMPRESSIVE AND RAREFACTIVE WAVES IN MAGNETOPLASMA WITH NEGATIVE IONS AND NONTHERMAL ELECTRONS

J. K. Chawla
Govt. R. R. College Alwar, Rajasthan, India-301001
Email: jitendra123chawla@yahoo.co.in

Study of ion–acoustic double layers in magnetized plasma with positive and negative ions and nonthermal electrons. The modified Korteweg-de Vries (m-KdV) equation is derived using reductive perturbation method (RPM). The effect of nonthermal electrons, magnetization, obliqueness angle (where obliqueness angle is the angle between wave vector and magnetic field) and negative ions on ion-acoustic compressive and rearafactive double layers are discussed in details. For a given set of parameter values, increases in the magnetization (the obliqueness angle), increases (decreases) the width of the compressive and rarefactive double layer, however the amplitude of the double layers have no effect.The amplitude and width of (Ar^+, F^-), (H^+, H^-) and (H^+, O_2^-) plasmas are discussed in details.

BPT-P-27

TEMPERATURE GUIDED CONFINING EFFECTS OF REALISTIC WALLS ON HELIUM GAS DYNAMICS AT LOW TEMPERATURES: UNRAVELING MOLECULAR MYSTERIES OF CRYOPLASMAS

Swati Swagatika Mishra, Sudeep Bhattacharjee
Indian Institute of Technology, Kanpur, Uttar Pradesh, 208016
E-mail: swatis@iitk.ac.in

Helium houses many peculiar phenomena owing to its light mass and small size that cause the onset of quantum behaviour even at a higher temperature (T) (~ 100 K) and atmospheric pressure. Therefore, in these temperatures, helium shows varying transport and structural phenomena with decreasing temperatures. Such behavioural changes of

helium get reflected in the cryoplasma produced in it, in terms of drastic dynamic and energetic changes below T = 50 K [1]. Further, these microplasmas are generated in dielectric barrier discharge electrodes (DBD), and the whole system is enclosed suitably in a metallic vessel. These confinements further complicate the system by restricting the molecular motion in the direction of confinement. Thus, in this presentation, we aim to present the molecular dynamics study of (i) the gaseous helium system in the temperature range of 150 K to 30 K and atmospheric pressure, and (ii) the effect of confinement on neutral helium gas in the aforementioned state points. These exercises are expected to connect plasma physics with molecular, chemical, and low temperature physics.

The confining effect of ideal reflective walls on the dynamics of hard sphere gaseous systems (argon) has been studied in depth at room temperature [2]. In order to incorporate the long range forces of gaseous interactions and gas – wall interactions, we study a helium gas system first as a bulk gas, and then in the presence of two parallel metallic (Fe) walls, that confine the gaseous system along X direction. The gaseous interactions are modelled using Lennard-Jones potential, and wall particle - gas particle interactions are guided by Morse potential.

We observe a visible transition in the gas behaviour and its transport phenomena as the temperature decreases below 50 K in both the bulk and confined systems. For in depth assessment of the transition, we examine gaseous potential energy, velocity autocorrelation function (VACF), mean square displacement (MSD), and time windows of ballistic to diffusive transition for both systems. The directional analysis of VACF and MSD in confined system shows the sub-diffusive modes present in the molecular motion. The time window of diffusive to sub-diffusive transition shows strong temperature dependence. We find concluding evidence of increasing temperature from 30 K to 150 K, causing increased confinement effect.

References:

[1] Noma *et al.*, Journal of Applied Physics, **109**, p 053303-1-6, (2011).
[2] Ghosh *et al.*, Phys. Rev. E **98**, p 052115-1-13 (2018).

BPT-P-28

ELECTROMAGNETIC WAVE TRANSPARENCY INDUCED IN A STRONGLY MAGNETIZED PLASMA

Devshree Mandal*[1], Ayushi Vashistha[1] and Amita Das[2]
[1]*Institute for Plasma Research, HBNI, Bhat, Gandhinagar – 382428*
[2]*Indian Institute of Technology, Delhi,India*
**E.mail: devshree.mandal@ipr.res.in*

Plasma is a medium where its constituents behave collectively. When perturbation of any kind i.e. electrical or magnetic nature is introduced in the plasma, charge particles of plasma try to shield these external perturbations. During this endeavour, current and charge densities are formed in the plasma. These current fluctuations further become the source of various fundamental modes of plasma itself. Dynamics of plasma changes by introduction of an external magnetic field. In the presence of a constant magnetic field, fundamental modes of plasma are enriched and several of them are hybrid in nature i.e. dynamics of electrons and ions both are involved. In this work, we are going to show the effect of strong magnetic fields on the plasma dynamics. This strong magnetic field is such that it doesn't give any chances to plasma species to form any current and charge sources. Any electromagnetic wave can propagate freely through such plasma without going through any dispersion. In our Particle- In- Cell (PIC) simulation study, we choose X-mode geometry i.e. ($\mathbf{k}\perp\mathbf{B_0}\perp\mathbf{E_l}$ (Laser Electric field)) and by applying strong magnetic fields such that ω_{ce} (electron cyclotron frequency) $>\omega_{ci}$ (ion cyclotron frequency) $>\omega_l$ (incident laser frequency), we observe near total transmission of an electromagnetic wave through the plasma. Further, theoretical analysis has shown that in the cases where $\omega_{ce}>\omega_{ci}>\omega_l$ has been followed, the resonances and cut-off frequencies approach each other and effectively the stop band width diminishes. This study finds its relevance in various astrophysical systems where strong magnetic field sources are present and radiation is continuously passing through the plasma present in such an environment. New magneto-optical devices can be fabricated based on this study.

References:

[1] Mandal, D., Vashistha, A. & Das, A. Electromagnetic wave transparency of X mode in strongly magnetized plasma. *Sci Rep* **11,** 14885 (2021). https://doi.org/10.1038/s41598-021-94029-3.

BPT-P-29

ULTRA-LOW EMITTANCE ELECTRON-BUNCH GENERATION IN PLASMA WAKEFIELD ACCELERATION

Sandeep Kumar,
Department of Physics, Manav Rachna University, Faridabad, Haryana, India

Among the plasma Wakefield acceleration scheme, Trojan horse scheme is a hybrid plasma Wakefield acceleration. In this method, laser controlled electron's release is directed into an e-beam driven plasma Wakefield acceleration. That paves the way for controllable, shapeable electron bunches with ultra-low emittance and ultra-high brightness. In this work, the trojan horse method and the effect of frequency-chirp ionization laser is analysed on electron bunch acceleration properties via two-dimensional particle in cell simulations. It is found that the electron injection and trapping process can be significantly influenced by introducing frequency-chirp in

ionization laser. The scheme is an ideal candidate for photon such as free-electron-lasers and those based on Thomson scattering and betatron radiation alike.

BPT-P-30

ARBITRARY AMPLITUDE ION-ACOUSTIC SOLITARY WAVES IN NEGATIVE ION PLASMA WITH RELATIVISTIC DEGENERATE ELECTRONS

KishanKumar [a)] and M. K. Mishra [b)]
[a, b)] Department of Physics, University of Rajasthan, Jaipur -302004, India
Email: [a)] kishanjindal08@gmail.com, [b)] mishramukesh105@yahoo.com

A negative ion plasma comprising non-degenerate positive ions, negative ions, and relativistically degenerate electrons is considered to study the large-amplitude ion-acoustic solitary (IAS) waves. Sagdeev'pseudopotential technique has been used for the existence of arbitrary-amplitude IASs, and the Mach number domain $(M_1 \le M \le M_2)$ is determined numerically in terms of various plasma parameters. It is seen that the compressive and the rarefactive IAS can exist in such plasma systems. Furthermore, the effect of various plasma parameters such as negative to positive ions density (f), degenerate electron density (k), relativistic factor (γ), temperature ratio (σ), the mass ratio (μ) and the Mach number (M) on the characteristic of IAS waves are also discussed. Our result may be helpful to understand the essentialaspect of nonlinear solitary waves in an astrophysical and space plasma, where negative ions are present.

BPT-P-31

TUNABLE DIFFUSIVE PROPERTY OF COMPLEX PLASMA DRIVEN BY MAGNETIZED WAKE

Biswajit Dutta, Nilakshi Das
Tezpur University, Tezpur, Assam, 784028
E-mail: biswaduttajit1995@gmail.com

Diffusion of a three-dimensional dust ensemble embedded in a flowing plasma is investigated as a function of magnetic field (B) and normalized ion flow velocity (M) using Langevin dynamics simulation. Here, we have modelled our system considering a binary Yukawa inter-particle interaction together with particle-wake interaction. It is found that the asymmetric wake potential created due to streaming ions drive the dusty plasma from sub-diffusive to the super-diffusive regime. A novel wake dominant regime is identified that shows super-diffusive behaviour for suitable adjustment of the magnetic field. Both Cross field ($D_\perp$) and parallel ($D_\parallel$) diffusion coefficients are

sensitive to magnetic field, even when the field strength is weak. The nature of dependence of the perpendicular and parallel diffusion coefficients on B depends on several factors like state of the system, ion flow velocity and effective interaction potential. The dependence of cross-field diffusion coefficient on magnetic field exhibits three distinct behaviours characterized by (a) B^{2-3} for ultra-low magnetic field and strongly correlated state, (b) $B^{0.1}$ for moderate magnetic field, and (c) classical B^{-2} for a relatively large magnetic field. Our analysis shows that the magnetic field is mediated via the streaming ions in the regime (a) and (b) of relatively low magnetic field where the dependence of diffusion coefficient on the magnetic field is faster than the usual classical regime.

References:

[1] T. Ott and M. Bonitz, Phys. Rev. Lett. 107, 135003 (2011)

[2] B. Dutta, P. Bezbaruah and N. Das, Physics of Plasmas, 2021,28, 083703

[3] Y. Feng, J. Goree, B. Liu, T. Intrator, and M. Murillo, Phys. Rev. E 90, 013105 (2014).

BPT-P-32

SIMULATING PLASMA DYNAMICS IN A MAGNETIC NOZZLE

Subhasish Bag and Vikrant Saxena

Department of Physics, Indian Institute of Technology Delhi (IITD), Hauz Khas, New Delhi-110016

E-mail: subhasishbag95@gmail.com

For deep space missions, electric propulsionbased thrusters are far more efficient than their chemical counterparts due to their very high fuel efficiency and operational longevity [1,2]. Some of the electric propulsion devices are based on the concept of magnetic nozzle (MN), which has a similar role like the classic de-Laval nozzle used in chemical thrusters. In a magnetic nozzle, the convergent-divergent magnetic field lines guide the plasma expansion by converting the random thermal energy of electrons into the directed kinetic energy of ions producing a significant amount of thrust [3]. Using classical trajectory simulations, we model the collision-less plasma expansion in a paraxial magnetic nozzle which has nearly uniform axial magnetic field over the radial plasma beam cross-section [4].

References:

[1] C. Charles, J. Phys. D: Appl. Phys., 42:163001 (2009).

[2] E. Ahedo, Plasma Phys. Controlled Fusion, 53:124037 (2011).

[3] Ioana A. Biloiu et al., Appl. Phys. Lett. 92:191502 (2008).

[4] Zhou J, Sánchez-Arriaga G, Ahedo E, Plasma Sources Science and Technology. 2021 Apr 15;30(4):045009.

BPT-P-33

NONLINEAR ELECTRON-ACOUSTIC WAVES WITH SCHAMEL-KAPPA DISTRIBUTED HOT ELECTRONS

Gurmant Kaur, Praveen Bala
Punjab Agricultural University, Ludhiana, Punjab 141027
E-mail: gurmant-2052002@pau.edu

Excess energetic (superthermal) particles have been found in different types of plasma environments, including astrophysical plasmas like the ionosphere, auroral zones, and laboratory plasmas. Superthermal particles may arise due to the effect of external forces acting on the natural space environment plasmas or to wave particle interaction. Plasmas with an excess of superthermal non-Maxwellian electrons are generally characterized by a long tail in the high energy region. Vasyliunas introduce the distribution function (Kappa distribution) of these superthermal particles (Vasyliunas 1968). Trapping of electrons has also been observed in space plasma and laboratories, where some plasma particles are restricted and bounce back and forth in a limited area. The formation of phase space holes caused by electron trapping in the wave potential may prevent electrons from following the Maxwellian distribution. The phase speed of the electron acoustic wave is much larger than the thermal speeds of cold electrons and ions, but is usually smaller than the thermal speed of the hot electron component in case of isothermal electrons. In the present investigation, electron-acoustic waves (EAWs) have been investigated in the plasma containing hot and cold electrons. The hot electrons are expected to follow non-Maxwellian-trapped electron distribution modelled by a kappa distribution function combined with Schamel distribution. By using appropriate stretched coordinates and reductive perturbation theory the Schamel-KdV equation for small but finite amplitude EAWs has been derived. The influence of superthermal and non-isothermal parameters on the present plasma model is investigated. The presented investigation may be helpful to understand the study of nonlinear waves in the astrophysical plasmas.

Keywords: Electron-acoustic waves, Schamel-kappa distribution, SchamelKdV equation, Reductive perturbation theory.

References:

[1] Vasyliunas V M (1968) A survey of low-energy electrons in the evening sector of the magnetosphere with OGO 1 and OGO 3. J Geophys Res.73: 2839-84.

BPT-P-34

ROTATIONAL PROPERTIES OF ANNULUS DUSTY PLASMA IN A STRONG MAGNETIC FIELD

Mangilal Choudhary, Markus H Thoma Markus
Institute of Advanced Research Gandhinagar
E-mail: jaiijichoudhary@gmail.com

The collective dynamics of an annulus dusty plasma formed between a co-centric conducting (non-conducting) disk and ring configuration is studied in a strongly magnetized radio-frequency (rf) discharge. A superconducting electromagnet is used to introduce a homogeneous magnetic field to the dusty plasma medium. In absence of the magnetic field, the dust grains exhibit thermal motion around their equilibrium position. The dust grains start to rotate in an anticlockwise direction with increasing magnetic field (B > 0.02 T), and the constant value of the angular frequency at various strengths of the magnetic field confirms the rigid body rotation. The angular frequency of dust grains linearly increases up to a threshold magnetic field (B > 0.6 T) and after that its value remains nearly constant in a certain range of magnetic field. Further increase in magnetic field (B > 1 T) lowers the angular frequency. Low value of the angular frequency is expected by reducing the width of the annulus dusty plasma or the input power. The azimuthal ion drag force due to the magnetic field is assumed to be the energy source which drives the rotational motion. The resultant radial electric field in the presence of a magnetic field determines the direction of rotation. The variation of floating (plasma) potential across the annular region at a given magnetic field explains the rotational properties of the annulus dusty plasma in the presence of a magnetic field.

BPT-P-35

A HEURISTIC STUDY OF NONLINEAR WAVE-PARTICLE INTERACTION IN AN UNMAGNETISED PLASMA

Priyangana Chatterjee, Arghya Mukherjee
Jadavpur University, Kolkata, W.B., India-700032
E-mail: priyanganachatterjee.diya@gmail.com

The study of nonlinear wave-particle interactions in plasma is a fascinating field of research in non-linear plasma physics. Here, we study the nonlinear dynamics of electrons, initially following a Maxwellian velocity distribution, in the presence of a nonlinear plasma wave travelling along one dimension, using an in-house developed test-particle simulation code. At the outset, linear analytical theory has been verified from the simulation results. Studies have been further extended to the non-linear regime

and the changes in the electron dynamics have been noted for a wide range of initial input parameters. We envisage to extend our research to the relativistic regime also.

BPT-P-36

NONLINEAR EVOULTION AND PHASE MIXING OF LOWER HYBRID MODES IN COLD PLASMA

MithunKarmakar, Chandan Maity, Sourav Pramanik
Sardar Vallabhbhai National Institute of Technology, Surat, Gujarat 395007
E-mail: mithun.k@phy.svnit.ac.in

We report the phase mixing process of lower hybrid modes in cold electron-ion plasma immersed in a uniform magnetic field. The nonlinear evolution of this low frequency mode is studied in the frequency range of $\Omega_{ci} \ll \omega \ll \Omega_{ce}$. In this range it is justified to treat the ions as un-magnetized and considering the contribution of electron inertia in the x-component to be negligible. The quasi-neutral plasma approximation is also relaxed. The dispersion relation for such mode can be written as { ω2=ω2pi (1+ω2peΩ2ce)}**. Simple perturbation technique is used to analyze the spatio-temporal evolution of such mode. It is shown that an initially excited lower hybrid mode gradually loses its coherent nature as a result of phase mixing. Eventually the wave breaks at an arbitrarily low amplitude. An estimate of the phase mixing time is provided which is found to increase as we increase the strength of the applied magnetic field. The results are of relevance to the field of space science and laboratory experiment.
**

$$\omega^2 = \frac{\omega_{pi}^2}{\left(1+\frac{\omega_{pe}^2}{\Omega_{ce}^2}\right)}$$

BPT-P-37

EFFECT OF TWO-TEMPERATURE ELECTRONS ON ION-ACOUSTIC SOLITARY WAVES IN A MAGNETIZED PLASMA

Jintu Ozah
Dibrugarh university, Dibrugarh, Assam 786004
E-mail: jintuozah@gmail.com

The characteristics of three-dimensional nonlinear ion-acoustic solitary waves are investigated in a magnetized plasma in presence of trapped electrons (two-temperature nonisothermal electrons). To carry out this investigation, we have derived Zakharov-Kuznetsov (ZK) equation using reductive perturbation approach. We have solved this

equation using the hyperbolic tangent method (tanh method) and a solitary wave solution has been obtained. From this solution, influence of different factors such as nonisothermal parameters for cold and hot electrons on phase velocity, soliton amplitude and width of solitary waves have been investigated. Our study may be useful in analyzing astrophysical and space environments, such as the magnetosphere of Saturn etc.

BPT-P-38

EFFECTS OF NEUTRAL COLLISIONS AND RADIATIVE HEAT-LOSS FUNCTIONS ON THERMAL INSTABILITY OF TWO-COMPONENT PLASMA WITH HALL CURRENT AND FINITE ELECTRON INERTIA IN HI REGION

Sachin Kaothekar[1,A], S. Mishra[2,3], and S. Phadke[4]
[1]Department of Physics,Prashanti Institute of Technology & Science, Ujjain-456664, M.P., India.
[2]Department of Physics, DAVV, Indore, M.P., India.
[3]Department of Physics, SICA, Indore, M.P., India.
[4]Department of Physics, Govt. Girls College, Dhar, M.P., India.
[a] E-mail: sachinmgi007@gmail.com

The effects of neutral friction, finite electron inertia, Hall current and radiative heat-loss function on the thermal instability of viscous two-component plasma has been investigated incorporating the effects of finite electrical resistivity, permeability and thermal conductivity. A general dispersion relation is obtained using the normal mode analysis method with the help of relevant linearized perturbation equations of the problem and a tailored thermal condition of instability is obtained. We find that the thermal condition of instability is tailored due the presence of radiative heat-loss function, thermal conductivity, finite electron inertia and neutral particle. The Hall current parameter influences only the longitudinal mode of propagation and it has no consequence on the transverse mode of propagation. For the case of longitudinal propagation we find that the condition of thermal instability is independent of the finite electron inertia, Hall current, magnetic field strength, finite electrical resistivity, permeability and viscosity of two-components, but depends on the radiative heat-loss function, thermal conductivity and neutral particle. For transverse mode of propagation we find that the condition of thermal instability depends on the finite electron inertia, magnetic field strength, radiative heat-loss function, thermal conductivity, neutral particle and finite electrical resistivity, but sovereign of Hall current, permeability, and viscosity of two-components. From the curves we find that the temperature dependent heat-loss function, thermal conductivity and viscosity of two-components shows stabilizing effect, while density dependent heat-loss function, finite electron inertia and finite electrical resistivity shows destabilizing effect. The effect of neutral collision frequency is destabilizing in longitudinal mode, but in transverse mode it shows stabilizing effect. This study helps in understanding the process of star formation in HI regions.

CATEGORY: BASIC PLASMA EXPERIMENT (BPE)

BPE-P-1

MULTI-FILAMENTARY W-BASED PLASMA SOURCE FOR LARGE VOLUME PLASMA DEVICE - UPGRADE

A.K. Sanyasi[*1], P. K. Srivastava[1], Ayan Adhikari[1,2], Pinakin Leuva[1], Prosenjit Santra[1], Ritesh Sugandhi[1,2], L. M. Awasthi[1,2], Bharat Doshi[1] and M. K. Gupta[1]

[1]Institute for Plasma Research, Bhat, Gandhinagar – 382428, India

[2] Homi Bhabha National Institute, Mumbai - 400085, India

E-mail[*]: amulya@ipr.res.in

A circular ($\phi \sim 1.8m$),large area, tungsten (W) - basedmulti-filamentary plasma source is designed, fabricated and installed successfully in Large Volume Plasma Device - Upgrade (LVPD-U) to facilitate production of cylindrically uniform, quiescent plasma ($\frac{\delta n_e}{n_e} \leq 0.5\,\%$) for carrying out various studies on plasma waves and instabilities e.g. whistlers, pressure driven instabilities etc. The plasma source consists of *162* number of hairpin shaped tungsten filaments (L~ $0.18m$ and ϕ~$5 \times 10^{-4}m$) respectively. The filaments are mounted on a pair of Molybdenum feed through (ϕ~ $0.008m$, Length~$0.15m$) facilitated with a chuck-nut fixing arrangement. The Mofeedthrough's are accommodated on *2* sets of *08* number of water-cooled specially designed ETP copper cassettes and are powered by a DC power supply ($10kA, 20V$). The water cooled air – vacuum power feeding system is designed in-house with *3D* shape. The plasma is produced by electron impact ionization of neutral Argon gas by applying a discharge voltage of *70V* between cathode and anode using a discharge power supply of rating ($1kA, 150V$) for a pulse duration of $t_{pulse} \sim 50\,ms$.

The conceived plasma source has enhanced emission area~ $4.58 \times 10^{-2}m^2$ targeting $\sim 10^{18}m^{-3}$ plasma density for high magnetic field plasma operations ($\leq 150G$) in LVPD-U. The source is versatile in the domains of choice of filament diameter, filament arrangement configuration and low to high power operations (10 – 180 kW). The plasma source is being characterized for different parametric operational regimes and the paper will discuss primarily, design features of the plasma source, its mechanical assembly, salient features of its operation and some basic plasma characteristics.

References:

[1] S. K. Mattoo et al Rev. Sci. instrum**72**, 3864 (2001).
[2] L. M. Awasthi et al 2003 Plasma Sources Sci. Technol. **12** 158.
[3] A. K. Sanyasi et al Phys. Plasmas **24**, 102118 (2017).
[4] A. K. Sanyasi et al 2021 Plasma Phys. Control. Fusion **63** 085008.
[5] Prabhakar Srivastav et al 2019 Plasma Phys. Control. Fusion **61** 055010.

BPE-P-2

ROLE OF WHISTLERS IN MITIGATION OF ENERGETIC (RUNAWAY) ELECTRONS

A.K. Sanyasi[*1], L. M. Awasthi[1,2],P. K. Srivastava[1], Ritesh Sugandhi[1,2],and D. Sharma[1,2]
[1]*Institute for Plasma Research, Bhat, Gandhinagar – 382428, India*
[2] *Homi Bhabha National Institute, Mumbai - 400085, India*
E-mail[*]: amulya@ipr.res.in

Whistlers is considered as one of the most fundamental electromagnetic wave observed and widely studied in magnetospheric, spaceand astrophysical plasmas. The most common drivers for the whistler excitation in plasma are energetic electrons, beams, pressure gradients, temperature anisotropies, loss-cone, electron reflection from magnetic mirrors etc. However, in the recent past whistler waves have assumed significancein tokamak plasmas with their recent experimental observations in DIII-D [1, 2] and further for their role in scattering of runaway electrons. Runaway electron physics has great significance in fusion plasmas as they can cause instabilities and further induce damage to the first wall. But, measurement of high frequency ($\omega_{Wh} \approx$ *0.5* ω_{ce}) whistlers in tokamaks is a challenge as it would require high sampling (GHz) of data and exact measurement of parallel wave numbers ($k_{\|}$) may not be possible and hence the analysis outcome will be based on several assumptions. Here, linear laboratory plasma devices exciting whistler waves in presence of energetic (tail) electrons can play a significant role of building a bridge of physics understanding extrapolated to tokamaks. Theoretically it has been shown [3] that the upper hybrid modes are rather stable in JET and ITER but whistlers in lower hybrid range may not be the case.

To an analogy of tokamak physics, we have carried out whistler experiments in large volume plasma device (LVPD) [4] and in the limit of quasi-linear analysis it is found that whistler destabilization has weaker temperature dependence ($\gamma_i \alpha\, T_e^{-0.5}$) in comparison to tokamaks ($\gamma_i \alpha\, T_e^{-1.5}$) [5]. It is understood that the whistlers (oblique) can induce substantial pitch angle scattering and wave-particle resonance due to its highly dispersive nature. It can be understood as, higher the whistler activity more probability of energetic electron scattering and vice-versa.

In this paperresults of controlled experiments carried out in LVPD will be discussed and the growth parameter of whistler modes will be compared to analogous parallels in tokamak physics.

References:

[1] Sponge D A et al Phys. Rev. Lett. **120**, 155002 (2018).

[2] Heidbrink W et al Plasma Phys. Control. Fusion **61** 014007 (2019).

[3] Guo Z et al Phys. Plasmas. **25** 032504 (2017).

[4] Sanyasi A K et al 2021 Plasma Phys. Control. Fusion **63** 085008.

[5] Fulop T et al Phys. Plasmas. **13**, 062506 (2006).

BPE-P-3

CONTINUOUS TEMPERATURE MONITORING SYSTEM FOR LARGE VOLUME PLASMA DEVICE - UPGRADE

D. Khanduri[1,*], R. Sugandhi[1, 2], P. K. Srivastava[1], A. Balaji[3], U. Pallapothu[3], A.Adhikari[1, 2], A. K. Sanyasi[1], and L. M. Awasthi[1, 2]
[1]Institute for Plasma Research, Gandhinagar, Gujarat 382428, India
[2]Homi Bhabha National Institute, Mumbai 400094, India
[3]SRM Institute of Science and Technology, 603203, Chennai, India.
E-mail[*]: dristikhanduri@gmail.com

Experiments in Large Volume Plasma Device[1] - Upgrade (LVPD-U) is being carried out for understanding physical phenomenon having relevance to Magnetospheric and fusion plasmas. The system is large and plasma operation requires several subsystems to work and being monitored simultaneously e.g. vacuum pumps, power supply, water flow, feed-back and system temperature etc. Due to continuous operation of various subsystems of high heat load, it is highly essential to have continuous monitoring of temperature for the performance and protection of the various critical components such as, magnet coils (P ~180kW), multi-filamentary plasma source, multi-cusp cathode plate($P \leq 200$kW), filament power supply (P~200kW), device inner wall etc. In order to monitor the temperature of various systems and subsystems,a low cost solution using data logger (Masibus Data logger 8030) with, indigenous software is developed and subsequently the system has been integrated to LVPD Machine Control System (MCS)[2][3]. The data logger provides 96 channel counts and is configured using manual as well as computerized interface along with, multiple types of temperature transducers inputs. The Optomuxprotocol[4] based serial interface, is utilized for remote monitoring and data archival where manual mode provides on-field display of temperature. However, absence of Optomux protocol driver in LabVIEW and compliance for MCS integration have motivated us for the development of new driver and application software for local and remote monitoring. For remote monitoring, the existing web based software (in JavaScript/NodeJS/Angular)[5], is enhanced and reconfigured to incorporate temperature data. The novelty of the work lies in the development of in-house software for temperature monitoring solution which is an essential system requirement for many plasma experiments dealing with high power. This has been achieved by use of legacy communication protocol with local monitoring solution in LabVIEW and remote using latest web-application frameworks. This paper discusses the system requirements, hardware and software architecture, present monitoring status and future scope of the work.

References:

[1]. S. K. Mattoo, V. P. Anitha, L. M. Awasthi, G. Ravi, and LVPD Team, Rev. Sc. Instrum., 72, 3864 (2001).
[2]. R. Sugandhi, P. K. Srivastava, A. K. Sanyasi, PrabhakarSrivastav, L. M. Awasthi, and S. K. Mattoo, Fus. Engg. Des, 112, 804-813, 2017.
[3]. R. Sugandhi, P. K. Srivastava, Prabhakar. Srivastav et al, Proc. 27th IAEA Fusion Energy Conference, Gandhinagar, 22-27 Oct 2018.
[4]. Data logger 8030, User's Manual.
[5]. R. Sugandhi, V. Soumya, M. Jha et al, Rev. Sci. Instrum. 92, 075102 (2021).

BPE-P-4

DESIGN OF PROCESS AUTOMATION SYSTEM FOR LARGE VOLUME PLASMA DEVICE UPGRADE

R. Sugandhi[1, 2,*], P. K. Srivastava[1], A. K. Sanyasi[1], A.Adhikari[1, 2],D.Khanduri[1],and L. M. Awasthi[1, 2]
[1]*Institute for Plasma Research, Gandhinagar, Gujarat 382428, India*
[2]*Homi Bhabha National Institute, Mumbai 400094, India*
E-mail: ritesh@ipr.res.in*

The machine control system (MCS) for the Large Volume Plasma Device Upgrade (LVPD-U) is responsible for the safe, protected, controlled and automated operation of the device. The LVPD-U has advanced from LVPD[1] and during the transition, has aimed for five-fold increase in discharge time (~50ms) and an order enhancement in plasma density (~10^{12}/cc) by argumentation of new plasma source and power supplies. The LVPD-U is operated in pulsed mode for the duration of 50ms in single pulse and burst mode of operations (burst of 8) with repetition rate of 1 second. In order to operate the device in the higher parametric configurationsfor advanced plasma investigation, it is required to switch from conventional manual mode (in LVPD) to automated operation of its various subsystemforenhanced safety and efficiency of utilization. It has motivated fortransitiontoward design and development of the process automation system[2] componentof MCS from conceptual architecture(reported earlier[2]). The lesson learned and experience gainedduring technology demonstrations and proof of concepts development for computerized operation of high current filament power supply[3] (20V/10kA), probe positioning system[4] (travel length ~1m, #12 Nos.),and web driven logging and configuration[5]have been utilized for the design of single consolebased fully automated system. The new development will cover the start, shutdown and pulse sequence of operation based on 5-layered information system architecture. In this context, necessary process artefacts have been prepared and PLC driven architecture for start and shutdownsequence has been selected to ensure end to end integrated solution. The novelty of the work lies in the systematic approach and integration of legacy system with newer technologies. This architecture is generic and has capabilities of its application to other experimental plasma devices of similar nature. The paper discusses the motivation, requirements, process diagrams, design architecture,selected tools and technologies,and obtained results.

References:

[1]. S. K. Mattoo, V. P. Anitha, L. M. Awasthi, et. al., Rev. Sc. Instrum., 72, 3864 (2001).
[2]. R. Sugandhi,P. K. Srivastava, A. K. Sanyasi,et. al., Fus. Engg. Des, 112, 804-813, 2017.
[3]. R. Sugandhi,P. K. Srivastava, A. K. Sanyasi,et. al.,FusEngg Des, 115, 49-55, 2017.
[4]. A. K. Sanyasi, R. Sugandhi, P. K. Srivastava, et. al., Rev. Sci. Instrum. 89, 055113, 2018.
[5]. R. Sugandhi, V. Soumya, M. Jha, et. al., Rev. Sci. Instrum. 92,075102, 2021.

BPE-P-5

WEB EDITOR FOR CONFIGURATION MANAGEMENT OF LABORATORY PLASMA EXPERIMENTS

V.Soumya[1, *], R. Sugandhi[2, 3], M. Jha[2], D. Khanduri[2], Ayan Adhikari[2, 3], P.K. Srivastava[2], A. K. Sanyasi[2], L. M. Awasthi[2, 3] and S. D. Panchal[1]

[1]*Graduate School of Engineering and Technology, GTU, Ahmedabad, Gujarat 382424*

[2]*Institute for Plasma Research, Gandhinagar 382428*

[3]*Homi Bhabha National Institute, Mumbai-400085, India*

E-mail[*]: vsoumya2295@gmail.com

The plasma physics experimental facilities around the world are subjected to continuous evolution across physics objective and engineering systems. The physics objective brings the change in operational configuration data whereas argumentation of new system or revision of the existing systems brings configuration changes at micro and macro stages of configuration management. This motivates the design and development of a framework for computerized configuration parameters handling. Towards standardization of configuration management, IEEE [1] has issued guidelines to handle configuration data and pathways to mitigate the issues. This model is applied in large scale machines such as ITER [2], WEST tokamak,and Stellarator W7-X [3], where the number of plant system are in large numbers and has complex parametric dimensions. The pulsed plasma experiment (laboratory scale) needs a simple yet generalized configuration management model. A configuration management software is thus developed for laboratory plasma machine such as LVPD [4] using relational algebra and set theory and integrated with existing web-based recording system [5] over open source and latest web frameworks (JavaScript/NodeJs/Angular). The developed software facilitates the experimental system configuration at user level using abstraction of system, subsystems, parameters, operational static and dynamic parametric data, parametric types, system inter-connections and process descriptions. The model is trained using existing configuration data of LVPD machine. The paper discusses the requirements, literature survey of existing tools and techniques, developed web-based editor software description, obtained results and lessons learnt.

References:

[1] IEEE Standard for Configuration Management in Systems and Software Engineering, IEEE Std-828-2012, 1-71, 2012.

[2] S. Chiocchio, E. Martin, P. Barabhaschi et. al., System engineering and configuration management in ITER, Fus. Eng. Des., 82. 548-554.

[3] G. Kühner, P. Hiemann, S. Heinzel et. al, Editor for system configuration and experiment program specification, Fus. Eng. and Des. 71. 225-230, 2004.

[4] S. K. Mattoo, V. P. Anitha, L M Awasthi, et. al., Large Volume Plasma Device, Rev. Sci. Instrum., 72, 3864, 2001.

[5] R. Sugandhi, V. Soumya, M. Jha, et al, Development of electronic record-keeping software for remote participation in Large Volume Plasma Device upgrade using Angular 2 and NodeJS web technologies, Rev. Sci. Instrum., 92(7):075102, 2021.

BPE-P-6

BROADBAND UV AND TEMPERATURE SENSOR PROBE FOR PLASMA STERILIZATION APPLICATION

*Kushagra Nigam, G. Ravi and S.K. Nema
Institute for Plasma Research, Bhat, Gandhinagar-382428
**E-mail: kushagra.nigam@ipr.res.in*

A low cost probe has been developed that can carry out local measurements of UV and temperature simultaneously. Low cost GUVA-S12SD photo-diode based UV and LM35 IC based temperature sensors have been used to design and develop the probe. The design of the probe is such that the sensors are not exposed to the harsh plasma environment. The probe has been developed primarily for characterization of a low temperature pulsed DC plasma used for sterilization of medical equipment and devices, where local point-to-point measurements are imperative; however it can be used in other plasma systems as well. The UV sensor has been tested against standard test sources of 254 nm (UV-C) and 365 nm (UV-A) wavelengths. These sources have been separately characterized using StellerNet EPP2000Spectrometer.Initial experiments carried out using the probe indicate uniformity of UV radiation intensity inside the plasma sterilization test chamber. Further experiments have been carried out to understand variation of UV radiation and temperature with gas pressure and discharge voltage. Detailed design of GUVA-S12SD and LM35IC based probe, calibration test results and experiment results will be discussed in this poster.

BPE-P-7

OBSERVATION OF DUST IN PLASMA TO DUSTY PLASMA TRANSITION IN HOLLOW ANODE DISCHARGE

Nidhi Patel[1] and G.Prasad
Institute for Advanced Research, Koba, Gandhinagar,Gujarat- 382 426
E.mail: nidhipatel.phd@iar.ac.in

The dust particles get levitated in the sheath region of plasmas formed in the laboratory. The dust particles get charged negatively. The direction of electric field should be in the same direction of gravity. However, the force on the negatively charged dust particles will be in opposite direction to direction of gravitation al field. Large size (heavy) dust particles get levitated deep inside the sheath and lighter particles float at sheath edge. This mechanism has been adapted in most of the laboratory experiments reported elsewhere. We report the experimental observation of dust particles gets charged in the plasma ejects out without finding a suitable strong electric field (sheath) for levitation. After increasing the discharge current, above the threshold limit, dust levitation is observed. We report the transition of dusty in plasma regime to dusty plasma regime in a glow discharge.

Argon plasma was produced in a vacuum chamber which was pumped down by rotary pump. Hollow anode plasma source was used to produce the plasma. We have used Alumina dust particles with size 2 to 100 μm were used in the experiment. These particles were placed in an aluminum hollow cylindrical crucible vertically below the hollow anode source with depth of 2 – 3mm. Initial experiments were carried out by placing the alumina particles on flat disc. We have observed dust particles ejected out from the flat disc in random direction and falling down. Later, we have used crucible shaped aluminum holder for dust particles. It has provided radially confining field for particle conferment. The levitation of dust particle is observed when the crucible is grounded or biased negatively. Levitation of dust particle were not observed if the aluminum crucible was left floating.

A systematic tracking of the dust particle with increase in discharge current was carried out. The Plasma parameters were measured in the specific parameter regime in order to get an estimate of Debye length for comparison. We have observed that the discharge current exhibit a hysteresis loop with discharge voltage. The dust in a plasma regime to dusty plasma regime is observed with a steep jump in the discharge current (200 - 250 mA). It is also coinciding with plasma plume extending out of the anode source and filling the entire chamber volume.

References:

1. Rocca et al., 790-797, 56(3), J. Appl. Phys, 1984.
2. H. M. Thomas et al., 19, 023702, Physics of Plasmas,2012

BPE-P-8

EVOLUTION OF SPONTANEOUS DUST DENSITY WAVES IN NANODUSTY PLASMAS UNDER STRONG HAVNES EFFECT

Bidyut Chutia*
Physical Sciences Division, Institute of Advanced Study in Science and Technology (IASST), Paschim Boragaon, Guwahati-781035, Assam, India
**E-mail: bidyut.chutia.jist@gmail.com*

In laboratory, reactive plasma media favors spontaneous growth of nanodust particles. Presence of nanodust particles in laboratory plasmas can lead to the formation of a highly dense nanodusty plasma that can strongly affect the discharge as well as plasma dynamics [1]. A highly dense nanodust cloud can enhance the Havnes parameter (ratio of dust density to ion density) which can have serious impact on the average dust charge and the dust acoustic (density) waves.

Here, the propagation of a self-excited dust density wave under a strong Havnes effect is studied experimentally. Initially, the growth kinetics of carbonaceous (a-C:H) nanoparticles in a capacitively coupled RF discharge (13.56 MHz) of Argon and Acetylene gas mixture is studied. The in situ grown particles produce a large 3D cloud with a dust density, measured to be of the order of 10^{13} m^{-3}. The cloud is illuminated by a green laser sheet (532 nm, 100 mW) and self-excited dust density waves (DDWs) are observed to propagate throughout the nanodust cloud for large distance ~ 19 cm. The wave dynamics is recorded by using a high-speed camera (Phantom Miro M110@400-1000 fps). The wave is propagating along the direction of gravity from the lower edge of the dust void. The detail spatiotemporal evolution of the DDW is performed using various techniques such as periodograms, Fast Fourier transformation and time-resolved Hilbert transformation. A dispersion relation of the DDW is obtained which is compared with a theoretical model to extract average charge on nanodust particle. Presence of a small finite electric field throughout the nanodusty plasma is confirmed. This electric field is the cause of the DDW excitation. As the nanodust density is quite high, a strong reduction of plasma electrons is expected and in turn the Havnes parameter reaches a large value (P= 15 – 32). The strong Havnes effect reduced the average charge on each nanodust particles to a very small value of (55 – 113) electronic charge only. As a result, the DDW is found to be propagating with a low phase velocity. The experiment also shows various interesting phenomena such as wave breaking/merging, high-amplitude shock like structure formation etc.

References:

[1] J. Berndt, E. Kovačević, I. Stefanović, O. Stepanović, S. H. Hong, L. Boufendi, and J. Winter, Contrib. Plasma Phys. **49**, 107 (2009).

BPE-P-9

NANODUPLEX: A NEW DUSTY PLASMA EXPERIMENTAL SETUP TO PRODUCE EXTENDED DUST CLOUDS USING REACTIVE ARGON ACETYLENE PLASMAS

BidyutChutia*, T. Deka, Y. Bailung, S. K. Sharma and H. Bailung
Affiliation: Dusty Plasma Laboratory, Physical Sciences Division, Institute of Advanced Study in Science and Technology (IASST), Paschim Boragaon, Guwahati-781035, Assam, India
**E-mail: bidyut.chutia.jist@gmail.com*

In this work, a large volume 3D dust cloud containing in-situ grown nanometer sized particles is produced in a newly developed versatile table-top experimental device, named nDuPlEx (nano Dusty Plasma Experiments) [1]. Carbonaceous nanoparticles having almost uniform size throughout the dust cloud are grown using capacitively coupled rf discharge in Ar-C_2H_2 gas mixture with low precursor gas flow rate (~ 2 sccm) and minimal rf power (~ 1 W). The vertical and radial extension of the dust cloud is 40 cm and 5 cm, respectively. The pure Ar plasma in the setup is characterized by measuring the discharge parameters as well as plasma parameters under different discharge conditions. The temporal evolution of average particle size is determined by analyzing the Scanning Electron Microscope (SEM) images of the particles. The dust density measured by using the laser extinction method, which is found to be of the order of 10^{16} – 10^{12} m^{-3} for discharge duration of (2 – 10) min. A spontaneous dust density wave (DDW) is also observed in the dust cloud.

References:

[1] B. Chutia, T. Deka, Y. Bailung, S. K. Sharma, and H. Bailung, Phys. Plasmas **28**, 063703 (2021).

BPE-P-10

HIGH CURRENT PULSED POWER SUPPLY SYSTEM FOR LARGE VOLUME PLASMA DEVICE-UPGRADE

P. K. Srivastava[1,*], R. Sugandhi[1, 2], A. K. Sanyasi[1], A.Adhikari[1, 2], and L. M. Awasthi[1, 2]
[1]*Institute for Plasma Research, Gandhinagar, Gujarat 382428, India*
[2]*Homi Bhabha National Institute, Mumbai 400094, India*
E-mail: pkumar@ipr.res.in*

The Large Volume Plasma Device (LVPD)[1] has been recently upgraded with installation of a new multi-filamentary plasma source, filament power supply, pulsed discharge power supply and pulsed solenoid power supply apart from upgraded PXIe based *40* channel data acquisition system. The up-gradation of LVPD system aimed at producing circular, uniform high density and quiescent plasma with enhanced plasma pulse duration of $\sim 50ms$ (Discharge Power Supply) from existing $9.2ms$. The experiments in LVPD are mainly focussed on plasma waves and instability studies, wave – plasma interaction, plasma transport across magnetic field etc. Apart from the high current long pulsed ($50ms$) discharge supply, LVPD required another high current long pulsed ($55ms$) power supply (Solenoid Power Supply) that can be employed for producing a strong transverse magnetic field via a varying aspect ratio solenoid called electron energy filter (EEF)[2].

The pulsed power supplies i.e. the discharge and solenoid power supplies are designed in LVPD, IPR with the functional parameters and specifications required as per the experimental needs. The system specifications were simulated in OrCAD's PSpice software limiting a maximum drop of output current to *5%* from its peak set value during the pulse. Discharge power supply design topology based on a capacitor bank of $C \sim 6.8F$, IGBT based switching and is capable of supplying an output current of $I_d \sim 1\ kA\ (max)$at $150V$.Similarly, the solenoid power supply is also based on design topologies with a continuously chargeable capacitor bank of $C \sim 5.66F$, capable of producing an output current of $I_{EEF} \sim 2.5\, kA\ (max)$ at $175V$.Both these power supplies are equipped with:(a) inbuilt capacitor bank charging power supplies, (b) suitable voltage and current protections for plasma and solenoid loads,(c) control knobs along with front panels indicators,(d) facilitation of local and remote control operations (e) short circuit and/or overload protection and (f) fibre optics interface for remote monitoring and control.

The power supplies are successfully fabricated, procured, installed and integrated with plasma operations in LVPD-U. The paper will discuss the engineering details, salient features, optimised performance and various modes of operation of these power supplies with plasma experiments in the conference. Apart from these our experience during the commissioning and testing phase in laboratory will also be presented.

References:

[1] S. K. Mattoo, V. P. Anitha, L. M. Awasthi, et. al, Rev. Sci. Instrum., 72, 3864, 2001.

[2] S. K. Singh, P. K. Srivastava, L. M. Awasthi, et. al, Rev. Sci. Instr. 85, 033507, 2014.

[3] P. K. Srivastava, S. K. Singh, A. K. Sanyasi,et.al, Rev. Sci. Instr.87, 073501, 2016.

BPE-P-11

UTILIZATION OF AN INERTIAL ELECTROSTATIC CONFINEMENT FUSION DEVICE AS A NEUTRON AND X-RAY SOURCE

D. Bhattacharjee[1], L. Saikia[1] and S. R. Mohanty[1,2]

[1] *Centre of Plasma Physics-Institute for Plasma Research, Nazirakhat, Sonapur, Assam, 782402*

[2]*Homi Bhabha National Institute, Anushaktinagar, Mumbai, Maharashtra, 400094, India.*

E-mail: darpan.bhattacharjee@cppipr.res.in

The conventional inertial electrostatic confinement fusion (IECF) operation is based on the application of high negative voltage to the central grid which results in the production of neutrons due to the fusion of lighter ions [1-3]. The neutron has enormous applications in diversified fields [4]. The device can also be used as an application based x-ray source by altering the polarity of the central grid. In this work, the electron dynamics during the positive polarity of the central grid have been studied by using an object-oriented particle-in-cell code (XOOPIC). The trapped electron density inside the anode is found to be of the order of 10^{16} m^{-3} during 10 kV simulation. The x-ray production, imaging and radiography have been investigated at different voltages and using different structure of the anode. The x-ray emitting zone have been studied via pinhole imaging technique. Lastly, the radiography of metallic as well as

biological samples have also been investigated. This study shows the versatile nature of the IECF device in terms of its applications, both in the field of neutron and x-ray.

References:

[1] R. Hirsch, Journal of applied physics 38, 4522 (1967).

[2] N. Buzarbaruah, N. Dutta, J. Bhardwaz, and S.R. Mohanty, Fusion Engineering and Design 90, 97 (2015).

[3] D. Bhattacharjee, N. Buzarbaruah, and S. R. Mohanty, "Neutron and x-ray emission from a cylindrical inertial electrostatic confinement fusion device and their applications," Journal of Applied Physics 130, 053302 (2021).

[4] G. H. Miley and S. K. Murali, Inertial electrostatic confinement (IEC) fusion (Springer, 2014).

BPE-P-12

EFFECT OF MULTIPLE GRID CONFIGURATION ON PLASMA PARAMETERS OF AN INERTIAL ELECTROSTATIC CONFINEMENT FUSION DEVICE

L. Saikia[1], D. Bhattacharjee[1], A. Maurya[1] and S. R. Mohanty[1, 2]

[1] *Centre of Plasma Physics-Institute for Plasma Research, Nazirakhat, Sonapur, Assam, 782402*

[2]*Homi Bhabha National Institute, Anushaktinagar, Mumbai, Maharashtra, 400094*

E-mail: lucky.saikia@cppipr.res.in

The Inertial Electrostatic Confinement Fusion (IECF) device is a fusion system in which ions are accelerated and fused at the central part of the device due to the application of an electrostatic field. It is mainly used as a portable neutron/proton/x-ray source which has multiple near term applications. In order to observe the modification in ion flow dynamics as well as change in plasma parameters, we have designed and installed two outer grids apart from the central cathode grid in the cylindrical IECF device. In this study, the ion confinement and the changes in the plasma parameters, such as plasma temperature, ion density, plasma potential, etc. have been investigated in the triple grid system in comparison to the single grid system during hot cathode discharge. The central cathode potential has been varied from low to high voltage to analyze the observed changes. In addition, the discharge phenomena during cold cathode discharge have also been studied and compared in both single and triple grid configurations of the device. This new configuration is believed to be more efficient in ion confinement and in increasing the ion beam energy than the conventional single grid system.

References:

[1] T. A. **THORSON** et al., “Convergence, Electrostatic Potential, and Density Measurements in a Spherically Convergent Ion Focus,” Phys. Plasmas, 4, 4 (1997).

[2] Masuda, Kai, et al. "Performance characteristics of an inertial electrostatic confinement fusion device with a triple-grid system." Fusion technology 39.3 (2001): 1202-1210.

[3] Buzarbaruah, Neelanjan, et al. "Characterization of discharge plasma in cylindrical IECF device." Proceedings of the tenth Asia plasma and fusion association conference: book of abstracts. 2015.

[4] Bhattacharjee, D., N. Buzarbaruah, and S. R. Mohanty. "Neutron and x-ray emission from a cylindrical inertial electrostatic confinement fusion device and their applications." Journal of Applied Physics 130.5 (2021): 053302.

BPE-P-13

PROTOTYPE AUTOMATED LINEAR AND ROTATIONAL PROBE DRIVE FOR LARGE VOLUME PLASMA DEVICE- UPGRADE

P. Chauhan[1], R. Sugandhi[1,2], A. K. Sanyasi[1], P. K. Srivastava[1], D. Khanduri[2], A. Adhikari[1,2], P. K. Leuva[1], M. K. Gupta[1], B. R. Doshi[1] and L. M. Awasthi[1,2]
[1]*Institute for Plasma Research, Gandhinagar 382421 India*
[2]*Homi Bhabha National Institute, Mumbai 400094 India*
E-mail[*] : pradeep@ipr.res.in

Large Volume Plasma Device- Upgrade (LVPD-U)[1] is a large sized, double walled, water cooled, cylindrical device dedicated for carrying out fundamental studies relevant to earth’s atmosphere and fusion plasmas. The SS304 vacuum vessel (L = 3m, Ø= 2m) is equipped with 94 ports to accommodate the diagnostics needed for plasma characterization. The need to equip the device with suitable probe drives for diagnostics movement has been felt since long. In the recent time, the device has been augmented with in-house developed, automated, linear probe positioning systems[2] in 12 numbers of its ports in horizontal plane. Subsequently design for another type of probe drive system capable of providing the linear as well as rotational movement has been commenced and a scale down version of the prototype is developed as a proof of concept to undertake its performance in air and vacuum for measurement accuracy and vacuum compatibility, especially for its novel vacuum seal. Presently, the developed prototype has been tested in air for its linear motion for a travel distance of approximately 35mm in length with accuracy of <1mm and rotational motion for 0-280^{o} in step size of 35^{o} using stepper motor, controller and software controlled, using LabVIEW based machine control system. The configuration parameters of the stepper motor has been optimized for smooth and silent movement of the linear and rotational drive. The system has also been tested for vacuum leak tightness of the seal in standalone mode and a leak rate of ~ 10^{-9} Torr-liters/sec has been obtained.This prototype will be installed soon in Double Plasma Device and will be tested for its performance in vacuum condition. Results on its performance in air as well as in vacuum will be reported. This paper will discuss requirements, literature survey, architecture, mechanical design, vacuum seal, electrical hardware and software and obtained results.

References:

[1] S. K. Mattoo, V. P. Anita, L. M. Awasthi et. al., Rev. Sci. Instrum 72, 3864 (2001)

[2] A. K. Sanyasi, R. Sugandhi, P. K. Srivastava et. al., Rev. Sci. Instrum, 89, 055113(2018).

BPE-P-14

INTERACTION OF A PRECURSOR SOLITON WITH A WAKE-FIELD IN A FLOWING DUSTY PLASMA

Krishan Kumar, Pintu Bandyopadhyay, Swarnima Singh, Abhijit Sen
Institute for Plasma Research, Bhat, Gandhinagar-382428, Gujarat
E-mail: krishan.kumar@ipr.res.in

We report experimental observations of the interaction of a precursor soliton with a wake structure in a flowing dusty plasma. The experiments are performed in an inverted pi-shaped dusty plasma experimental (DPEx) device, and the dusty plasma is made in a DC glow discharge Ar plasma using micron size Kaolin particles [1]. Two copper wires installed radially on the cathode serve as charged objects in the plasma environment. Precursor solitons and wakes get excited when the dust fluid flows supersonically over these objects [2,3]. In the frame of the fluid, the solitons propagate in the upstream direction, whereas the smaller amplitude wake structures propagate in the downstream direction. A soliton, excited by one of the obstacles, interacts with the wake structure excited by the other obstacle in the region between the two charged objects. After the interaction, the soliton is seen to merge with the smaller amplitude wake structure and to propagate in the same direction. The resultant amplitude and the velocity of the combined structure increases after the interaction. The results are explained theoretically using numerical solutions of a model forced Korteweg–deVries equation that is driven by two source terms.

References:

[1] S. Jaiswal, P. Bandyopadhyay, and A. Sen, Rev. Sci. Instrum. **86**, 113503 (2015).

[2] S. Jaiswal, P. Bandyopadhyay, and A. Sen, Phys. Rev. E 93, 041201 (2016).

[3] G. Arora, P. Bandyopadhyay, M. G. Hariprasad, and A. Sen, Physics of Plasmas 23,100705 (2016).

BPE-P-15

TRANSITION OF A MONOLAYER CRYSTAL TO A LIQUID-SOLID COEXISTENCE STATE IN A COMPLEX PLASMA

Swarnima Singh[1,2], Krishan Kumar[1,2], M.G. Hariprasad[1,2], A. Saravanan[1], P. Bandyopadhyay[1,2] and A. Sen[1,2]
[1]*Institute for Plasma Research, Bhat, Gandhinagar-382428*
[2]*Homi Bhabha National Institute, Training School Complex, Anushakti Nagar, Mumbai-400085*

We report an experimental investigation of the transformation of a 2D monolayer crystal to a self-sustained solid-liquid phase coexistence in a dusty plasma system. The experiments are performed in a glow discharge Argon plasma, which is produced in an L-shaped Dusty Plasma Experimental (DPEx-II) device by applying a DC voltage between a disc-shaped anode and a grounded tray-shaped cathode. Initially, a monolayer crystal is formed by using mono-dispersive MF particles at a discharge voltage of 400 V and neutral gas pressure of 6 Pa. The monolayer gets converted to a two-phase coexistence state when the gas pressure is reduced beyond a threshold value. The central region of the coexistence state consists of a molten liquid surrounded by a crystalline periphery. Prior to this transition, the particles exhibit a self-excited horizontal oscillation with a frequency of ~30 Hz at the center. Various structural and thermodynamics quantities like inter particle distance, bond order parameter, dust-temperature, and Coulomb coupling parameter are calculated over the entire range of neutral gas pressure. These estimated quantities differ significantly when the system migrates from a monolayer to a phase coexistence state. Similar behavior of phase coexistence state is also seen when the discharge voltage is reduced gradually from a threshold value for a given neutral gas pressure. The formation of ion wakes resulting from a non-reciprocal force triggers the Schweigert instability, which is responsible for the coexistence of the liquid-solid phases in our dusty plasma system.

BPE-P-16

DESIGN CONSIDERATION FOR A LINEAR MAGNETIZED PLASMA DEVICE

Dibyajyoti Bora and Subir Biswas
Institute of Advanced Study in Science and Technology, Guwahati-781035, Assam, India
E-mail: dibyajyoti95bora@gmail.com, subirb@iasst.gov.in

The complicated nature of magnetically confined fusion devices like tokamak and stellarator and the simultaneous occurrence of various wave modes in them do not offer the opportunity to study any particular wave mode exclusively. A linear magnetized plasma device however, enables successful isolation and study of different wave and

instability modes and their non-linear behavior in magnetized plasma regime in a controlled manner. Several laboratories both in India and abroad are working on various experimental investigations in linear magnetized plasma with different magnetic field configurations and plasma sources depending on their experimental aim [1-3]. Here, the design of such a linear plasma device and its set of magnetic field coils for producing a continuous uniform magnetic field inside the vacuum chamber will be described. For the production of plasma we use a filament (tungsten) assisted DC plasma source which is biased negatively with respect to a positively biased stainless steel circular mesh placed inside the chamber. Basic plasma parameters such as electron density and temperature are measured using single Langmuir probes inserted from radial ports of the device.

References :

[1] R. Pal, S. Biswas et. al., Rev. Sci. Instrum. 81, 073507 (2010).

[2] W. Gekelman, H. Pfister et.al., Rev. Sci. Instrum. 62, 2875 (1991).

[3] S. Bose, M. Kaur et. al, Rev. Sci. Instrum. 86, 063501 (2015).

BPE-P-17

NOVEL EXPLANATION OF THE COLD PULSE PROPAGATION PHENOMENON INDUCED BY GAS PUFF IN ADITYA-U TOKAMAK

Tanmay Macwan[1,2], Harshita Raj[3], Kaushlender Singh[1,2], Suman Dolui[1,2], Sharvil Patel[1,4], Ankit Kumar[1,2] , P Gautam[1], J Ghosh[1,2], R L Tanna[1,4], K A Jadeja[1,5], K M Patel[1], Rohit Kumar[1], Suman Aich[1], Umesh Nagora[1,2], M B Chowdhuri[1], R Manchanda[1], Nandini Yadava[1,4], Ritu Dey[1,2], Kiran Patel[1,2], S. K. Pathak[1, 2], M. K. Gupta[1], K. Tahiliani[1], P. K. Chattopadhyay[1,2], A Sen[1,2], Y C Saxena[1,2], R Pal[6]

[1] Institute for Plasma Research, Gandhinagar 382 428
[2]Homi Bhabha National Institute (HBNI), Mumbai 400 085
[3]EPFL, Route Cantonale, 1015, Lausanne, Switzerland
[3] Pandit Deendayal Petroleum University, Gandhinagar 382 007
[4] Institute of Science, Nirma University, Ahmedabad 382 481, Gujarat, India
[5] Department of Physics, Saurashtra University, Rajkot, Gujarat, India
[6]Saha Institute for Nuclear Physics, Kolkata 700 064
Email: tanmay.macwan@ipr.res.in

Cold pulse propagation (CPP) phenomenon has eluded a convincing explanation for the past ~ 25 years. The fast increase in the core temperature observed in CPP in response to the edge cooling is counter-intuitive to the current understanding of the plasma transport, which is believed to be dominated by local turbulence. In ADITYA-U, CPP is induced by short bursts of hydrogen/deuterium gas puffs, each puff injecting ~ 10^{17}-10^{18} molecules. It is shown that the sharp rise in the chord averaged density with every injection is necessary for the rise in the core temperature. Further, the rise in the core temperature is shown to depend on the chord averaged plasma density before injection and the amount of injected gas. The increment in the core density and core temperature is seen to increase with the amount of injected gas molecules, while the rates of rise of density and temperature remain the same. The sharp density rise and hence the CPP is explained by a combination of the fast reduction in the ion orbit loss due to a decrease in the radially outward electric field and an increase in the Ware pinch of the particles due to a rapid increase in the loop voltage.

BPE-P-18

INITIAL PLASMA EXPERIMENTS IN SIMPLE TIGHT ASPECT RATIO MACHINE ASSEMBLY

T. Ram[1, 2], Jagbandhu kumar[1], P. K. Sharma[1, 2], Raju Daniel[1, 2]
[1]*Institute for Plasma Research, Bhat, Gandhinagar, Gujarat 382428, India*
[2]*Homi Bhabha National Institute, Training School Complex, Anushakti Nagar, Mumbai 400094, India*
E-mail: tulchhi.ram@ipr.res.in

A device STARMA (acronym for simple tight aspect ratio machine assembly) [1] is developed to studyelectron cyclotron resonance (ECR) produced plasma in small aspect ratio devices. It is a low aspect ratio (A) device, with A=1.5, having a major radius of 10.4cm and minor radius of 6.8cm.A 2.45GHz, 6kW CW magnetron source is employed to produce plasma using ECR techniques. The 2.45GHz magnetron source requires a toroidal magnetic field of 875G for first harmonic breakdown [2] which is realized with sixtoroidal field coils. The magnetic field coils are charged using a capacitor bank power supply which gives a time varying toroidalmagnetic field. The helium plasma is formed for ~70-80ms having electron density ~$5x10^{16}m^{-3}$ and electron temperature ~11eV. The plasma parameter is studied at different parameters to understand the production of ECR plasma with different neutral background which impacts the collision frequency [3].The temporal variation of the toroidal magnetic field forms the ECR plasma with ECR layer moving spatially in time and this provides an opportunity to understand the spread in the peak density profile between the ECR layer (875G) and upper hybrid layer.

References:

[1] Jagabandhu Kumar, T Ram. Development of Simple Tight aspect ratio Machine Assembly (STARMA) for Basic Plasma experiments (IPR library Technical Report 2021).

[2] Bornatici, M. Theory of electron cyclotron absorption of magnetized plasmas. Plasma Physics 24, 629–638 (1982).

[3] P K Sharma et al 1997 Plasma Phys. Control. Fusion 39 1669.

BPE-P-19

EXPLORING POSSIBILITY OF ETG SUITABLE PROFILES IN VARYING RATIO OF TRANSVERSE TO LONGITUDINAL MAGNETIC FIELD IN LVPD-U

Ayan Adhikari[1, 2], A. K. Sanyasi[1], L.M. Awasthi [1, 2], P. K. Srivastava[1], Ritesh Sugandhi[1,2] and Mainak Bandyopadhyay[1,2]
[1]*Institute for Plasma Research, Gandhinagar, Gujarat 382428, India*
[2]*Homi Bhabha National Institute, Mumbai 400094, India*
E-mail: ayan.adhikari@ipr.res.in

The Large Volume Plasma Device-Upgrade (LVPD-U) is a water cooled, double walled, cylindrical device of dimension (ϕ = 2m, and L = 3m). It facilitates a Large Area Multi-filamentary Plasma Source (LAMPS), a large solenoid called as electron energy filter(EEF), two high current pulsed power supplies (2.5kA/100V and 1kA/120V) for energizing the EEF and for striking the plasma discharge, and 12 numbers of automated linear probe drives. The LAMPS consists of hairpin shaped filaments (n=162, Ξ=0.5mm, L=18cm, W-make) and these are mounted in front (Ξz =15 cm) of the cusped anode plate of LAMPS. The 1.8m diameter EEF, which is mounted at axial centre of the device produces a transverse magnetic field of ≤250G. The EEF divides the LVPD-U plasma into three distinct regions of 1) Source 2) EEF and 3) Target respectively. The purpose of transverse field here is to control transport of plasma from source to target plasma region.

The pulsed Argon plasma (t_{disch}~50ms) is produced for discharge parameters (V_d~ -70V, P_{Ar}~ 4 x10^{-4} mbar and B_z~ 6.2G). The radial confinement is provided by a set of 10 discrete garlanded coils while axial confinement by a pair of SS304 cusped plates mounted at immediate back of filaments and extreme end of the device respectively. The plasma parameters like plasma density, n_e, floating potential, V_f, and electron temperature, T_e and their AC counterparts are estimated. The experiments are carried out for investigating the evolution of plasma for varying ratio of transverse (B_x) to ambient (B_z) magnetic fields. The plasma scenarios for EEF ON and OFF cases have been explored in source and target plasmas. We could see that EEF not only cools down electron temperature but also reduces plasma density in the target plasma. The obtained values of electron temperature and plasma density in the source and target plasmas are 4.5eV, 2eV and 4x10^{17}m^{-3} and 2.5x10^{17}m^{-3} respectively. The radial profiles of electron temperature and plasma density shows typical scale lengths of electron temperature and plasma density as L_T ~61.5cm, and L_n~ 133cm respectively in the core region of target plasma for Bx/Bz~19. For this scenario, the threshold condition, Ξ=L_n/L_T>2/3 for ETG turbulence is satisfied. Interestingly, for EEF OFF case, no fluctuations are excited in the core plasma region (x ≤ 50 cm)of both source and target plasmas but when EEF is switched on, significant level of fluctuations are detected. A detailed comparison of equilibrium profiles and excited gradient scales with excited fluctuations will be presented in the conference.

BPE-P-20

UNDERSTANDING DENSITY DEPLETION IN CROSS-FIELD DIFFUSED PLASMA OF LVPD-U

Ayan Adhikari[1, 2], A. K. Sanyasi[1], L. M. Awasthi[1, 2], P. K. Srivastava [1], Ritesh Sugandhi[1, 2] and Mainak Bandopadhyay[1, 2]
[1]*Institute for Plasma Research, Gandhinagar, Gujarat 382428, India*
[2]*Homi Bhabha National Institute, Mumbai 400094, India*
E-mail: ayan.adhikari@ipr.res.in

The pulsed Argon plasma (Δt_{disch}~50ms) is produced for discharge parameters (V_d~ -70V, P_{Ar}~ 4 x10^{-4} mbar and B_z~ 62.G) in LVPD-U. The plasma in LVPD-U is divided into three different plasma regions of source, EEF and target plasmas because of the presence of a finite width (Δz = 4cm), large electron energy filter (EEF) at its axial centre. The EEF is capable of producing transverse magnetic field (≤ 250G) in the device whereas, the axial magnetic field is produced by a set of 10 garlanded coils over the length of the device. The experiments are carried out to understand the evolution of plasma in source and target plasmas for the varying ratio of transverse (B_x) to ambient (B_z) magnetic fields.

While pursuing plasma evolution, we encountered an interesting phenomenon of density depletion in the target plasma. We observed that plasma density gets depleted temporally when the ratio of Bx/Bz>16.5. In order to confirm whether it has any correlation with the process of plasma formation itself, we compared the profiles of target region with that of source region and interestinglyfound them uncorrelated. On further expanding these investigations, we observed that the reason behind temporal depletion of plasma density may have some correlation with the modification in diffusion rate of plasma across the EEF. Validation of hypothesisand its relation with temporal modification of cross field diffusion requires further investigations viz., 1) eliminating capacitance between plasma and the insulator of EEF jacket which is a Teflon material, by biasing the EEF conductors to negative potential, and 2) incorporate a pair of biased electrodes within EEF to modify the ratio of parallel and perpendicular diffusion through EEF.The former case we believe may confirm the role of EEF boundary as a negatively charged sheet and probably may quantify its contributiontowards depletion of plasma density in the target region while in the latter case where a pair of electrodes are either biased positively or negatively, the role of parallel and transverse diffusion in depletion of plasma density may be explained. These investigations may help us in identifying the mechanism of refilling the target plasma column with bulk plasma electrons. Detailed results on these investigations will be presented in the conference.

BPE-P-21

THREE DIMENSIONAL DUST CLOUD IN DC GLOW DISCHARGE PLASMA

Sachin Sharma[1], G Veda Prakash[2], Meenakshee Sharma[3], Sayak Bose[4], Sanat Kumar Tiwari[1]
[1]*Indian Institute of Technology Jammu, Jammu & Kashmir, India, 181221*
[2]*Department of Energy Science and Engineering, Indian Institute of Technology Delhi, Hauz Khas, New Delhi, India, 110016*
[3]*Institute for Plasma Research, Bhat, Gandhinagar, Gujarat, India, 382428*
[4]*Columbia Astrophysics Laboratory, Columbia University, 550 West 120th Street, New York, NY, USA, 10027*
E.mail: 2020rph1040@iitjammu.ac.in

We report three-dimensional dust cloud formation in an Argon gas plasma using a DC-glow discharge experiment. In cathode-grounded configuration, a hemispherical dust cloud is observed around the edges of the circular cathode. The preliminary observation suggests the dust cloud formation of size 6-8 cm in diameter and approximately 5 cm in depth. The temperature and density of Argon plasma are in ranges of 2-6 eV and 10^8 - 10^9 cm^{-3} respectively. The typical discharge parameters are: the discharge voltage ranging from 290 - 320 Volt, discharge current ranging from 20 – 50 mA and the typical gas pressure of 1.2 x 10^{-1} mbar. We plan to study fluid-like collective behavior with such a widened cloud of dust particles [1,2].

References:

[1] Turbulence in strongly coupled dusty plasmas using generalized hydrodynamic description, Phys. of Plasmas, **22**, 023710, 2015.

[2] Suppression of Rayleigh Taylor instability in strongly coupled plasmas, **21**, 062102, 2014.

BPE-P-22

TEMPERATURE ANISOTROPY DIRECTED PARTICLE TRANSPORT IN A PLASMA CONFINED IN A DIPOLE MAGNETIC FIELD

Ayesha Nanda and Sudeep Bhattacharjee
Department of Physics, Indian Institute of Technology Kanpur, Kanpur - 208016, India
E-mail: ayesha@iitk.ac.in

Anisotropy in temperature prevails in natural environment such as space and astrophysical plasma, and in laboratory plasma. Temperature anisotropy being a free energy source not only influences the wave propagation by modifying their dispersion relations, but also induces various instabilities [1]. The interplay of this free energy source with the inhomogeneous plasma parameters [2] have revealed possible

explanations to heating and particle acceleration problems and is still an intriguing question of research.

The temperature anisotropy is an intrinsic characteristic of magnetized plasmas and arises due to unequal charge distribution along two directions – parallel and perpendicular to the magnetic field. Several works have been carried out on different phenomena such as plasma heating, wave generation and instabilities arising from the anisotropy in temperature. But the problems have been mostly addressed with a unidirectional magnetic field, where both the perpendicular directions are dealt with equal probability (by equipartition theorem) [3]. But the most natural magnetic field configuration in space is a dipole magnetic field [4], which is not unidirectional. The anisotropy arising in a dipole field with reference to parallel component must be due to two perpendicular directions with different energy distributions, thereby different probability current density and transport mechanism.

For accurate understanding of the anisotropy induced wave generation and particle acceleration, investigation on one of the fundamental properties such as electrical conductivity is inevitable. To address the problem, a mathematical model is formulated using the momentum equation, by considering the net velocity due to all possible particle drifts. The vivid theoretical development incorporating temperature anisotropy in various conductivity terms like Pedersen, Hall and longitudinal in a dipolar magnetic field supported by experiments at various spatial positions will be presented in detail in the conference.

References:

[1] M. F. Bashir et al, Phys. Plasmas, **17**, 102112, (2010).

[2] H. Naim et al, Phys. Lett. A, **377**, 234, (2013).

[3] B. Remya et al, J. Geophys. Res., **118** p 785-793, (2013).

[4] A. R. Baitha et al., Plasma Res. Express, **1**, 045005 (2019).

BPE-P-23

DESIGN AND DEVELOPMENT OF MULTI-GAP PSEUDOSPARK DISCHARGE BASED PLASMA CATHODE ELECTRON SOURCE FOR EUV/SOFT X-RAY RADIATION GENERATION

Varun[1,2], Navin Kumar Sharma[3], Akhilesh Mishra[1,2], Ram Prakash Lamba [1,2] and Udit Narayan Pal[1,2]

[1]*CSIR-Central Electronics Engineering Research Institute, Pilani, Rajasthan- 333031*

[2]*Academy of Scientific and Innovative Research (AcSIR), Ghaziabad, Uttar Pradesh- 201002*

[3]*Devi Ahilya Vishwavidyalaya, Indore, Madhya Pradesh-452001*

E-mail: varundixit992@gmail.com/udit@ceeri.res.in

The pseudosparkdischarge based devices has gain much attention in various growing applications in the field of high-power plasma switches, electron-beam lithography, plasma processing, extreme ultraviolet sources, intense X-ray source, and microwave radiation source [1]-[3]. In the recent decade, the research and development of the pseudosparkdischarge based plasma cathode electron (PD-PCE) source is more focus toward the generation of high density and energetic electron beam for the application of the surface modification and EUV/Soft X-ray radiation emissions [4]-[5]. In fact, PS discharge based devices have capability of the generation of high current density ($\geq 10^4$A/cm^2), high power density (~10^9 W/cm^2) and high brightness (~10^{12} A/m^2 rad^2) with low emittance (~15mm mrad) electron beam [1]-[2].

In this research work, the simulation and experimental analysis of discharge characteristics of the PD-PCE source has been performed at different operating parameters (breakdown voltage (5-25 kV), external storage capacitance (500 pF-12 nF), gases and pressure (5-100 Pa)) and geometrical parameters (electrodes aperture diameter and sequence, gap distance and number of gaps). Simulation investigation has been performed using 2-D electrostatic plasma simulation OOPIC^{TM}PRO which shows the significant dependence of the discharge initiation, electron beam generation and its propagation on the electrode apertures and potential distribution inside the chamber of PD-PCE source. In fact, electron beam generation and propagation is a complex discharge process which is influenced by geometrical and operating parameters [6]-[7]. It has been observed that the sequence of electrode aperture diameter can create the problem of quenching in the rise of electron beam current. This can be further avoided by increasing the gas pressure and varying the geometrical parameters. Furthermore, the experimental investigation indicates that the generation of high energetic pulsed electron beam in the hollow cathode phase and its current can be controlled by the external circuit parameters. The PD-PCE sourced energetic and high density electron beam has been utilized for the generation of the EUV/Soft X-ray radiations.

References:

[1] J. Christiansen *et al.*, Für Phys. A Atoms Nucl. **290**, 35 (1979).
[2] A.W. Cross *et al.* J. Phys. D. Appl. Phys. **40**, 1953 (2007).
[3] U. N. Pal *et al.*, IEEE Trans. Electron Devices **67**, 5600 (2020).
[4] X. Cao *et al.*, Vacuum **184**, 109914 (2021).
[5] D. Bowes *et al.*, Nucl. Instrum. Methods Phys. Res. B, Beam Inter. Mater. At., **335**, 74 (2014).
[6] Varun *et al.*, IEEE Trans. Electron Devices **67,** 1793 (2020).
[7] Varun *et al.*, IEEE Trans. Electron Devices **67**, 2182 (2020).

BPE-P-24

REALIZATION OF NONLINEAR DEMAGNIFICATION IN PLASMA-BASED ION BEAM OPTICS

Sushanta Barman,[1] Sanjeev K. Maurya,[2] and Sudeep Bhattacharjee[1]
[1]*Indian Institute of Technology-Kanpur, Kanpur 208016, India*
[2]*Tata Institute of Fundamental Research, Colaba, Mumbai 400005, India*
E-mail: sushanta@iitk.ac.in

The demagnification (*DM*) of an electrostatic lens is a crucial parameter, which decides its efficiency and applicability in various areas [1, 2]. For electrostatic lens systems employed in charged particle optics, the *DM* factor is determined by the geometry and the voltage ratios of the lens elements. It is usually a constant for a set of fixed potentials applied to the electrodes. But in optics, several unconventional lenses such as liquid [3], metamaterial [4], and dielectric lenses [5] can have nonlinear demagnification due to the change in the inherent properties of the lenses such as mechanical and electrical properties, structure, and refractive index. However, despite these studies, the possibility of realizing nonlinear *DM* factor for electrostatic lenses by tuning the object beam size without modifying the inherent properties of the lens has not been realized earlier.

Recently, we have reported that the *DM* factor can vary nonlinearly when the object beam size is reduced to below the plasma Debye length [6], although the underlying physics was not explained. In this work, we have investigated experimentally, the effect of the plasma parameters and sheath nonlinearity, which controls the profile of the ion emission surface, on the *DM* factor. More importantly, the influence of the plasma sheath on radial and axial variation of the electric field in the region of the micro-beam aperture has been determined, which plays a critical role in the *DM* factor. We have observed that in plasma-based focusing systems, for extraction aperture sizes smaller than the plasma Debye length, the *DM* factor becomes nonlinear due to the sheath nonlinearity and enhanced penetration of the electric fields through the sheath region, which is originated because of the inadequate shielding of fields. The strength of nonlinearity depends upon the extraction aperture size and plasma Debye length, as confirmed from theoretical modeling and experimental results. The realization of nonlinear reduction of the *DM* factor can help to obtain nanometer-size beams in Maxwell-Boltzmann systems even for higher beam current, a unique finding for plasma-based charged particle focusing systems.

References:

[1] Wohlfart et al., Physical Review A **77**, 031404 (2008).
[2] J. M. Amini, C. T. Munger Jr, and H. Gould, Physical Review A **75**, 063416 (2007).
[3] L. Dong, A. K. Agarwal, D. J. Beebe, and H. Jiang, Nature **442**, 551 (2006).
[4] Wang et al., Nature Nanotechnology **13**, 227 (2018).
[5] Cao et al., Scientific Reports **5**, 1 (2015).
[6] S. K. Maurya, S. Barman, N. Pan, and S. Bhattacharjee, Physics of Plasmas **26**, 063103 (2019).

BPE-P-25

COLD ATMOSPHERIC PRESSURE PLASMA JETS: RONS DYNAMICS AND ELECTRIC FIELD ASYMMETRY

Deepika Behmani and Sudeep Bhattacharjee
Department of Physics, Indian Institute of Technology, Kanpur, Uttar Pradesh: 208016, India
E-mail: deepika@iitk.ac.in

Cold atmospheric pressure plasmas jets (C-APPJs) have become a subject of intense research interest due to their diverse applications in the area of surface treatment [1] and biomedicine [2]. These plasmas are non-equilibrium in nature ascribed to different electron (6000 K) and ion temperature (300 K) [3], and their low gas temperature makes them suitable for biological cells and tissues treatment. These plasmas are produced in an ambient environment and their direct interaction with air provides rich gaseous chemistry resulting in formation of reactive oxygen and nitrogen species (RONS) such as OH, HO_2, H_2O_2, NO, and N_2O_5 [4]. Thereactive species and their dependence on the plume electric field play an important role in biomedical applications. The electric field fluctuations can distort the electric field distribution function (EEDF) that can change rate coefficients of chemical reactions involving RONS, thereby affecting the biomedical applications. Therefore, it is crucial to study the electric field fluctuations and asymmetry, and their impact on RONS dynamics.

In this experiment, the plasma is ignited by applying a sinusoidal voltage (V_{pp}~ 15 kV and ν ~ 10 kHz) inside a glass capillary tube and the plasma comes out from the orifice of the capillary with the flow of gas in the form of jet [3,5]. The current study aims to map the electric field along the axial and poloidaldirections of the plasma jet by employing a two-pin probe and deducing the spatial asymmetry of the electric field along the plasma plume. A theoretical zero-dimension global model has also been developed that predicts the generation and dynamic behaviour of RONS including positive and negative ions. The electron and the ion density obtained from the global model have been used in the fluid model that contains coupled power balance equation, continuity equation, and Poisson equation, to determine the local plasma potential. The experimentally obtained electric field is corroborated with the electric field obtained from the solution of the Poisson equation. We aim tofind the connection between the time scale of electric field fluctuations and RONS generation, and the impact of fluctuations on the production of active species. Hence, the current study is important for the optimization of C-APPJs and their implementation for applications.

References:

[1] S. Yonson, S. Coulombe, V. Leveille, and R. L. Leask, J. Phys. D: Appl. Phys. **39** 3508 (2006)
[2] D. Mance, R. Wiese, T. Kewitz, and H. Kersten, Eur. Phys. J. D **72** 98 (2018)
[3] D. Behmani, K. Barman, and S. Bhattacharjee 2021 AIP Adv. **11** 085128 (2021)
[4] L. Lin and M. Keidar, Appl. Phys. Rev. **8** 011306 (2021)
[5] K. Barman, D. Behmani, M. Mudgal, S. Bhattacharjee, R. Rane and S. K. Nema Plasma Res. Express **2** 02500 (2020)

BPE-P-26

A DBD PLASMA BASED PACKED BED DISCHARGE SYSTEM USEFUL FOR EFFECTIVE VOCS REDUCTION

Ramavtar*, Kiran, and Ram Prakash
Department of Physics, Indian Institute of Technology Jodhpur,
N.H. 62, Nagaur Road, Karwar, Jodhpur, Rajasthan, 342037
**Email: jangra.1@iitj.ac.in*

It is well-known that carpets, building materials, furniture, office, equipment, detergents, paints, glues, solvents or fungicides emit a variety of volatile organic compounds (VoCs) and there is a surge in demand to develop innovative devices and systems to mitigate the issue. Packed bed discharge systems are being intensively researched internationally for VOCs reduction in the environment due to their exceptional performance in degrading VOCs into non-toxic components [1]. In this study, a coaxial cylindrical packed bed discharge system using glass beads as packing material has been researched to degrade VOCs that is powered by a bipolar pulsed power supply. It is a single-stage reactor in which the packing material is directly placed in the plasma discharge zone. The presence of packing material is expected to change the chemical features within the discharge zone, such as oxidation and destruction pathway, generation of by-products, and so on [2]. The developed system is optimized in terms of discharge characteristic parameters and power consumption. Ozone generation characteristics is also analysed. The results showed that a DBD packed bed reactor operated with a bipolar pulse power source produces powerful immediate discharge and energetic particles, which could be effectively used for VOCs degradation.

References:

[1] S. Xu, J. C. Whitehead, and P. A. Martin, "CO_2 conversion in a non-thermal , barium titanate packed bed plasma reactor : The effect of dilution by Ar and N_2," *Chem. Eng. J.*, vol. 327, pp. 764–773, 2017, doi: 10.1016/ j.cej. 2017. 06.090.

[2] S. K. P. Veerapandian, C. Leys, N. De Geyter, and R. Moren, "Abatement of VOCs using packed bed non-thermal plasma reactors: A review," *Catalysts*, vol. 7, no. 4, pp. 1–33, 2017, doi: 10.3390/catal7040113.

CATEGORY: NUCLEAR FUSION TECHNOLOGY (NFT)

NFT-P-1

TWEAKING FOR LOOP VOLTAGE PROFILE OF OHMIC TRANSFORMER POWER SUPPLY IN ADITYA-U TOKAMAK

Shivam Kumar Gupta, Kunal S Shah, M N Makwana, B V Nair, S Nair, Rohit Kumar, R L Tanna, Joydeep Ghosh and Aditya-U Team
Institute for Plasma Research, Bhat near Indira Bridge, Gandhinagar, Gujarat (India) 382428

Tokamak works on a principle of transformer, the Central Solenoid (primary coil) and a single turn plasma column (secondary coil) [1]. A time-varying current in the central solenoid generates a voltage in the plasma column ring, called loop voltage (LV), which breaks the neutral gas into ions and electrons, drives current through the plasma.Time-varying current in the ADITYA-U Tokamak, central solenoid is set by the Ohmic Transformer Power Supply (OTPS). The rating of OTPS 20kA, 2kV 12-pulse dual converter-based power supply [2].

Voltage profile generated across the Central solenoid (OT) is also represented as a primary loop voltage (PLV). Duration of the PLV profile is ~ 400ms. Initially,by inserting the external resistance the value of PLV is ~12kV, which induces the peak loop Voltage of ~20V in plasma column ring. After that PLV is controlled by switching resistances and corresponding LV brought to the value of ~1.5 V. During OTPS operation, it is observed that, after 100ms of loop voltage profile, voltage magnitude droops with a constant rate. This type of loop voltage profile is not desirable for plasma operation.

To overcome this problem, we analysedand concluded that the pre-defined reference and control circuitry needs to be tuned with OTPS. Hence, tweaking in the control circuitry so that existing hardware drives the current closely as per reference. Also the configuration of current reference profile for the required loop voltage was carried out in OTPS.We found some satisfactory results of constant Loop Voltage. The parameter configuration, tuning and experimental results will be concluded in this poster.

References:

[1] J A Romero, JET-EFDA Contributors, Nuclear Fusion. Vol. 50, 115002, 2010.

[2] V. Balakrishnan, C.N. Gupta, R.K. Sinha, Plasma current and position feedback control in ADITYA Tokamak, Fusion Engineering and Design, Volumes 66–68, 2003,Pages 809-813,ISSN 0920-3796.

NFT-P-2

DESIGNOF SUPPORT STRUCTURE FOR THE WAVEGUIDE SYSTEM FOR MICHELSON INTERFEROMETER SYSTEM FOR SST-1

Pratibha Gupta, Manoj Kumar Gupta, Bharat Doshi, Abhishek Sinha, S.K.Pathak
Institute for Plasma Research, Bhat, Gandhinagar-382428
E-mail: pgupta@ipr.res.in

Michelson diagnostichas been installed on SST-1 (Steady State Superconducting Tokamak) at IPR (Institute for Plasma Research). The diagnosticis being used for measuring broadband ECE (Electron Cyclotron Emission) emissions from SST-1. This diagnostic system has waveguides which are laid down from diagnostic lab to SST-1 port no. 12. The number of support structure columns to support this systemwas optimized. The waveguides were clamped in place by waveguide holders which were fabricated in-house. Channels were selected to act as a support base for waveguides. Efforts were made to mountthe support structure columns in a manner to avoid fouling with other subsystems in SST-1 hall.The support structure designwas found to be within the acceptable safety limits. Detailed design will be described in this paper.

NFT-P-3

UPGRADE IN SOFTWARE BASED INTERLOCK FOR ICRH DAC FOR EXPERIMENTS

Ramesh Joshi, H. M. Jadav, Manoj Singh, Kishore Misra, Sunil Kumar & High Power *ICRH Systems Division*
Institute for Plasma Research, Bhat, India
E-mail: rjoshi@ipr.res.in

Different experiments have been performed with an established technique for ion cyclotron heating of tokamak plasma [1]. In order to run various tokamak experiments using the ICRH DAC system, it needs to upgrade the software interlock in the existing control system. There is a requirement of having a different amplitude pulse to share ICRH RF power for various experimental conditions. It needs the facility of adjustable rise and decay in pulse development using software for various duty cycles and amplitudes which has been modified and integrated successfully. It is needed to implement another interlock to stop delivering power when plasma is not available in the tokamak which has been implemented in 1KHz time scale. This utility will facilitate not even suspension of digital pulse operation but multiple analog sync pulses have been stopped immediately. Few modifications have been implemented for central control system message communication required during operation. In this paper we explain the necessary modifications made in the previously developed VME based real

time operating and control system to cater experiment requirements which is successfully tested during recent tokamak testing campaigns.

References:

[1] Engineering design report (EDR) of ICRH-SST1, SST-2.03-050199-RF Group.

NFT-P-4

SOFTWARE MODIFICATIONS IN ICRH DAC FOR 45.6MHZ SYSTEM

Ramesh Joshi, H. M. Jadav, Sunil kumar& High Power ICRH Systems Division
Institute for Plasma Research, Bhat, India
E-mail: rjoshi@ipr.res.in

Ion Cyclotron Resonance Heating (ICRH) [1] for high power RF experiments has been developed for Tokamak. Data Acquisition and Control system (DAC) for ICRH system has been commissioned with a new concept of low cost design in the 3 amplifier stages of RF amplifiers up to 200kW of RF power. PLC based DAC instrumentation is used which includes 32-analog input channels, 32-digital input channels, 16-digital output channels and 16-analog output channels for the measurement and control of the system parameters. Control System Studio (CSS) is used to develop the application for user interface that can easily glue with the EPICS variable. The implemented software has been modified in terms of data acquisition using NI LabVIEW to avoid synchronization in data triggered by PLC to NI DAQ module using software communication and calibration module has been upgraded for precise data storage for after shot analysis.

NI DAQ card has been used for data archival in two different ways, one with hardwired trigger from PLC channels and another using software trigger event with EPICS variable. CALab is used to trigger data acquisition event using EPICS variable in order to synchronize data monitoring with data acquisition. Data visualization and plotting is modified using LabVIEW which uses a separate calibration module for acquired row data. Spline interpolation method is used for calibration of nonlinear range of data for acquired signals. This paper describes the modification in software communication and data storage and calibration scheme.

References:

[1] Engineering design report (EDR) of ICRH-SST1, SST-2.03-050199-RF Group.

NFT-P-5

CONCEPTUAL DESIGN OF SIGNAL CONDITIONING AND INTERLOCK OF 82.6GHZ GYROTON BASED ECRH SYSTEM

Harshida Patel[1], J Patel, D Purohit, K G Parmar, Hardik Mistry, B K shukla and ECRH Group
Institute for Plasma research, Near Indira bridge, Bhat Gadhinagar-382480
[1]*Email: harshita@ipr.res.in*

An 82.6GHz Gyrotron is being upgraded with high power according to the need of SST-1 tokomak experiments.82.6GHz Gyrotron based ECRH system would be used various plasma experiment in SST-1 tokomak. . Electron Cyclotron Resonance Heating system (ECRH) is one of the important heating system for super conducting steady state Tokomak (SST-1).In order to analyze performance as well as for the operation of the system, it is essential to monitor .acquire different system parameters along with an interlocking systems to operate system in fail safe manner. ECRH system develops its own data acquisition and control system to execute the task of data acquisition from sub- system like different auxiliaries power supplies, cooling system, high power measurements and safety interlocks for Gyrotron. Signal conditioning is medium between the control system and auxiliaries system. Fiber based design concept is used for all conditioning and interlocks for ECRH system. Different types of Analog and digital conditioning cards are developed with optical fiber based isolation. There are 60-70 no's of signals monitors and control from different auxiliaries system.Paper will discuss the design idea and layout of front end electronics of ECRH DAC system and explain its working.

NFT-P-6

INTERFACE OF ANODE POWER SUPPLY WITH 42GHZ GYROTRON FOR DUAL PULSE OPERATION IN SST TOKAMAK

Harshida Patel[1],DPurohit,J Patel, N Rajan Babu, K G Parmar, Hardik Mistry, B K shukla and ECRH Group
Institute for Plasma research, Near Indira bridge, Bhat Gadhinagar-382480
[1]*Email-harshita@ipr.res.in*

A 42GHZ Gyrotron based ECRH system on SST -1 has been used for various experiments like start up and heating of plasma experiments. The 42GHz Gyrotron delivers 500KW power at ~42KV DC beam voltage and +22KV anode voltage. Electron Cyclotron Resonance Heating system (ECRH) is one of the important heating system for super conducting steady state Tokomak (SST-1). The Dual pulse operation of Gyrotron are very important Plasma experiment need in SST-1 tokomak. First pulse is used for pre ionization and second pulse for plasma heating. New anode power supply is specially developed to fulfill these requirements. Parameters of power supply

are +30KV /100mA. The main interfacing signals are analog control to set required voltage and digital for high speed switching and control the power supply. The power supply has been fully integrated with Gyrotron tube and operates remotely with PXI based data acquisition control system on SST tokomak. Dual pulse operation of Gyrotron on SST-1 tokomak has been demonstrated successfully.This paper will discuss interface of power supply with ECRH systems.

NFT-P-7

OVERHAULING OF POWER TRANSFORMER 132KV / 11KV, 15000KVA AT 132KV IPR SUBSTATION

Prakash Parmar, Chandra Kishor Gupta, Supriya Nair, Chirag Bhavsar
Institute for Plasma Research, Near Indira Bridge, Bhat, Gandhinagar
E-mail: pkparmar@ipr.res.in

IPR has 132 KV, 3ph, 50Hz line coming from 220 kV substation at Ranasan through the single circuit overhead line. Maximum contract demand of IPR is 6 MVA. The Substation at IPR covers various equipment such as Power Transformers, Circuit Breakers, Isolators, Earth Switches, Lightning Arresters, Current Transformer, Potential Transformer, Control and Relay panel and Grounding System rated for 145 kV. There are five Power Transformers of different rating installed in substation which convert 132 KV voltage into 11 kV and 22 kV voltage. This is feed to corresponding 11 kV Bus (S1-S6) and 22 kV (S11-S14). The distribution system at IPR involves various voltage levels. All high power electrical loads are supplied from a 132 kV switchyard through 5 power transformer feeders with associated 11 kV and 22 kV systems. Further distribution in LT (415 V) supplies to various low power loads.

The TR#3 and TR#4 power transformer of rating 132kV/11kV, 15 MVA was installed and commissioned, back in the year 2000, to cater to the continuous loads SST#1 auxiliary systems as well as that of IPR campus.

This paper presents the procedures for major overhauling, gasket replacement and testing of power transformer. Transformer maintenance at regular intervals is very important which includes the major Overhauling. Overhauling of a large transformer is very complex which will be explained in easy steps in this paper.

References:

[1] Power Transformers Principles and Applications – John J. Winders, Jr
[2] NFPA70B – 2006, Recommended Practice for Electrical Equipment Maintenance.
[3] IEEE 902-1998 – Guide for Maintenance, Operation and Safety of Industrial and commercial Power System.

NFT-P-8

FOCUSING OF HIGH CURRENT ION BEAM BY APERTURE DISPLACEMENT TECHNIQUE

Mukti Ranjan Jana
Institute for Plasma Research, Bhat, Gandhinagar – 382428
E-mail: mukti@ipr.res.in

The objective of ion beam focusing is to minimise beam divergence. This leads to improvement in the beam transmission, reduces heat loadings on different components of the injector and duct, neutral beam injection port of tokamak e.g. SST-1. Parameters of ion beam focusing are determined by the dimensions of the ion extractor grids, beamline, injection port, and the distance of the target plasma from the ion extractor grid. The beamline is composed of an ion source, ion extraction system, neutralizer, bending magnet, ion dump, V-target, cryopump, gas feed system, cooling, and power supply system. The placement and dimensions of these components have been optimized for their individual performance and for the influence they have on each other as an integral component of the beamline. The beam enters the plasma at a tangency radius of 98 cm by inclining the beamline by 27o w.r.t major radius at the injection port. SST-1 entrance duct is at 5.4 m and the major radius of the plasma is at 7 m from the earth grid. PNBI port access is 27 cm (W) × 60 cm (H). Reserving minimum and optimized space for mounting cooling panels, the net available access for transmission is ± 9.5 cm horizontally and ± 20 cm vertically. In order that duct walls are within tolerable heat load (10 MW/m2), beam transmission power loss is ~ 150 kW per MW neutral beam power, we fix horizontal focal length (f_h), lie at the entrance of the duct and vertical focal length (f_v) at the major radius of a tokamak plasma. This procedure fixes f_h~ 5.4 m and f_v~ 7m. Focusing of beamlets of the beam to a common point or a line can be achieved by shaping the grids in a suitable manner. The simplest way is to give a requisite amount of curvature to shaped extractor grids. This method is suitable for low power, short duration beams. In this case, curvature remains stable. For large rectangular extraction area (dictated by rectangular duct at tokamak entrance), shaped grids are not suitable for focused, long pulse high power ion beam because differential heat deposited on grids lead to differential changes in the curvature of grids builds up of stress at the edges where grids face a fixed boundary of the mounting support structures. Further, it is difficult to achieve two focal length parameters, f_h and f_v with one mechanical process. This paper will describe in detail of achieving two focal lengths parameters. We have selected two processes: (1) offsetting the apertures of deceleration grid (or earth grid) w.r.t acceleration grid to obtain one focal length and (2) combination of both apertures offsetting and splitting the grid in two halves and inclining at an angle of 1.07^o to obtain second focal length parameter. We use offsetting method for f_h and combination method for f_v. The maximum offset in direction is ~ 400 µm.

NFT-P-9

QUANTUM COMPUTER USING PROTEIN SYNTHESIS AS BLOCKCHAIN TECHNOLOGY

A.B. Rajib Hazarika
Department of Mathematics, Diphu Government College, Diphu Assam, India-782462
E.mail: drabrh_dgc5163@rediffmail.com , drabrh02@gmail.com

The application of protein based blockchain technology is studied with equal amount of Amino acids and peptides to form paired assets coexisting to provide entanglement at any time which are the most essential element in our life. The blockchain of polypeptides and amino acids acts as bio quantum computer.The most energy efficient quantum computers. The study uses quantum cryptography to understand the entanglement process.

Keywords: *Quantum cryptography, biological quantum computer,blockchain*

NFT-P-10

OVERVIEW OF THE RECENT INVESTIGATIONS ON THE SURROGATE-PARTICLE-IRRADIATION IN TUNGSTEN PLASMA-FACING-MATERIALS

P.N. Maya[1, *]and S.P. Deshpande[1,2]
[1]*Institute for Plasma Research, Gandhinagar, Gujarat 382428, India*
[2]*Homi Bhabha National Institute, Anushaktinagar, Mumbai, Maharashtra, -400094 India*
E-mail:pnmaya.n@gmail.com, pnmaya@ipr.res.in*

One of the major challenges in the realization of a fusion power reactor is the long-term operation of the in-vessel components under high neutron and heat flux.At present, there exists no fusion relevant test facility that can simulate the simultaneous heat and the neutron loads that a component will get exposed under the reactor-relevant conditions. Therefore, accurate predictive modelling is the only option to validate the material properties under such extreme conditions. Although there is no single recipe to do this, the general approach requires a set ofexperimentally validated and benchmarkedmodelsthat can link the atomistic features of radiation cascade and residual defects formed in a few pico-seconds to macroscopic material failure happening over several full-power years of operation. Surrogate particle-irradiation using ions, electrons, γ-rays and fission neutrons can notonlyvalidate such models but also provide insightsabout different mechanisms of multi-scale processes leading to their failure.In this context, we present the ongoing activities in tungsten plasma-facing material which is one of the most promising candidates for both first-wall and divertor of the fusion power reactors due to its high melting point, low erosion yield and low

affinity for hydrogen. However, the simultaneous exposure of the neutrons and γ-particles create radiation damage in tungsten which can adversely affect its otherwise favourable properties. Under the IAEA-CRP project (No. 18180/R0) extensive ion irradiation experiments and modelling were carried out involving different irradiation facilities across India and these results have conclusively shown that contrary to the popular understanding, the choice of ion mass and energy do play a critical role in the defect created in tungsten [2,3,4]. These studies have also brought out novel features of the atomistic strain-driven gas diffusion in metals which might explain the fundamental features of blister formation, gas permeation in advanced metal-membranes, gas-target formation etc [5]. These experiments have also shown for the first time a direct atomistic observation of the conjecture of the vacancy nucleation during the non-conservative motion of grain boundary during recrystallization [6]. We also present the planned experimental efforts on the gamma and fission neutron irradiation and apotentialscopeof activities to create statistical failure models for fusion reactor materials by compiling large volume experimental and modelling data, their visualization and the methods of deduction using various statistical and AI-based techniques.

References:

[1]. S. P. Deshpande et al., book chapter, Atomic and Plasma-Material Interaction Data for Fusion, IAEA Vol. 18, 3-44, (2019)

[2]. P.N. Maya et al.,(2019) Nucl. Fusion 59 076034

[3]. P.N. Maya et al., *Studies on the Role of Ion Mass and Energy in the Defect Production in Irradiation Experiments in Tungsten*, Nuclear Fusion, Accepted, Oct (2021)

[4]. P. Sharma et al., Microscopy and Microanalysis (2019), 1–7

[5]. P.N. Maya et al., (2021) Nucl. Fusion 61 036007

[6]. P.N. Maya et al., Materials Letters 283 (2021) 128801

NFT-P-11

MECHANICAL DESIGN OF PROTOTYPE CENTER STACK (PCS) FOR SPHERICAL TOKAMAK BASED TECHNOLOGIES DEVELOPMENT

A.K. Verma, S. Ranjithkumar, Prasada Rao P, Shiju Sam, Y.S.S. Srinivas, E.Rajendra Kumar
Institute for Plasma Research, Bhat, Gandhinagar-382428, Gujarat, India
E-mail: adityakumar@ipr.res.in

Spherical Tokamak (ST) is a special type of magnetic confinement configuration-based Tokamak which is being pursued to develop fusion energy for commercial power production on afast track approach. STs are smaller in size as compared to conventional tokamaks. STs have theleast possible bore in the center because of which the resultant plasma shape is nearly spherical. Thecompactness and modular features make this machine very attractive.

The main components of ST are Center Stack (CS) (an integrated structure consisting of TF innerlegs, Ohmic coil and their casing), TF outer legs, Vacuum Vessel, auxiliary powers sources andsupport structures. Design and fabrication of the Center Stack (CS) assembly is one of the mostcritical & challenging system (in magnetic and mechanical aspects) of Spherical Tokamak configuration. The study of small scalecenter stack with TF outer legs has been attempted in this project and a Prototype of Center Stack (PCS) has been designed. Further, it is planned to construct aPCS assembly to validate the indigenous design.

PCS consists of two sets of coils- Toroidal Field (TF) coils and Ohmic (OH) coil. The OH and TFcoils are mainly designed to produce 0.025 volts.sec and 0.1 Tesla magnetic field (at its majorradius) respectively. The power supply for the TF coil to generate the required field is rated for8.5kA. The ripple is checked by simulation and is <1% with six TF coils connected in series. TheOH power supply is rated for 10 kA that produces required flux.

Each TF coil consists of 3 turns which are connected electrically in series. The trapezoidal shaped (38 mm radial width) inner turns are considered for the design in order to achieve high packingfraction. The inner legs are connected to the outer legs via radial and flexible U connectors. Thecross-section of 50 x 10 mm2 copper conductor is considered for the TF outer turns. OH coil iswound in 2 layers with 143 turns in each layer. A square cross-section conductor of 5.6 x 5.6 mm2with a central cooling hole of 2.5 mm diameter is considered for the OH coil winding. Anappropriate support structure of SS304 is also designed for the PCS coils and assembly.This poster describes the mechanical design of PCS coils, support structure, components arrangement and assembly sequence of coils.

NFT-P-12

DESIGN OPTIMIZATION OF PROTOTYPE CENTER STACK (PCS) TOROIDAL FIELD COILS

S. Ranjithkumar, A.K. Verma, Prasada Rao P., Shiju Sam, Y.S.S. Srinivas, E.Rajendra Kumar
Institute for Plasma Research, Bhat, Gandhinagar-382428, Gujarat, India
E-mail: ranjith@ipr.res.in

A Prototype Centre Stack (PCS) is being designed and developmentat Institute for Plasma Research (IPR) as a part of R&D activities in Spherical Tokamak (ST) technologies. One of the major challenge in the Spherical Tokamaktechnologies is design and development of center stack, which consists of inner legs of TF coil, the Central Solenoid coil and the casing as an integrated component.

The PCS system consists of six number of TF coils made of ETP copper, with three turns per coil, all connected in series. Each TF coil is made of two parts – the inner leg and the outer leg, possessing three turns each. The inner leg of the TF coil isstraight, with trapezoidal cross section, and all the 18 inner leg turns together form a circle at the inner bore region. The outer leg has a D-shaped configuration and the turns arerectangular in cross section. The turns are sufficiently insulated from each other using G-10 material.

The TF coil is subjected to electromagnetic forces and thermal loadsduring operation. During the design optimization various combinations of inner to outer leg connections were attempted and based on a thorough study, the orientation of TF coil as well as the connection between the inner and outer leg (using a U bend connection at top region) was finalized. The support structure of the machine is designed mainly considering the loads experienced by the TF coil.

The coil operates at 8.5kA to produce a field of 0.1Tesla at the major radius of 0.28m. Considering the nominal operational requirement with a specified time duration, the rise in temperature of the TF coil is ~4°C per shot. However, considering eight hours of operation of ST for 30 back to back shots in a day, active cooling by water circulation has been considered for inner legs of the coil. The bulk of electromagnetic load on the coil is radially inward direction which is restricted by the G10 rod at the centre of the bore.

This poster discusses the design optimization and analysis of the TF coils in PCS machine, including the iterations carried out in the process of design. Electromagnetic and thermal analysis has been performed on the coil using ANSYS Mechanical, Multiphysics and Maxwell software modules. In addition, the cooling requirement is also envisaged for the continuous operation of the coil.

NFT-P-13

R&D IN FABRICATION OF CENTER STACK FOR SPHERICAL TOKAMAK TECHNOLOGIES DEVELOPMENT

Shiju Sam, A.K. Verma, S. Ranjithkumar, Prasada Rao P., Y.S.S. Srinivas, E. Rajendra Kumar
Institute for Plasma Research, Bhat, Gandhinagar-382428, Gujarat, India
E-mail: shiju@ipr.res.in

The Center Stack (CS) assembly is one of the important systems of Spherical Tokamak configuration. Its compact design makes this spherical compact configuration attractive. Efforts have been carried out in order to study and design a typical Prototype Center Stack (PCS) Assembly which consists of components such as toroidal field (TF) coils, ohmic (OH) coil, tension cylinder, center stack casing and support structure arranged in a limited volume. As a result, achievement of dimensional accuracy with strict control on tolerances at each stage of the manufacturing, during and after assembly becomes a challenge. In the PCS design, a single complete TF Coil made of ETP Copper is formed by connecting the three inner TF turns with the outer leg while the OH coil is formed by winding an insulated continuous square cross-section ETP Copper conductor (5.6mm x 5.6mm), having a throughout opening of 2.5mm diameter in the center, over an insulated tension cylinder of SS 304.

Small mock-ups of TF inner turn and OH coil (both 300 mm length) were fabricated to assess the fabrication feasibility of the designed TF inner turn & OH coil for possible challenges and to improve design. The TF inner turn has a water cooling tube of 4mm OD along its entire length on one side which needs to be brazed. The TF inner turn small samples were fabricated through two routes: (a) TF inner turn made by machining ETP Copper bar with a slot for fitting the 4mm OD copper tube with 0.9mm wall thickness and brazing it on the surface along the entire length; (b) TF inner turn made by machining ETP Copper bar with a throughout hole of 4mm diameter for cooling made by wire-cut EDM and Copper tubes brazed on both ends. Both these mock-ups were checked for dimensional measurements and brazed joints were tested for leak through helium leak detection in vacuum mode. No degradation was found in the helium background leak rate (1.6 x 10-9 mbar.l/s) at anywhere on the brazed region. The OH coil mock-up was fabricated by winding a solid bare copper conductor (6mm x 6mm) on 3.5 inch SS 304 pipe of with conductor entry exit attachment for the end connections. This coil was checked for dimensional measurements only. Most of the achieved dimensions in the three mock-ups were within 0.5mm of the specified dimensions while other deviations were less than 1mm.

Fabrication of these small mock-ups provided needed R&D experience in validating the design of PCS coils from fabrication aspect. This poster highlights the challenges addressed in the fabrication of these mock-ups and inputs obtained related to achievable and permissible tolerances in these components on the shop floor to finalize design details for fabrication.

NFT-P-14

ELECTRICAL DESIGN OF CENTER STACK FOR SPHERICAL TOKAMAK BASED TECHNOLOGIES DEVELOPMENT

Prasada Rao P, Y.S.S. Srinivas, A.K. Verma, S. Ranjithkumar, Shiju Sam, E.Rajendra Kumar
Institute for Plasma Research, Bhat, Gandhinagar-382428, Gujarat, India
E-mail: prasad.rao@ipr.res.in

In the present world, to fulfill the fast growing energy requirements, Fusion Energy is the one of the best choices. Spherical Tokamak (ST) is one of its kind which is being pursued for commercial production of fusion energy. In ST, Center Stack (CS) is the major component with many challenges in design because of its limited bore area.

In IPR, efforts are in progress to develop a Prototype Center Stack (PCS) with TFcoils. PCS consists of Toroidal Field (TF) inner legs and outer legs, Ohmic (OH) coil and their casing. In the present design, the targeted TF field at the major radius is 0.1T. The design of TF has six number of coils in which each coil consists of three turns. The current required to produce 0.1T at major radius is ~ 8.5kA. The ripple in the optimized design is less than 1% at major radius. The OH coil is wound in two layers with an input peak current of ~10kA. To finalize the insulation material and thickness, the electric field stresses are analyzed in all critical areas. Based on this analysis, the polyester glass fiber tape, G-10, Teflon are selected as insulating materials for these coils. Further, Vacuum Pressure Impregnation (VPI) process is also recommended during fabrication.

Present poster describes the electrical insulation design for the TF and OH coils. Details of estimation of TF field & ripple at major radius and estimation of resistance of joints in the coils are also presented.

NFT-P-15

ERECTION, INSTALLATION, TESTING AND COMMISSIONING OF 1600KVAR, 11KVAPFC SYSTEM

Chirag B. Bhavsar, Prakash Parmar, C.K Gupta, Supriya Nair
Email: chirag@ipr.res.in

Electrical Power Distribution System in IPR comprises of 132 kV Substation suppliedby dedicated 2 GVA SCC line by the Grid Operator (UGVCL). The 132 kVsubstation hosts four 132 kV / 11.5 kV main step down transformers of 31.5 MVA, 37.5 MVA and 2 x 15 MVA and one 132kV/22 kV step down transformer of rating 31.5 MVA. The total installed capacity of around 130 MVA caters to bothsteady/ continuous power demand (~6 MW) and pulse power demand (~50 MW) of the

Institute. The power demanded by the systems is supplied at 11 kV, 22kV & 415V voltage levels. Requirement of Automatic Power Factor Capacitor (APFC) System have a numerousadvantages like power factor correction, reducing reactive power & I2R Power loss &KVA loading of Transformers loss and high PF using full capacity of power systemnetwork. A high power factor eliminates penalty charges and give incentive amountabove required value. The APFC device calculates the reactive power consumed by asystem's inductive load and compensates the lagging power factor using capacitancefrom a capacitor bank.

This paper covers Erection, Installation, testing and commissioning of 1600KVAr, 11kV Automatic Power Factor Capacitor (APFC) System.

NFT-P-16

STRUCTURAL DESIGN OF WINCH SYSTEMFOR REMOTE HANDLING APPLICATION

Manoah Stephen M, Ravi Ranjan Kumar, Naveen Rastogi, Krishan Kumar Gotewal, Jignesh Chauhan
Institute for Plasma Research, Gandhinagar-382421, Gujarat, India
E-mail: manoah@ipr.res.in

Failed in-vessel components replacements requires lifting, hauling and holding heavy payload plasma facing components with the help of winch system and multi-joint maintenance manipulator. Basically winch recounts an integrated assembly which consists of a drum, sheaves carrying wire ropes and actuated by some form of power units. Winches are hoisting, pulling and holding equipment’s in which a tensioned wire rope is winded round a rotating drum. The selection of drum/ wire rope configuration, transmission drive and actuators depends upon the designed application.

This paper presents the structural design of a winch system, which consists of rotating drum, pulleys, wire rope self-reversing screws and actuators with braking system. A dual design approach, design by formula and design by analysis in combination with two standards SAA and DNV are used to achieve the optimised design solution. Design by formula was used to arrive at preliminary design of drum, wire rope, actuators with brakes, spooling system, and transmission system. Further design by analysis is used to optimise the design of drum for different loading condition and payload capacity of 50 kg. A combination simulation platform based on ANSYS workbench and Rigid Body Dynamics are used for optimisation and selection of suitable actuator components. Finally a structural design is arrived by demonstration of proposed approach in design of winch system with desired constraints.

Keywords— winch system; sheaves; wire rope; remote handling**.**

NFT-P-17

SST-1 CRYOGENICS PLANT MONITORING SYSTEM USING EPICS OPC

V.B. Patel[1], A.L. Sharma[1], H.H. Chudasma[1], H. Masand[1], I.A Mansuri[1], J.J. Patel[1], M.K. Bhandarkar[1], P. Gaddam[1,] P.N. Panchal[1],R.J. Patel[1], T.S. Rao[1], V.L.Tanna[1], K. Mahajan[1] and SST1 Cryogenics Team

[1]Institute for plasma research, Bhat, Gandhinagar, 382428

E-mail: vishnu@ipr.res.in

SST-1 Cryogenics plant with 1.3 kW at 4.5K capacityis installed at IPR to supply liquid helium to magnet system of SST-1 tokomak. The plant consists of Purifier, Coldbox, Compressor system and Distribution system. These systems are having individual PLC and connected in a master slave architecture with cold box PLC which is acting as a master.An overall supervisory control system is setup using Citect SCADA while some of the PLCs are being monitored using Wonderware software from Schneider Electricals.

Normally a SST-1 campaign lasts for around 1 month that includes magnet cool-down, plasma experiment and magnet warm-up period. During this period monitoring of SST-1 cryogenics plant at anytime from anywhere in the institute is realized by incorporating EPICS SCADA into the system without disturbing the existing software setup.

This paper presents challenges in integration of EPICS OPC client with Wonderware FS Gateway which is part of Wonderware SCADA package. This EPICS OPC client acts as an EPICS IOC server to make data available to any EPICS client such as CS-Studio BOY, data-archiver, data browser etc. over channel access.

NFT-P-18

COMPARATIVE STUDY ON THERMAL PROPERTIES OF DIFFERENT GRADES OF HIGH DENSITY GRAPHITE

ArunPrakash Arumugam*, K.P. Singh, P. Patel, S. Khirwadkar, D.C. Raval and Z. Khan

Institute for Plasma Research, Bhat, Gandhinagar-382428, Gujarat

**Email: arun@ipr.res.in*

Beryllium, Tungsten and Carbon are typically considered as armour material for Plasma Facing Component (PFC) of Fusion devices. Each of these three candidate materials has some inherent advantages and dis-advantages. Their application as armour material in Tokamak depends on the specific operational requirements. Carbon based materials, namely; Graphite and Carbon Fiber Composites (CFC) are the preferred armour materials in present day Tokamaks. As Graphite being a high

temperature material, it is widely used as an armour material for first wall in Tokamaks. High thermal shock resistance and low atomic number of carbon are the most important properties of graphite for its application as an armour material in many Tokamaks. High density graphite of grade FP479 is chosen as plasma facing armour material in SST-1 Tokamak. About 1,200 kg of graphite material will be used as plasma facing material in SST-1 tokamak in the form of shaped tiles. There are about 3800 numbers of graphite tiles of different sizes bolted on 132 numbers of PFC copper modules. Selection of graphite is based on criteria involving different thermo-physical properties. Some of the important requirements are: thermal conductivity, ash content, open porosity, flexural Strength, etc. Thermal properties of graphite plays a major role in graphite selection. Hence graphite thermal properties are measured experimentally. Thermal properties of graphite such as Thermal Conductivity, Thermal Diffusivity and Specific heat are measured from room temperature to high temperature using laser flash technique at HTTD, IPR.Commercially available high density graphite grades around the world were chosen to compare the thermal properties at room temperature and elevated temperature. Three grades of high density graphite chosen for the study are (i) FP479 grade manufactured by Schunk Kohlenstofftechnik GmbH Germany, (ii) IG430 from Toyo Tanso, Japan and (iii) DXN from Graphite India Ltd., India. This paper will discuss about the experimental results of thermal properties of different grades of high density graphite at various temperature and the variation of thermal properties with temperature.

NFT-P-19

DESIGN AND SIMULATION OF TWO-WAY RF COAXIAL SWITCH FOR ICRH EXPERIMENTS

*Uttam Kumar Goswami, Nikhil Vispara, Raj Singh and P. K. Atrey
Institute for Plasma Research (IPR), Gandhinagar, India
E-mail: uttam.goswami@ipr.res.in

The increasing need for fusion plasma research in the ICRF domain necessitates the use of a high-power RF switch. The high-power RF switches aren't indigenously available due to technical design constraint & fabrication complexities. An innovative RF switching system has been designed and simulated by electro-mechanical approach with high & long-term reliability. The design concept enables RF coaxial switches to be produced with very high operating life (million cycles), maintaining no increase in contact resistance and reliability over time. The paper presents the design aspects of 3-1/8 inch coaxial RF transfer switch for applications in ICRH 50-ohm transmission lines, primarily to improve the system performance and when failures occur, enabling emergency repairs by facilitating quick checks under actual operating conditions. The designed switch is double-pole, double throw configuration, which enable the changing

of coaxial connections between RF transmitters and antenna or dummy loads with a minimum changeover time. The unique internal construction will make this switch a very cost-effective. The switch is designed to support 20 kW RF power and anticipated to operate in the frequency range of 10 to 100 MHz, with a reflection coefficient (S_{11}) -32 dB and the transmission coefficient (S_{21}) -0.005 dB in normal operation. The CST EM solver has been used to investigate the RF electric field distribution in the designed coaxial RF transfer switch and the simulation results are validated in the fabricated switch.

References:

[1] Sanket Chaudhary, Atul D Varia, Fiazuddin Shaik, SV Kulkarni and ICRH Group; "*Design and Simulation of RF Switch & Impedance matching in T-Junction Transmission line*", Research report: IPR/TR-285/2014, May 2014.

NFT-P-20

STUDIES OF EDGE PLASMA PARAMETER IN ADITYA-U TOKAMAK USING UEDGE CODE

Ritu Dey[1], Tanmay M. Macwan[1,2], Harshita Raj[3], M. B. Chowdhuri[1], Joydeep Ghosh[1,2], R. L.Tanna[1], R.Manchanda[1], Deepti Sharma[1], T. D. Rognlien[4]

[1] Institute for Plasma Research, Gandhinagar 382428, India

[2]Homi Bhaba National Institute, Anushakti Nagar, Mumbai 400094, India

[3]EPFL, Route Cantonale, 1015, Lausanne, Switzerland

[4]Lawrence Livermore National Laboratory, Livermore, CA 9455, USA

E-mail: ritu.dey@ipr.res.in

In the core-edge region of a tokamak, the magnetic flux surfaces are closed on themselves, and charged particles move along the field lines and are confined to the flux surfaces. Outside of the last closed flux surface (LCFS), there are open flux surfaces, and they are in direct contact with material walls/limiter/divertor of the fusion reactor. Due to the changes of magnetic field lines from closed to open there are various time-scale and length-scale are involved in edge plasma transport. So the study of edge region of tokamak plasma is very challenging. We report the analysis of edge plasma parameters in ADITYA-U tokamak plasma using the UEDGE code. UEDGE, which is a two dimensional edge plasma fluid transport code, is applied for ADITYA-U limiter configuration. The simulated radial profiles of electron density and temperature are compared with the recent experimental measurements. The details of this investigation will be presented at the conference.

NFT-P-21

INSTALLATION AND COMMISSIONING OF THE ARC DETECTION SYSTEM FOR PF BUS BARS IN SST-1 CRYOGENICS INTERFACE

H. Nimavat, H. Dalicha, N. Ramaiya, D. Sonara, R. G. Trivedi, R. Manchanda, V. L. Tannaand D. Raju
Institute for Plasma Research, Bhat, Gandhinagar
Email: hiren@ipr.res.in

In order to detect unpredicted Arcs either due to Paschen Discharge or any other electrical ground faults in the superconducting (SC) current feeders system (CFS), an optical fibre based flash arc detection system is introduced in SST-1. From the recent event of flash arcs between PF3 SC feeders and cryostat ground, this system will work as precautionary measures to mitigate any major damages inside the Cryostat by identifying arcs if any phenomena happen again. To visualise the condition of flash arcs in a vacuum, a lab-scale cryostat is developed and the arc detection system is tested for low energy flash arcs. This system of arc detection is unique in its class as it is made to detect vacuum arcs mostly as well as it will collect direct or indirect light from very cold surfaces where SC magnet cable in conduit conductors (CICC) bus bars are connected with SC current feeders or current leads (CL). The difference between a normal flash arc detector and this arc detector for SST-1 is the complexity of optical fibres mounting in vessel-in-vessel type vacuum chambers, coupling loss reduction as well as detection of vacuum arcs from ultra-cold surfaces. Light is to be detected from inside SST-1 cryostat vessel which is already in the CFS vacuum chamber. As per requirement, optical fibres are mounted on vacuum compatible optical feed-throughon PF ducts of Cryostat inside CFS and routed in vacuum to optical window. This paper will describe lab-scale tests and installation of fibre optic arc detection system in CFS chamber.

Reference:

(1) Development of Arc Detection System for RF source and Microwave Componentspresented by Hrushikesh Dalicha et al, in PSSI-19.

NFT-P-22

PIPING LAYOUT OF CRYOGENIC EXPERIMENTAL SET-UP FOR 3-STREAM PLATE-FIN HEAT EXCHANGER

O Chandratre[1], Vivek Sharma[2], A K Sahu[1], H Kavad[1]
[1]*Institute for Plasma Research, Bhat, Gandhinagar 382428*
[2]*NIT, Rourkela, Odisha*
E-mail: omkar.chandratre@ipr.res.in

The indigenous IPR helium refrigerator/liquefier (HRL) plant being developed at Gandhinagar, Gujarat, for tokamak application, has Vacuum-brazed Al-plate-fin heat exchangers. These are some of the most important components of the cold box of the

HRL. These Heat Exchangers will be used at cryogenic temperature and are generally made of aluminum alloy (Al3003/Al5052) considering high thermal conductivity, good machinability and good mechanical strength at low temperature. A 3-stream plate-fin heat exchanger (HE), to be used for HRL plant, has been designed and manufactured indigenously. This is a vacuum-brazed counter-flow type with serrated fins of fin density ~700fins/m. The performance test of this 3-stream heat exchanger has been done at cryogenic temperature. The piping design and layout has been done carefully to take care the operating pressure and thermal stresses [1,2]. The piping layout has been analyzed using CAESAR II software for stress analysis for both room temperature and 80 K operational situations. The details of these will be presented in this poster.

Keywords: Piping analysis, Cryogenic temperature, heat exchanger

References:

[1] Process plant layout and piping design, Bausbacher,ED and Hunt,Roger,PTR Prentice Hall 1993.

[2] Piping and pipeline calculation manual construction, design fabrication and examination,Ellenberger,J.Phillip,publish by Elsevier2010.

NFT-P-23

PARAMETRIZATION OF OHMIC TRANSFORMER POWER SUPPLY FOR ADITYA-U TOKAMAK

K S Shah, M N Makwana, Shivam Kumar Gupta, B V Nair, S Nair, R L Tanna,
Joydeep Ghosh, and Aditya-U Team
Institute for Plasma Research, Bhat near Indira Bridge, Gandhinagar, Gujarat (India) 382428

Ohmic Transformer Power Supply (OTPS) consists of 11kV VCB, Converter Transformers, 12-pulse dual converter, Controller, sequencing and logic Panels operated through VME interface and DC Isolators. OTPS is rated for +/- 20kA, 2.2kV with wave shaping circuit consisting of DC VCB, 1200µF Capacitor bank, and 1.8Ω Resistor Bank, and associated Switches for commutation purposes [1].

Plasma Loop Voltage (V_L) is controlled through appropriate resistance connections for R1, R2 & R3 as per plasma experiment requirement. For Aditya-U Operation R1 is connected at 0.84/ 0.72Ω tapping, R2 is connected at 0.48/ 0.36Ω tapping and R3 is connected at 0.06Ω tapping which gives peak V_L of ~ 20-25V. According to experimental requirement,the V_L profile for gas breakdown and subsequent plasma ramp-up phase is set by inserting resistances (R1, R2, R3) in the waveshaping circuit through ignitrons at appropriate timing intervals(T1, T2, T3) respectively[2]. During the plasma flat-top phase, a certain minimum V_L is required which is obtained using negative converter operation. A negative Converter is used to maintain a constant di/dt thereby affecting a certain minimum VL. Signal I_{OT} reference is configured at VME GUI to effect required I_{OT} profile as required for necessary di/dt to maintain V_L.VME system output is connected to respective controllers through optocouplers.

R1, R2, R3 resistances tapping alongwith their switching instants T1, T2, T3 configuration and I_{OT} reference parameter settings at VME GUI as required for different Plasma Loop Voltage (V_L) are depicted and described in this Poster.

References:

[1] V. Balakrishnan, C.N. Gupta, R.K. Sinha, Plasma current and position feedback control in ADITYA Tokamak, Fusion Engineering and Design, Volumes 66–68, 2003,Pages 809-813,ISSN 0920-3796.

[2] Bhatt, S B &D.Bora, &C.N.Gupta, et al., (1989). Aditya: The first Indian Tokamak. Indian Journal of Pure and Applied Physics. 27. 710.

NFT-P-24

SIMULATION OF UNIAXIAL COMPRESSION TESTS ON CERAMIC PEBBLE BEDS FOR ITS MECHANICAL CHARACTERIZATION

Maulik Panchal[*,1], Harsh Patel[1], Paritosh Chaudhuri[1,3]
[1]*Institute for Plasma Research, Bhat, Gandhinagar-382 428, India*
[3]*Homi Bhabha National Institute, Mumbai - 400 085, India*
E-mail[*]: maulikpanchal@ipr.res.in

The lithium-based ceramic materials in the form of nearly spherical-shaped particles have been selected as a tritium breeder in the solid breeder blankets of the future fusion reactor. The pebbles are packed in a canister in the state of random close packing. The uniaxial compression test is one of the well-known techniques for the mechanical characterization of granular material such as pebble beds. In this work, the uniaxial compression tests have been simulated using the Discrete Element Method (DEM) to generate the stress-strain response of different pebble beds. The mono-sized, binary-sized and poly-dispersed assemblies of pebble beds have been considered for simulation studies. The effect of size ratio and size variation on the stress-strain response of the pebble bed has been examined. During the cyclic loadings of the pebble bed assemblies, the effect of external load on the micro-information like contact force, coordination number, etc. has been investigated. The predicted values of the effective modulus of elasticity of pebble beds by DEM simulation have been compared with the experimentally obtained values from the literature.

NFT-P-25

AN ARTIFICIAL INTELLIGENCE BASED SOLUTION FOR SST1 TOKAMAK BUILDING MONITORING

Agraj Abhishek, Abhishek Sharma, Gaurav A. Garg, Hitesh H. Chudasama, Daniel Raju, Manika Sharma
Institute for Plasma Research, Bhat, Gandhinagar382428, Gujarat, India
Email: agraj@ipr.res.in

Closed circuit television (CCTV) has been around for nearly two decades and hasgrown multifoldwith the advancement of IP enabled cameras, larger bandwidths andfaster INTERNET speeds. Security camera surveillance is a valuable asset forlaboratories and keeps experiments, equipment, intellectual property and researcherssafe. SST 1Tokamak building being one of the most important experimental placesat IPR campus, needs continuous monitoring and surveillance. So, we have come upwith a Convolutional Neural Network (CNN) based software solution which takesinput from CCTV cameras and raises an alarm when any intruder or object of interestis detected for an undefined hour. The software solution also ensures the security andsafety of researchers and equipment during ongoing experiments by detectingabnormal events like fire etc. The software accuracy is more than 97%, with a veryhigh sensitivity/ specificity value of 94.9% and 98.6%.

NFT-P-26

UHV TESTING OF PROTOTYPE STEERABLE ECRH LAUNCHER

Hardik Mistry, Dharmesh Purohit, Siju George, Harshida Patel, Jatin Patel, K G Parmar, Dilip Raval, Manoj Kumar Gupta, B K Shukla
Institute for Plasma Research, Bhat, Gandhinagar-382428, Gujarat, India
E-mail: hardik.mistry@ipr.res.in

Electron Cyclotron Resonance Heating (ECRH) can be used for various experiments on the tokamak. It is primarily used for pre-ionization, heating, current drive and Neo-classical tearing Mode (NTM) suppression. Suppression of NTMs can be achieved by controlling the localized EC power deposition in the plasma at the island locations. This can be accomplished by real time steering of EC beam in the poloidal plane. A new prototype ECRH launcher is developed which will enable the beam steering in poloidal and toroidal directions. The launcher system consists of plane mirror, profiled mirror, steering mechanisms, bellow, servo motors and rotary encoders. High speed accurate mirror movement under UHV is a major technical challenge for development of steerable launcher. The UHV compatibility of the launcher has been tested in a

specially designed vacuum chamber. The ultimate vacuum level of 4×10^{-9} mbar has been achieved after baking the whole assembly at 150 °C for approximately 48 hrs. The temperature of was continuously monitored by temperature sensors during the baking cycle. The mirror movements of the movable (flat) mirror along poloidal and toroidal axis was also checked under UHV. Accuracy of ~0.03° and repeatability of ~0.01° were achieved for both the axis.The poster describes the design of the launcher, testing procedureand various tests carried out under UHV in a specially designed vacuum vessel.

NFT-P-27

DEVELOPMENT OF CALIBRATION UNIT FOR CALORIMETRIC PULSED POWER MEASUREMENT OF HIGH POWER MICROWAVE SOURCE

Hardik Mistry, Harshida Patel, Jatin Patel, DharmeshPurohit, K G Parmar,B K Shukla

Institute for Plasma Research, Bhat, Gandhinagar-382428, Gujarat, India

E-mail: hardik.mistry@ipr.res.in

ECRH is one of the main heating systems of tokamaks. ECRH system comprises of high power microwave source (Gyrotron), matching optics unit (MOU), transmission line, polarisers, mitre bends, RF switches and launcher.The high power microwave beam generated by Gyrotron is launched into the plasma. The power measurement of microwave beam is important for carrying out controlled plasma experiments. The pulsed power of the Gyrotron can be measured by calorimetric method. In this method, the high power generated by Gyrotron is launched into the dummy load and the energy is absorbed by the flowing water. The inlet and outlet temperature of the flowing water is continuously measured and the output power of the Gyrotron is estimated by measuring the area of the temperature difference signals. Calibration with known energy is required to obtain the calibration factor.

The calibration unit with the arrangement of the heater is developed which can provide 10kJ of thermal energy. Design and fabrication of probe assembly significantly effects the temperature response and measurement accuracy. The effect of probe material and wall thickness on the thermal response of the probe is studied through finite element simulations. The calibration unit is tested at different (10LPM and 21 LPM) flow rates and different power levels for checking the consistency of the measured area values.The poster describes the Gyrotron’s power measurement procedure, the design of calibration setup, critical aspects of the system and initial experimental results.

NFT-P-28

IMPLEMENTATION OF THREE-DIMENSIONAL SIMULATIONS FOR SCRAPE-OFF LAYER TRANSPORT IN INBOARD LIMITED ADITYA-UPGRADE PLASMA CONFIGURATION

Arzoo Malwal[1,2], Devendra Sharma[1,2]

[1]*Institute for Plasma Research, Bhat, Gandhinagar, Gujarat 382428, India*

[2]*Homi Bhabha National Institute, Training School Complex, Anushakti Nagar, Mumbai 400094, India*

E-mail: arzoo.malwal@ipr.res.in

The magnetically confined plasmas display distinct transport characteristics in the open field line zone of the Scrape-off layer of the modern magnetic confinement fusion devices as compared to transport in the core region of closed magnetic surfaces. The magnetic configuration of Aditya-Upgrade is implemented for SOL transport studies by means of 3D coupled plasma-neutral simulation code combination EMC3-EIRENE [1]. This fresh implementation of Aditya-Upgrade additionally considers plasma limited by the inboard located belt limiter where poloidally local plasma surface interaction characteristics can be simulated for investigating issues of diffusion-driven radial transport [2, 3] or a partial detachment like the behaviour of plasma flow approaching the belt limiter. The present implementation has covered defining the configuration in magnetic flux surface aligned coordinate system to compute plasma transport with the effect of boundary for plasma, and neutrals, generated by the inboard located limiter target as well as the device first wall. The distribution of geometrical and physical parameters of the plasma configuration, transformed from the magnetic flux coordinates to the physical coordinates, and their localized behaviour about the inboard limiter generated plasma boundary will be presented and discussed.

References:

[1] Sahoo, B. P., Sharma, D., Jha, R. Feng, Y. Flow structure and shear generation in the 3D SOL of a circular tokamak plasma in Aditya. Nuclear Fusion 55, (2015).

[2] Sahoo, B. P., Sharma, D., Jha, R. Feng, Y. 3D Monte-Carlo study of toroidally discontinuous limiter SOL configurations of Aditya tokamak. Physics of Plasmas 24, (2017).

[3] B. LaBombard et al 2000 Nucl. Fusion 40, 2041.

NFT-P-29

PERFORMANCE STUDY OF METAL HYDRIDE REACTOR EQUIPPED WITH SPIRAL HEAT EXCHANGER

Sudhir Rai, Amit Sircar
Institute for Plasma Research, Gandhinagar, Gujarat 382-428, India
E-mail: sudhirrai@ipr.res.in

Hydrogen is being considered as a potential candidate for alternative fuel due to its high energy density per weight and no emission of pollutants. Storing and transportation of hydrogen efficiently and effectively is a challenge for its safe and economical applications. Among the storage technologies, solid-state hydrogen storage methods using Metal Hydrides (MH) have attracted considerable attention owing to their relatively higher volumetric storage density, safety and lower cost.One key issue for MH hydrogen storage systems is to achieve rapid hydrogen charging/discharging rates under the appropriate operating conditions.Often, the heat transfer rate is thecontrolling variable for absorption and desorption due to limited heat transfer within hydride bed.

A multi-dimensional, unsteady, non-isothermal mathematical model rigorously accounting for the reaction kinetics and heat & mass transfer mechanisms during the hydrogen absorption and desorption processes in MH storage system has been used to analyse metal hydride storage system equipped with spiral heat exchanger.The performance study has been carried out to minimize total storage time.Hydrogen absorption time mainly depends onthe successful heat removal from the bed.Analysis of temperature evolution inside bed with different supplied pressure has been carried out. The spiral heatexchanger is tested for its performance at various supply pressures, pitch, and cooling/heating fluid temperature. Thisperformance analysis helped in optimizing operation parameters forsignificant improvements of the time of storage and discharging of hydrogen.

NFT-P-30

CONCEPTUAL DESIGN OF GLOW DISCHARGE CLEANING SYSTEM FOR SMALL SCALE-SPHERICAL TOKAMAK

M. S. Khan, Ranjith Kumar, Shiju Sam, Y S SSrinivas, Ziauddin Khan, E. Rajendra Kumar
Institute for Plasma Research, Bhat, Gandhinagar-382428
Email: Khan@ipr.res.in

A Small Scale Spherical Tokamak (SS-ST) is being designed at IPR with the objective to produce low aspect ratio plasma and perform various basic plasma experiments to generate database in support of compact fusion. DC glow discharge cleaning (GDC) technique[1], using hydrogen has been planned for wall conditioning of the SS-ST Tokamak to reduce low z impurities residing on the walls of vacuum vessel[2].

SS-ST will include two movable anodes at the two locations 180° apart from two top ports of the machine. During glow discharge cleaning (GDC), the anodes will be inserted in to the machine from the top port up to 10 cm below the axis of the machine. The length of the exposed anode will be 20 cm. A dedicated DC power supply with all safety control system will be connected to the anode. In this paper, we presented the conceptual design of glow discharge cleaning system for Small Scale Spherical Tokamak (SS-ST).

References:

[1] Modelling of tokamak glow discharge cleaning I: physical principles, Plasma Phys. Control. Fusion **57** (2015) 025008 (14pp).

[2] Wall conditioning in fusion devices and its influence on plasma performance, Plasma Phys. Control. Fusion **38** (1996) 1503–1542. Printed in the UK.

NFT-P-31

LAYOUT OF CRITICAL PERIPHERAL EQUIPMENT'S FOR INDIGENOUS HELIUM REFRIGERATOR/LIQUEFIER PLANT

Hitesh R Kavad, A K Sahu, R Bhatasana, H Dave, O Chandratre, N Kumar, Prashant Singh, Priyanka Brahmbhatt

Institute for plasma research, Gandhinagar-382428

E-mail: hitesh.kavad@ipr.res.in

A helium refrigerator/liquefier plant of cooling power 200 W at 4.5 K for Tokamak is being developed at IPR. Critical peripheral equipment and systems like bearing gas supply, cooling water circulation, liquid nitrogen supply, vacuum pumping systems and instrumentation air line for helium plant has been designed, fabricated and tested at IPR. Addition to this high pressure line and low pressure line for connection of helium compressor with cold box, are also designed, fabricated and tested for the IPR's indigenous helium plant. These systems include many instrumentations for measurement of pressure drops, temperatures, flow rates and pressures which are linked to the control system of helium plant operation. Requirements of these instrumentations have been generated considering different critical operations of the plant. Pressure test for above all lines are done as per ASME requirements and then thorough leak tests have been done. Some pipe lines have been insulated to reduce ambient heat transfer. This paper will give details of these.

References:

[1] Kays WM, London AL. 1984 Compact heat exchangers. In: McGraw-Hill series in mechanical engineering. *New York: McGraw-Hill Book Co*.J.

NFT-P-32

STATUS OF AUXILIARY POWER SUPPLIES FOR ITER PROTOTYPE RF SOURCE

Hrushikesh Dalicha*, Gajendra Suthar, Kartik Mohan, Rohit Agarwal, Rajesh Trivedi, Kumar Rajnish, Raghuraj Singh, Aparajita Mukherjee

ITER-India, Institute for Plasma Research, Gandhinagar, India 382428

E-mail: hrushikesh.dalicha@iter-india.org

ITER-India, IPR has developed a dedicated test facility for testing of MW level RF source and associated components [1] [2]. The test facility includes MW level RF source, high power dummy load, transmission line components including mis-match lines comprising of stub and phase shifter, data acquisition & control system, auxiliary power supplies, high voltage power supply (HVPS), AC power distribution network, active water-cooling and air-cooling system etc. The same facility will be used in future for testing of RF sources related to ITER deliverables.

Prototype RF source consists of two identical amplifier chains and one combiner. Each chain is having one solid state amplifier and two tube based amplifiers. The tube-based amplifiers require DC biasing for the electrodes with specific protection and response for operational need. There are four types of biasing power supplies required for RF tube which are, Anode, Screen grid, Control grid and Filament. Among the mentioned power supplies, Screen grid, Control grid and Filament power supplies are considered as auxiliary power supplies. To meet the above requirement, one set of each, Screen grid power supply (HPA2 – 1500V/3.3A, HPA3-2000V/10A) and Control grid power supplies (HPA2&HPA3 – 500V/12A) are procured and tested successfully.

The detailed test plan, test setup and test results (i.e., ripple in output, rise time & fall time slew rate measurement, protection validation, remote operation and signal response time) will be presented.

References:

[1] Aparajitamukherjee et al., Status of R&D activity for ITER ICRF power source system, Fusion Engineering and Design 96–97 (2015) 542–546.

[2] Rajesh trivedi et al., Outcome of R&D program for ITER ICRF Power Source System, Preprint, FEC-2018.

NFT-P-33

AMPLITUDE ANDPHASE CONTROL USING I-Q MODULATOR: APROTOTYPE DEVELOPMENT

DipalSoni, Kumar Rajnish, Sripraksh Verma, Raghuraj Singh, R.G. Trivedi and Aparajita Mukherjee
ITER-India, Institute for Plasma Research, Block-A, SangathSkyz, Bhat-Motera Road,
Koteshwar,Ahmedabad – 380005, Gujarat
E.mail: dipal.soni@iter-india.org

The Ion Cyclotron Heating and Current Drive (ICH &CD) system for ITER application is being designed, fabricated and commissioned to couple 20 MW Radio Frequency (RF) power into ITER plasma for heating and driving plasma current in the frequency range of 35-65MHz [1]. There will be 8 RF sources to generate total 20 MW of RF power. There is also one prototype RF source which will be used as spare. Each RF source will be capable to deliver 2.5MW output power at Voltage Standing Wave Ratio (VSWR)2:1 having bandwidth of 2MHz as per ITER requirement. Each RF source consists of two parallel amplifier chains of 1.5MW RF power level and a combiner at the output side to generate 2.5MW power.

Development activities related to prototype RF source is initiated. To provide 2.5MW constant RF output power to ITER is utmost requirement of RF source. To maintain amplitude and phase as per experimental requirement, different control loops like amplitude control loop and phase control loop are under development. At present low power control element like, voltage variable attenuator and voltage variable phase shifter are used to control requested amplitude and phase for the individual RF chain. I-Q modulator may be a better option instead of using voltage-controlled attenuator and phase shifter as low power control element to control the amplitude and phase of the RF chain. This paper describes the basic experimental test resultsof analog I-Q modulator.

References:

[1] SRD 51(SRD-51 (ICH&CD) from DOORS (28B33K v6.0) (current)).

NFT-P-34

TESTING OF HIGH-POWER AMPLIFIER AT 1.5MW FOR CONTINUOUS WAVE (CW) OPERATION

Raghuraj Singh, Aparajita Mukherjee, R.G. Trivedi, Kumar Rajnish, Akhil Jha, Manoj Patel, Gajendra Suthar, DipalSoni, Sriprakash Verma, Kartik Mohan, Rohit Agrawal, Rohit Anand, HrushikeshDalicha and Paresh Vasava

ITER-India, Institute for Plasma Research, Gandhinagar, India 382428

E-mail: raghuraj.singh@iter-india.org

ITER-India is developing 2.5 MW Radio Frequency (RF) source having 1dB bandwidth of ±1MHz in the frequency range 35-65 MHz for ITER application. It has to provide constant output power of 2.5MW at any frequency within the specified range on match and mismatched load having voltage standing wave ratio (VSWR) 2:1 at any phase of reflection coefficient [1]. Eight such RF sources will be used to meet total 20MW of RF power requirement for plasma heating and current drive experiment. Each 2.5MW RF source consists two chains of RF amplifiers capable to deliver 1.5MW and a 3dB hybrid combiner. A Research & Development (R&D) chain of 1.5MW RF power based on Diacrode technology is tested on matched and mismatched load (VSWR 2:1) after setting the 1dB bandwidth of ±1MHz [2] [3].

During testing of R&D chain of amplifiers, it was observed that to achieve 1dB bandwidth of ±1MHz at 65MHz is not possible due to higher level of harmonics while moving from 65 to 66MHz. Therefore, it was decided to check the bandwidth at 60MHz because the requirement for ITER experimental frequency lies in between 40-55MHz. Hence, rigorous testing of Diacrode based R&D amplifiers chain was completed successfully, with 1dB bandwidth at ±1MHz for more than 1.5MW/2000s on matched load. The detailed test results will be presented in this paper.

References:

[1] SRD 51(SRD-51 (ICH&CD) from DOORS (28B33K v6.0) (current)).

[2] Aparajita Mukherjee et al., Status of R&D activity for ITER ICRF power source system, Fusion Engineering and Design 96–97 (2015) 542–546.

[3] Rajesh Trivedi et al., Outcome of R&D program for ITER ICRF Power Source System, Preprint, FEC-2018.

NFT-P-35

DEVELOPMENT OF WATER-COOLED BLEEDER HEATSINK FOR PROTOTYPE AUXILIARY POWER SUPPLIES

Paresh Vasava, HrushikeshDalicha, Rohit Anand, Rajesh Trivedi, Kumar Rajnish, Raghuraj Singh, Aparajita Mukherjee

ITER-India, Institute for Plasma Research, Gandhinagar, India 382428

E-mail: paresh.vasava@iter-india.org

ITER-India has developed a dedicated test facility for testing of 1.5 MW R&D RF source. The RF source is 3-stages cascaded amplifiers; pre-driver, driver and final stage, based on solid state technology and vacuum tubes (Diacrode / Tetrode). The test facility includes high power RF Dummy load, transmission line system including mis-match lines comprising of stub and phase shifter, AC power distribution network, Control Unit, Auxiliary power supplies (Control Grid power supply, Screen Grid power supply, Filament power supply), High Voltage power supply etc. The same facility will be used in future for testing of RF sources at 3MW level related to ITER deliverables.

Prototype RF source consists of two identical amplifier chains and one combiner at the output side. Each amplifier chain is comprising of one solid state amplifier (HPA1) followed by two tube-based amplifiers (HPA2 & HPA3). Auxiliary power supplies consisting of 6 nos. of DC power supplies are required for HPA2 and HPA3. Out of which 4 nos. of power supplies need bleeder circuit with total power rating of ~8kW. For such high-power heat dissipation, active water cooling is required for thermal management. A dedicated water-cooled heat sink has been designed, developed and tested successfully.

The detailed design, simulation and test data will be presented.

References:

[1] Aparajita Mukherjee et al., Status of R&D activity for ITER ICRF power source system, Fusion Engineering and Design 96–97 (2015) 542–546.

[2] Rajesh Trivedi et al., Outcome of R&D program for ITER ICRF Power Source System, Preprint, FEC-2018.

NFT-P-36

RAMI ANALYSIS FOR UPPER PORT 09 AND PERFORMING FMECA TO FIND OUT THE EXPECTED CRITICALITY MATRIX

Suraj Pillai [a], Siddharth Kumar[a], Sandip Roy[a], Hitesh Pandya [a,b]
[a]*ITER-India, Institute for Plasma Research, Bhat, Gandhinagar Gujarat 382424, India.*
[b]*Institute for Plasma Research, Bhat, Gandhinagar Gujarat 382424, India.*
E.mail: Suraj.pillai@iter-india.org

Upper port plug 09 is serving to host diagnostic and service systems, to provide neutron shielding and to perform plugging function. It has two tenants namely XRCS-Edge and High Field Side Reflectometry (HFS-R). UP09 system provides supporting structure for tenants as well as to do the port integration throughout three distant port areas in the upper port: the port plug, interspace support structure and port cell. Upper port 09 shouldbe highly reliable, efficient and safe device built to producea quantitative and qualitative predefined output. It has to be available for experiments whenever needed with low operation and maintenance cost. Thus, a RAMI (Reliability, Availability, Maintainability and Inspectibility) analysisis a part of design and manufacturing review process during ITER component product lifecycle [1]. This aims to provide designers and engineers for the optimum design, appropriateoperation, testing and maintenance programmes.In this poster asa part of RAMI analysis functional breakdown analysis is done to understand thebasic function and associated components [2].To define risks of failures of the system, the most probable risks of component failures were identified in parallel with RBD (Reliability Block Diagramme)-analysisusing Blocksim software. This Software provides a comprehensive platform for system reliability, availability, maintainability and related analyses that allows you to model the most complex systems and processes using discrete event simulation and computation for repairable and nonrepairable systems. This is used to find out the initial and expected availability and reliability of UP09. Failure mode effect and criticality charts were prepared, major riskswere identified and risk mitigation measures were proposed. Thus, expected criticality matrix was plotted based on severityandoccurrence.These results and integrative concepts can help in better control of technical risk which makes it possible tohave better guarantee that this device meets project requirements with respect to reliability (continuity of correct operation), availability (readiness for correct operation), maintainability (ability to undergo repairs and modification) and Inspectibility (ability to undergo visits and controls).

Keywords: RAMI analysis, FMECA analysis, Fusion, Upper Port.

References:

[1] Suraj et al,"A Study on irradiated welding joints in ITER materials and its effects on FMECA analysis of ITER components". Fusion engineering and Design (2019).

[2] Van Houtte D, ITER RAMI Analysis Program IDM document (28WBXD _v4.3) (2011).

NFT-P-37

INVESTIGATION OF STRUCTURAL INTEGRITY OF SWIFT HEAVY ION IRRADIATED AL2O3

Paramita Patra1,*, Sejal Shah1,2,3†, M. J. Singh1,2, I. Sulania4, S. Kedia4, F. Singh4
1ITER-India, Institute for Plasma Research, Ahmedabad-380005, India
2Institute for Plasma Research, Ahmedabad-380005, India
3Homi Bhabha National Institute, Anushakti Nagar, Mumbai-400094, India
4Material Science Group, Inter-University Accelerator Center, New Delhi, 110067, India
*Email: *paramita.patra-pdf@iter-india.org, †sshah@iter-india.org*

The harsh radiation of nuclear reactors may alter the structural properties of insulating materials, used in high voltage systems of the reactors [1,2]. Therefore, it is essential to ensure the performance of the insulators for high doses of radiation over a long period of time. However, it is not possible to perform this study by replicating the exact radiation environment of the reactors, we have used the surrogate technique of swift heavy ion (SHI) beam irradiation to simulate the radiation condition [3].

We have chosen alumina (Al2O3) for our study as it is widely used in the high voltage applications of fusion reactors. In this work, 100 MeV Au ion, with fluences of 1×1011 to 1×1014 ions/cm2 has been used to study the irradiation impact on the structural properties of alumina. The range of the ion beam in alumina is estimated to be 8.3 µm using SRIM code. Estimated electronic and nuclear energy losses are 22.59 keV/nm and 0.4 keV/nm, respectively. The radiation damage in terms of displacement per atom (DPA) is calculated for fluences1×1011 to 1×1014 ions/cm2, which are in the range of 9.28×10-5 to 9.28×10-2, respectively for selected insulator and ion [4]. Structural modification after the SHI irradiation is investigated by Grazing Incident X-Ray Diffraction (GIXRD) and Photoluminescence Spectroscopy (PL). The XRD measurement is performed at a grazing angle of 1 degree (X-ray attenuation length ~1.0 µm in Al2O3) within the projected range of 100 MeV Au ion in Al2O3. XRD patterns show a gradual decrease of peak intensity with the increase in ion fluences attributed to the atomic disorder in the material resulting from the SHI irradiation. PL spectra of pristine and irradiated samples show two distinct emission bands at ~ 679 nm and ~ 695 nm with an excitation wavelength of 442 nm using He-Cd laser system. The intensity of these bands decreases with an increase in ion fluences, is corroborating the GIXRD results. The obtained results will be presented and discussed in detail.

References:

[1] Sejal Shah, D. Sharma, D. Parmar, H. Tyagi, K. Joshi, M. Bandyopadhyay, C. Rotti, A. Chakraborty, Fusion Eng. & Design **113**, p 6-15, (2016).
[2] Sejal Shah, H. Tyagi, D. Sharma, D. Parmar, K. Joshi, K. Patel, A. Yadav, R. Patel, M. Bandyopadhyay, C. Rotti, AIP Conference Proceedings, AIP Publishing **1869**, p 060004, (2017).
[3] S. Kumar, Sejal Shah, I. Sulania, F. Singh, A. Chakraborty, Ceramics International **45**, p 20346, (2019).
[4] Paramita Patra, Sejal Shah, M. Toulemonde, I. Sulania, F. Singh, manuscript under review (August 2021).

NFT-P-38

DEVELOPMENT OF 16 CHANNEL CURRENT MEASUREMENT MODULE FOR SSPA

Manojkumar Patel, HrushikeshDalicha, Gajendra Suthar, Akhil Jha, Kumar Rajnish, Raghuraj Singh,R.G. Trivedi and Aparajita Mukherjee
ITER-India, Institute for Plasma Research, Block-A, SangathSkyz, Bhat-Motera Road, Koteshwar,Ahmedabad – 380005, Gujarat
E.mail: manoj.patel@iter-india.org

The Ion Cyclotron Heating and Current Drive (ICH &CD) system for ITER application is being designed, fabricated and commissionedto couple 20 MW Radio Frequency (RF) power into ITER plasma for heating and driving plasma current in the frequency range of 35-65MHz [1].Each RF source will be capable to deliver 2.5MW output power at Voltage Standing Wave Ratio (VSWR) of 2.0 having bandwidth of ±1 MHz as per ITER requirement. Each RF source consists two parallel amplifier chains of 1.5MW and combine to generate 2.5MW power using 3 dB hybrid combiner.In the present configuration, two tube based tuned amplifiers, i.e. driver (150 kW) and final (1.5 MW) stage amplifiers are driven by a wideband Solid State Power Amplifier (SSPA) having power handling capability of around 8 kW.

In the present design, 16 RF amplifier modules are required to combine for achieving 8 kW of RF power. Each module should be protected by over current protection to prevent any failure in amplifier module. Current measurement cards are designed and developed to fulfill such requirement. Closed loop current transducer sensors are used for DC current to DC voltage conversion and interlock cards are integrated to generate fault signal in case of SSPA module current crosses the threshold value.

This paper describes the design & test results of current measurement cards.

References:

[1] SRD 51 (SRD-51 (ICH&CD) from DOORS (28B33K v6.0) (current))

NFT-P-39

DEVELOPMENT OF PLC BASED CONTROL SYSTEM FOR REMOTE OPERATION OF 200KV HIGH VOLTAGE POWER SUPPLY

Kumar Saurabh, Amal S, Aritra Chakraborty, Paul Christian and Ashok Mankani
Institute for Plasma Research, Gandhinagar-382428
E.mail: saurabh@ipr.res.in

A PLC based control system is developed and integrated with the 200kV HVPS for the remote operation and monitoring. Digital and analog signals are integrated with the PLC system and output command signal are communicated with the control card using relay based system. The work involves configurations and principles of the control system which is based on PLC and HMI. The control system includes inbuilt processor-supporting both analog and digital inputs, motion system (gear assembly, servo motors), IO modules & visualization (HMI). In this work PLC is programmed using ladder diagram and HMI is designed with hotspots, buttons and active points to control operations. This PLC - HMI based control system can operate the HVPS manual intervention this system is convenient to install and maintain, stable to work, reliable to operate and precise to control.

References:

[1] 200kV, 15mA High Voltage DC power supply Characterization at (InPAC-2019)” at IUAC, New Delhi, India (18-21 November, 2019). Amal S, Kumar Saurabh, Urmil Thaker, Aritra Chakraborty, Paul Christian, Ashok Mankani1and UjjwalBaruah.

[2] "Design and test results of 200kV 15 mA High Voltage DC Test Generator", Amal.S, UrmilThaker, Kumar Saurabh, UjjwalBaruah, Pages: 312 to 338 in The Book: "Plasma and Fusion Science, from Fundamental Research to Technological Application", Apple Academic Press.

[3] Design and Test Results of a 200kV, 15mA High Voltage Test Generator (NF139) at PLASMA 2014”. 2014 at Mahatma Gandhi University, Kottayam, Kerala, India (8-11 December 2014).

[4] “Design and Development of 200kV, 15mA High Voltage Power Supply (NF-011) at PLASMA 2013”. at KIIT University, Bhubaneshwar, India. (3-6 December 2013).

NFT-P-40

DEVELOPMENT OF ARCHITECTURE FOR CONTROLLINGELECTRICAL MOTORS OF ITERSECONDARY COOLING WATER SYSTEM

Jinendra Dangi[*1], A.G. Ajith Kumar[1], D. K. Gupta[1], Nirav Patel[1]
[1]*ITER-India, Institute for Plasma Research, Bhat Gandhinagar-382428, India*
[*1]*E-mail:jinendra.dangi@iter-india.org*

ITER Secondary Cooling Water System (SCWS) designed and supplied by ITER-India, consisting of Component Cooling Water System, Chilled Water System and Heat Rejection System, is one of the major consumers of electrical power at ITER site, with the total installed power during the first plasma operation phase estimatedat 38MWe andthe large capacityelectrical motors (upto1.4 MWe/ 6.6 kV capacity) are the dominant consumers among all.

The major technical challengesencountered during the design werethe optimization and the integration of SCWS electrical network with ITER steady state electrical network load centres to achieve both physical and functional controls remotely, apart from ensuringsafe operations of SCWS asynchronous motors. The control philosophies were developed to control the electrical machines through intelligent electronic devices, plant control system, hardwired logicsetc. The starting methods either through direct online starters, soft starter and variable frequency drives were established for electrical motors considering reliability aspects along with process requirements. Effective and efficient monitoring provisions were made through switchgear and/or plant control system to have continuous monitoring of healthiness of equipment,along with monitoring critical parameters during operation. The operation and controlofmedium voltage and low voltage electrical machines during various scenarios and modes of operations through independent local control panelslocated in the close vicinity of their respective machines were also considered in the design.

This paper highlightsthe architecture developed and the interfaces established during design toensure optimized, occupationally safe, effective, and reliable operation of the SCWS electrical machines, complying with IEC standards, ITER electrical guidelines, European directives, legal requirementsand safety regulations applicable to ITER site.

NFT-P-41

RF DESIGN OF POWER LEVEL 2.5 MW COMPATIBLE TRANSMISSION LINE COMPONENTS

Akhil Jha, Rohit Anand, P. Ajesh, Paresh Vasava, Ulhas K. Dethe, Sunil Dani, R.G. Trivedi, and Aparajita Mukherjee
ITER-India, Institute for Plasma Research, Gandhinagar, India 382428
E-mail: akhil.jha@iter-india.org

ITER-India is developing an ICRF source with a power level of 2.5 MW in the frequency range of 35-61 MHz for ITER application. It has to provide a constant output power of 2.5MW at any frequency within the specified range on a match and mismatched load having voltage standing wave ratio (VSWR) 2:1 at any phase of reflection coefficient [1]. Eight such RF sources will be used to meet a total 20MW of RF power requirement for plasma heating and current drive experiment. Each 2.5MW RF source consists of two chains of RF amplifiers capable to deliver 1.5MW and a 3dB hybrid combiner. During the R&D phase the single-chain amplifier was tested for the power level of 1.5 MW at VSWR 2:1 in continuous wave (CW) mode with the indigenously developed 12inch transmission line components containing directional couplers, gas barriers, straight sections, 90° elbows, shorted variable stub, variable phase shifter, etc. All these 12inch transmission line components were tested at the power level of 1.5 MW with VSWR 2:1 in CW mode [2] [3].

In the next phase, to test the RF source at the power level of 2.5 MW with VSWR 2:1, the design of these transmission line components has been upgraded for the given power level and load condition. A detailed analysis is performed to check the RF performance of these transmission line components at the given power level and load condition. It is required to keep the magnitude of E-field level inside the transmission lines below 2 kV/mm to have sufficient margin with the breakdown strength of dry air i.e. 3kV/mm. Therefore, several modifications have been performed in the design of existing transmission line components.

This paper discusses the detailed simulations results of the 12inch transmission line components performed using commercial software CST MWS.

References:

[1] Bertrand Beaumont et al., Status of the ITER Ion Cyclotron H&CD, EPJ Web of Conferences 157, 02002 (2017)
[2] Aparajita Mukherjee et al., Status of R&D activity for ITER ICRF power source system, Fusion Engineering and Design 96–97 (2015) 542–546
[3] Rajesh Trivedi et al., Outcome of R&D program for ITER ICRF Power Source System, Preprint, FEC-2018.

NFT-P-42

DEVELOPMENT AND INTEGRATION OF MODULAR CONTROL AND ACQUISITION SYSTEM FOR LASER ABSORPTION SPECTROSCOPY IN ROBIN

Kartik Patel[1], Himanshu Tyagi[2], Manas Bhuyan[2], Hiren Mistri[1], Ratnakar Yadav[2], Kaushal Pandya[1], MJ Singh[2], Mainak Bandyopadhyay[2], Arun Chakraborty[1]
[1]Institute for Plasma Research, Gandhinagar, India
[2]ITER-India, Institute for Plasma Research Gandhinagar, India.
E-mail: kartik.patel@ipr.res.in

Negative Ion based inductive coupled plasma sources operate under high RF power and HV for plasma productionand beam transport. ROBIN [1] ion source is currently in operation at IPR, Gandhinagar with an aim to achievestable negative ion production and beam extraction. In order to obtain high extracted current densities, it isnecessary to lower the work function of the surface of the Plasma grid. This is accomplished by coating thesurfaces with Caesium. A specific diagnostic is needed which can quantify Caesium within the experimentalsystem. Laser Absorption Spectroscopy (LAS) diagnostic uses a tuneable laser diode (LD852-SE600) to obtain the high-resolution absorption spectrum of the Caesium 852 nm line along a line of sight to measure Cs densityat the ground state. The laser absorption technique is optimised for the diagnostics of neutral caesium densitiesclose to the extraction surface at which negative ions are generated.

To study the systematic density variation of Cs, the temperature and current through the laser diode need to becontrolled precisely as this affects the laser diodes optical power. The Photodiode receives the optical signalthereby giving an estimation of Cs density in the plasma source. In order to perform the seamless remote operationof LAS, a dedicated Data acquisition system is needed which can be triggered from central DACS duringoperations. For this purpose, a discrete controller is developed based on USB based interface with the LabVIEWplatform. This avoids the usage of any industrial vendor-provided controller for the laser diode thereby providing a cost-effective solution. The operation of LAS along with data acquisition has been performed using thedeveloped Data Acquisition system.

The LabVIEW based controller has been developed and tested with the LAS in ROBIN. The developed controlleris able to interface multiple components and provide an integrated HMI to the experimentalists. Precise controlof the current and temperature of a laser diode with an accuracy of less than ±0.01% has been achieved. Similarly,data from the photodiode is acquired with a minimum resolution of 10ms on the same platform. The entire setuphas been integrated with ROBIN DAC [2] system for synchronized operations. Data is logged in Shot wise and day wise modes for proper post-analysis.

This paper presents the details of the work done in developing the system with test results and experiences.

References:

[1] K Pandya et.al, "System up gradation for Surface Mode Negative Ion Beam Extraction Experiments in ROBIN", Fusion Engg. Design, 114, 187–191 (2017).

[2] J. Soni, et.al "Conceptual design, implementation and commissioning of data acquisition and control system for negative ion source At IPR" AIP Conference Proceedings, 1390 (2016), p. 624.

NFT-P-43

DESIGN & DEVELOPMENT OF OPERATIONAL PROTECTION AND INTERLOCK CIRCUIT FOR VACUUM PUMPING SYSTEM OF TWIN SOURCE (TS)

Hardik Shishangiya[1], Deepak Parmar[1], R. Yadav[1], R Pandey[2], J. Bhagora[1], K Joshi[1], M Bhuyan[1], A. Gahlaut[2], M. Singh[1], M. Bandyopadhyay[1,3] and A. Chakraborty[1]

[1]Iter-India, Block-A, SangathSkyz, Bhat-Koteshwar Road, Koteshwar, Ahmedabad – 380 005, India

[2] Institute for Plasma Research, Bhat, Gandhinagar, Gujarat- 382015

3Homi Bhabha National Institute, Anushaktinagar, Mumbai, Maharashtra 400094

E-mail: hardik.shishangiya@iter-india.org

Operations on Twin Source (TS) [1] experimental setup have been initiated recently with an aim to understand the methodology to establish matching and inductively couple RF power from one generator to two source drivers, a configuration similar to be that adopted for multi driver ion sources with large extraction areas. For operations this set up uses a combination of two rotary and two turbo molecular pumps of 2500 l/s pumping speed each not only to achieve the desired vacuum of 10-6 mbar prior to operation but also to pump out the gas actively fed into the source prior to operations. The pumps are isolated from the vessel using ISO 500 gate valves. The entire sequence of operation of the pumps and the desired interlocks for protection are controlled through an indigenously developed data acquisition and control system.

This paper/poster discusses the design and development of such a system with inbuilt features related to protection and interlock for reliable and safe operations.

References:

[1] Two RF driver based negative ion source experiment, IEEE Trans. Plasma Sci. 42 (March) (2014) 624.

NFT-P-44

TWIN SOURCE PLASMA OPERATION USING 40 KW, 1 MHZ SOLID STATE HIGH FREQUENCY POWER SUPPLY

Manas Bhuyan[1%], Ravi Pandey[2],Jignesh Bhagora[1], Mahesh. Vuppugalla[2], Ratnakar Yadav[1], Himanshu. Tyagi[1], S. Gajjar[1], D. Upadhyay[1], Hardik. Shishangiya[1],Bhavesh Prajapati[2], M. N. Vishnudev[1], Deepak Parmar[1], Agrajit Gahlaut[2], Hiren Mistri[2], Kaushal Joshi[1], Kaushal Pandya[2], Mainak Bandyopadhyay[1,3], N P Singh[1], Mahendrajit Singh[1] and Arun Chakraborty[1]

[1]ITER India, Institute for Plasma Research, Bhat, 382428, Gandhinagar, India.
[2]Institute for Plasma Research, HBNI, Bhat, 382428, Gandhinagar, India.
[3]HomiBhabha National Institute (HBNI), BARC, Anushaktinagar, 400094, Mumbai, Maharashtra, India.
E-mail: [1%]manas.bhuyan@iter-india.org

TWIN source [1, 2, 3, and 4] is an indigenously built two driver based RF negative ion source with the purpose of gaining experience in operation, optimisation, extraction and acceleration of H^- beams from a scaled up version of the present single driver ROBIN test bed. The inductively coupling of RF power to produce plasma in the source uses a scheme of two drivers in series fed power from a single RF generator with a suitable matching network. This scheme is relevant towards operation of the next version of the source which is an 8 driver RF source with 8 drivers fed power simultaneously using 4 RF generators in the INTF test stand. The experience gained on TWIN is of immense relevance to shorten the operational and optimisation time on INTF. It also severs as a test bed towards configurational optimisation of indigenously built 1 MHz 200 kW RF generators. Experiments have been initiated on the TWIN in the configuration mentioned above by coupling the source to the first generation of indigenously built solid state 40 kW RF generator[5]. The present paper will report on the operational and optimisation experiences of an experimental campaign where 40 kW RF power coupled to the two drivers to produce plasma densities of the order of $10^{16}/m^3$on the TWIN source. The source filling pressures were in the range of 0.4 -1 Pa and the plasma densities were measured using Langmuir probes. The next step is to couple the source to a 180 kW RF generator to reach the desired powers of 80 kW per driver followed by coupling the source to a 3 grid extractor and accelerator system to produce 35 mA/cm^2 H^- beams on the calorimeter.

References:

[1] M. Bandyopadhyay, M.J. Singh, G. Bansal, A. Gahlaut, K. Pandya, K.G. Parmar, J. Soni, I. Ahmed, G. Roopesh, C. Rotti, S. Shah, A. Phukan, R.K. Yadav, A.K. Chakraborty, Two RF driver based negative ion source for fusion R&D, IEEE Trans. Plasma Sci. 40 (2012) 2767–2772.

[2] M. Bandyopadhyay, R. Pandey, S. Shah, G. Bansal, D. Parmar, A. Gahlaut, J. Soni, R.K. Yadav, D. Sudhir, H. Tyagi, K. Pandya, K.G. Parmar, H.S. Mistri,

M. Vuppugalla, A.K. Chakraborty, Two RF driver based negative ion source experiment, IEEE Trans. Plasma Sci. 42 (March) (2014) 624.

[3] Ravi Pandey, M. Bandyopadhyay, R. Yadav, D. Parmar, H. Tyagi, H. Shishangiya, S. Shah, D.S. Kumar, A. Gahlaut, M. Vuppugalla, J. Soni, J. Bhagora, G. Bansal, K. Pandya, A. Chakraborty, Indigenousmanufacturing realization of TWIN source and it's Auxiliary, IEEE Trans. Plasma Sci. 2375–2380 (July) (2017).

[4] R. Pandey et. al, Indigenous Manufacturing realization of TWIN Source, 2017 J. Phys.: Conf. Ser. 823, 012029, doi:10.1088/1742-6596/755/1/011001.

[5] S. Gajjar et.al. Experimental results of 40 kW, 1 MHz Solid State High Frequency Power Supply with Inductively Coupled Plasma, AIP Conference Proceedings 2373, 100002 (2021); https://doi.org/10.1063/5.0057477.

NFT-P-45

REMOTE TUNING SYSTEM FOR RF MATCHING NETWORK OF TWIN SOURCE USING STEPPER MOTOR

V. Mahesh[1], A. Gahlaut[1], D. Parmar[2], B. Prajapati[1], H.Shishangiya[2], M. Bandyopadhyay[2], M.J. Singh[2] and A. Chakraborty[1]
Institute for Plasma Research, Gandhinagar, Gujarat - 382428, India
Iter-India, IPR, Koteshwar, Ahmedabad – 382424, Gujarat
E-mail: vmahesh@ipr.res.in

Impedance tuning over a limited dynamic range is essential to establish the most optimal coupling of RF power in ion source. In TWIN Source (TS) [1], the RF power from the generator is interfaced to the ion source Antenna with a matching network in between. The matching network is a combination of impedances of capacitors and transformer. While the impedance of the transformer is fixed, the impedance tuning can only be done using capacitors with a combination of fixed and variable capacitors when the parameters like RF power, gas pressure, RF frequency etc. are varied. However, due to the limited range of the variability of the capacitance, it is important to have a precise control and backlash free mechanism, to arrive at the appropriate impedance with a tolerance on the capacitance value within +/- 10%. Also, the matching network is enclosed with RF shielding to reduce the effect of RF radiation and the output of the matching network is connected to the RF coil at HV (~30kV) potential.

Realization of such a mechanism has been implemented in the operation of the Twin Source (TS)[1], where RF power from a single, 0 - 180 kW RF Generator, operational in the frequency range of 0.9-1.1 MHzcouples to two ion source antennas, connected in series/ parallel configuration. The mechanism consists of Stepper motors which are coupled to variable capacitors using RF & HV compatible insulators, HMI in which

GUI has been prepared to provide required input to tune the capacitors and PLC system to control the stepper motors. RF shielding of stepper motors, PLC system and the cables has been incorporated to avoid any RF disturbances.

The paper will discuss in detail about the system design, programming logic, integration and commissioning in TS RF matching network.

References:

[1] Two RF driver based negative ion source experiment, IEEE Trans. Plasma Sci. 42 (March) (2014) 624.

NFT-P-46

EXPERIENCE OF MANUFACTURING BEAM LINE COMPONENTS FOR ITER DNB

H Patel[1], J Joshi[1], M J Singh[1], M. V. Nagaraju[1] , A Chakraborty[1], J Chareyre[2],B Schunke[2] , C Rotti[2], E Pfaff [3], J Schäfer[3], M Krohll[3], C Eckardt[3]

[1]ITER-India, Institute for Plasma Research, Gandhinagar - 382428, Gujarat, India

[2]ITER Organization, Route de Vinon-sur-Verdon –CS90046,13067 St Paul-Lez-Durance – Cedex, France

[3]PVA Industrial Vacuum System GmbH, Im Westpark 10-12, D 35435, Wettenberg, Germany

E-mail: hitesh.patel@iter-india.org

The diagnostic neutral beamline (DNB) is expected to deliver 100 keV, 18–20A beam of hydrogen neutrals to the ITER plasma to diagnose the He ash content in the ITER Machine. DNB system consists of several Beam Line Components (BLCs) installed in Neutral Beam Vessel. BLCs mainly includes, Neutralizer (to neutralize the negative ions produced by Ion Source), Residual Ion Dump (to remove the residual ions from the mixed beam of ions and neutrals existing from the Neutralizer) and Calorimeter (for beam diagnosis).

BLCs are designed w.r.t ITER Structural Design Criteria for In Vessel Components (SDC-IC) and manufactured to meet EN/ISO standards, ITER Vacuum Handbook and ASME codes requirements. Several non-conventional manufacturing technologies in the areas of materials, machining, welding have been developed during the course of the manufacturing of these components. These BLCs are in advance stage of manufacturing. Some of the crucial technologies developed as prototype and applied to the production of the actual components includes; 1) Production of CuCrZr alloy with strict control over chemical composition and specific mechanical properties in aged condition, ii) deep hole drilling of Neutralizer Panels with specific drift control < 500 microns over a length of 1.5 m 3) Electron Beam welding (EBW) of 25 mm thick CuCrZr panels for RID 4) realization of Heat Transfer elements for Calorimeter etc.

During the course several modifications had to be undertaken to ensure the desired requirements without compromising on the stringent testing and quality requirements and have resulted in an extensive database which will be of use for similar technologies applied to various components of fusion machines.

The paper shall present the overall experience of the manufacturing and technology development / prototyping, supplemented by the handling of the QA/QC activities from the ITER perspective. A specific emphasis will be placed on handling of the non-conformances and the deviations that are inherent part of any technology intensive projects.

NFT-P-47

DESIGN DEVELOPMENT OF DNB VACUUM VESSEL FOR ITER

Ashish Yadav[1], Jaydeep Joshi[1], Mahendrajit Singh[1], Arun Chakraborty[1]
[1]ITER-India, Institute for Plasma Research, Gandhinagar, Gujarat – India
ashish.yadav@iter-india.org

DNB Vessel is a 9 m long, 5 m height and 5 m of width rectangular vacuum enclosure to house~~s~~ the beam line components of the neutral beam system. The integrated assembly of DNB vessel consist of (1) main shell (size 9m × 5m × 5m) with appropriately sized and located stiffeners along with end flange (9 m × 5m with a thickness of 200 mm) welded along it periphery, (2) a detachable top lid (9 m × 5m with a thickness of 115 mm). Such a configuration with a detachable top lid allows for easy insertion as well as removal of internal components during installation and maintenance phases. DNB vessel has the suitable openings in terms of large and medium size ports to enable mounting of the high voltage bushing, front end components, hydraulic connections, cryolines, gas feed lines, actuator feedthroughs and diagnostics.

Being a safety important component and first confinement barrier for ITER environment, RCC-MR code has been used for the design and analysis of the DNB vessel. One of the major design challenges was to limit the deflection requirements (less than 1mm near beam-source support location and less than 5mm to the overall vessel), while adhering to the metallic seal compression requirements, design verification as per the load combinations, and interface management.

Apart from the engineering design, manufacturing feasibility is also important from the fact that based on the RCC-MR requirements, full penetration welding is incorporated into the design (total weld length > 130m) for all the vacuum boundary welds and fillet welds (total weld length >250m) for stiffeners welding. Due to the large number of welds and therefore huge weld deposition and the heat input, especially on the stainless steel structure, the challenges related to distortion control amplify by several factors. To mitigate the risks related to welding distortions thereby ensuring a reduction in the post-fabrication machining activities and hence the costs, a computational assessment for predicting the welding distortion for different welding sequences has been made and has resulted in optimization of the manufacturing strategy of this vessel.

The objective of this paper is to present the analysis, design optimization and manufacturing feasibility assessement of the DNB vacuum vessel in line with the ITER functional and operational requirements.

NFT-P-48

COMPARISON OF TOPOLOGIES FORTWIN SOURCEHVDC TRANSMISSION LINE

Vishnudev M N[a,b], Deepak Parmar[a], HardikShishangiya[a], Santosh C. Vora[b],AgrajitGahlaut[c], MainakBandyopadhyay[a,c,d], Arun Chakraborty [a,c]
[a]*ITER-India, Institute for Plasma Research, Bhat, Gandhinagar Gujarat 382424, India*
[b]*Dept of Electrical Engineering, Institute of Technology, Nirma University, Ahmedabad 382481, India*
[c]*Institute for Plasma Research, Bhat, Gandhinagar Gujarat 382424, India*
[d]*HBNI, Anushakti Nagar Mumbai, 400094, Maharashtra, India*

In neutral beam system negative ion extraction and acceleration plays very important role.This makes the HVDC transmission line for extraction and acceleration system very crucial component in neutral beam system. Hence it is very important to compare different topologies of HVDC transmission lines in neutral beam systems. By comparison we can get rough estimate of transmission line parameters, cost, complexity and other un envisaged points in its implementation.TWIN source is a two driver based negative ion source currently operational at IPR [1]. The two driver RF negative ion source test bed aimsto extract and accelerate H- ion beams up to 50 keV. In such negative ion sources, grid breakdown is a routine phenomenon during system conditioning and operation phases. During the grid breakdown event, there are chances that electrostatic energy stored in the transmission line is dumped in the grids, which may possibly damage them. In case of NNBI system with long high voltage transmission line, contribution for the stored energy emanates from their inter-conductor capacitance, an important transmission line lumped parameter.

Estimation of inter conductor capacitance for vertical topology and its benchmarking with experimental measurements was done earlier[2]. Also the experimental estimation of stored energy for 1m prototype and estimation of stored energy for whole length of transmission line was done for vertical topology. In this paper/poster we explore the comparison of vertical and equilateraltriangle topology in terms of transmission line parameter.Also modelling of vertical topology is attempted.Theanalytically estimated inter-conductor capacitance for equilateral triangle topology is benchmarked with a simulation in COMSOL.

Keywords: Twin source, negative ion source, RF, stored energy, breakdown, transmission line.

References:

[1] M. Bandyopadhyay, R.Pandey, S.Shah, G.Bansal, D.Parmar, A.Gahlaut, J.Soni, R.K.Yadav, D.Sudhir, H.Tyagi, K.Pandya, K.G.Parmar, H.S.Mistri, M. Vuppugalla and A.K.Chakraborty, "Two RF Driver Based Negative Ion Source Experiment", IEEE Transactions on Plasma Science, 42, 624, March (2014).

[2] Vishnudev M N, Deepak Parmar, HardikShishangiya, AgrajitGahlaut, V Mahesh, M. Bandyopadhyay and Arun Chakraborty, "Estimation of inter-conductor stray capacitance for HVDC transmission line of negative neutral beam injector", AIP Conference Proceedings 2373, 100006 (2021) https://doi.org/10.1063/5.0057755.

NFT-P-49

MODIFICATION IN PERIOD OF SAWTOOTH OSCILLATION AFTER GAS PULSE INJECTION IN ADITYA-U TOKAMAK

Suman Dolui[1,2] ,Tanmay Macwan[1,2], Kaushlender Singh[1,2], Ankit Kumar[1,2],Sharvil Patel[3], Suman Aich[1,2] ,Rohit Kumar[1], Laxmikant Pradhan[1], Ankit Patel[1], Kalpesh Gadoliya[1], K. A. Jadeja[1],K. M. Patel[1] ,R.L. Tanna[1], Joydeep Ghosh[1,2] and ADITYA-U Team[1]

[1]*Institute for Plasma Research, Bhat, Gandhinagar, Gujarat 382428*

[2]*Homi Bhabha National Institute (HBNI), Mumbai 400 085*

[3]*Pandit Deendayal Petroleum University, Gandhinagar 382007, India*

E-mail: suman.dolui@ipr.res.in

The sawtooth instability [1] in tokamak plasma results in periodic relaxations of the core plasma density and temperature. Observation of sawtooth oscillation in soft-X ray signals coming from plasma core is very common in Aditya-U tokamak. A typical sawtooth cycle consists of three phases: A ramp phase, precursor phase with growth of internal kink mode and fast collapse phase. Enhancement of sawtooth ramp phase has been observed in Aditya-U tokamak After injection of short gas pulse (~1ms), which contain (0.2-1.2)*10^18 hydrogen or deuterium molecules. It is observed that increase in chord-averaged density is followed by the enhancement of sawtooth ramp phase with each gas pulse. The fast collapse phase of the sawtooth cycle is well explained by the partial re-connection model [2]. And no change in fast collapse phase is observed with gas pulse unlike the ramp phase. The physics of this phenomenon is not fully understood till now. This study will explain how the fast propagation of cold pulse [3] with gas injection, changes the local gradients of temperature and current density near the q=1 surface [4] and as a consequence enhance the sawtooth ramp phase [4].

References:

[1] J. Wesson, 2004, Tokamaks, 3rd edition, Clarendon Press, Oxford.

[2] Model for the sawtooth period and amplitude ; F Porcelli*et al* 1996 *Plasma Phys. Control. Fusion* **38** 2163.

[3] Gas-puff induced cold pulse propagation in ADITYA-U tokamak ; Tanmay Macwan*et al* 2021 *Nucl. Fusion* **61** 096029.

[4] Observation of Sawtooth Oscillations in the COMPASS Tokamak ;WDS'13 Proceedings of Contributed Papers, Part II, 67–72, 2013.

NFT-P-50

DESIGN OF A BALL PEN PROBE FOR THE MEASUREMENT OF EDGE ION TEMPERATURE IN ADITYA-U TOKAMAK

Ankit Kumar[1,2], Kaushlender Singh[1,2], Suman Dolui[1,2], Tanmay Macwan[1,2], Pramila Gautam[1], Rohit Kumar[1], Suman Aich[1,2], Laxmikant Pradhan[1], Ankit Patel[1], Kalpesh Gadoliya[1], K. M. Patel[1], K. A. Jadeja[1], R.L. Tanna[1], Joydeep Ghosh[1,2] and ADITYA-U Team[1]

1Institute for Plasma Research, Bhat, Gandhinagar, Gujarat 382428

2Homi Bhabha National Institute (HBNI), Mumbai 400 085

E-mail: Ankit.kumar@ipr.res.in

Ion temperature plays a significant role in tokamaks, e.g., the phenomenon of plasma rotation, plasma detachment and turbulence transport [1, 2] are found to be correlated with ion temperature. However, the underlying correlation behind the dependence of these phenomenon on the ion temperature is not fully understood yet [1, 3]. Measurement of ion temperature is not very straightforward as compared to electron temperature, which can be measured with Langmuir probes. In this paper, development of a "Ball pen probe" for ADITYA-U tokamak is presented, which measures the temperature of the main ion species present in the plasma [4, 5]. This probe also measures the plasma potential directly [6]. In this paper, we will present the design of the Ball pen probe and the technique used to measure edge ion temperature through it.

The ball pen probe for ADITYA-U tokamak is fabricated using a hollow cylindrical of MACOR ceramic (alumina). This ceramic tube can accommodate up to 3 probes simultaneously, at a time. The probe-tip material is Molybdenum having a melting point of 2896K. The probe-tip is cylindrical in shape having a diameter of 2.9 mm. Due to the unique shape, ball pen probe collects only the ions from the plasma [5,6]. A ramp voltage having a frequency of 4KHz, when biased with the probe, gives the I-V characteristic curve. The ion temperature of the plasma at a particular radial position, can be obtained from the I-V curve [4-6]. Repeating the temperature measurement at different radial position will provide the edge temperature profile of the main ion present in the plasma.

References:

[1] Rice J.E. et al 2008 Plasma Phys. Control. Fusion 50 124042.

[2] Gaurav Shukla et al 2019 Nucl. Fusion **59** 106049.

[3] Burrell K H et al 2009 Nucl. Fusion 49 085024.

[4] Thesis: SOUMEN GHOSH/ Study of Localized Potential Structure and Heating in Expanding Helicon Plasma.

[5] J. Adamek, J. Stöckel, I. Duran, M. Hron, R. Panek, M. Tichý, R. Schrittwieser, C. Ioniţă, P. Balan, E. Martines, G. Van Oost, Czech. J. Phys. 55, 235 (2005).

[6] R. Schrittwieser, C. Ioniţă, J. Adamek, J. Stöckel, J. Brotánková, E. Martines, G. Popa, C. Costin, L. van Peppel, G. Van Oost, Czech. J. Phys 56, B145 (2006).

NFT-P-51

DESIGN AND INSTALLATION OF TRIPLE LANGMUIR PROBE FOR DIRECT MEASUREMENT OFEDGE DENSITY AND TEMPERATURE IN ADITYA-U TOKAMAK

Kaushlender Singh[1,2], Suman Dolui[1,2], Ankit Kumar[1,2], Tanmay Macwan[1,2], Pramila Gautam[1], Rohit Kumar[1], Suman Aich[1,2], Laxmikant Pradhan[1], Ankit Patel[1], Kalpesh Gadoliya[1], K. M. Patel[1], K. A.Jadeja[1], R.L. Tanna[1], Joydeep Ghosh[1,2] and ADITYA-U Team[1]
1Institute for Plasma Research, Bhat, Gandhinagar, Gujarat 382428
2Homi Bhabha National Institute (HBNI), Mumbai 400 085
E-mail: Kaushlender.singh@ipr.res.in

Langmuir Probe is one of the fundamental and well-established diagnostics used for measuring plasma parameters like electron temperature, density, and potential [1]. To remove various complications in sweep generation and data analysis of single and double Langmuir probe and for instantaneous measurement of electron temperature and density, Triple Langmuir probe (TLP) was invented. This method does not require any kind of voltage sweep, frequency, or switching and provisions can be easily made to have a direct display of density and temperature [2]. A TLP systemis specially designed and installed in ADITYA-U tokamak to explore the plasma properties of edgeregion (region near the last closed flux surface, LCFS). The probe tips can be moved radially insidethe LCFS up to 3 cm. The dimension of the probes are chosen based on the existing edge plasmaparameters of ADITYA-U. Plasma density ne~ (0.1-0.2)*1019 m-3, and electron temperature Te ~10-20 eV are measured in the typical discharges of ADITYA-U at the LCFS. Apart from using thesystem as TLP, the individual probes are also used as single Langmuir probes (SLPs) to obtain, density, temperature and the poloidal electric field and its fluctuations. Comparative studies ofmeasurement of plasma parameters using the TLP and SLP have been carried out. Furthermore,using the TLP system, a reduction in the poloidal electric field is observed during the fuel gas-puff inthe plasma discharge. The detailed probe construction process and analysis of various events duringthe gas-puff in the edge plasmas of ADITYA-U tokamak will be presented in this paper.

References:

[1] Biswas S. et al, Journal of Applied Physics **118**, 063302 (2015).
[2] Chen Sin-Li, and Sekiguchi T., Journal of Applied Physics 36, 2363 (1965).
[3] Godyak V. A. and Alexandrovich B. M., Journal of Applied Physics **118**, 233302 (2015).
[4] Riccardi C. et al, Review of Scientific Instruments 72, 461 (2001).

NFT-P-52

DESIGN OF LASER INDUCED BREAKDOWN SPECTROSCOPY (LIBS) BASED WALL MONITORINGDIAGNOSTICS FOR ADITYA-U TOKAMAK

Bharat Hegde[1,2], Ashok Kumar[1,2], Ankit Kumar[1,2], Kaushlender Singh[1,2], Suman Dolui[1,2], Tanmay Macwan[1,2], Rohit Kumar[1], Suman Aich[1,2], Laxmikant Pradhan[1], Ankit Patel[1], Kalpesh Gadoliya[1], K.M. Patel[1], K. A. Jadeja[1], R.L. Tanna[1], Joydeep Ghosh[1,2] and ADITYA-U Team[1]
[1]*Institute for Plasma Research, Bhat, Gandhinagar, Gujarat 382428*
[2]*Homi Bhabha National Institute (HBNI), Mumbai 400 085*
E-mail: bharat.hegde@ipr.res.in

In tokamak, due to several transport phenomenon, energy and particle flux coming from core of theplasma interacts with the first wall i.e. limiter and other plasma facing components [1]. This interaction leads to several complications such as erosion, impurities production, fuel retention andco-deposition etc. [1, 2]. Impurities generated due to these plasma wall interactions (PWI's) maycause unanticipated variation of discharge parameters and cause hurdles in the day-to-day tokamakoperations [3]. Impurities on the surface of vessel can be studied using passive spectroscopytechnique using a laser of appropriate power, after each plasma discharge. The laser excites/ionizesthe impurities and forms a localized plasma near the surface. Light emissions from this plasma ischaracteristic of composition of plasma and hence the impurities. This is known as Laser InducedBreakdown Spectroscopy (LIBS) technique [4, 5].

In this paper, we aim to design the LIBS experimental setup by determining specifications of the laser, spectrometers and required mechanical components for in-situ monitoring of wall conditioningof ADITYA-U tokamak**.**

References:

[1] Zhaou D. et al. *Rev. Sci. Instrum.* **89**, 073501 (2018); https://doi.org/10.1063/1.5024848.

[2] P Liu et al. *Plasma Phys. Control. Fusion* **60** 085019 (2018); https://doi.org/10.1088/1361-6587/aace83.

[3] S. Brezinsek*et al Nucl. Fusion* **53** 083023 (2013); https://doi.org/10.1088/0029-5515/53/8/083023.

[4] Anabitarte F. et al. *IRN Spectroscopy Volume* (2012), Article ID 285240; https://doi.org/10.5402/2012/285240.

[5] B. Kearton and Y. Mattley, "Laser-induced breakdown spectroscopy:Sparking new applications," *Nature Photonics, vol. 2, no. 9, pp. 537–540*, (2008); https://doi.org/10.1038/nphoton.2008.173.

NFT-P-53

FEASIBILITY STUDY AND DEVELOPMENT OF A DIAGNOSTIC FOR MEASUREMENT OF TOROIDAL ASYMMETRY IN THE RADIATION DURING DISRUPTIONS IN ADITYA-U TOKAMAK

Ashok Kumar[1,2], Bharat Hegde[1,2], Ankit Kumar[1,2], Kaushlender Singh[1,2], Suman Dolui[1,2], Tanmay Macwan[1,2], Pramila Gautam[1], Rohit Kumar[1], Suman Aich[1,2], Laxmikant Pradhan[1], Ankit Patel[1], Kalpesh Gadoliya[1], K. M. Patel[1], K. A. Jadeja[1], R.L. Tanna[1], Joydeep Ghosh[1,2] and ADITYA-U Team[1]

[1]*Institute for Plasma Research, Bhat, Gandhinagar, Gujarat 382428*

[2]*Homi Bhabha National Institute (HBNI), Mumbai 400 085*

E-mail: ashok.kumawat@ipr.res.in

In tokamaks, plasma disruption is a calamitous event which could be a major reason to disturb the plasma confinement. Therefore, to understand the plasma disruptions and diagnose it in tokamaks is an essential task. In this project, we will study the variation in radiation power in toroidal direction during the plasma shots in ADITYA-U tokamak and visualize either this incident radiation power distribution is symmetric or asymmetric.

During disruption, plasma disappears in a few milliseconds. Hence in a few time a large energy is fallen on the internal components (like limiters diverters, inner wall) and can damage them. So, to mitigate disruptions massive gas particles/ solid pallets are inserted [1], so that energetic charged particles lose their energies during collisions in form of radiation due to deceleration. So, after disruption mitigation, we will also find symmetry in radiation distribution[2] in toroidal direction. For this we will identify a suitable bolometer with justification and preliminary design (detectors, electronics, placement on the machine etc.)[3] to study the toroidal radiation distribution symmetry and other possible studies.

References:

[1] Nicolas commaux et al Physics of Plasmas **21**, 102510 (2014); https://doi.org/10.1063/1.4896721.

[2] M. Lehnen*et al* 2015 *Nucl. Fusion* **55** 123027.

[3] Ratneshwar Jha et al 2012, Bolometer for fusion plasma Diagnostics, 10.5772/33466.

NFT-P-54

DEVELOPMENT ANDMEASUREMENT OF 2.45 GHZ, UHV COMPATIBLE RF WINDOW FOR ECR SYSTEM

K. K. Ambulkar[1], P. R. Parmar[1], A. L. Thakur[1],P. K .Sharma[1,2]

[1]*Institute for Plasma Research, Bhat, Gandhinagar 382428, India*

[2]*Homi Bhabha National Institute, BARC Training School Complex, Anushakti Nagar, Mumbai 400094, India*

E-mail: kiran@ipr.res.in

Electron Cyclotron Resonance (ECR) system [1] produces pre-ionized plasma and also used to drive plasma current non-inductively, which would increase the pulse length of plasma current up to few seconds. The magnetron based RF source at 2.45GHz is used to produce the ECR plasma.

To isolate the Ultra High Vacuum (UHV) environment of the tokamak and the transmission line at the atmospheric pressure, it is must to have the vacuum barrier between the tokamak and the transmission line. The RF vacuum window with a high return loss and low insertion loss for microwave at frequency 2.45GHz is designed, analyzedand presented earlier [2].The development of the UHV compatible RF window is the multidisciplinary problem wherein various aspects such as RF, Mechanical and Thermal have to be considered. The alumina metallized ceramic having alumina content of 99.7% is brazed with a copper metal cylinder in the vacuum furnace which acts as a vacuum barrier. The assembly and relevant testing details are reported. The low power rf measurement using Vector Network Analyzer is discussed along with the high power test.

This paper presents and discusses the development and measurement of 2.45GHz, UHV compatible RF window for ECR system.

References:

[1] P. K. Sharma et al., “ECR System At 2.45 GHz For Small Scale Spherical Tokamak,” in34th National Symposium on Plasma Science & Technology (PLASMA 2019) (Poster NF-240).

[2] Yogesh M. Jain, K. K. Ambulkar, Jagabandhu Kumar, P. K. Sharma, “Design and Multiphysics Analysis of a 2.45 GHz, 25 kW CW RF Window for Small Scale Spherical Tokamak” in 34th National Symposium on Plasma Science & Technology (PLASMA 2019) (Poster NF-309).

NFT-P-55

SMALL ASPECT-RATIO NUCLEAR TOKAMAK AS FUSION FISSION HYBRID

Pranjal Singh[1], Prabhat Ranjan[2], Nirav Bhaliya[1], Gaurav Singh[1], Jay Joshi[1], Kamya Chandrasekhar[1], Chandresh Shah[1], Manoj Srivastava[1], Akash Singh[1]

[1]*Albot Technologies Pvt. Ltd., Pune, Maharashtra, India*

[2]*DY Patil International University, Akurdi, Pune - 411044, Maharashtra, India*

E-mail: pranjal@albot.io

Compact volume neutron sources have number of applications ranging from medical isotope production to fuel breeding. A high yield of neutron flux can be achieved from small size tokamak devices wherein fast neutrons are produced from fusion of hydrogen nuclei.

The paper presents a novel modular design of **S**mall **A**spect-ratio **N**uclear **T**okamak as Fusion Fission Hybrid (SANT-FFH) capable of producing large flux of high energy neutrons to fulfill the limited availability of nuclear fuels simultaneously in hybrid model.

To demonstrate the proof of the concept project Sanalayan aims to deliver SANT-FFH. The design parameters of SANT-FFH based on the operational limits of magnetic confinement based compact fusion devices will be discussed in the presentation.

NFT-P-56

COMPENSATION OF FAST FEEDBACK CORRECTION MAGNETIC FIELD ON MAGNETIC DIAGNOSTIC IN ADITYA-U TOKAMAK

Rohit Kumar[1,*], Shivam Gupta[1, 2], R.L Tanna[1], S.K Jha[1], Suman Aich[1, 2], Tanmay Macwan[1, 2], Kunal Shah[1], M.N Makwana[1], Supriya Nair[1], Kaushlender Singh[1, 2], Suman Dolui[1, 2], Kaushal Patel[1], Kumarpal Jadeja[1] and J Ghosh[1, 2]

[1]*Institute for Plasma Research, Bhat, Gandhinagar 382428, Gujarat, India.*

[2]*HBNI, Training School complex, Anushakti Nagar, Mumbai 400085, India.*

E-mail: rohit.kumar@ipr.res.in

Real-time plasma position control [1] in ADITYA-U is based on the technique of using light intensity signals provided by pair of photodiodes. Correction in the plasma position is governed by the operation of Fast Feedback (FFB) coils in real-time using plasma position signal.The drawback of this method is that the position measurement results is affected by perturbations of the plasma edge by gas-puffs. Alternatively, Mirnov probes serve as sensors for the estimation of plasmaposition for the cross examination of plasma discharge parameters.

In the ADITYA-U tokamak, the magnetic diagnostic are significantly affected by the vessel eddy current due to different time varying magnetic fields. The plasma position measurement using Mirnov probe is reliable upto some extent as the signals are affected by the eddy currents induced by the variations of FFB currents. To eliminatethe deviation of plasma position caused by the FFB coils, the responses of the magnetic probes to theFFB coils at different frequencies are studied with a view to compensate for the pick-up fluxes.

In this work, the response function [2] is developed which provides a means to examine the effect of FFB coil field to calculate the absolute sensitivity of each Mirnov probe in the presence induced vessel eddy currents. The information derived in the calibration process can be used in equilibrium reconstructions to separate signals due to externally produced eddy currents at Mirnov probes, without determining the eddy current profile.

References:

[1] Rohit et al., "Real-time feedback control system for ADITYA-U horizontal plasma position stabilisation" Fusion Engineering and Design 165 (2021) 112218.

[2] J. Spaleta et al., “Magnetic probe response function calibration for plasma equilibrium reconstruction of CDX-U”, Rev Sci Inst. 77, 10E305 (2006).

NFT-P-57

A METHOD FOR PREPARATION OF ELECTRICAL CONTACT ON CARBON MATERIAL

K.P Singh[1,*], Priyanka Patel[1], Tushar Patel[1], Samir S Khirwadkar[1,2], Amardas Alli[3]

[1]*High Temperature Technologies Division, Institute for Plasma Research, Bhat, Gandhinagar 382 428*

[2]*Homi Bhabha National Institute, BARC Training School Complex, Anushakti Nagar, Mumbai 400094*

[3]*Inspection and Quality Division, Institute for Plasma Research, Bhat, Gandhinagar 382 428*

[*]*E-mail: kpsingh@ipr.res.in*

The present work describes a method of making electrical contact on carbon material especially graphite and CFC material. The direct joining of copper with carbon is not possible as there is no wetting between these two materials. Another problem is having a large thermal mismatch (CTE of carbon to copper is 1:16) between these two materials. Hence, an intermediate material is required to first metallize the graphite surface. Titanium as being an active metal that is commonly used for surface activation on graphite material. Titanium material has been coated by magnetron sputtering technique prior to copper coating on the carbon material. The metallized titanium surface has been further uniformly coated by OFHC copper material to have proper thermal and electrical contact. Proper masking is made to avoid coating on the unwanted region. Electrical contact has been made by soldering on the metallized coated area. The multi-layered coating surface has been characterized by optical microscopy and electrical resistivity by four probe resistivity measurement technique. Electrical resistivity is simulated by using COMSOL Multiphysics. The details of experimental works are presented in the paper.

CATEGORY: INDUSTRIAL PLASMA APPLICATION, PLASMA PROCESSING AND SOCIETAL BENEFIT OF PLASMA (IPS)

IPS-P-1

EMERGENCE OF NANOSCALE FEATURES USING LOW-ENERGY IONS PRODUCED BY PLASMA SOURCE

Sukriti Hans[1, 2], Mukesh Ranjan[1, 2]
[1]*Institute for Plasma Research, Bhat, Gandhinagar, Gujarat,India-382428*
[2]*Homi Bhabha National Institute, BARC Training School Complex, Anushaktinagar, Mumbai, Maharashtra, India-400094*
Email: sukritihans21@gmail.com

Irradiating surfaces with low energy ions produced by plasma source results in the formation of large variety of nanoscale features which has attracted much interest innanopatterning [1,2]. In the last decade, many investigations have focused on Silicon because of its technical applications. It has been found that, at low ion incident angles, the surface remains flat up to a certain critical angle after which the nanoripple formation starts. Along with that, triangular features are also observed which have not been investigated so far. These triangular features depend on ion beam irradiation parameters such as ion species, ion energy, angle of incidence and fluence etc.In this work, we report the investigation on the ion-beam induced triangular features using plasma source on silicon surfaces by varying different ion beam parameters. These triangular features start evolving after 200 eV energy leading to well enhanced features at 300eV and with increase in energy the base length of these features increases from 160 nm at 300 eV to 450 nm at 500 eV, after which these features don't appear. They are found in two categories: elevations and depressions. It is found that there is more number of elevations than depressions when angle of incidence was varied and this number increases up to 67^{o} and decreases afterwards [3].

Dispersion is found to be the responsible mechanism for the formation of these triangular features on ripple patterns [4].This is confirmed in our experiments by varying the ion fluence. With increase in the ion fluence, the lateral length of the triangular features increases whereas the base angle inside them remains constant. This trend isobserved for all the ion energies studied here.The evolution of these triangular features can be described by modified AKS equation. Numerical simulations are performed using this modified equation and results are consistent with our experiments. The performed simulations indicate that, curvature dependent sputtering and dispersion mechanisms seem to be the leading process in formation of the triangular features. Also these features show stronger lateral dependency on the angle of incidence [3].

References:

[1] A. Keller, S. Facsko, Materials (Basel). 3 (2010) 4811–4841.

[2] J. Muñoz-García, L. Vázquez, M. Castro, R. Gago, A. Redondo-Cubero, A. Moreno-Barrado, R. Cuerno, Mater. Sci. Eng. R Reports 86 (2014) 1–44.

[3] S. Hans, M. Ranjan, Surf. Sci. (2021) 121951.

[4] K.M. Loew, R.M. Bradley, Phys. Rev. E 100 (2019) 012801.

IPS-P-2

THE ANTIMICROBIAL EFFICACY OF ARGON COLD ATMOSPHERIC PLASMA JET ON MULTIDRUG-RESISTANT BACTERIA ISOLATED FROM HUMAN BLOOD

Sarthak Dasa*, Veda Prakash Gajulab, Sarita Mohapatrac, Satyananda Karb

[a]*School of Interdisciplinary Research, Indian Institute of Technology (IIT) Delhi, Hauz Khas, New Delhi –110016, India*

[b]*Department of Energy Science and Engineering, Indian Institute of Technology (IIT) Delhi, Hauz Khas, New Delhi –110016, India*

[c]*Department of Microbiology, All India Institute of Medical Sciences (AIIMS), New Delhi – 110029, India*

**Email id: sarthakdas.sd7@gmail.com*

Recently, the emergence of multidrug-resistant bacteria has led to rise in morbidityand mortality rate. The conventional antimicrobial techniques have trailed in combatting andpreventing the growth of these multidrug-resistant species. One of the possible solutions tothe ongoing situation is cold atmospheric plasma (CAP) technology. To understand theefficacy of CAP on multidrug-resistant bacteria, a cold atmospheric plasma jet (CAPJ) withan AC source (0-7.5 kV at 25 kHz) was indigenously developed. The bacteria E. coli(resistant to drugs ceftazidime, ciprofloxacin, cefoperazone sulbactam, and piperacillintazobactam) and S. aureus (resistant to cefoxitin, cotrimoxazole, ciprofloxacin, erythromycin,and penicillin) isolated from human blood following the standard operating procedure weretreated by argon CAPJ operating at 6.5 kV with variation in treatment distance (1 and 2 cm)and time (30 to 300 s). For E. coli, with an increase in CAP treatment time from 30 to 300 s,an increase in inactivation area from 1.413 to 7.848 cm2 and 0.714 to 7.033 cm2 at treatmentdistance 1 cm and 2 cm, respectively, was observed. Whereas, for S. aureus, with an increasein CAP treatment time from 30 to 300 s, an increase in inactivation area from 0.521 to 5.9045cm2 and 0.458 to 4.193 cm2 at treatment distance 1 cm and 2 cm, respectively was observed.The higher inactivation at a higher treatment time might be due to longer interaction of CAPreactive species (Ar*, OH, O1) with the bacteria cell wall and cellular components. Also, thehigher inactivation at less treatment distance might be attributed to the decrease in intensityof reactive species along the length of the CAP plume. Moreover, a higher inactivation wasobserved in E. coli than

S. aureus due to the difference in the cell wall structure. Theexperimental outcomes with indigenously developed CAPJ show high efficacy in theinactivation of multidrug-resistant bacteria and thus fortify the utilization of CAP as analternate antimicrobial technique.

IPS-P-3

EFFICACY AND BIOSAFETY EVALUATION OF COLD ATMOSPHERIC PLASMA FOR HAND STERLIZATION

Abu Sufiyan Chhipa[a], VikasRathore[b], Snehal Patel[a], PritiMehta[a], AkshayVaid[b], ShitalButani[a]*
[a]*Institute of Pharmacy, Nirma University, Ahmedabad, Gujarat*
[b]*Facilitation Centre for Industrial Plasma Technologies (FCIPT), Gandhinagar, Gujarat*

Objective: The present study was carried out to evaluate the disinfecting effects of Helium generated cold atmospheric plasma (He-CAP).The study further explored the biosafety profile of He-CAP on animal models and human volunteers.

Methodology: Disinfecting effects of He-CAP was evaluated on two bacterial strains namely: gram positive *Staphylococcus aureus* and gram negative *Pseudomonas aeruginosa.* Optimization of working parameters was done by testing the bactericidal efficiency against different combination of working parameters (exposure time, plasma flow rate and applied voltage). Cell membrane integrity was evaluated by the amount of protein leakage and scanning electron microscopy. For biosafety evaluation, MTT assay was performed to assess any cytotoxicity caused by the He-CAP exposure in human cell line. *In vivo* biosafety evaluation was performed on mice. Sensitivity and irritation (erythema and edema) caused by plasma on ear lobes (site of application) was measured.Histopathological analysis of the exposed ear lobes was performed. Further, Draize test was performed on albino rabbits for the assessment of dermal toxicity. Finally, plasma exposure (at the optimized combination of parameters) was given to human volunteers and grading of erythema and edema was done.

Results and conclusion: Isolated strains of bacteria were identified and verified. Optimization of working parameters showed that He-CAP highest bactericidal efficacy at flow rate 5 LPM, 5 minutes exposure and applied voltage at 2.50kV, when the distance between the plasma plume and bacterial culture was maintained at 10 mm. He-CAP resulted in significant membrane rupture, evident from protein leakage and SEM images. Biosafety evaluation of He-CAP showed no significant cytotoxicity in MTT assay. No signs of skin irritation and sensitivity on experimental animals. Histopathological analysis showed no signs of inflammation or tissue injury. Also, no signs of sensitivity or irritation were observed in human volunteers. In conclusion, He-CAP can be further explored for their bactericidal effects and can be used as an effective alternative to conventionally available disinfecting agents.

IPS-P-4

SURFACE PROPERTIES OF PULSED PLASMA ION NITRIDED INCONEL 601 ALLOY

Ravindra Kumar
Department of Physics, Birla Institute of Technology, Mesra, Jaipur Campus, Rajasthan-302017
Email: ravindrauniversal@gmail.com

In this study Inconel 601 alloy was plasma nitrided at different process temperatures to modify the surface properties. Inconel alloys are widely used material for various applications such as; chemical processing plants, gas turbine, heat exchanger and nuclear industries due to its excellent corrosion resistance and resistance to heat properties [1]. It's having such excellent properties but shows poor wear resistance and lower surface hardness [2]. After plasma ion nitriding, surface properties were investigated by various characterization techniques such as; scanning electron microscope (SEM), micro-hardness measurement, X-ray diffraction (XRD) and wear resistance properties by pin on disk method. A thin nitrided layer ~2-4 µm was observed under surface morphological images. It was observed that, surface micro-hardness increases after PIN process. The volume loss and wear rate were found to decreases after plasma nitriding process. The minimum wear rate ~1.06 x 10^{-4} mm^3/Nm was found in the samples of Inconel 601 alloys, which samples were nitrided at 350 ^{0}C. The SEM images agreed with the trends of our calculated values of wear rate with some anomaly.

References:

[1] Characterization of nitrogen-bearing surface layers on Ni-base super alloys, Wear, **263**, 625, (2007)

[2] Nitriding kinetics of Inconel 600, Surface and Coatings Technology, **226**, 92–99, (2013)

IPS-P-5

EFFECT OF GAS ENVIRONMENT DURINGSULFURIZATION PROCESS OF CZTS THIN FILM ON SOLAR CELL PERFORMANCE

Sagar Agrawal[*,a,b], RinkalKanani[a],
[a]*Institute for Plasma Research, Gandhinagar, Gujarat, India, 382428*
[b]*HomiBhabha National Institute, Anushaktinagar, Mumbai, Maharashtra, India, 400094.*
Email: sagar@ipr.res.in

Cu_2ZnSnS_4 (CZTS) is a well-known absorber layer which has proven its potential in thin film solar cell with a record efficiency of 11%[1]. The unique features of CZTS lies in its' high absorption coefficient of 10^4 cm^{-1}, an optimum band gap of 1.4-1.5 eV,

natural abundance and its non-toxic constituents [2][3]. Despite these attractive properties of CZTS for light harvesting, performance of CZTS layer as an absorber depend on many factors like, defects, grain size, grain boundaries, energy states, optical and structural properties, etc. Properties of CZTS layer depends on its process parameters, like elemental ratio of precursor, annealing rate, temperature, annealing time, annealing environment, etc.

In this work CZTS layer of up to one micron thickness was preparedby sulfurization (annealing in sulfur vapor + gas environment) of a precursor prepared using magnetron co-sputtering of Cu, Zn and Sn on soda lime glass. Annealing environment was changed by varying the gas (Argon / Nitrogen) during the sulfurization process to study the effect of gas environment on CZTS cell performance. Cells prepared using nitrogen gas sulfurization is found to be more efficient as compared to argon gas sulfurization. This could be because of the higher thermal conductivity of nitrogen gas which lead to the larger grain size and so higher short circuit current. A highest efficiency of ~5% has been achieved using nitrogen as annealing environment. These results will be presented and discussed in detail.

References:

[1] M.A. Green, E.D. Dunlop, J. Hohl-Ebinger, M. Yoshita, N. Kopidakis, X. Hao, Solar cell efficiency tables (version 56), Prog. Photovoltaics Res. Appl. 28 (2020) 629–638. https://doi.org/10.1002/pip.3303.

[2] H. Katagiri, K. Jimbo, S. Yamada, T. Kamimura, W.S. Maw, T. Fukano, T. Ito, T. Motohiro, Enhanced conversion efficiencies of Cu2ZnSnS4-based thin film solar cells by using preferential etching technique, Appl. Phys. Express. 1 (2008) 0412011–0412012. https://doi.org/10.1143/APEX.1.041201.

[3] H. Katagiri, Survey of development of CZTS-based thin film solar cells, ICP 2012 - 3rd Int. Conf. Photonics 2012, Proc. 517 (2012) 345–349. https://doi.org/10.1109/ICP.2012.6379533.

IPS-P-6

AN ACTIVE ARC SENSING AND CONTROLLING TECHNIQUE FOR PLASMA NITRIDING PROCESS

Keena Kalaria, Naresh Vaghela and Suryakant B. Gupta
Institute for Plasma Research, Bhat, Gandhinagar-382428
Email: keena@ipr.res.in

Carburizing, nitrocarburizing, or gas nitriding are traditional techniques used for the surface hardening processes. But those seeking precise control of diffusion layer formation, case depth, and preserving component dimensions are increasingly turning to advanced Plasma Nitriding process. Plasma Nitriding can significantly enhance wear and fatigue resistance that results into improved reliability and durability of the stainless steel. Pulsed DC power supply offer precise control of plasma nitriding parameters than conventional DC power supply. Using Pulsed DC power supply, the process parameters can be changed in a wide range by independently varying duty cycle and frequency or both. In addition, the reduction of current limiting resistance in Pulse DC Power Supply also help to save energy.

It is well known that during the plasma nitriding process, arcing is observed initially on the components due to the dust particles/oil/grease present on it. The arcing has to be suppressed because if the plasma goes to the arc mode, it may damage the components surface. Hence, active arc suppression is necessary during plasma nitriding process. This poster describes the design, development and implementation of an active arc sensing and control circuitry for the Pulsed DC Power Supply. An electronic circuit has been designed indigenously and integrated with the IGBT based Pulsed DC power supply for the Plasma Nitriding application. Furthermore, the circuit also does the measurement and monitoring of the peak current flowing in the load circuit during the plasma nitriding process. The objective of the proposed circuit is to prevent over currents caused by the arc discharge and thus leading to a significant improvement of performance of the Plasma Nitriding system.

IPS-P-7

STUDIES ON THE ROLE OF AXIAL MAGNETIC FIELD FOR LINE AND RING CUSP MAGNETIC CONFIGURATIONS IN A LOW ENERGY ION SOURCE

Bharat Singh Rawat[1, 2], S. K. Sharma [1, 2], B. Choksi[1], P. Bharathi[1], B. Sridhar[1], L.N. Gupta[1], D. Thakkar[1], S.L. Parmar[1], V. Prahlad[1] and U.K. Baruah[1, 3]

[1]Institute for Plasma Research, Bhat, Gandhinagar, Gujarat 382428

[2]Homi Bhabha National Institute, BARC Training School Complex, Mumbai, 400094

[3]ITER-India, Bhat-Motera Road, Ahmedabad, Gujarat 382424

Email: bharat.rawat@ipr.res.in

Low energy multi cusp ion sources have applications in various area like electric propulsion and material studies [1]. A line cusp ion source, developed at IPR, has shown excellent performance in extracting argon ion beam of current up to 240 mA at beam energy of 1650 eV and discharge loss ≥ 1500 W/A . In thruster applications, the discharge loss (inverse of discharge efficiency) is one of the important criteria for the ion source due to the limitation of available power in space. Ring cusp ion sources have been considered most suitable for thruster applications due to their low discharge losses [2]. Studies have indicated that the number of magnetic field lines connecting cathode to the extraction grids play an important role in reducing the discharge loss. The line cusp configuration does not provide such magnetic field lines in the axial direction. The Line cusp ion source is not very suitable in thruster applications due to their high discharge loss. The existing line cusp ion source is planned to upgrade with a ring cusp configuration. In this work, we shall present the initial experimental studies on the role of axial magnetic field and simulation studies on the confinement of primary electrons under line cusp and ring cusp configurations using CST studio [3].

References:

[1] J. S. Sovey, "Improved ion containment using a ring cusp ion thruster.," *NASA Tech. Memo.*, 1982, doi: 10.2514/6.1982-1928.

[2] D. M. Goebel, R. E. Wirz, and I. Katz, "Analytical ion thruster discharge performance model," *J. Propuls. Power*, 2007, doi: 10.2514/1.26404.

[3] D. Systems, "CST studio suite." 10, rue Marcel Dassault CS 40501 78946 Vélizy-Villacoublay Cedex, France, 2019, [Online]. Available: https://www.3ds.com/products-services/simulia/products/cst-studio-suite/.

IPS-P-8

LOW TEMPERATURE PLASMA CARBURIZING OF AUSTENITIC STAINLESS STEEL 316L

Ghanshyam Jhala, Vijay Chauhan, Pravin Dwivedi and Alphonsa Joseph

Institute for Plasma Research, Bhat, Gandhinagar-382 428, Gujarat, India

Email: grzala@ipr.res.in

Austenitic stainless steels are the most widely used corrosion-resistant materials in various sectors of industries, due to their excellent chemical and metallurgical properties. The food, pharmaceutical, chemical, pulp and paper, and petrochemical industries depend heavily on austenitic stainless steels because of their corrosion resistance yields low maintenance, lack of product contamination, high cleanability, and long life.

However, despite of many advantages the application of austenitic stainless steel is limited due to its low mechanical properties like hardness and wear resistance. In industries there are few technologies like carburizing and nitriding which improve the surface hardness and wear resistance of austenitic stainless steel.

In this study, efforts have been made to improve the surface hardness and wear resistant of austenitic stainless steel 316L by low temperature plasma carburizing process. The carbon expanded austenite produced on the surface of the steel sample by diffusing the carbon atom in to the surface with the help of plasma. To maintain the corrosion resistance of the steel after carburizing process low temperature for the process was selected (425, 450 and 475oC) at which chromium remains in the solid solution form thus it retains the corrosion resistance of the steel. Process was carried for 15 hours. The carburized sample was characterized for surface hardness, layer thickness, surface roughness and the phases formed during the processes.

It was found that there is an increase in surface hardness after this treatment. Carburized layer thickness increases with increasing temperature. Expanded austenite was confirmed through X-ray diffraction. There was increase in corrosion resistance when treated at 450oC.

IPS-P-09

STUDY ON SYNTHESIS OF TITANIUM NITRIDE NANOPARTICLES FROM WASTE TITANIUM SCRAPS BY THERMAL PLASMA ARC DISCHARGE METHODAND ITS MAGNETIC PROPERTIES

L. Kumaresan and G. Shanmugavelayutham*
Plasma Processing Laboratory Department of Physics, Bharathiar University,
Coimbatore - 641046, Tamil Nadu, India
Email: sgsvelu@buc.edu.in

Thermal plasma method is most interesting and effective technology for metal recovery, recycling process from bearing ores and metal waste scraps. Titanium nitridenanoparticles (TiN NPs) is an interestingceramic materialas it displays many other attractive features such as high hardness, good electrical conductivity, relatively high chemical inertness, very high melting point and favorable optical properties. TiN NPs, which combine large surface areas with good electrical conductivity is ideal for use in super-capacitors. The present work is to synthesis pure TiN NPs from waste titanium scraps by thermal plasma arc discharge method.Phase, elemental composition and morphology of the synthesized sample were characterized by XRD, EDS and TEM analysis. In addition to the above, the magnetic properties of the samples were investigated by vibrating sample magnetometer (VSM). From this study, the results indicate that the processed NPs are in pure phase whichexhibitscubic and spherical morphology. The magnetic properties, such as, saturation magnetization (M_S) and coercivity (H_C) were estimated and reported. The M–H loopsof TiN NPsrevealed soft ferromagnetic nature and comparatively very high M_S and H_C values.

Reference:

[1] S. B. Tharchanaa, K. Priyanka, K. Preethi, and G. Shanmugavelayutham, Mater. Technol. **36**, 97 (2021).

[2] S. Yugeswaran, P. V. Ananthapadmanabhan, L. Kumaresan, A. Kuberan, S. Sivakumar, G. Shanmugavelayutham, and K. Ramachandran, Ceram. Int. **44**, 14789 (2018).

[3] E. M. Koushika, G. Shanmugavelayutham, P. Saravanan, and C. Balasubramanian, Mater. Manuf. Process. **33**, 1701 (2018).

IPS-P-10

INVESTIGATION OF GAS DIFFUSION BARRIER AND ANTIFOULING PROPERTIES OF PLASMA TREATED LOW DENSITY POLYETHYLENE FOR PACKAGING APPLICATIONS

Purvi Dave*[1, 2], Balasubramanian C[1, 2], Sukriti Hans[1, 2] and S. K. Nema[1, 2]

[1]*Institute for Plasma Research, Atmospheric Pressure Plasma Division, Gandhinagar, India*

[2]*Homi Bhabha National Institute, Anushakti Nagar, Mumbai, India*

E-mail: purvi@ipr.res.in

Low Density Polyethylene (LDPE) is widely used material for food packaging applications. Shelf life of the packed food depends on many factors such as exposure to light, oxidative environment, microbes and temperature [1-2]. Both gas diffusion barrier property and antifouling properties are important for ensuring better food quality inside the packaging for a long time. Plasma treatment is an eco-friendly process used for modifying surface of polymeric materials at room temperature. In the present work LDPE surface is treated with Oxygen + HMDSO (Hexamythyl Disiloxane) plasma using capacitively coupled radio frequency (13.56 MHz) configuration. Prior to deposition, LDPE surface is activated using oxygen plasma. Surface energy calculated using OWRK model is found increased by two times after plasma treatment. Properties of SiOxCyHz film deposited by PECVD method is studied as a function of RF power. LDPE surface is characterized using video contact angle goniometer, Fourier Transform Infrared Spectroscopy (FTIR), Atomic Force Microscopy (AFM), Scanning Electron Microscopy (SEM) for wettability, surface chemistry and surface morphology respectively. Oxygen Transmission Rate is determined by pressure difference method and antifouling property is evaluated by plate counting method. Nine fold reduction in oxygen transmission rate is observed in SiOxCyHz coated LDPE packaging film. Results of antifouling properties of plasma treated LDPE surface are underway.

References:

[1] Malhotra B, Keshwani A and Kharkwal H (2015) Antimicrobial food packaging: potential and pitfalls. Front. Microbiol. 6:611. doi: 10.3389/ fmicb.2015.00611.

[2] Antimicrobial-coated films as food packaging: Yezhi Fu Edward G. Dudley A review, Compr Rev Food Sci Food Saf. 2021;20:3404-3437.

IPS-P-11

STUDY OF CHARACTERISTICS OF PLASMA ANTENNA

Manisha Jha[1, 2], Nisha Panghal[1], Unnati Patel[1], Rajesh Kumar[1, 2]
[1]*Institute for Plasma Research, Bhat, Gandhinagar, Gujarat 382428*
[2]*Homi Bhabha National Institute, BARC Training School Complex, Mumbai, Maharashtra 400094*
E-mail: manisha.jha@ipr.res.in

Plasma antenna has been modeled for VHF range in CST with varying the length, radius and pressure of the plasma antenna tube. The plasma antenna characteristics have been studied in terms of S11, VSWR and radiation pattern. A plasma antenna consists of Argon gas filled in a borosilicate tube of a particular length and radius at a particular pressure. The plasma properties depend upon the discharge condition like gas nature, pressure. In CST, the plasma characteristics are calculated using Drude model.

References:

[1] H. Ja'afar, M.T. Ali N. A Halili, Hanisah. Mohd Zali, A. N Dagang, "Analysis and Design between Plasma antenna and Monopole Antenna," IEEE International Symposium

[2] ANDERSON, T. Theory, measurements, and prototypes of plasma antennas. In IEEE Antennas and Propagation Society International Symposium (APSURSI). Memphis (TN, USA), 2014, p. 567–568. DOI: 10.1109/APS.2014.6904614

IPS-P-12

BULK RATE SYNTHESIS OF METAL-OXIDE NANOMATERIALS FOR TREATMENT OF WASTEWATER AND OTHER BIOMEDICAL APPLICATIONS

Mizanur Rahman[1], Deepak B. Pemmaraju[2]& M. Kakati[1]
[1]*CIMPLE-PSI Laboratory, CPP-IPR, Sonapur 782402, Assam, India*
[2]*Department of Pharmacology & Toxicology, NIPER Guwahati 781101, Assam, India*
E-mail :mayur@cppipr.res.in

The absence of controlled nanoparticle production methods with bulk production rates has often hindered actual utilization of nanomaterials in many prospective fields, especially in large-scale applications like water treatment and environmental engineering. Synthesis is also critical for hydrogen evolution reactions (HER), cancer treatment by photo-thermal therapies (PTT), or other plasmonic applications. Therefore, the search for alternative materials synthesized through fast and relatively simple techniques to replace expensive and scarce noble metals is still on high demand. In a novel plasma-chemical reactor configuration developed by us, the argon/oxygen plasma streamlines engulf a large metal plate to quickly oxidize the top surface and

sublimate, from which metal-oxide (WO_3 and MoO_3) nanomaterials are synthesized maximum upto 750 g/h. Blue-black coloured plasmonic nanosheets of sub-stoichiometric molybdenum oxide (MoO_{3-x}) were synthesized simply by injecting additional hydrogen gas into the plasma chamber. This step successfully introduced controlled surface oxygen vacancies through intercalation of low energy hydrogen atoms into the material crystal, all accomplished during a unique one-step process. Both metal oxides demonstrated efficient photo-catalytic, antibacterial, and absorption properties, which may lead to highly desirable multi-functionality during wastewater treatment. The defect-rich metal-oxide materials were perfectly dispersible in an aqueous solution. They had a strong absorption in the NIR (near-infrared region) regime. Therefore, we have observed the plasmonic structures in killing the skin cancer cells *in-vitro* when exposed to a NIR light source (808 nm) through photo-thermal mediated ablation. Moreover, the materials were observed to be magnetic at room temperature conditions. Considering the ferromagnetic properties, they may be controlled with a suitable magnetic field for targeted delivery during the PTT, thereby aiding as an *in-situ* NIR light responsive nano-probes that have a profound value in biomedical applications, especially in cancer treatment.

IPS-P-13

SPHEROIDIZATION OF METAL POWDERINMETHANE-CARBON DIOXIDE PLASMA JETAT ATMOSPHERIC PRESSURE

Yugesh.V[1*], Amarnath. P[1], Yugeswaran. S[1], Ananthapadmnabhan. PV[2]
[1] *Department of Physics, Pondicherry University, Puducherry–605014, India*
[2] *President, Power beam Society of India, India*
E-mail: yugeshv@gmail.com

Thermal plasma technology is the one of the prominent methods used in material processingdue to its high temperature and high energy density [1].Compared to the conventional plasma forming gases, the enthalpy and thermal conductivity of the methane (CH_4)-carbon dioxide (CO_2) mixture is higher than at the same temperature [2]. The thermophysical properties of CH_4 -CO_2 mixture at high temperature is a good option for material processing.In this attempt, a low power DC non-transferred arc plasma torch was designed to produce a stable CH_4 -CO_2 plasma jet for the spheroidization of metal powders. The reaction chemistry of the plasma jet has been controlled by the selection of CH_4 and CO_2 gas composition in order to process the metal powders without oxidation. The plasma torch was operated at different power levels with optimum gas flow rates. The electro-thermal efficiency of the plasma torch was in the range of 30-70%. Presence of active species and the temperature profile of the plasma jet along the axial direction has been studied through emission spectroscopy. Effect of plasma power and the plasma gas composition on spheroidization of metal powders will be presented in detail.

References:

[1] J. Trelles, C. Chazelas, A. Vardelle, and J. Heberlein, "Arc plasma torchmodeling," Journal ofthermal spray technology, vol. 18, p 728–752, (2009).

[2] Treatment of refractory powders by a novel, high enthalpy dc plasma, J. Phys. D: Appl. Phys. 46, 224019, (2013)

IPS-P-14

EFFECT OF CHARGE EXCHANGE COLLISIONS ON VELOCITY DISTRIBUTION OF N_2 AND N_2^+ FOR SELECTIVE EXTRACTION OF ENERGETIC SPECIES FOR COLD PLASMA FOOD PROCESSING

M. Perumal and Suraj Kumar Sinha,
Department of Physics, Pondicherry University, Pondicherry-605 014, India
E-mail : perumalphy@gmail.com

Cold plasma food processing (CPFP) is an emerging chemical-free technique that uses energetic ions, radicals, and UV radiations for physicochemical modification and microbial inactivation of various food products. Due to a lack of knowledge of active species generation mechanisms for a specific application, many CPFP devices are being investigated, adding complexity. In addition to this, low energy efficiency and high processing cost are preventing its industrial application. The present numerical investigation demonstrates that, by utilizing charge exchange collisions between N_2 and N_2^+inside the cathode sheath, a desired active species with specific energy can be selectively generated and extracted for the treatment. This concept was applied to a starch sample for physicochemical modification under typical glow discharge plasma using air as the feed gas. The use of air as feed gas reduces operating costs drastically, and energetic N_2 as active species improved the process energy efficiency to 40%. Thus, the present research may lead to a versatile CPFP device with high energy efficiency and low operating cost.

IPS-P-15

NITROGEN FIXATION THROUGH SUBMERGED THERMAL PLASMA PROCESS

Nanditta Nandy*, Indumathy B, Amarnath. P, Yugeswaran. S
Department of Physics, Pondicherry University, Puducherry–605014, India
E-mail : nanditalipi9999@gmail.com

In the nitrogen fixation process, the atmospheric nitrogen is converted to more reactive nitrogen compounds like ammonia, nitrates and nitrites. There is a huge demand of such nitrous compounds in medicine, fertilizers and chemical industries. Plasma assisted nitrogen fixation is done in two ways: one is the nitrogen reduction for ammonia synthesis and the other is oxidation to produce NO_X. Among different plasmas, thermal plasma uses oxidation process. In spite of the advantages like use of air as feedstock and being environmentally friendly, thermal plasma suffers a setback due to its high energy consumption and low production rate. Submerged thermal plasma is emerging as a new energy efficient green technology that has found many applications. In addition of having the above benefits of thermal plasma, its localized high enthalpy produces highly reactive species such as atomic oxygen and vibrationally excited nitrogen molecules which highly contributes on the production of NO_X in water phase. In addition to that the overall cold reactor provides high quenching rates that favors the NO_X formation. Keeping these advantages in view, a low power hollow cathode plasma torch (power range 10kW) is developed that can able to work in submerged conditions for the production of NO_X. Electrothermal efficiency and enthalpy of the plasma torch was characterized for Ar+N_2 and Ar+Air gas compositions. Reactive species, electron density and the temperature of plasma jet was determined by optical emission spectroscopy method. Generation of reactive species such OH, H_2O_2 and O_3 during the submerged plasma treatment was quantified by trapping reagent method, colorimetric method and indigo trisulfonate assay method, respectively. Concentration of nitrites and nitrates are analyzed by Ion chromatography method. Experimental results revealed that the formation of NOx was relatively higher in Ar+Air gas composition as compared to Ar+N_2 gas mixture. The maximum production rate of 9.42 g/hr achieved at Ar+Air plasma at 4.4 kW power.

IPS-P-16

STABILITY OF AL AND AG METALLIC THIN FILM MIRRORS IN SPACE ENVIRONMENT UNDER IMPLANTATION OF LOW ENERGY HYDROGEN AND HELIUM IONS FROM MICROWAVE PLASMAS

Krishn Pal Singh and Sudeep Bhattacharjee
Department of Physics, Indian Institute of Technology-Kanpur, Kanpur (U.P.) India, 208016
E-mail: krishnp@iitk.ac.in, sudeepb@iitk.ac.in

The space environment has long been a subject of interest to the scientific community because of its direct or indirect impact on our earth atmosphere or in missions related to earth exploration. The spacecrafts, satellites, and solar orbiter have been deployed in space to gather information about the solar activity or to study the solar environment in order to achieve deeper understanding about its impact on earth atmosphere [1]. These space investigating tools encounter the solar wind particles (mainly high energy protons and alpha particles) and cosmic rays (protons, electrons and heavy ions) coming from the distant stars and galaxies. The performance of optical components used in space vehicles is therefore subjected to degradation in harsh space environment [2]. Hence, prior knowledge of irradiation effect of proton and helium ions on Al and Ag could be useful for their possibility of being used in the space environment and for making sustainable metallic mirrors.

In this regard, following study has been carried out according to the European space agency program, which was planned to explore the solar activity by sending a sun orbiting satellite i.e., solar orbiter (SOLO) to its closest distance (0.28 AU at perihelion) [3]. The effect of bombardment of helium ions on reflectivity of Ag and Al MTFs has been investigated using Lambda 950 UV-VIS-NIR spectrophotometer in the wide range covering from ultraviolet to near infrared (200-2500 nm) region of the electromagnetic spectrum, by varying ion energy (0.5 - 3 keV) and dose {(1.1-1.56) × 10^{16} cm^{-2}}. The fluence of helium ions was chosen according to the four (1.1 × 10^{16} cm^{-2}) and six (1.56 × 10^{16} cm^{-2}) years journey of solar orbiter. It has been observed that the reflectivity of both the MTFs does not show the significant impact of implantation in the whole range of investigation and opens the channel of utilization of these MTFs to provide more stable MTFs for the mission.

In the conference, the effect of low energy hydrogen and helium ion irradiation on reflectivity of Al and Ag MTFs will be presented.

References:

[1] M. Pelizzo, A. J. Corso et al., Opt. Express **19**, 14838–14844 (2011)
[2] M. Pelizzo, A. J. Corso et al., ACS Appl. Mater. Interfaces **10**, 34781– 34791 (2018).
[3] A. D. Rousseau et al., Proc. Of SPIE., **5900**, 590004 (2005).

IPS-P-17

DESIGN AND CHARACTERIZATION OF COLD ATMOSPHERIC PRESSURE PLASMA SOURCES SUITABLE FOR FOOD AND AGRICULTURE APPLICATIONS

PritiPal[1,2], VishaliSingh[1], ShubhanshuNema Bhatiyara[1],Navin Kumar Sharma[3], Shikha Misra[2], Ravindra Kumar[2], Alok Mishra[2],Rajendra Kumar Verma[2],Udit Narayan Pal[2,3]Shivendra Maurya[1,2]and Ram Prakash Lamba[1,2]

[1]*CSIR- Central Electronics Engineering Research Institute, Pilani, Raj.-333031*

[2]*Academy of Scientific and Innovative Research (AcSIR), Ghaziabad, Uttar Pradesh- 201002*

[3]*Devi AhilyaVishwavidyalaya, Indore, Madhya Pradesh-452001*

E-mail: pritipal1998@gmail.com,rplamba@ceeri.res.in

Non-thermal plasma technology is environmentally friendly processing method that has a wide range of applications and meets the need of the food and agriculture industry [1]. Several non-thermal technologies have been tested in the food industries to prevent the food waste and to improve food production. Nonthermal surface decontamination procedures are ideal for a range of applications, including those in which it is critical to maintain the quality and nutritional properties of food products, which are frequently compromised by excessive heating. Furthermore, cold atmospheric pressure plasma (CAP) is an excellent method for increasing seed germination and seedling growth in agriculture [2]. The plasma-activated water (PAW) is a promising alternative to traditional food sanitizers and fertilizers. The PAW serves as a medium for transporting the plasma-generated species to the food and seeds [3].

The present work focuses on the design and characterization of CAP sources (excited by the short pulse electrical power and microwave power) suitable for food processing, seed germination enhancement, plant growth enhancement, food packaging, and sterilization. Different types of cold atmospheric pressure plasma jets (C-APPJ) have been designed, developed and characterized [4]. The developed C-APPJ have been used to investigate the seed germination and seedling growth parameters. Different types of the seed have been treated with the C-APPJ sources and comparative study have been carried out for the germination rate, root/shoot length and root/shoot weight of the seedlings, water-holding and moisture content, etc. Investigations have also been carried out for the measurement of different properties of PAW, like conductivity, pH, Turbidity, ORP, TDS, Nitrite, Nitrate, and Ammonia contents, and compared with the normal untreated water. It has been observed that after receiving cold plasma treatment, seedling development and health appear to improve. The seed's ability to absorb water has improved, and its root, shoot weight has increased compared to the control seed. Further characterization studies are underway to optimize the portable CAP sources for its potential applications in food and agriculture sectors.

References:

[1] D. Bermúdez-Aguirre, “Advances in cold plasma applications for food safety and preservation.”

[2] N. N. Misra, et al., *Food Eng. Rev.*,**3**, p. 159–170, (2011).

[3] Q. Wang and D. Salvi, Curr. Opin. Food Sci., vol. 42, pp. 51–60, Dec. 2021.

[4] N. K. Sharma, S. Misra, Varun, and U. N. Pal, Phys. Plasmas, vol. 27, no. 11, 2020.

IPS-P-18

DESIGN AND DEVELOPMENT OF COLD ATMOSPHERIC PRESSURE PLASMA JETS SUITABLE FOR BIOMEDICAL APPLICATIONS

Navin Kumar Sharma[1], Shikha Misra[2], Priti Pal[2,3], Ravindra Kumar[2], Alok Misra[2], Mahendra Singh[2], Ram Prakash Lamba[2,3], Murali M Pandey[4],Yaduvendra Choyal[1] and Udit Narayan Pal[2,3]

[1]*Devi Ahilya Vishwavidyalaya, Indore, Madhya Pradesh-452001*

[2]*CSIR- Central Electronics Engineering Research Institute, Pilani, Rajasthan. -333031*

[3]*Academy of Scientific and Innovative Research (AcSIR), Ghaziabad, U.P. - 201002*

[4]*Birla Institute of Technology and Science, Pilani, Pilani Campus, Rajasthan– 333031*

E-mail: navinshrma48@gmail.com, udit@ceeri.res.in

Cold atmospheric pressure plasma (CAP) sources have gained much interest among the researchersfor their potential applications in the area of biomedical, food, agriculture, etc. [1]. The key components of the CAP sources are ultraviolet radiation, neutral and charged particles, electromagnetic fields, reactive species, etc., which unlock the door for the applications in the field of plasma medicine [2,3]. Cold atmospheric pressure plasma jet (C-APPJ) is one of the CAP sources which gains enormous attentiondue to remarkable characteristics for the delivery of reactive oxygen and nitrogen species (RONS) in the small and confined regions [4]. In the recent past, research works have been carried out for utilizing the C-APPJ in wound healing, cancer treatment, drug delivery, etc. [6-7, 5, 2].

In the present work,efforts have been made for the indigenous design, development and characterization of dielectric barrier discharge(DBD) based C-APPJs at CSIR-CEERI.The generation and the propagation mechanism of the C-APPJs in the different geometrical configurations (tapered structure geometry of dielectric tube, straight cylindrical geometry, etc.) and operating conditions have been investigated. A detailed plasma simulation and experimental comparativeanalysis for the discharge formation and generation of plasma plumes in different C-APPJs have been carried out.The tapered structure of nozzle facilitates the high speed of gas as compare to inlet, which would be more focused to propagate toward the nozzle exit and results the fine and stable plasma plume, while the strait cylindrical nozzle producesthe wide plasma plume. The plume interacts with the air molecules and produces the reactive oxygen and nitrogen species (RONS). The presence of different species in the C-APPJ have been diagnosed using the optical emission spectroscopy (OES). The electrical and optical diagnostics have confirmed the formation of cold plasma plume and the generationof the metastable, hydroxyl (OH), NO, RONS, electromagnetic fields, UV radiation, etc. Further, efforts are underway for utilizing the developed C-APPJ in biomedical application.

References:

[1] G.Y. Park, et.al, Plasma Sources Sci. Technol. **21**, p. 043001 (2012)
[2] K. D. Weltmann and T. von Woedtke, *Plasma Phys. Control. Fusion*, **59**, no.1, Art. 014031, (2017).
[3] M. Keidar, et al, Phy. *of Plas*. **20**, Art.057101,(2013).
[4] S Reuter, et. al, J. Phys. D: Appl. Phys., **51**, no. 23, Art. 233001, (2018).
[5] S Bekeschus, et al. Redox Biology, **46**, Art. 1021116, (2021).
[6] Navin. K. Sharma, S. Misra, Varun, and U. N. Pal, Phy. of Plas., **27**, no. 11, Art. 113502, (2020).
[7] Navin K. Sharmaet al., IEEE. Trans. Plas. Sci. **49**, p 2799-2805, (2021).

IPS-P-19

DESIGN AND DEVELOPMENT OF DIELECTRIC BARRIER DISCHARGE BASED EFFICIENT VACUUM ULTRAVIOLET (VUV), FAR UV-C, AND UV EXCIMER RADIATION SOURCES

Navin Kumar Sharma[1], Surbhi Bidawat[2], Shikha Misra[2,]Shyam Sundar Jaiswal[2], Varun[2,3], Niraj Kumar[2,3], Ram Prakash Lamba[2,3], and Udit Narayan Pal[2,3]
[1]*Devi Ahilya Vishwavidyalaya, Indore, Madhya Pradesh-452001*
[2]*CSIR- Central Electronics Engineering Research Institute, Pilani, Rajasthan-333031*
[3]*Academy of Scientific and Innovative Research (AcSIR), Ghaziabad, U.P. - 201002*
E-mail: navinshrma48@gmail.com, udit@ceeri.res.in, rplamba@ceeri.res.in

There are resurgent requirement of mercury free Vacuum ultraviolet (VUV), Far Ultraviolet-C (UV-C) and Ultraviolet (UV) radiation sources in different industrial and societal applications such as surface modification, semiconductor treatment, surface disinfection, microbial inactivation,water purification, food packaging, etc.[1,2].In the past two decades, excimer sources established as a most promising incoherent sources for the efficient generation of VUV/Far-UV-C/UV radiations [3-5]. The intense emission characteristics of the different excimer/ exciplex molecules uplifted the development of such sources.Different excitation mechanism has been used for the operation of excilamps. Among these, dielectric barrier discharge (DBD) and micro-hollow cathode discharge based excilamps are efficient and therefore have gained much attention among the researchers [4-5]. Recent investigations show that the far UV-C radiation (207-222 nm) are very effective for inactivation of pathogens including Corona viruses, and also very much safe for the human [2].

In the present work, efforts have been made for the design and development of dielectric barrier discharge (DBD) based efficient Vacuum ultraviolet (VUV), Far Ultraviolet-C (UV-C) and Ultraviolet (UV) radiation sources and their potential societal and industrial applications. Plasma simulations have been carried out for the investigation of the discharge characteristics and the effect of the operating parametersfor efficient generation of VUV/ Far-UV and UV radiationsin the co-axial and flat geometrical configurations. The analysis has been carried out using the different noble gases and their mixture with halogen gases.

References:

[1] M.I. Lomaev, E.A. Sosnin, V.F. Tarasenko, Prog. in Quant Elect., **36**p. 51-97 (2012).

[2] David Welch et.al. *Sci Rep* **8,** 2752 (2018).

[3] U. N. Pal*et al.*, Plasma Sci. and Tech. **1**, P 635 (2013).

[4] U. N. Pal *et al.*, IEEE Trans. Plasma Sci. **39**, p. 1475 (2011).

[5] V. F. Tarasenko and E. A. Sosnin,Opt. Technol. **79**, p. 653-658 (2012).

IPS-P-20

HIGH VOLTAGE AND HIGH FREQUENCY PULSE POWER SUPPLY FOR PLASMA APPLICATIONS

A K Dhakar[1], S K Rai[2], M Mishra[3]and U N Pal[4]
[1,4]*CSIR-CEERI, Pilani, India*
[2]*EE Department, BKBIET, Pilani*
[3]*BITS-Pilani, Pilani Campus, India*

High voltage and high frequency pulse power supplies are the essential need of the plasma based devices for various applications. This paper included the design and experimental validation of the forward topology based high voltage and high frequency pulse power supply. The pulsar has voltage variation up to 5 kV with frequency variation up to 25 kHz. The pulse width of produced pulses is less than a microsecond. The pulsar has capability to produce both positive and negative pulses just by reversing the secondary winding of the pulse transformer. The experimental validation is done with the DBD load.

Keywords: Plasma Devices, DBD, Pulse Power Supply, Forward Topology

IPS-P-21

PLASMA JET INTERACTION WITH GB-SCC (ITOC-03) CELL LINE

A.Vaid[1*], K. Pansare[1,2], S.Singh[2], R.Rane[1], A. Visani[1], M. Ranjan[2,3], C.Krishna[2,3], R. Sarin[3,4]
A. Joseph[1,3]
[1] *Institute for Plasma Research, Gandhinagar, Gujarat, India*
[2] *Chilkapati Lab, TMC, ACTREC, Kharghar, Navi Mumbai-410210, India*
[3] *Homi Bhabha National Institute, Mumbai-400094, India*
[4] *ICGCLAb, TMC, ACTREC, Khargar, Navi Mumbai-410210, India*
*E-mail: akshay@ipr.res.in

Non-thermal plasma has found its applications in many biomedical fields. These fields include wound healing, blood coagulation, cancer treatment, skin treatment, root canal treatment, etc. The study on cancer using non-thermal plasma has started about a decade ago and is gaining prominence. One of the non-thermal plasma sources is the Atmospheric Pressure Plasma Jet (APPJ) developed by PSED, IPR. In this work, we have accessed the in-vitro efficacy in gingivobuccal squamous cell carcinoma (GB-SCC). We have found that plasma jet shows a pronounced inhibitory effect on GB-SCC at the treatment time of 4 to 5 minutes. We have also measured the concentration of ROS/RNOS in the medium in which the cells are grown and found that their concentration increases with an increase in treatment time. Results will be discussed in detail during the presentation.

IPS-P-22

GERMINATION ENHANCEMENT OF TOMATO AND CAPSICUM SEEDS USING DIELECTRIC BARRIER DISCHARGE (DBD) PLASMA TREATMENT

R.Rane[1*], A. Vaid[1], R.Parihar[1], P.Maila[1], A. Visani[1], A. Vikram[2], A. Joseph[1], M.Kumar[2]
[1] *Institute for Plasma Research, Gandhinagar, Gujarat, India*
[2] *Dr. Y. S. Parmar University of Horticulture and Forestry, Nauni, Solan- 173230, Himachal Pradesh, India*
*E-mail: ramu@ipr.res.in

Plasma treatment of seeds has the potential to improve germination yields and kill fungal spores present on seed coats. The dielectric barrier discharge (DBD) based atmospheric pressure plasma system has been developed at PSED, IPR. The system consists of a plasma treatment area of 75 x 25 cm. The seeds to be plasma treated are spread uniformly on the electrodes. The tomato and capsicum seeds were treated at different plasma exposure times using air plasma. The surface morphology of plasma-treated seeds is studied by Scanning Electron Microscopy (SEM) while hydrophilicity of the surface is studied by water contact angle measurement. The plasma-treated capsicum and tomato seeds showed around 30-40 % improvement in germination

percentage. The plasma-treated surface of the seed becomes more hydrophilic which helps in improving germination percentage and speed of the germination.

IPS-P-23

ON UTILIZATION OF DIELECTRIC BARRIER DISCHARGE PLASMA FOR BENEFIT OF MANKIND

Anand Kumar Srivastava
Birla Institute of Technology Mesra (Ranchi),
Jaipur Campus, Jaipur, Rajasthan 302017, *India*
E-mail: aksrivastava@bitmesra.ac.in

Plasma "The fourth state of matter" is an ionized gas and comprising of constituents like electrons, ions, neutral particles, radicals, UV radiation, chemical species, EM fields etc. The plasma research is an important part for harvesting energy like sun through nuclear fusion reactor. The fusion energy is enormous and will certainly fulfill the energy requirements of mankind. Further with several advancements, laboratory plasma sources have been explored for various industrial applications for benefit of society. The cold plasma produced at atmospheric-pressure are playing a crucial role societal plasma application. They are extensively proposed for various daily-life applications such as water/air purification, pollution-control, plasma-television, lightening, plasma-medicine, material treatment, food sterilization, agriculture, aerodynamics etc. Dielectric barrier discharge (DBD) plasma-sources are the potential candidates among various atmospheric pressure plasmas due to their flexible design, uniformity, and scalability. Different DBD geometries have been designed and characterized suitable to particular application. We have also performed E-field simulations to support experimental observations. It is observed that the optimization of DBD parameters is required to achieve improved source efficiency. The paper presents various prospects of DBD plasma sources relevant to its exploration for benefit of mankind or society.

References:

[1] J.R. Roth, 'Industrial Plasma Engineering,' Bristol, U.K.: IOP, **1**, Principles, (1995).

[2] R. Brandenburg, Plasma Sources Sci. Tech., **26**, No.5,p1-29 (2017).

IPS-P-24

PURE AND SAMARIUM INCORPORATED LITHIUM TITANATE AS LOW ACTIVATION CERAMICS FOR BREEDER BLANKET APPLICATION

S.K.Sinha
Department of Physics, Birla Institute of Technology, Mesra, Patna campus, India-800014
Email: sk.sinha@bitmesra.ac.in

High activation energy of blanket ceramics material for breeding of tritium has been a problem in tritium production. Li^6 available in Li_2TiO_3 (Lithium Titanate Ceramics) is capable in producing tritium by the high energy bombardment of neuron. Activation Energy for the lithium Titanate prepared by solid state method has been reported in the range of 0.14 to 0.18 eV. Achieving such as high input energy in getting the Tritium require very high temperature of Breeder blanket and this high requirement of initial input energy raise a big question of feasibility of breeder blanket reaction.

To reduce the required activation energy, in present work the material fabrication is carried out by adopting sol. gel. method of fabrication of nano ceramics. Since activation energy of a ceramics is linked with the materials electrical conductivity and permittivity. It has been reported by many workers [1-3] that activation energy depends of the dopants as the dopants have capability to influence the conductivity as well as dielectric constatnt. A proper selection of dopant makes the total charge in the material to contribute positively.

Samarium being lanthanide series of material having a few favourable feature to contribute in reduction of activation energy of Li_2TiO_3. Sm^{+2} being helpful in increasing the electrical conductivity of the material and as a result it reduces the activation energy of lithium titanate.Sm^{+2} doped Li_2TiO_3 ceramics pebbles were prepared by sol gel technique followed by urea – acetone spherodization method. Activation energy was calculated by taking help of impedance analyser and a computer program. The activation energy was found to decrease by 20% after incorporation of Samarium in lithium titanate.

References

[1] Kopasz, J. P., Miller, J. M., & Johnson, C. E. (1994). Tritium release from lithium titanate, a low-activation tritium breeding material. *Journal of nuclear materials*, *212*, 927-931.

[2] Kumar, M., Sinha, R. K., Yadav, S., Sinha, S. K., & Raole, P. M. (2017). Preparation of Ca modified Li2TiO3 ceramics pebbles and its activation energy calculation. *International Journal of Materials Engineering Innovation*, *8*(3-4), 273-281.

[3] Sharma, P., & Uniyal, P. (2017). Investigating thermal and kinetic parameters of lithium titanate formation by solid-state method. *Journal of Thermal Analysis and Calorimetry*, *128*(2), 875-882.

IPS-P-25

TISSUE THICKNESS PLAYS AN IMPORTANT ROLE IN PENETRATION OF COLD ATMOSPHERIC PLASMA IN TUMOR TISSUES RESECTED FROM GLIOMA PATIENTS

Yogesh Aggarwal, Akshay Vaid, Jyotirmoy Banerjee, P.S. Chandra, Alphonsa Joseph, Ramakrishna Rane, Anand Visani, Manjari Tripathi, Ramesh Doddamani, Aparna Dixit
All India Institute of Medical Sciences, New Delhi
Email: yogeshaggarwal19@gmail.com

Purpose: Cold atmospheric plasma (CAP) is a promising adjunctive therapy for the treatment of gliomas as it specifically targets cancer cells through generation of reactive oxygen and nitrogen species (RONS). A significant number of patients with glioma experience seizures even after surgery, primarily due to incomplete resection of the tumor. Treatment of tumor bed with CAP post resection provides an opportunity to reduce recurrence in patients with glioma. The effectiveness of CAP in deeper layers of human tissue remains a challenge and very few studies have investigated CAP tissue penetration in resected brain tissues. This study was designed to study the efficacy of CAP to penetrate resected tissues obtained from glioma patients by measuring the levels of RONS in tumor tissues of different thickness.

Method: Helium CAP jet with Voltage set at 4 kV and Gas flow rate (GFR) at 3 LPM was used in this study. Surgically resected tumor tissue specimens from ten glioma patients were obtained. Tumor tissue (~10 mm thickness) or 600 µm-thick slices, prepared using vibratome, were treated with plasma jet for 5 min and intracellular RONS levels were measured.

Result: Increase in intracellular RONS was observed in both glioma tissues (0.1064 ± 0.0436 nmoles/mg) and slices (0.175 ± 0.075 nmoles/mg) on plasma jet treatment as compared to untreated tissues (0.0584±0.0127 nmoles/mg) and slices (0.072 ± 0.015 nmoles/mg) respectively. However, glioma slices with lesser thickness showed higher percentage increase in RONS (133.31 ± 54.85 %) compared to glioma tissues with higher thickness (81.35 ± 53.57 %).

Conclusions: The magnitude of effect of plasma jet is higher in thinner tumor samples as compared to the thicker samples. Thus, penetration depth of CAP is a critical factor that needs to be considered for the treatment of tumor bed in patients with glioma. CAP could be used as a potential adjunct therapy post-resection for a seizure-free surgical outcome in patients with glioma.

CATEGORY: PLASMA DIAGNOSICS (PDG)

PDG-P-1

STUDY AND CHARACTERIZATION OF HYDROGEN / ARGON / NITROGEN PLASMA PRODUCED BY ELECTRON CYCLOTRON RESONANCE USING DOUBLE LANGMUIR PROBE

S. K. Jain[1],[2], [a], Rekhya Naika[1], Manish Pathak[1], Rajnish Kumar[1], Dharmraj V. Ghodke[1], Vijendra Prasad[1], Purushottam Shrivastava[1]

[1]*Raja Ramanna Centre for Advanced Technology (RRCAT), Indore - 452 013, India*

[2]*Homi Bhabha National Institute, Training School Complex, Anushakti Nagar, Mumbai - 400 094, India*

[a]*E-mail : skjain@rrcat.gov.in*

Development of various types of H-/H+ ion sources like filament heated arc based ion source, RF based ion source and electron cyclotron resonance (ECR) ion source is being pursued at Raja Ramanna Centre for Advanced Technology, Indore as a front end source for the pulsed proton accelerators. The ion sources are tested and characterized for its plasma parameters with operating conditions at various stages. The most preferred device used for plasma parameters characterization is Langmuir probe [1, 2, 3, 4]. In ECR ion source, plasma is produced using hydrogen / argon / nitrogen as feeding gas. The produced plasma is characterized at different input power by varying inlet gas pressure, using Langmuir probe, under tunable magnetic field, produced by an electromagnet, for flat as well as mirror configuration. The probe is placed 20 mm inside to the plasma chamber i.e. away from the ECR surface where electrons are heated. Due to this, the effect of the mirror magnetic field is not seen much on plasma parameters. It has been observed that at a constant input gas pressure, with increasing microwave power, the rate of ionization does not increase significantly. However, at given constant input microwave power, with increasing input gas pressure, the rate of ionization increases. This paper discusses the details of recorded results of ECR plasma source by using Langmuir probe for acquiring data in the form of current-voltage curve at various operating parameters like input microwave power, different filling gas pressures etc. for hydrogen / argon / nitrogen feed gas.

References:

[1] F. F. Chen, R. H. Huddlestone, and S. L. Leonard, “Plasma Diagnostics Techniques” (Academic Press, New York, 1965).

[2] J. D. Swift, and M. J. Schwar, “Electrical Probes for Plasma Diagnostics” (Elsevier, New York 1969).

[3] I. M. Hutchinson, “Principles of Plasma Diagnostics” (Cambridge University Press, New York, 1987).

[4] N. Hershkowitz, “Plasma Diagnostics” (Academic Press, New York, 1989).

PDG-P-2

ELIMINATING FLUX CONTRIBUTED BY EXTERNAL CURRENTS AND EDDY CURRENT FROM MAGNETIC PROBE MEASUREMENT IN SST-1 DISCHARGES

Sameer Kumar, Kumudni Tahiliani, Surya Kumar Pathak, Daniel Raju, Praveena Kumari, Vismaysinh D Raulji , Praveenlal Edappala, Ashish Ranjan, Jasraj Dongde and SST -1 Team
Institute for plasma research, Bhat, Gandhinagar
Email: skjha@ipr.res.in

Poloidal field of plasma current is useful quantity for estimating plasma parameters like plasma position and shape. It is measured by discrete magnetic probes along apoloidalboundary of plasma current. The voltage signal in magnetic probes is contributed not only by plasma current but also by the current in external circuits (VF coils, ohmic coils and RCC coils) and eddy current on SST-1 vessel. The contribution of these external currents needs to be eliminated from the probe signal to achieve an accurate measurement of poloidal field.

An integrator is connected to magnetic probes to convert voltage signal intopoloidal field or flux. The integrated output of the probe is represented as weighted sum of current of external circuits and a convolution integral of current and anexponential function $e^{(-\alpha\tau)}$ [1-2]. Their weights are determined in non-plasma shots in which all external currents are present except plasma current. The contribution of external current are estimated from the obtained weights and measured external currentsand then eliminated from the probe measurements for every plasma shot.

References:

[1] S. K. Saha, R. Kumar, and A. K. Hui, Rev. Sci. Instrum. **72**, 4289 (2001).

[2] Kumar S, Jha R, Lal P, Hansaliya C, Gopalkrishna M V, Kulkarni S and Mishra K 2010 *Rev. Sci. Instrum.* **81** 123505

PDG-P-3

DENOISING THE NOISY PLASMA IMAGES CAPTURED THROUGH WOUND OPTICAL FIBER BUNDLE

Abhishek Sharma, Agraj Abhishek, Gaurav A. Garg, Surajkumar Gupta, Manoj Kumar, Manika Sharma
Institute for Plasma Research, Bhat, Gandhinagar-382428,
Email:abhishek.sharma@ipr.res.in

Visible image acquisition is one of the activities during Plasma experiments todiagnose Tokamak Plasma. It plays an important role in diagnostics for Plasma basedstudies to measure plasma movement, plasma size etc. Due to the presence of strongmagnetic fields in and around Tokamak, the camera cannot be directly kept inside theTokamak. To solve this problem wound optical fiber bundle is used, which transportsthe Plasma images from inside of the machine to the camera outside. But optical fiberbundle has a problem of inheriting spatial noise into the image. Due to the orientationand edges of fibers, a honeycomb like structure is induced on image. Denoising refers to removal of unwanted noise from image to improve its PSNR (Peak signaltonoiseratio). Noisy image needs to be denoised first for further studyof plasma. It is also one of the major preprocessingsteps. Different denoisingalgorithms and spatial filters has been used to produce different results. The resultsare then compared to find the best algorithm to denoise the image.

PDG-P-4

IMAGING DIAGNOSTICS IN SST-1

Suraj Kumar Gupta, Vishnu Chaudhari, Manoj Kumar,
Institute for Plasma Research, Bhat, Gandhinagar India.
E-mail : skgupta@ipr.res.in

There are several diagnostics installed in SST-1 tokamak to study the plasma movement, behavior and characteristics of the plasma. For plasma movement and plasma wall interactions imaging diagnostics is used in SST-1. This diagnostics consists of imaging lenses, wound imaging fiber bundle, relay lens and GigE based mirror-less camera. The assembly is installed at port no. 08 (which is tangential) of the machine. Data acquisition is done in industrial PC with the help of Lab-View based software. The software is synchronized with SST-1 central server. Camera is triggered by the pulse of the central server which is routed through function generator. The camera records the frame at the timed interval of 30 mili-seconds. Data is saved on PC after the completion of the plasma shot.

Various narrow band filters can be used to monitor the specific impurity or elemental distribution during the plasma discharge and evolution. Carbon filter can acquire C II (singly ionized carbon) images, oxygen filter can acquire oxygen impurities, in the torus during the shot. H-alpha filter can be sued to capture the plasma column movement and interaction with the plasma facing components.

References:

[1] Design of a wide angle infrared thermography and visible diagnostic for JET, *Association EURATOM-CEA, CEA/DSM/DRFC, CEA Cadarache, France,* E Gauthier et Al.

[2] A visible light high-speed imaging system and tomographic reconstruction of plasma emissivity on the J-TEXT tokamak, Minghui Xia et al, Fusion Engg & Design

[3] Installation of a fast framing visible camera on KSTAR Rev. Sci. Instrum., 79 (10) (2008), p. 1056

PDG-P-5

STUDY OF A PROTOTYPE METAL FOIL BOLOMETER

Devilal Kumawat[1], Kumudni Tahiliani[1], Praveen Lal E.V[1], Prabal Biswas[1], Suresh I[1], Santosh P Pandya[1], Manoj K Gupta[1], S.K. Pathak[1,2]
[1]Institute for Plasma Research, Bhat, Gandhinagar, Gujarat, 382428, India
[2]Homi Bhabha National Institute, Mumbai, 400 094, India
Email: devilal.kumawat@ipr.res.in

A thin metal foil is used as a broadband radiation absorber from the ultraviolet to soft x-ray radiation in a metal foil bolometer, which is used for the measurement of the total radiation loss from the tokamak. The metal foil bolometer plays a vital role in establishing the local energy balance and study of plasma-wall interaction in the tokamak. The bolometer is composed of three layers, a platinumabsorber foil, kapton dielectric, and a 50 Ω meander resistor made of platinum.

A prototype metal foil bolometer is calibrated in the lab and the calibration constantsviz. thermal resistance, cooling time, and heat capacity are determined.To determine the temperature coefficient of resistance of the bolometer a RTD and IR thermography are used. ANSYS analysis on prototype bolometer is performed to validate the experimental data. The prototype metal foil bolometer has been tested for different incident powers.

References:

1. E.R Muller, and F. Mast, J applied Physics, 55(7), 1984
2. J. Schivell, Rev. Sci. Instrument, 59(8), 1988

PDG-P-6

DYNAMICS OF SLOW AND FAST COMPONENTS IN LASER PRODUCED PLASMA OF CARBON AND RUBY

Archana Kushwaha[a]*, Satchi Kumari[b] and Alika Khare[c]
[a]*Indian Institute of Information Technology, Guwahati*
,[b]*Central University of Jharkhand, Ranchi*
[c]*Indian Institute of Technology, Guwahati*
**E-mail: archana@iiitg.ac.in*

Laser produced plasma (LPP) is a very promising field due to its enormous applications in thin film deposition, X-ray production, ion production, identification of materials etc1. It exhibits an interesting feature of double and triple peak in its time-of-flight signals2,3. The slow component is attributed to maximum radiation absorption during the laser pulse. Whereas, the fast components appear at the end of the laser pulse and contains information about plasma dynamics. The analysis of these peaks can provide in depth knowledge about LPP behaviour which in turn governs all the applications. To study these dynamics in detail, we have selected two entirely different compositions first one is carbon-nitrogen system and another is alumina doped with chromium (Ruby). Double peak and triple peak features were observed in both the cases.

In case of carbon plasma, time-resolved imaging and spectroscopy techniques were used to study this peculiarity4. It has been observed that the expanding plume splits into two parts (at 0.05μs) forming a slower component, close to the target and a faster component, away from the target. The slower component contains atomic and ionic emission that vanishes earlier inferring a relatively lower lifetime of primarily ejected atoms and ions. The faster component is the result of collisions between the particles (ions and atoms) in the plume and the ambient N2 gas. Further, at ~0.3 μs, a third component of the plasma emission appears on the back of the leading component of the expanding plume. It arises due to formation of C2 and CN molecules in the plasma having comparatively longer lifetime. A fluctuation in temporal variation of velocity of the C2 molecule is also observed at ∼0.35 μs which actually corresponds to triple peaks in TOF signal and confirms re-splitting at later stage.

In spite of having very different composition, interestingly, Ruby plasma also showed the double and triple peak behavior in Langmuir probe diagnostic5. It confirms two velocity components for the constituent species at early stage. The first peak is very sharp (~ 0.5 μs) and slow peak is relatively broad (~ 5 μs). The triple peak was observed at 50 mm away from the target due to further re-splitting of plume. The physics of plume splitting in LPP of carbon and ruby, shall be compared and discussed in details.

References:

[1] Laser-Induced Plasmas and Applications, L. J. Radziemski and D. A. Cremers (1989).

[2] J. Phys. D: Appl. Phys. **54,** 37, LT01, p 1-5, (2021).

[3] Phys. Lett. **73,** 2, p 163-165, (1998)

[4] J. Appl. Phys. **105**, p 044902-044905, (2009)

[5] J. Instr. **7,** 5, p C05017, p 1-9, (2012)

PDG-P-7

INITIAL RESULTS OBTAINED FROM NEAR-INFRARED SPECTROSCOPIC SYSTEM ON ADITYA-U TOKAMAK

N. Ramaiya[1], R. Manchanda[1], M. B. Chowdhuri[1], N. Yadava[2], S. K. Pathak[1], R. L. Tanna[1], K. A. Jadeja[1], K. M. Patel[1], R. Kumar[1], S. Aich[1], and J. Ghosh[1]

[1]Institute for Plasma Research, Gandhinagar – 382428, India

[2]Institute of Science, Nirma University, Ahmedabad – 382481, India

Email: nilam@ipr.res.in

Near-infrared (NIR) spectroscopic studies of tokamak plasma has become currently important as the UV-Visible spectroscopy faces many issues emerging in the harsh environments of tokamaks, like ITER, producing burning plasma [1]. These issues are, as suggested from the results obtained from the DT operation phases on the TFTR and JET tokamaks, related to the performance degradation of optical components, e.g., windows and fibers, under high neutron, plasma particle and γ-ray fluxes [2, 3, 4]. It has been observed that even in harsh environmental conditions, optical material and component properties are not much degraded in the NIR range, having its diagnostics concept almost similarto aUV-Visible spectroscopic system. Therefore, NIR spectroscopy is an effective technique which can be used to carry out plasma control and performance measurements in fusion grade plasmas [5, 6].

Considering that, a near-infrared spectroscopic system has been developed on ADITYA-U tokamak [7] having capability of producing shaped plasma in the divertor configuration. It consists of a 0.5 m spectrometer with image sensor PyLon-IR: 1024-1.7, a linear InGaAs photodiode array. The sensor is having 1024 × 1 pixels with each pixel with size 25 μm × 500 μm. The spectrometer is equipped with three gratings, 300 grooves/mm blazed at 1700 nm, 600 grooves/mm blazed at 1000 nm, and 1200 grooves/mm blazed at 750 nm. To carry out initial measurements from the tokamak, radiation is collected using an optical fiber with 1 mm core diameter and 0.22 numerical aperture. A collimating beam probe having a lens with 19 mm focal length and 11 mm diameter is connected at the front end of the fiber and views the edge plasma radially. For the first time, a survey spectrum in the NIR wavelength range has been obtained from ADITYA-U plasma using this diagnostic system. The spectral lines such as C I, C II, N I, Li I, He I, and $H_\alpha$have been clearly observed in the survey spectrum. By using the ionization per photon (S/XB) factors available in the ADAS system [8] for these observed lines, particle influx measurements have been estimated and compared with influx measurements done using a visible spectroscopic system. The details of the newly installed NIR spectroscopic diagnostic system, initial survey spectrum, and influx measurements are presented.

References:

[1] G. Vayakiset *al*., Fusion Sci. Technol. **53,** 699 (2008)
[2] A. Ramsey, Rev. Sci. Instrum. **66**, 871 (1995)
[3] A. C. Maas *et al*., Fusion Eng. Des. **47**, 247 (1999)
[4] T. Shikama, Nucl. Fusion **43**, 517 (2003)
[5] V. A. Soukhanovskii*et al*., Rev. Sci. Instrum**79**, 10F539 (2008)
[6] V. A. Soukhanovskii*et al*., Rev. Sci. Instrum. **85**, 11E418 (2014)
[7] R. L. Tanna*et al.*, Plasma Sci. Technol. **20**, 074002 (2018)
[8] H. P. Summers, The ADAS User Manual, version 2.6, http://adas.phys.strath.ac.uk (2004)

PDG-P-8

FABRICATION, INSTALLATION, DATA ACQUISITION OF DIAMAGNETIC LOOP IN ADITYA-U TOKAMAK

S. Aich[1,2,*], K. Singh[1,2], S. Dolui[1,2], J. Ghosh[1,2], K. Galodiya[1], T. M. Macwan[1,2], R. L. Tanna[1], R. Kumar[1], H. Mandliya[1], A. Kumar[1], Praveenlal E. V.[1], Ankit Kumar[1,2], K. A. Jadeja1, K. Patel[1], and ADITYA-U team
[1]*Institute for Plasma Research, Gandhinagar, Gujarat - 382428, India*
[2]*Homi Bhabha National Institute Anushaktinagar, Mumbai, Maharashtra − 400094, India*
**Email: suman.aich@ipr.res.in*

The measurement of the stored energy of a tokamak plasma resolves many gaps between the energy input and its utilisation during plasma discharges and so it plays a crucial role for the diagnosis of the plasma [1]. One of simple techniques for the measurement of the stored energy of tokamak plasma is diamagnetic loop measurement method. A diamagnetic loop is a single turn conducting wire, encircling the plasma ring poloidally and it essentially measures the toroidal magnetic field both at the presence and absence of plasma [2]. A processing of the acquired data gives the estimation of stored energy inside the plasma. New diamagnetic loops, along with diamagnetic compensation loops, are designed, fabricated and installed in Aditya-U tokamak, which is a medium size machine with major and minor radii 75 cm and 25 cm respectively. The corresponding data of the diamagnetic and compensation loops during plasma discharge is acquired and found to contain several noise pick-ups. The noise is then substantially reduced by the use of proper electronics and hence a cleaner data is acquired using a dedicated data acquisition system. This work summarises an entire idea of designing a magnetic diagnostics – starting from basic considerations to the final data acquisition. As a consequence, several interesting and impactful conclusions are achieved.

References:

[1] WESSON, J., Tokamaks, Oxford, Clarendon (1997).
[2] HUTCHINSON, I. H., Principles of Plasma Diagnostics, Cambridge University Press, Cambridge (1987).

PDG-P-9

IMPURITY TRANSPORT IN ADITYA-U TOKAMAK WITH INDIGENOUSLY DEVELOPED SEMI-IMPLICIT IMPURITY TRANSPORT CODE

Nandini Yadava[1, 2], J. Ghosh[3, 4], M. B. Chowdhuri[3], Ashoke De[1], R. Manchanda[3], N. Ramaiya[3], K. Shah[5], S. Patel[5], S. Purohit[3], M. K. Gupta[3], U. C. Nagora[3], S. K. Pathak[3], K. A. Jadeja[3], K. M. Patel[3], Ankur Pandya[6], R. Kumar[3], Tanmay Macwan[3, 4], S. Aich[3], Suman Dolui[3, 4], Kaushlender Singh[3, 4] R. L. Tanna[2, 3] and Aditya-U Team[3]

[1]*Department of Aerospace Engineering, Indian Institute of Technology Kanpur, Kanpur-208 016, Uttar Pradesh, India*
[2] *Institute of Science, Nirma University, Ahmedabad 382 481, Gujarat, India*
[3]*Institute for Plasma Research, Bhat 382 428, Gandhinagar, India*
[4] *HBNI, Training School Complex, Anushakti Nagar 400 085, Mumbai, India*
[5]*Department of Physics, Pandit Deendayal Petroleum University, Raisan, Gandhinagar 382421, India*
[6] *Institute of Technology, Nirma University, Ahmedabad 382 481, Gujarat, India*
E-mail: nandini7754@gmail.com

Impurity gas seeding, i.e., injection of non-fuel gases in tokamak plasmas, has several applications. One of the important applications is to reduce heat load on plasma facing components during disruptions. Further, optimized seeding also leads to improved confinement like radiative improved (RI) and detached H-mode. Neon, Argon, Lithium and Nitrogen are most common candidate for gas seeding into tokamak plasmas. The impurity transport, i.e., how the particles of these injected gases behave in the hot tokamak plasma, becomes important to study when exploring different plasma phenomenon happening due to impurity seeding. To simulate the radial transport of these above-mentioned species, an indigenous code has been developed. The main crux of this code resides in the semi-implicit numerical method for solving the transport equation while producing the simulated radial profiles of different impurity ions [1]. The current version of the code is capable of producing radial emissivity profiles of Oxygen (Z=8), Carbon (Z=6) and Neon (Z=10) impurity ions. The results will be than compared with experimentally obtained emissivity profiles. In the current paper, the detailed code development and analysis for Neon will be presented. Along with that, the estimated emissivity of Ne^{1+} is compared with experimentally observed visible spectral line of Ne^{1+} at 377.7 nm.

References:

[1] Bhattacharya, Amrita, et al. "A study of the von Neumann stability analysis of a semi-implicit numerical method applied over the radial impurity transport equation in tokamak plasma." *Journal of Fusion Energy* 37.5 (2018): 211-237.

PDG-P-10

OPTICAL DIAGNOSTICS OF PLASMA DISCHARGE INSIDE LIQUID DURING THE SYNTHESIS OF AU/CUO NANOCOMPOSITES

Palash Jyoti Boruah*, Parismita Kalita, Rakesh Ruchel Khanikar, H. Bailung

Institute of Advanced Study in Science and Technology (IASST), Paschim Boragaon, Guwahati-781035, Assam, India

E-mail: palashjyoti.dhe@gmail.com

Over the past few years, the technique of plasma discharge inside liquids has been immensely engaged in the fabrication of nanomaterials due to their growing demand in our day-to-day life. The main advantage of the technique is the flexibility in controlling both the physical (plasma parameters) and chemical (liquid parameters) properties, which provides fine-tuning required for the shape and composition of nanomaterials. Previous studies reveal the behavior of plasma becomes quite complicated when interacting with liquid as it involves dissociation, electrochemical reactions, heating, local evaporation, ion bombardment etc. [1,2]. However, to understand the fabrication mechanism using this process, it is essential to investigate the role of different plasma parameters.

A plasma – liquid reactor is developed to generate a plasma between two vertically pointed copper electrodes inside deionized water and an ionic liquid ($HAuCl_4$, which acts as a precursor for Au nanoparticles). When the discharge is generated in deionized water, CuO nanospindles are formed due to the evaporation of Cu atoms from the electrodes. While, in $HAuCl_4$ solution, Au/CuO nanocomposites are formed. The colour of the plasma appears green, which indicates the emission of copper atoms. Optical emission spectra (OES) indicate the presence of atomic oxygen, hydrogen (H_α and H_β), Cu I and Cu II lines. The intensity of the H_α line is observed to increase more than tenfold for discharge in $HAuCl_4$ solution compared to that in deionized water. The electron/excitation temperature (T_e) of the plasma is determined from the relative line intensities of the Cu I lines, as reported in our previous work [3]. In both conditions, the value of T_e goes beyond 8000 K. Therefore, high energy electrons can easily vaporize the electrode materials as their energy exceeds the boiling point of copper (2835 K). For the discharge in ionic liquid, T_e is higher than deionized water. The electron density (N_e) also goes beyond 10^{19} m^{-3}. The electron/excitation temperature and density provide an idea of the formation process of the nanocomposites.

References:

[1] Decoupling interfacial reactions between plasmas and liquids: Charge transfer vs plasma neutral reactions, J. Am. Chem. Soc. **135**, 16264, (2013)

[2] Plasma-liquid interactions: A review and roadmap, Plasma Sources Sci. Technol. **25**, 053002, (2016)

[3] Novel single-step synthesis and shape transformation of Au/CuO micro/ nanocomposites using plasma-liquid interaction, Nanotechnology **32**, 245601, (2021)

PDG-P-11

STUDY OF TEMPORAL PROFILES OF ELECTRIC FIELDAND PLASMA TEMPERATURE IN SOL REGION OF ADITYA-U TOKAMAK

Abha Kanik[1], Arun Sarma[1,2], Joydeep Ghosh[3], Tanmay Macwan[3,4], Sharvil Patel[5], R. L. Tanna[3], Minsha Shah[3], Kalpesh Galodiya[3], Kumarpal Jadeja[3], Kaushalendra Singh[3,4], Suman Duloi[3,4], Ankit Kumar[3,4], Suman Aich[3], Rohit Kumar[3], Kaushal Patel[3]and ADITYA-U Team[3]

[1]*UPES, University of Petroleum and Energy Studies, Bidoli, Uttrakhand-248007*

[2]*NECTAR, 2nd Floor ViswakarmaBhawan, Shaheed Jeet Marg, New Delhi 110016, India*

[3]*Institute for Plasma Research, Near Indira Bridge, Gandhinagar District, Gujarat-382428*

[4]*Homi Bhabha National Institute, Mumbai, Maharashtra-400094*

[5]*Pandit Deendayal Energy University, Knowledge corridor, Gandhinagar, Gujarat-382007*

E-mail: abhakanik@gmail.com

Langmuir probes are one of the basic diagnostic to understand the properties of plasma because of its simple circuitry and also due to the advantage of localized measurement with good spatial and temporal resolution. Different configurations of Langmuir probes under a spectrum of experimental parameters are employed to study interested plasma domains.Overcoming the limitations of a big device like tokamak, a disc Langmuir probe system is designed and developed to study of the Scrape off Layer (SOL) plasma. The probes estimates the temporal evolution of not only the local electric fields but also aids in understanding edge behaviour during fuel gas and impurity injection.

Radially movable disc probes made of Graphite having 6 mm diameter wereoperated in the SOL region of ADITYA-U tokamak and biased at1 kHz frequency, thereby having optimum measurements of plasma parameters in typical plasma shot of ~300 ms. Experiments were carried out in hydrogen plasma and deuterium plasma in two sets at fix radial location. First, to measure radial profiles of potential in the edge plasma region of ADITYA-U tokamak, that will give the radial electric fields and second to estimate the localized plasma temperature and density.Temperature and density recorded from disc probes at r = 26 cm are 2.3 eV and 1 - 3^{17} m^{-3} respectively. In this paper we present the studies of the temporal profiles of electric field in SOL region as well as the correlation of plasma temperature (and density) with respect to other plasma events.

References:

[1] A comparative study of sheath potential profile measurements with laser-heated and current-heated emissive probes, Review of Scientific Instruments **87**, (2016)

[2] Emissive probes, J P Sheehan and N Hershkowitz, Plasma Sources Sci. Technol. **20** (2011)

[3] Overview of operation and experiments in the ADITYA-U tokamak, R.L. Tanna et al (2019) Nucl. Fusion **59** 112006

[4] A set-up for a biased electrode experiment in ADITYA Tokamak, PraveshDhyani et. al. Meas. Sci. Technol. **25** (2014)

PDG-P-12

OBSERVATION OF ANOMALOUS DOPPLER RESONANCE EFFECT IN ADITYA-UPGRADE

Varsha.S.[1,2] , Santosh Pandya,[1] S.K.Pathak[1,2] , Umesh Nagora[1], Jayesh Raval[1], M.K. Gupta[1], K.Tahiliani[1], R.L.Tanna[1], Rohit Kumar [1], Suman Aich[1], J.Ghosh[1] and Aditya-U Team[1].
[1]Institute for Plasma Research, Bhat, Gandhinagar – 382 428.
[2]Homi Bhabha National Institute, Mumbai, India.
Email: varsha@ipr.res.in

This paper describes the experimental observation of Pitch angle scattering events through the Anomalous Doppler Resonance (ADR) of relativistically high energy electrons in the Aditya-Upgrade tokamak. These observations are investigated primarily using the ECE signals. However, correlative understanding of the events is obtained from the HXR diagnostics while “PREDICT” code is used to simulate and investigate these events. A steep jump with 20 – 40% rise in the ECE amplitude is observed during the occurrence of the pitch angle scattering (PAS) event along with oscillatory behaviour in the HXR signals. The occurrence of the instability in its different forms and the possibilities of its occurence are discussed in the paper.

PDG-P-13

PLASMA POSITION MEASUREMENTS FOR SST1 DISCHARGES USING FUNCTION PARAMETERIZATION (FP) METHOD

Sameer Kumar, Kumudni Tahiliani, Daniel Raju, Surya Kumar Pathak, Jayesh Raval, Praveenlal Edappala, Suresh I, Devilal Kumavat, Ashish Ranjan, Jasraj Dongde and SST -1 Team
Institute for plasma research, Bhat, Gandhinagar
Email: skjha@ipr.res.in

Plasma position (Rc,Zc) can be expressed in terms of poloidal field of plasma current. Poloidal field is measured by discrete magnetic probes arranged along the poloidal boundary of plasma. Function parameterization method is employed to determine plasma position for SST-1 discharges. FP method obtains mapping between physical parameters (Rc, Zc) and measurements from a model or experiments [1-3]. Database of simulated measurements is formed.Collinearity among the measurements is removed and its dimension is reduced by principal component analysis (PCA). Functions for the physical parameters are obtained from the simulated measurements (Regression Analysis). Physical parameters (Rc, Zc) are determined from the experimental measurements and obtained function.

References:

[1] B. J Brams, Plasma Phys, Control. Fusion, Vol.33, No.7(1991), pp 715-748.
[2] B.J. BRAAMS, W. JILGE, K. LACKNER, NUCLEAR FUSION, Vol.26, No.6 (1986)
[3] Y Guo1, B J Xiao1,2 and F Yang, Plasma Phys. Control. Fusion 55 (2013) 035006 (7pp)

CATEGORY: LASER PLASMA, PULSED POWER AND OTHERS (LPP)

LPP-P-1

THZ GENERATION VIA GAUSSIAN LASER INTERACTION WITH VA-CNTS

Sandeep Kumar[1], Shivani Vij[2], Niti Kant[1] and Vishal Thakur[1]
[1]*Department of Physics, Lovely Professional University, G.T. Road, Phagwara - 144411, Punjab, India*
[2]*Department of Applied Sciences, DAV Institute of Engineering & Technology, Jalandhar, 144008, India*
E-mail: sanphymagic@gmail.com

In this neoteric analysis, we study the nonlinear interaction of Gaussian laser beam with the array of vertically aligned carbon nanotubes (VA-CNTs) for the terahertz (THz) generation. The VA-CNTs are gown over the dielectric substrate. The Gaussian laser beam propagates through the array of VA-CNTs to exert a nonlinear ponderomotive force on the electrons of CNTs. The laser beam provides a nonlinear resonant velocity to the electrons of CNTs, at the modulation frequencyω_m. As a result, nonlinear current density is produced in the system. This is responsible for the THz generation. The impact of dimensions of CNTs, on the normalized THz amplitude has also been observed in this analysis.

Keywords: VA-CNTs, THz radiation, dielectric surface, Gaussian laser, and nonlinear ponderomotive force.

LPP-P-2

ELECTRONBERNSTEIN WAVE EXCITATION BY NONLINEAR INTERACTIONS OF TWO LASER BEAMS IN A COLLISIONAL NANOCLUSTER PLASMA

Ashish Varma[a] and Asheel Kumar
Plasma Physics Research Group, Department of Physics, University of Allahabad, Prayagraj, India-211002
[a]*Email: varmaashish331@gmail.com*

An analytic formalism is developed to study electron Bernstein wave excitation by two copropagating high power super-Gaussian laser beams in a collisional nanocluster plasma.The medium is assumed to contain spherical plasma plume ball of nanocluster. As the electric field of two laser beams interact with nanoclustered plasma, it would cause the beat wave frequency. The laser beat wave exerts a nonlinear ponderomotive force on electron cloud of clustered plasma that in turns lead to excite the electron Bernstein wave in the laser field polarizations direction.The effective finite

y-component of the beat wave experiences group velocity and it might cause convective losses. The spatial shape of electron Bernstein wave normalized potential and power profile promises better excitation mechanism in nanoclustered plasma as compared to only plasma medium.It is observed that excitation is much enhanced when the laser beat frequency lies near the effective plasmons frequency of nanoclustered plasma. The excitation is detuned by varying the laser mode index, clustered radius, collisional frequency, parameter b.

Keywords: Electron Bernstein wave, Plasmon frequency, Nanocluster plasma, Ponderomotive force, Beat wave, Supper-Gaussian laser beam, Collisional, Excitation

LPP-P-3

EXCITATION OF ELECTRON BERNSTEIN WAVE BY BEATINGOF TWO HIGH POWER LASER BEAMS IN A COLLISIONAL PLASMA

Arvind Kumar and Asheel Kumar*
Plasma Physics Research Group, Department of Physics,
University of Allahabad, Prayagraj, India-211002
**Email:1222arvind@gmail.com*

In this present study, a theoretical model has been investigated for excitation of electron Bernstein wave in collisional plasma with dc magnetic field by nonlinear interactionsof two cosh-Gaussian laser beams. The beat wave has frequency and wave vector exerted a nonlinear ponderomotive force on electrons. This nonlinear force has potential to drive electron Bernstein wave in collisional plasma with dc magnetic field.An analytical formalism is developed for power going into the electron Bernstein wave with respect to total laser power. The variation of normalized potential and power distribution profile as a function of beam direction, normalized beat wave frequency, and normalized collisional frequency is demonstrated to excite electron Bernstein wave under resonance conditions. The spatial shape of laser beam, optimum laser beam width parameter, decentred parameter, extreme value of electron thermal velocity, and cyclotron frequency is proposed for much more excitation. This proposed theory of electron Bernstein wave excitation may be relevant applicable for plasma heating.

Keywords: Electron Bernstein wave, cosh-Gaussian laser beams, Beat wave, Ponderomotive force, Collisional plasma, decentred parameter

LPP-P-4

ELECTRON ACCELERATION BY TIGHTLY FOCUSED RADIALLY POLARIZED LASER PULSE IN AN ION CHANNEL

Ram Jeet* and Asheel Kumar
Plasma Physics Research Group, Department of Physics, Science Faculty, University of Allahabad, Prayagraj-211002
**Email- rjpatel896@gmail.com*

We examine the electron acceleration by tightly focused radially polarized laser beam in a preformed ion channel. The tight focusing and polarization of laser beam takes the advantage of extremely intense and asymmetric fields. The longitudinal electric field component at the beam center helps in trapping of electrons. For effective acceleration, the preformed ion plasma channel behaves as an applied external magnetic field. The electrostatic space charge field of this preformed ion channel helps in trapping of electrons and confined them to the accelerating phase. The gain in the energy of the electron is due to the fact that the radial component of electric field become zero on the propagation axis and only longitudinal component survives which accelerates the electrons in the longitudinal direction to high energy. The electrostatic space charge field assists in confining the motion of electrons from transverse oscillation and inject them to accelerating field which causes a resonance between electric field of laser and electrons. Because of combined role of tightly focused radially polarized laser and ion channel the electrons can gain energy of the order of GeV.

Keywords: Tightly focused laser beam, Radially Polarized laser beam, Ion channel, Electron acceleration.

References

[1] S.V. Bulanov, F.F. Kamenets, F. Pegoraro and A.M. Pukhov, Phys. Letters A, 195 (1994) 84.

[2] N.A. Bobrova, P.V. Sasorov, C. Benedetti, S.S. Bulanov, C.G.R. Geddes, C.B. Schroeder, E. Esarey and W.P. Leemans, Phys. Plasmas, **20** (2013) 020703.

[3] Y.I. Salamin, Optics Lett. **31** (2006) 2619.

LPP-P-5

SECOND HARMONIC GENERATION BY OBLIQUE INCIDENT GAUSSIAN LASER BEAM IN PLASMA

Vinay Sharma[1], Vishal Thakur[1], Arvinder Singh[2] and Niti Kant[1]*
[1]*Department of Physics, Lovely Professional University, G.T. Road,Phagwara -144411, Punjab, India.*
[2]*Department of Physics, NIT Jalandhar-144011, India*
E-mail: nitikant@yahoo.com

In present study the efficiency of second harmonic generation (SHG) for oblique incident intense laserin plasma medium has been investigated for optimum values of different laser parameters. Earlier studies shows that the efficiency of the second harmonic pulse depends upon the angle of incidence and vanishes at normal incidence. Using paraxial approximation, the expression for amplitude of SHG has been derivedand solved mathematically. Wiggler magnetic field is applied to provide additional momentum to the photons of second harmonic pulse, to satisfy the phase matching conditions. Variation of normalized efficiency, for SHG, with normalized intensity of fundamental laser, with normalized plasma frequency and normalized wiggler magnetic field has been studied. Optimizing the values of angle of incidence and other laser parameters results anappreciable gain in the efficiency of second harmonic pulse.

Key words: Second harmonic generation, oblique incident laser, wiggler magnetic field, plasma frequency.

LPP-P-6

PROPAGATION DYNAMICS OF SINGLE AND LATERALLY COLLIDING LASER PRODUCED PLASMAS

Shilpa S.[1] and Pramod Gopinath [1,2]
[1]*International School of Photonics*
[2]*Inter University Centre for Nanomaterials and Devices*
Cochin University of Science and Technology, Kochi 682022, India
**Email: pramod@cusat.ac.in*

The propagation dynamics of single and laterally colliding laser produced aluminium plasmas were investigated using fast imaging and spectroscopic techniques. The collision of two laser produced plasmas resulted in the formation of stagnation region in between the collision front. Time gated Intensified Charge Coupled Device (ICCD) imaging was used to study the temporal evolution of plasma. Time resolved spectroscopy was used to obtain information about the distribution of neutral as well as the ionic species in collision process of laterally colliding plasmas and single plasmas.

Greater concentrations of ionic species were found in stagnation region than single plasma. Electron density and temperature were also calculated from the emission spectra. Colliding plasma plumes have higher temperature and increased electron density. Time resolved fast imaging clearly depicted the greater lifetime and plume front velocity of colliding plasmas compared to that of single plasmas.

LPP-P-7

ELLIPTICALLY POLARIZED THZ RADIATION GENERATION IN OBLIQUELY MAGNETISED PLASMA

Dinkar Mishra and Bhupesh Kumar
Department of Physics, University of Lucknow – 226007
Email: dinkarmishra.edu@gmail.com

Today, THz generating radiation sources can be realized using short and intense laser pulses propagating through magnetised and un-magnetised plasmas under appropriate conditions. Significant research has been done in generating linearly polarized THz radiation using short laser pulses in axially and perpendicularly magnetised plasma. It is shown that when a short and intense circularly polarised laser pulse is propagated along x-direction, through the homogenous plasma in presence of an arbitrarily oriented static magnetic field in y-z plane, both elliptically and linearly polarized THz radiation are generated under appropriate conditions. Generation of such THz radiation may be attributed to the coupling of arbitrarily oriented magnetic fields with transverse and axial components of quiver velocity of plasma electrons. Intensity of elliptically polarized THz radiation obtained analytically (6.18 x 1010 W/cm2) has been validated using 3-D particle in cell simulation (1.66 × 1011W/cm2) and found to be of the same order.

References:

[1] Tajima T and Dawson J Phys. Rev. Lett. 43, 267 (1979)
[2] Peñano J, Sprangle P, Hafizi B, Gordon D and Serafim P Phys. Rev. E 81 026407 (2010)
[3] Saroch A and Jha P Phys. Plasmas 24 (2017) 124506
[4] Dinkar M, Pooja S, Saumya S, Bhupesh K and Pallavi J Plasma Res. Express 3 025002 (2021)

LPP-P-8

HEATING OF ELECTRONS BY INTERACTION OF HIGH INTENSE ULTRA-SHORT LASER PULSES IN NANOPARTICLES

S P Mishra* and Ashish Varma

Department of Physics, K. N. Govt. P. G. College, Gyanpur-Bhadohi, U.P., 221304

**Email: drspmishra2001@rediffmail.com*

In this present theoretical study, we investigate the evolution of electron heating by interaction of high intense ultra-short laser pulses in nanoparticles. The interaction of laser electric field profile with electronic clouds of nanoparticles causes the oscillatory velocity to the electrons. This oscillatory velocity might be produced the heating. The pulse parameters evolution such as normalized energy of the pulse, pulse width, position of the pulse center and reflectivity coefficient of the medium is investigated theoretically on plasma generation. The graphical discussions were promised to achieve extreme heating rate at resonance condition surface plasmon frequency.

Keywords: Ultra-short laser pulse, Nanoparticles, Oscillatory velocity, Surface plasmon frequency, Heating

LPP-P-9

HIGH-ORDER HARMONIC GENERATION FROM STRONGLY OVERDENSE PLASMAS IRRADIATED BY ASYMMETRIC LASER PULSES

Deep Kumar Kuri

Department of Physics, Digboi College, Digboi, Assam – 786171, India

E-mail: deepkuri303@gmail.com

The recent advances in laser technology has made possible the interaction of highly intense short laser pulses with matter [1]. Such interactions can generate high-order harmonics which has been an active field of research due to its potential applications towards the production of extreme ultraviolet (XUV) pulses [2-4]. The shape of the laser pulse can play an important role in laser-plasma interactions which might have a significant effect on the generation of high-order harmonics [5]. Here, I have numerically studied the high-order harmonic generation in the interaction of intense strongly overdense plasmas with intense short temporally asymmetric laser pulses having an unequal rise and fall time.

References:

[1] M. D. Perry and G. Mourou, *Science* **264**, 917 (1994).
[2] S. V. Bulanov, N. M. Naumova, and F. Pegoraro, *Phys. Plasmas* **1**, 745 (1994).
[3] R. Lichters, J. Meyer-ter-Vehn, and A. Pukhov, *Phys. Plasmas* **3**, 3425 (1996).
[4] G. D. Tsakiris, K. Eidmann, J. Meyer-Ter Vehn, and F. Krausz, *New J. Phys*. **8**, 1 (2006).
[5] W. P. Leemans, P. Catravas, E. Esarey, C. G. R. Geddes, C. Toth, R. Trines, C. B. Schroeder, B. A. Shadwick, J. van Tilborg, and J. Faure, *Phys. Rev. Lett.* **89**, 174802 (2002).

LPP-P-10

COMPARATIVE STUDY OF WAKEFIELD GENERATION IN HOMOGENEOUS AND INHOMOGENEOUS PLASMA

Saumya Singh and Bhupesh Kumar
University of Lucknow, Lucknow, 226007
Email: saumyasingh.phy@gmail.com, bhupeshk05@gmail.com

Interaction of short and intense laser pulse (~TW) with plasma, leads to transverse and longitudinal wakefield generation in plasma. These wakefields oscillate at plasma frequency. A constant axial magnetic field has been applied to enhance the laser-plasma interaction time. At the same time plasma channel helps in controlling the pulse diffraction beyond Rayleigh length within plasma. The transverse wakefield has been compared for homogeneous and inhomogeneous plasma (plasma channel). We report the enhancement of electric and magnetic wakefield by ~77% in the inhomogeneous plasma as compared to homogeneous case.

References:

[1] Phys. Rev. Lett. **43** 267-270 (1979)
[2] Europhys. Lett. **94**, 15001-15006 (2011)
[3] Rev. ST Accel. Beam **8**, 071301-071307 (2005)
[4] Phys. Plasmas **24**, 013102-013107 (2017)

LPP-P-11

3D SIMULATION STUDIES OF A DOUBLE-SIDED LINEAR INDUCTION MOTOR FOR ELECTROMAGNETIC LAUNCH APPLICATIONS

AnanyaKundu, Arvind Kumar, AnkurJaiswal, PrasadRao P, Vilas C Chaudhari, RambabuSidibomma, Y.S.S. Srinivas, E.Rajendra Kumar
Institute for Plasma Research, Bhat, Gandhinagar-382428, Gujarat, India
E-mail: ananya@ipr.res.in

The research and technologies employing Linear Induction motor (LIM) are gaining popularity in several applications including transportation, conveyor systems, liquid metal pumping, electromagnetic launching. These applications need higher linear trust in a controlled manner to satisfy the operational requirements. As part of a sanctioned project at IPR, a LIM based electromagnetic launching system of 8 kN force is being developed. To meet the requirement, a double-sided vertical LIM based electromagnetic launching system has been designed.

In a LIM, the stator consists of a three-phase winding of copper coils placed linearly in the slots of a core, made up of stacked and laminated CRNGO (cold–rolled non-grain

oriented) sheets. The rotor of a single-sided LIM is a metallic carriage plate placed above the core with a small air gap. The rotor is electromagnetically coupled to the stator and experiences the thrust force when the three-phase winding is energized. Due to the mechanical coupling of the rotor to the payload, the thrust is transferred to the payload. The double-sided LIM arrangement is more efficient as the flux utilization is better and the undesirable vertical component of the thrust is nullified.

In the present work, a 3D conceptual model of double-sided LIM in vertical configuration along with a carriage plate placed in the air-gap between two LIMs is prepared. In the slotted structure of the core domain, double layer winding of the coils is modelled. Finite element based (FEA) simulations are carried out with different stator currents of 50 Hz frequency to estimate the linear thrust on the carriage plate. Based on the outcome of the simulation, the design of the carriage and its support structure are optimized for the application. The stator coils are connected as per the three-phase winding in the simulation and other coil parameters like the number of turns in each coil, conductor cross-section etc. are used as inputs to the simulation.

This poster presents the details of the 3D simulation (COMSOL) adopted for the estimation of the magnetic flux density, induced current density and the linear thrust experienced by the carriage plate placed in the air gap of a double-sided LIM in vertical configuration. The effect of the variation of stator current on the thrust force on the carriage plate, for a fixed air gap, is also studied in this work.

LPP-P-12

AN ALTERNATIVE APPROACH FOR BIOSCOURING AND BLEACHING OF KNITTED COTTON FABRIC IN SINGLE PROCESS USING AIR PLASMA

T.Anupriyanka and G.Shanmugavelayutham*

[1]*Plasma Physics Laboratory, Department of Physics, Bharathiar University, Coimbatore-641046, Tamilnadu, India*

E-mail: sgsvelu@buc.edu.in

Surface modification of the knitted cotton fabric with chemicals, acids which are hazardous to the environment is a big issue today. Before dyeing, the knitted fabric was scoured and bleached using sodium hydroxide, surfactants, soaps, hydrogen peroxide, sodium silicate and organic stabilizers. Thus the fabric preparation involves wet processing with chemical and liquor baths, several washing and rinsing techniques that generates waste water effluents [1- 3]. Plasma method is a green, dry process, eco-friendly, single step process without the usage of chemicals that can alter the surface properties without major change in bulk performance of textile materials. In addition to that huge variety of chemically active functional groups can be incorporated into the surface [4]. The present work is to modify the surface of the knitted cotton fabric by air plasma treatment with operating parameters such as exposure time, discharge potential and base pressure are kept constant as 10mins, 200 V and 18 Pa respectively. The change in the chemical and morphological properties have been investigated by ATR-FTIR, SEM analyses and reported.

References:

[1] T.Anupriyanka, G.Shanmugavelayutham, BornaliSarma, M.Mariammal, A single step approach of fabricating PET fabric by using low pressure plasma for oil-water separation,Colloids and Surfaces A 600 (2020) 124949.

[2] Muhammad Naveed, Plasma treatment as green technology for dyeing of textile fabrics,Trends in Textile Engineering &Fashion Technology,2, 2 (2018) 168-173.

[3] A J S Ferreira, M B Goede, N T Vila, M G Silva, S Fiori, T A Nascimento, M Fernandes &A P Souto,Surface activation of textile fibers by plasma DBD for dyeing with teak leaf,IOP Conf.Series:Materials Science and Engineering, 460(2018) 1-6.

[4] Saied Jamaliniya, Nezam Samei & Sheila ShahidiUsing low temperature plasma for surface modification of polyester fabric : dyeing and printing improvement, The Journal of The Textile Institute, 2(2019) 1-5.

LPP-P-13

INFLUENCE OF AN AXIAL MAGNETIC FIELD ON PULSED PLASMA STREAM

A. Ahmed*, S. Singha, S. Borthakur, N. K. Neog and T. K. Borthakur
Centre of Plasma Physics- Institute for Plasma Research,Nazirakhat, Sonapur-782402, Kamrup, Assam
E-mail : tridip@cppipr.res.in

The influence of an external axial magnetic field on plasma stream in a pulsed plasma accelerator (PPA) is studied in this work. Generally, the pulsed coaxial plasma accelerator produces high density plasma stream by utilizing self-generated **J×B** thrust to accelerate plasma inside of annulus of a coaxial electrode assembly [1,2]. On application of external magnetic field, the characteristics of the plasma stream in PPA changes. In this work, a pulsed magnetic field is applied parallel to the plasma stream flow to study its effect on emission processes of different ionized and neutral argon species by OES under different discharge conditions such as pressure and discharge voltage. The plasma density, temperature and intensity variation of transitions from different energy states are estimated and analyzed under different experimental conditions. Intensity distribution profiles of spectral lines shows significant enhancement in emission from neutral atoms as compared to those from ionized

species. A time evolution study is also carried out to gather information regarding the variation of the plasma stream at different times of its evolution by using delay triggering of the optical spectrometer. The delay triggering is carried out in a time span of 50 – 300 µs in steps of 50 µs. The temporal evolution study shows a decrease in plasma density from 1.96×10^{21} m^{-3} at 50 µs to 1.23×10^{20} m^{-3} at 300 µs and excitation temperature from 0.86 to 0.77 eV [3]. The energy density of the plasma stream shows a time-dependent decreasing nature during the observed time span.

References:

[1] A. I. Morozov, Sov. J. Plasma Phys., 16, p 131-146 (1990)

[2] S. Borthakur et al., IEEE Trans. Plasma Sci., 45, p 1769-1775 (2017)

[3] A. Ahmed et. al., Phys. Plasmas., 28, 023109 (2021)

LPP-P-14

INVESTIGATIONS OF COMPLEX FAST ELECTRON TRANSPORT PHENOMENA IN INTENSE ULTRASHORT LASER FOIL INTERACTION

T. Mandal[*1,2], V. Arora[2], A. Moorti[1,2] and J. A Chakera[1,2]

[1] *HBNI, Training School Complex, Anushaktinagar, Mumbai 400 094*

[2]*Laser Plasma Division, RRCAT, Indore 452013*

E-mail : tirtham@rrcat.gov.in

Investigating intense, ultrashort laser foil interaction through fast electron generation is important for fundamental understanding of laser coupling in extreme condition as well as for various potential future applications. When an ultrashort (tens of fs) intense (peak intensity $>10^{19}$ W/cm^2) laser interacts with sharp density gradient plasma, it generates stream of high current (peak current ~MA) highly energetic (keV to MeV) fast electrons which propagate through dense matter. Use of thin foil target allows one to detect the escaped fast electrons for investigating the transport of fast electrons through dense matter. Fast electron transport and their escape from target surface is affected by different complex processes including refluxing and reacceleration. As the electrons reach the target rear surface, they setup a strong quasistatic sheath field (strength ~TV/m) which restricts the escape of further electrons and are reflected back into the target. Similar sheath fields are also generated at target front surface. Therefore the electrons will travel back and forth within the target known as ‘refluxing’ which is most prominent in thinner foils. Further, this process can result in relatively higher electron energy through re-acceleration if the laser pulse duration is larger than twice the electron traverse time through the target foil and the recirculating electrons remain within the dimension of laser focus. Role of refluxing and reacceleration in fast electron transport is investigated by measuring electron angular and spectral distribution as a function of pulse duration, focal spot and target thickness.

The experiments were performed at a laser intensity of ~4x10^{19} W/cm^2 achieved by focussing the 25 fs Ti:sapphire laser pulse on 2-7 µm Cu foil to a focal spot of ~5µm. The fast electrons were measured using a phosphor screen-CCD combination whereas the spectrum was measured using a magnetic spectrograph. The laser intensity was varied using three ways viz. by varying laser pulse energy at fixed pulse duration, varying the laser pulse duration for fixed laser energy, and varying the laser focal spot for fixed laser pulse duration and energy. It was observed that in all methods of changing laser intensity, the overall charge, maximum energy and temperature reduces with decrease in laser intensity. However, the rates of decrement in three methods are different. In case of laser focal spot variation, the decrease rate is slowest whereas for pulse duration variation, the decrease rate is in between of laser pulse energy variation and focal spot variation. The observation of slow decrease of electron properties with laser intensity in case of pulse duration or focal spot variation is due to reacceleration of electrons possible at longer pulse duration and larger focal spot. Further, it was seen that the electron charge increased for increase in target thickness as the sheath field strength is weaker in thicker target and therefore causing less refluxing. Next electron spectrum analysis has shown that the temperature for thinner target foil was slightly higher than comparatively thicker target (e.g. temperature for Cu 2 µm : ~0.55 MeV compared to ~0.43 MeV for Cu 7µm at intensity~ 4x10^{19} W/cm^2) showing a clear demonstration of re-acceleration phenomena. The detailed experimental results and understanding of transport processes will be presented.

LPP-P-15

UNDERSTANDING GRAZING INCIDENCE INTERACTION THROUGH FAST ELECTRON GENERATION IN THIN FOIL AT EXTREME INTENSITIES

T. Mandal[*1,2], V. Arora[2], A. Moorti[1,2] and J. A Chakera[1,2]
[1] *HBNI, Training School Complex, Anushaktinagar, Mumbai 400 094*
[2]*Laser Plasma Division, RRCAT, Indore 452013*
E-mail : tirtham@rrcat.gov.in

Understanding laser matter coupling in intense, ultrashort laser foil interaction has been a topic of active research investigation for decades for unraveling interaction issues as well as for many potential future applications. Particularly the interaction at grazing incidence (incidence angle ≥70º) attracts special attention due to generation of strong surface fields and interaction of electrons with this field leading to improvement in the electron beam parameters. The study is also important to understand the generation and transport of fast electron in the context of hollow re-entrant cone target proposed for the fast ignition where electrons are generated in cone sidewalls at grazing incidence.

The experiment was performed at grazing angle of incidence of ~70° and oblique incidence angle of ~45° with 150 TW Ti:sapphire laser (of energy ~2.2 J, pulse duration~25 fs) focussed onto thin Cu foil target at a peak intensity of ~7 x 10^{19} W/cm^2. The electrons were detected along front as well as rear direction using phosphor screen-CCD combination setup along laser direction. For 45° incidence angle, the electrons were emitted along nearly laser direction in the target rear surface. However, when the incidence angle was increased to ~70°, the rear fast electrons were found to be more inclined towards target surface direction along with improvement in flux and divergence. The electron charge (energy >350 keV) increases by ~2X from ~2±0.2 nC to 4±0.6 nC with increase in incidence angle from ~45° to ~70°. The divergence angle also reduced from ~94°±5° to ~65°±5° on increasing the incidence angle. Next, for 70º incidence angle, the rear escaped electron charge increased from 4 ± 0.6 nC to 4.9±0.7 nC and 6.4 ± 0.9 nC on increasing the target thickness from 7µm to 25 µm and 50µm respectively. At grazing incidence interaction, highly collimated electrons were also generated along front target surface direction. Divergence of front surface electrons was much lower ~7º.

For oblique incidence interaction, JxB was main fast electron generation mechanism producing electrons along laser direction. With the increase in incidence angle charge of the electrons increased whereas the divergence decreased. Increase in charge is due to enhanced JxB acceleration possible at longer laser propagation length in preplasma. Reduction in divergence can be explained due to electron collimation effect by self-generated magnetic field (~MG order) at longer target length experienced by electrons due to grazing incidence. Further, at such high incidence angle, surface fields are also generated effectively which also adds up in deviating the electrons along surface direction. The surface field effect is more pronounced for front surface electrons where we observed highly collimated electrons along surface direction. The detailed experimental results and understanding of physical processes will be presented.

LPP-P-16

SELF-FOCUSING OF AN AMPLITUDE MODULATED LASER FILAMENT IN A MAGNETIZED PLASMA

Raju Ram Meena[1,2]

[1]*Faculty of Physical Science, Dr. A. P. J. Abdul Kalam University, Indore-452016*

[2]*Department of Physics, ShyamLal College (Delhi University), Delhi-32*

E-mail: rajurammeena1988@gmail.com

Laser interactions with plasma have been a fascinating area of research due to its application in fusion and accelerator technology. For most of the applications it is necessary to preserve the laser properties in plasma. Plasma is a nonlinear optical medium, which can excite higher order electric susceptibility during laser propagation. These higher order nonlinearities may assist to guide the laser in plasmas. In this work, we study the self-focusing of a laser amplitude modulated filament in a magnetized plasma. The laser filament with non-uniform distribution ofintensity exerts a ponderomotive force on electrons and sets in an ambi-polar diffusion of the plasma. The ambient tmagnetic field, however, strongly inhibits the process, when the electron Larmor radius is comparable to or shorterthan the laser spot size. As the plasma density is depleted, the laser beam becomes more self-focused. This studyaddresses a significant enhancement in the laser self-focusing rate by including the amplitude modulation of the laser beam.

References:

[1] D. N. Gupta, K. Avinash, and H. Suk, Laser and Particle Beams **31**, 307 (2013).

[2] M. Singh and D. N. Gupta, Proc. SPIE **9654**, 96541R (2015).

LPP-P-17

SELF-FOCUSING OF LOWER MODES OF BESSEL BEAMS: MOMENT THEORY APPROACH

Proxy Kad[1], Arvinder Singh[2]
Dr. B.R. Ambedkar National Institute of Technology, Jalandhar-144011 (Punjab),India
E-mail : proxykad59@gmail.com[1], arvinders@nitj.ac.in[2]

In the present work, the self-focusing of laser beam having Bessel-Gaussian profile has been studied in plasma taking into account the relativistic non-linearity. A non-linear second order differential equation determining the evolution of spot size has been obtained using the moment theory approach. The differential equation has been solved numerically using the Runga-Kutta method and the variation in the spot size of laser beam with distance of propagation of laser beam inside plasma has been obtained. The variation of spot size has been observed for different parameters of laser and plasma.

LPP-P-18

LASER-CLUSTER INTERACTION IN A STATIC MAGNETIC FIELD WITHOUT DIPOLE APPROXIMATION

Kalyani Swain[1,2] and Mrityunjay Kundu[1,2]

[1]*Institute for plasma research (IPR), Bhat, Gandhinagar, Gujarat-382428, India*

[2]*Homi Bhaba National Institute (HBNI), BARC Training School Complex, Anushaktinagar, Mumbai, Maharashtra 400094*

E-mail : kalyani.swain@ipr.res.in

The concept of electric dipole approximation may be applied in the case of laser-matter interaction when the target size is much smaller than the laser wavelength (λ). Atomic clusters have the advantages of both gas and solid targets with size on the order of nanometer scale, which is very small compared to λ, and the criteria of dipole approximation is well satisfied. Dipole approximation assumes that the laser field is spatially homogeneous, and thus magnetic field component of the laser is neglected. We have performed the study of laser interaction with deuterium cluster for a linearly polarized laser by taking the laser magnetic field into account with an additional static external magnetic field of tens of kilo-Tesla. Considering the dipole approximation for a laser intensity 7.31×10^{16} W/cm^2 and λ = 800nm (Ti:sapphire laser), we find that the laser energy absorption is significantly enhanced (~ MeV range) compared to the earlier reported works[1]. Under this situation, the forward excursion (z) of the electron along laser propagation quickly achieves the order of λ, and the relation $z/\lambda \ll 1$ (condition for dipole approximation) weakly holds. Hence, the dynamics of the electron is again analyzed without dipole approximation, and amazingly much higher values of energy absorption is obtained near the electron-cyclotron resonance as compared to the dipole approximation.

References:

[1] S. S. Mahalik, M. Kundu, Phys. Rev. A 97, 063406 (2018)

[2] A. Ludwig, J. Maurer et al., Phys. Rev. Lett. 113, 243001 (2014)

LPP-P-19

SELF-FOCUSING OF BESSEL-GAUSSIAN LASER BEAM IN COLLISIONLESS PLASMA

Aman Bhatia, Arvinder Singh
Dr. B R Ambedkar National Institute of Technology, Jalandhar Punjab, 144011
E-mail : amanb.ph.19@nitj.ac.in

In the present investigation, the self-focusing of laser beam in the ponderomotive plasma has been observed. The laser intensity distribution is taken to be Bessel-Gaussian profile. The ponderomotive force tends to generate a density gradient in plasma which further modifies the refractive index of plasma and lead to laser self-focusing. The differential equation for spot size of laser beam has been derived by using the method of moments and also incorporating WKB approximations. The numerical formulation of the differential equation has been done by Runge-Kutta fourth order method. The variation of the self-focusing of laser beam with propagation distance has been observed for different laser and plasma parameters.

LPP-P-20

PARAMETER OPTIMIZATION FOR TERAHERTZ RADIATION GENERATION FROM LASER-PULSE INTERACTION WITH ELECTRON-HOLE PLASMAS

M. C. Gurjar and D. N. Gupta
Department of Physics and Astrophysics, University of Delhi, Delhi-110007, India
E-mail : princeposwak2@gmail.com

When a short laser-pulse interacts with a semiconductor, different electronic mechanisms are excited, depending on the sample semiconductor. For narrow band-gap semiconductors, free electrons inside the solid can directly absorb laser energy and form hot electron-hole plasma. At high energy, the electron-hole plasma created on the surface of the solid will induce emission of electromagnetic radiation through the nonlinear current generation. We use a simple, two-fluid model for the collective electromagnetic response of an electron-hole plasma, which treats the electron and hole components as a two-species plasma system. The laser exerts a ponderomotive force on electrons and holes. The carriers oscillate with oscillatory velocity at the laser frequency. The plasma density perturbation coupled with the oscillatory velocity produces a nonlinear transverse current with nonzero curl. This nonlinear current drives coherent THz radiation. An analytical expression of the THz fields is obtained by solving Maxwell and hydrodynamic equations with appropriate boundary conditions. The systematic analysis of this mechanism shows an efficient and tunable source of

THz radiation, which varies with various parameters such as the density modulation, laser intensity and other laser parameters.

References:

[1] D. Dragoman and M. Dragoman, Prog. Quantum eElectron. **28**, 1 (2004). M.C. Gurjar, K. Gopal, D.N. Gupta, V.V. Kulagin, Europhysics Letters **133** (1), 14001 (2021).

[2] D. N. Gupta, Plasmonics **16** (2), 419 (2021).

LPP-P-21

A STUDY AND SIMULATIONS OF PLASMA OPENING SWITCH FOR HIGH VOLTAGE AND HIGH CURRENT APPLICATIONS

Kanchi Sunil[1], Rohit Shukla[1,2], Archana Sharma[1,2]
[1]*Homi Bhabha National Institute Mumbai-400094,*
[2]*Pulsed Power & Electro-Magnetics Division, Bhabha Atomic Research Centre Facility, Atchutapuram, Visakhapatnam, Andhra Pradesh, India-531011,*
E-mail: sunilkanchi8125@gmail.com

In pulsed power systems, plasma opening switches (POS) plays a major role in designing compact inductiveenergy storage systems for generation of high voltage and high current with fast rising pulses for the applications like flash radiography, high energy plasma physics, X-ray generation, Z-pinch, X- pinch and fusionresearch [1]. In the POS, the plasma source plays an important role to form a short circuit path during conduction phase for which plasma should have sufficient density, charge, mass, velocity and spatial distribution. This is to attain large bipolar current needed before the POS begin to open [2]-[3]. In this paper, the POS conduction and opening phases with different models like bipolar model, magnetic pressure model, snow plough model and erosion model will be discussed [1], [4]-[5]. The design criteria and simulations of density, velocity variations along the axial length of plasma source inside the designed POS will be reported. The sufficient conditions and necessary criterion for the design of plasma opening switch, the electric field and voltage variations inside the POS with plasma source simulations will be reported.

References:

[1] E. A. Guenther, M. Kristiansen, and T. Martin, *Advances in Pulsed Power Technology: Vol. 1: Opening Switches*. New York: Plenum Press, 1987.

[2] P.Stevenson, “Novel plasma sources for plasma opening switches,” PhD thesis, Loughborough University, 2002.

[3] S. Kohno, Y. Teramoto, I. Lisitsyn, S. Katsuki, and H. Akiyama, “Cable gunsas a plasma source in a plasma opening switch,” *IEEE Transactions on PlasmaScience*, vol. 27, no. 3, pp. 778–785, 1999.

[4] S.V.Loginov, “Plasma Dynamics in Opening Switches,” *IEEE Transactions onPlasma Science*, vol. 36, no. 2, pp. 494–497, 2008.

[5] J. W. Schumer, et al, “MHD-to-PIC Transition forModeling of Conduction and Opening in a Plasma Opening Switch,” *IEEE Trans.Plasma Sci.*,, vol. 29, no. 3, pp. 479–493, 2001.

LPP-P-22

ENHANCED ELECTRON ACCELERATION IN A SUBCRITICAL DENSITY ION CHANNEL USING CHIRPED LASER PULSE

Harjit Singh Ghotra
Advanced Study Hub (ASH), Theoretical and Computational Research Form (TCRF), Near GT Road
Jalandhar-144001, Punjab, India
E-mail : harjit.ghotra@yahoo.com

A substantial enhancement in electron energy upto GeV order is realized in a performed ion channel by using chirped circularly polarized laser pulse. The presence of chirp parameter as well as the spaced charge field induced by the propagation of chirped CP laser pulse play a crucial role in enhancing the electron energy. The electron energy gain appears to be more sensitive to changes in the chirp parameter from linear to quadratic to least sensitive to the CP laser pulse's limited transformed frequency. To improve electron acceleration, the chirp parameter is tuned with the subcritical density in performed ion channel.

In a recent work, the combined involvement of a tightly focused radially polarized laser and an ion channel for electron energy increase on the order of GeV was examined [1]. The effect of linear and nonlinear chirp types of laser pulses on electron acceleration is discussed [2].

References:

[1] Electron acceleration by a tightly focused laser pulse in an ion channel, Eur. Phys. J. D, **75**(10), 268 p 1-7, (2021)

[2] Multi-GeV electron acceleration by a periodic frequency chirped radially polarized laser pulse in vacuum, Laser Phys. Letters, **13**(6), p 065402, (2016).

LPP-P-23

ROLE OF SATURABLE INDUCTOR FOR IMPROVING THE COMMUTATION LOSSES IN HIGH POWER PSEUDOSPARK SWITCH

Akhilesh Mishra[1,2], Shikha Misra[1], B. L. Meena[1], Ram Prakash Lamba[1,2] and Udit Narayan Pal[1,2]

[1]*CSIR- Central Electronics Engineering Research Institute, Pilani, Rajasthan-333031*

[2]*Academy of Scientific and Innovative Research (AcSIR), Ghaziabad, Uttar Pradesh-201002*

E-mail: akhileshmishra056@gmail.com/udit@ceeri.res.in

The pseudospark switches have the extraordinary capabilities of high power handling with fast current rise, making them ideal for many fast pulse power applications [1-2]. However, the commutation losses increase at very high power which limits its performance and life. In the present work, efforts have made to reduce the commutation losses by introducing a saturable inductor in series with the anode of the multi gap multi aperture pseudospark switch (MGMA-PSS). Electrical modelling has been carried out to investigate the switching characteristics of the MGMA-PSS with and without the saturable inductor. Also, saturable inductor offers a high impedance (~up to few of ohm) during the commutation process of the PSS before saturation [3-5]. Further, the effect of the saturable inductor is analyzed by using MATLAB simulation software and results have been found satisfactory. It is observed that the use of saturable inductor in the circuit can delay the rate of current rise. The operational behavior of a PSS with saturable inductor shows the change in the impedance and reduces the switching loss during its breakdown [3]. Experimental studies have also been carried out at different operating conditions which confirmed the improvement in the switching losses using saturable inductor in the test circuit. Such quantitative investigation would be very much useful in design and development of efficient PSS for high pulsed power application.

References:

[1] K. Frank et al. IEEE Trans. Plasma Sci., vol. 17, no. 5, pp. 748–753, 1989.

[2] U. N. Pal et al. IEEE Trans. Electron Devices, vol. 67, no. 12, pp. 5600–5604, 2020.

[3] W. Ding et al. IEEE Trans. Plasma Sci., vol. 47, no. 10, pp. 4572–4578, 2019.

[4] H. Yin et al. J. Appl. Phys., vol. 90, no. 7, pp. 3212–3218, 2001.

[5] R. P. Lamba et al. Plasma Sources Sci. Technol., vol. 27, no. 3, 2018.

LPP-P-24

ENERGETIC PROTONS FROM A LASER EXPLODED MICROSPHERE WITH DENSITY GRADIENTS

Ankita Bhagawati, Nilakshi Das
Dept. of Physics, Tezpur University, Napaam, Tezpur-784028, Assam (India).
E-mail : ankita8@tezu.ernet.in

The up-and-coming laser-plasma-based ion-accelerators have captivated significant interest owing to their compact size and cost-effectiveness. Some applications like fast-ignition of fusion fuel, hadron therapy of tumors, etc. require further development in the quality of ion beams in terms of maximum energy and beam flux. A tunable ion source with improved beam properties can be made possible by identifying and controlling the inherent ion acceleration mechanisms. It is evident from previous literature that a deviation from the well-studied and robust Target Normal Sheath Acceleration (TNSA) mechanism is essential for the production of ion beams with narrow band-width energies and low divergence. The suppression of the sheath field can be realized by using targets having a decreasing density gradient in the rear side [1].

Utilizing this information, we have adopted a model with a non-uniform density spherical target with the density peaked at the centre and dropping isotropically towards the periphery. Such a target may be produced by availing the inevitable presence of the pre-pulse, which readily ionizes the solid target and explodes it to create density gradients inside it [2]. In the present work, we have used 3D PIC simulation to analyze the underlying proton dynamics when an intense femtosecond pulsed circularly polarized laser is incident on a pre-exploded hydrogen microsphere. Two types of density profiles- a linear and a Gaussian profile are compared with the homogeneous target. The Gaussian profile is more effective in terms of the suppression of the sheath electric field [3]. We also saw crucial dependence of the steepness of the density profile on the acceleration processes involved. A smaller density gradient leads to a near-isotropic expansion of the target, whereas a steeper density gradient favours the formation of shocks in the decreasing density profile. Well-collimated proton bunches of energies exceeding 100 MeV are obtained, which show energy scaling better than the TNSA protons.

References:

[1] Ion acceleration from laser-driven electrostatic shocks, *Phys. Plasmas* **20(5)**, p 056304, (2013).

[2] Optimizing laser-driven proton acceleration from overdense targets, *Sci. Rep.* **6**, p 29402, (2016).

[3] Laser-accelerated protons using density gradients in hydrogen plasma spheres, *J. Plasma Phys.* **87(4)** (2021).

LPP-P-25

GOLD ASSISTED HOLE-BORING SCHEME FOR ION ACCELERATION IN PARABOLICALLY DECREASING BACKGROUND DENSITY PLASMA PROFILE

Nivedya Krishnan
Amity Institute of Applied Sciences, Amity University Noida,201301
Email: nivedyakrishnan97@gmail.com

Radiation pressure hole boring ion acceleration is studied with Gold-Carbon-Hydrogen (GCH) foil. Laser quickly converts the foil into an overdense plasma which then is accelerated to high velocity. The generated quartet sheets of electrons, protons, carbon and gold ions are variably accelerated owing to their different charge-to-mass ratio by the strong laser and electrostatic fields. Gold ions facilitates the dragging due to inertia and further elongates the space charge field. In the foil's frame, the fast-moving ultra-intense space charge field reflects the upstream background plasma protons. The protons of the plasma are imparted with approximately double the momentum depending upon the density profile of the background plasma. The field structure elongation is studied vis-à-vis the laser normalized amplitude. Ions in the range of hundreds of MeV can be generated by employing the scheme. The parabolic profile is found to be the most suitable under the practical parameters.

LPP-P-26

MODELING OF ULTRASHORT TWO COLOUR PUMP-INDUCED THERMAL STRAIN PROPAGATION IN GE [111]

R. Rathore*[a,b], H. Singhal[a,b] and J. A. Chakera[a,b]
[a]*HBNI, Training School Complex, Anushaktinagar, Mumbai 400094*
[b]*Laser Plasma Division, RRCAT, Indore 452013*
[*]*E-mail: ranjana@rrcat.gov.in*

Germanium is a promising material for high speed metal–oxide–semiconductor transistors and silicon-based optoelectronics as it provides a much higher carrier mobility than Si. But heat dissipation remains a bottleneck for next-generation optoelectronic devices. Thus, technologies enabling faster heat dissipation are necessary for performance improvement. In order to understand the heat dissipation in Ge, we deposit heat at the surface of the sample using an ultrashort (~50fs) optical pump (800nm/400nm) pulse and track its dissipation in real-time using time-resolved x-ray diffraction (TXRD) technique, by recording XRD patterns at different delays (~5ps). Here, the Cu K_α laser plasma x-ray probe is generated by the interaction of ultrashort laser with Cu wire[1]. It has ultrashort pulse duration (~100fs), narrow bandwidth (~7eV @ 8.047keV) and high peak brilliance (~10^{17}photons/(s-0.1%BW-

mm^2-mrad^2)). TXRD is advantageous as it provides a nondestructive way to probe heat dissipation by directly monitoring optical pump-induced thermal strain[2].

In this paper, the simulation results on thermal strain propagation by laser heating in Ge [111] crystal and its comparison with experimental results is presented. The changes in the XRD pattern of a pumped sample can be correlated with the evolution of thermal strain in the sample. The experimentally observed XRD patterns from strained sample are simulated using Takagi-Taupin (TT) equations. The strained crystal is modeled by assuming three crystalline layers of different thicknesses and 'd' spacing on top of pristine crystal. Top strained layer is formed by the laser absorption which has largest strain and smallest thickness. Bottom strained layer has smallest strain and largest thickness. This layer is generated by propagation of strain. Middle layer is the transition layer. The point spread function (PSF) of experimental setup is calculated by convolving it with the simulated XRD pattern for pristine sample to match with experimentally observed XRD pattern. The XRD pattern for the strained crystal is simulated by taking appropriate thicknesses, strain values of different crystalline layers in our model and by convolving with PSF to obtain the best possible fit of the diffracted signal. In the case of 400nm pump, smaller absorption depth (15nm vs 100nm) results in larger strain (4×10^{-3} vs 1×10^{-3}) at initial time compared to 800nm pump even at the same pump fluence (6.5 mJ/cm^2). The thermal strain propagation velocity is calculated to be ~3×10^5cm/s in both the pump cases which is comparable to longitudinal acoustic velocity (5.5×10^5cm/s). The present study paves the way for an improved understanding of heat transport in Ge induced by ultrafast laser pulses which will assist in the design of optoelectronic devices. The detailed experimental and simulation results will be presented.

References:

[1] R. Rathore et al., J. Appl. Phys., **126**, 105706, (2019).

[2] R. Rathore et al., J. Appl. Cryst., 54, https://doi.org/10.1107/ S160057672 1010281, (2021)

LPP-P-27

ELECTRON ACCELERATION BY HERMITE COSH GAUSSIAN LASER BEAM IN VACUUM WITH GEV ENERGY GAIN

Ashok Kumar Pramanik[1], Niti Kant[1], Harjit Singh Ghotra[1,2]and Jyoti Rajput[1]
[1]*Department of Physics, Lovely Professional University, G.T. Road Phagwara 144411, Punjab, India;*
[2]*Advanced Study Hub (ASH), Theoretical and Computational Research Form (TCRF), Near GT Road Jalandhar-144001, Punjab, India*
E-mail: akphmp@gmail.com

Electron acceleration with low order mode of Hermit-cosh-Gaussian (HChG) laser beam is investigated theoretically in vacuum. HChG laser beam possesses more power and have a capability to focus earlier than the Gaussian laser beam. Even, at low power such laser beam produces a high energetic electron beam. This is the beauty of HChG laser beam. The decentered parameter "b" associated with this beam plays a key role on electron acceleration. It is observed that by changing decentered parameter for a fixed intensity parameter $a_0 = 20$and laser spot-size $r_0 = 75$, Hermite function order $s = 1$,can result in electron energy gains of the order of GeV.

In a recent work, the electron acceleration and energy gain investigated theoretically by using cosh Gaussian laser beam in vacuum [1]. The distinct TEM mode indices dependent electron acceleration using Hermite Gaussian laser was explained [2].

LPP-P-28

EXPERIMENTAL STUDY OF POWER FREQUENCY BREAKDOWN CHARACTERISTICS OF VARIOUS SF_6 ADMIX IN NON-UNIFORM FIELDS

Vinod Kumar Gandi[1], Rishi Verma[1,2], Manoj Kumar Warrier[1,2],
Gursharn Singh[1,2] and Archana Sharma[1,2]
[1]*Homi Bhabha National Institute, Mumbai- 400094, India*
[2]*Bhabha Atomic Research Centre, Visakhapatnam-531011, India*
E-mail: gvinodsrkr@gmail.com

Sulphar hexafluoride (SF_6) gas is a potent greenhouse gas, and there has been research into more environmentally friendly alternative gas as a replacement to SF_6 in HV equipment. The research into alternative gases has shown that SF_6 admix have a promising dielectric property as comparable to pure SF_6. In this work, power frequency breakdown characteristics ofvarious SF_6 admix (SF_6/N_2, SF_6/dry air and SF_6/Ar) is tested using HV co-axial sparkgap switch with different % by vol of SF_6 under non-uniform field background (Point-Plane configuration). The experimental work is

performed with 5%, 10%, 25% and 50% by vol of SF_6 for pressure levels between 5 psi to 30 psi in gap length of 4 mm. The breakdown voltage of the SF_6/N_2 and SF_6/dry air mixture with 5% SF_6 is found to be ~50% of pure SF_6 under the same experimental conditions. Furthermore, SF_6/N_2 and SF_6/dry air mixture shows a saturated growth trends with increase in %SF_6. In case of SF_6/Ar admix the growth rate of breakdown voltage is greatly reduced at higher pressure with low % by vol of SF_6. A comprehensive experimental and theoretical investigations reported herein presents the application feasibility of these admix as a replacement to SF_6.

LPP-P-29

HEATING OF ELECTRONS BY INTERACTION OF HIGH INTENSE ULTRA-SHORT LASER PULSES IN NANOPARTICLES

Shri Prakash Mishra, Ashish Varma
Department of Physics, K. N. Govt. P. G. College, Gyanpur-Bhadohi, U.P., 221304
Email: spmishra2001@rediffmail.com

In this present theoretical study, we investigate the evolution of electron heating by interaction of high intense ultra-short laser pulses in nanoparticles. The interaction of laser electric field profile with electronic clouds of nanoparticles causes the oscillatory velocity to the electrons. This oscillatory velocity might be produced the heating. The pulse parameters evolution such as normalized energy of the pulse, pulse width, position of the pulse center and reflectivity coefficient of the medium is investigated theoretically on plasma generation. The graphical discussions were promised to achieve extreme heating rate at resonance condition surface plasmon frequency.

CATEGORY: SPACE, ASTROPHYSICAL AND IONOSPHERIC PLASMA (AIP)

AIP-P-1

EQUATORIAL PLASMA BUBBLES OVER INDIA DURING 2017 - A QUALITATIVE ANALYSIS

Sunil Kumar Chaurasiya[1], Kalpana Patel[1], Abhay Kumar Singh[2]
[1]*SRM Institute of Science and Technology, Delhi-NCR Campus, Modinagar, Ghaziabad, U.P. -201204*
Email: spacek.kalpana@gmail.com
[2]*Atmospheric Research Lab., Department of Physics, Banaras Hindu University, Varanasi - 221005*
Email: singhak@bhu.ac.in

Equatorial plasma bubbles (EPBs) are plasma density depletions and accompanying plumes of irregularities that give rise to severe radio signal disruptions [1-2]. These EPBs are mostly observed in the pre-midnight period [3]. They are generally connected with tropical spread F (ESF) or tuft structures. They are principally seen in the F-region of the ionosphere at lower scope areas and it is a direct result of the wavering phenomena occurring in the ionosphere.

In this study, we have attempted to present the structures and construction of EPBs and their specific qualities for the low solar activity period of 2017, over India. To study the characteristic of plasma bubbles in the topside ionosphere, we have analyzed a large database of post-sunset plasma density measurements acquired by the Defense Meteorological Satellite Program (DMSP) during a low solar activity period of 2017. The observed results are discussed according to the other reported results.

Key words: Ionosphere, Spread-F, Plasma bubble, solar activity, R-T instability.

References:

[1] Burke, W. J. et al., ***J. Geophys. Res***. 108(A5), 1221, (2003).
[2] Aarons J., ***Space Sci. Rev***. 63, 209, (1993).
[3] Patel, K and Singh A.K., ***Earth System Sciences,*** 119 (2), 211-220, (2010).

AIP-P-2

KINETIC SCALE DENSITY FLUCTUATIONS TO STUDY SOLAR CORONAL HEATING

Bheem Singh Jatav
Department of physics, Sikkim University, Gangtok, Sikkim.

We study the kinetic scale density fluctuations for understanding the solar coronal heating, when the background plasma density is modified by parallel ponderomotive force and Joule heating. The Kinetic Alfven wave plays a prominent role for solar coronal hearing and particle acceleration in space plasma. Numerical method has been used to analyse the evolution of KAW in solar corona [1]. The kinetic scale density fluctuation spectrum follows Kolmogorov scaling in inertial range [2]. Steepened spectrum has been achieved in the dispersive range, which is continues in the dissipation range. Our obtained results reveal that the kinetic scale density fluctuations plays an important results for transferring the energy from larger length scales to smaller length scales in solar coronal plasma, which is responsible for solar coronal heating.

References:

[1] Singh, H.D. and Jatav, B. S.,: RAA, 2019, 19, 7, 93.

[2] Sahraoui, F., Goldstien, M. L., Robert, P., Khotyaintsev, Y. V.: Phys. Rev. Lett. 102 (2009) 231102.

AIP-P-3

A STUDY ON THE VERTICAL COUPLING OF THE MESOSPHERE-THERMOSPHERE SYSTEM USINGTIMED-SABER SATELLITE DATA

Sandhya K Nair, Tarun Kumar Pant, Kishore Kumar K. and Vineeth C.
Space Physics Laboratory, Vikram Sarabhai Space Centre, Trivandrum, Kerala, India-695022

The Solar and geomagnetic activity modulates atmosphere-ionosphere coupling processes from top and lower atmospheric processes from below. The vertically propagating atmospheric waves play an important role in the coupling of atmosphere ionosphere system through wave saturation-dissipation processes as they carry energyand momentum. We have examined the day-to-day variability of temperature in the mesosphere-thermosphere-ionosphere system using TIMED SABER satellite data. TIMED satellite, which can measure the temperature profile from lower stratosphere to lower thermosphere daily and globally. The TIMED SABER data for the month of

December atvarious altitude levels in the stratosphere-mesosphere-thermosphere, reveal that their exits large spatial and temporal variation in temperature. The spatial variation, inparticular with altitude, in temperature is found to be as large as ~ 40 to 50 degree K.In order to examine the variability in temperature in terms of wave propagation, aregion around the equatorial region is selected and various modes of wavespropagation have been examined therein. Quasi 2.5, 8 and 13 days of periodicities areprominently seen in the data with significant vertical propagation through altitude.These waves and the changes in temperatures have been analysed vis-a-vis wind andother upper atmospheric processes. The outcome of this analyses will be presentedduring the conference.

AIP-P-4

STUDY OF CHARACTERISTICS OF IONOSPHERIC IRREGULARITIES USING GNSS TECHNIQUES OVER EQUATORIAL ANOMALY REGIONVARANASI

Sanjay Kumar, Mukulika Mondal and A. K. Singh

Atmospheric Research Lab., Department of Physics,

Banaras Hindu University, Varanasi - 221005, India.

Email: singhak@bhu.ac.in

Ionospheric irregularities are referred to as plasma density irregularity which causes fluctuation in phase and amplitude of radio signals passing through them and phenomena is known as scintillation [1]. Fluctuation in phase and amplitude of radio wave due to presence of ionospheric irregularities/ plasma bubbles causes failure of radio technological navigation system and hence affect human life [2-3]. Phase scintillation is always accompanied by amplitude scintillation but not vice-versa. Our aim is to study plasma bubbles, produced mainly at the post sunset time of a day will be studied since November 2020 to October 2021 over Varanasi using multi-frequency GNSS receiver Septentrio PolarX5S installed on the terrace of the Department of Physics, BHU. We have chosen solar minimum period of 25th solar cycle to see the dependence of ionospheric scintillation occurrences on solar activity over equatorial anomaly region Varanasi. To study the solar activity dependence, we have taken solar indices of Sun Spot Number (SSN) and $F_{10.7}$ (solar radio flux at 10.7 cm)over Varanasi and observe the variation of amplitude scintillation index S_4 with these indices individually. Year is divided into three seasons namely Summer (May, June, July, August), Winter (November, December, January, February) and Equinox (March, April, September, October) to observe the seasonal variation of occurrences of scintillation. Highest scintillation activity is observed during the equinox season. Diurnal analysis shows that scintillation activity is more prominent during the nighttime hour. Further, to observe the effect of geomagnetic storm on scintillation, we have chosen quiet days ($K_P < 4$) and disturbed days of this duration and observed the difference between two. Various geomagnetic indices like K_P, DST, B_Z, E_Y have been used.

Keywords: Ionospheric irregularities, GPS, Scintillation

References:

[1] Aarons J., ***Space Sci. Rev***. 63, 209 (1993).
[2] Burke, W. J. et al., ***J. Geophys. Res***. 108(A5), 1221 (2003).
[3] Singh, R. P. et al., ***Ann. Geophys***. 22, 2849–2860 (2004).

AIP-P-5

STUDY THE EFFECT ON THE IONOSPSHERE DURING SOLAR ECLIPSE OF 21 JUNE 2020 USING VLF WAVE

S. B. Singh and A. K. Singh
Atmospheric Research Lab., Department of Physics,
Banaras Hindu University, Varanasi - 221005, India.
Email: singhak@bhu.ac.in

A solar eclipse provides an opportunity to study the behavioral changes of properties of the ionosphere in the day time like as night time's conditions for a short time. During the Solar eclipse the radio communication and satellite navigation's are disturbed [1, 2]. Each eclipse has its different property due to occurrence time of the year, the solar disk occultation degree, time of the day, atmospheric weather, and location (latitude and longitude) of the observations on the Earth [3].

In this study, we have used VLF wave's observation and its emissions during the solar eclipse of 21th June 2020. As the Sun was eclipsed, the night time's condition is generated in the day time and VLF Tweeks and whistlers are observed. The analysis of the Tweeks shows the variation in the ionospheric reflection heights (~ 8-11 km) and electron density (~ 3-2 el/cm^{-3}). The eclipse- imposed modifications in the VLF transmitter's signal HWU (18.3 kHz) and NWC (19.8 kHz) display an average growth of 2.8 dB and 0.8 dB respectively in the signal strength during the solar eclipse period.

References:

[1] Smith, L.G., Journal of Atmospheric and Solar -Terrestrial Physics, 34(4), 601–611(1972).
[2] Singh, et al., J. Geophys. Res. 116, doi: 10.1029/2011JA016641 (2011).
[3] Baran, et al., Advances in Space Research, 31(4), 989–994 (2003).

AIP-P-6

THE SELF-GRAVITATIONAL JEANS INSTABILITY IN MAGNETIZED DUSTY PLASMA WITHCHARGE GRADIENT AND POLARIZATION FORCES AND NONTHERMAL EFFECTS

Shweta Jain[1] and Prerana Sharma[2]
[1]Physics Department, N.S.C.B. Govt. P.G. College, Biaora, M. P. - 465674, India
[2]Physics Department, Ujjain Engineering College, Ujjain, M. P. - 456010, India

A theoretical framework has been developed using three fluid theory to study the Jeansinstability in magnetized collisional dusty plasma accounting for superthermal effects ofelectrons and nonthermal effects of ions. The dynamics of the dust is described by dustpolarization force, dust charge gradient force, dust thermal speed and the dust neutral collisions.The general dispersion relation for the Jeans instability has been derived considering theperturbation to propagate in form of plane wave. The new expression for the modified Debyelength resulting from the nonthermal behavior of electrons and ions and the dust charge gradientforce is found to be appeared in the dispersion relation. The expression for Jeans instabilitycondition and critical wave number is presented to establish the dominance of nonthermalparameters as well as dust polarization and charge gradient force. The analytical and numericalestimation of the instability growth rate is done in both the parallel and perpendicular directionof propagation. The importance of our study to the formation of planetesimals and collapse ofinterstellar clouds in star forming regions is discussed. We discuss the implication of our results.

Keywords: Charge gradient force, non-thermal ion distribution, polarization force, selfgravitationalJeans instability, magnetized dusty plasma.

AIP-P-7

HIGH FREQUENCY ELECTRON ACOUSTIC SHOCK WAVES IN NON-MAXWELLIAN PLASMA

Rajneet Kaur*and N. S. Saini
Department of Physics, Guru Nanak Dev University, Amritsar-143005, India
**Email: rajneetkaur909@gmail.com*

There has been a large interest in studying the electron acoustic waves in plasmas due to its confirmation by satellite observations in theauroral and other regions of the magnetosphere.Electron-acoustic waves may exist in plasmas consisting of two distinct temperature (cold and hot) electrons in which the cold electrons provide the inertia and the restoring forcecomes from the pressure of the hot electrons. Along with two

electron population, presence of magnetic field-aligneddrifting electrons in the upper region of magnetosphere can be considered as source ofenergy for the excitation of electron acoustic waves.In this investigation, we have analysed the electron acoustic (EA) shocks in a plasma composed of cold inertial electrons, cool electron beam, hot electrons modeled by non-Maxwellian distribution and stationary background of positive ions penetrated by an electron beam. To the best of our knowledge, the characteristics of shock waves governed by deriving nonlinear Burgers equation by employing the reductive perturbation method. By taking into account the effect of electron beam and other plasma parameters on the characteristics of electron acoustic waves, shock structures are analyzed.It is shown that the combined effects of electron beam, hot to cold electron number density ratio, temperature ratio and viscosity significantly modify the propagation properties of the EA shock waves. The work presented in this investigation may be useful to studying the salient features of EA shocks dynamics in various plasma environments such as astrophysical/spaceplasma and earth's magnetosphere.

AIP-P-8

SOLAR WIND PLASMA CATEGORIZATION BASED ON THE SW PARAMETERS AT 1AU

Priyank Srivastava, A.K. Singh
University of Lucknow, Lucknow, 226007
E-mail : rajat.priyank44@gmail.com

The parameters defining the Solar wind are SW Plasma Temperature (K), SW Proton density (N/cm^3), SW plasma speed (km/s), Flow pressure, Plasma beta. There are mainly three primary forms of solar wind plasma: coronal-hole plasma, streamer-belt plasma, and ejecta [1]. Coronal-hole plasma, also known as rapid solar wind, is produced by the interaction of open field lines with low-lying closed loops on the floor of a coronal hole [2]. Plasma from the streamer belt is frequently referred to as the slow solar wind and solar transients like coronal mass ejections are related with ejecta. But, streamer-belt plasma is further subdivided into two groups: (a) streamer -belt, (b) sector reversal regions [3]. In the data time series, streamer belt plasma intervals are classified as helmet streamers or pseudostreamers. Helmet streamers emerge on the Sun when a loop arcade separates two coronal holes with opposing magnetic polarities. There is a period of plasma surrounding the sector reversal of a helmet streamer that has extremely low proton-specific entropy, high-number densities, either no electron strahl or a very intermittent electron strahl, a low alpha-to-proton density ratio, and often a very low velocity [4]. Sector reversal regions will be used to describe these periods of different plasma.

References:

[1] Richardson, I. G., E. W. Cliver, and H. V. Cane, J. Geophys. Res., **105**, 18-203, (2000)

[2] Cranmer,S.R.,LivingRev.SolarPhys.,**6**, 3, (2009)

[3] Foullon, C., et al., Atrophys. J., **737**, 1, (2011) Astrophys. J., 737, 1 .

[4] Wang, Y.-M., R. Grappin, E. Robbecht, and N. R. Sheeley Jr., Astrophys. J., **749**, 182, (2012)

AIP-P-9

EFFECT OF POLARIZATION FORCE ONDUST ACOUSTIC ALFVÉNDRESSED SOLITONS

Sunidhi Singla and N. S. Saini,
Department of Physics, Guru Nanak Dev University, Amritsar-143005, India.
Email: singla.sunidhi94@gmail.com

In dusty plasmas, various kinds of forces act on a dust particles, such as electromagnetic force, drag force, gravitational force, thermophoretic force and radiation pressure force. Over the last many years, there has been an increasing interest in the study of influence of polarization force on different kinds of nonlinear structures in a dusty plasma. The polarization force in dusty plasmas arises due to the change in plasma density on two sides of the dust grains. This can be caused by finite dust pressure. As a result of this density non-uniformity, the Debye shield of dust grains no longer remains spherical. This leads to a partial charge separation, thus creating an electric field. This electric field can oppose or enhance the external electric field, which is parallel electric field in the present investigation. For the last many years, a great deal of attention has been focused to study the linear and non-linear dynamics of dust kinetic Alfven (DKA) waves in a dusty plasma. Dust grains are very sensitive to the perturbations in the external applied magnetic field which is naturally available in most of the space plasmas and in laboratory plasmas. The perturbations in the magnetic field generate the dust kinetic Alfven waves (DKAWs) via polarization drift of dust fluid. Dust dynamics modifies the dispersion relation for the kinetic Alfven waves. In a dusty plasma, when the dust is considered as cold and stationary, dust modified kinetic Alfven waves arise with frequency in the range. But, for finite dust temperature, dust kinetic Alfven waves arise with frequency less than the dust cyclotron frequency. For dusty plasmas, comprising of negatively (positively) charged dust grains, the Debye shielding distance is determined by the number density and temperature of positively charged ions (electrons). However, for a fixed value of other parameters, the strength of polarization force remains the same for a plasma, containing either positively or negatively charged dust grains, and is always directed opposite to the electric field. The observations of various satellite missions have confirmed the omnipresence of non-

Maxwellian particles with suprathermal tails at higher energies in most of the astrophysical and space environments. Such kinds of nonthermal particles are naturally found in solar wind, Jupiter, and Saturn environments. The non-Maxwellian hybrid distributions involving two commonly adopted distribution functions for describing the plasmas are the kappa distribution, (first time introduced by Vasyliunas for modelling the OGO 1 and OGO 2 solar data), and the highly non-Maxwellian distribution profile with bump on the tail proposed by Cairns et al. The contribution of higher-order nonlinearity and dissipation effects to form dust acoustic kinetic Alfven dressed solitons is investigated by using the reductive perturbation technique from the solutions of higher order KdV-type equation in a polarised plasma. The findings of this investigation might be useful to understand the propagation of dust kinetic Alfven nonlinear structures in different space and astrophysical environments.

AIP-P-10

INTERACTION BETWEEN ION ACOUSTIC SOLITONS IN A QUANTUM PLASMA WITH TWO SPIN DEGENERATE ELECTRONS

Manveet Kaur[1] and N. S. Saini[1]
[1]*Department of Physics, Guru Nanak Dev University Amritsar-143005, INDIA*
E-mail: manveetsandhu7@gmail.com

Dense quantum plasmas have emerged as an active field of research due to their great pertinence in different areas of practical importance and in dense astrophysical plasmas such as white dwarfs [1]. In dense quantum plasmas, at extremely high number densities, the de-Broglie wavelength associated with the charge particle becomes comparable to the inter-particle distance. The spin effects are considered as one of quantum plasma's most important properties due to great significance of highly magnetized quantum plasmas. The interaction of solitons is a phenomenon that usually occurs in various plasma environments. The way of interaction of two solitons can be assorted as head-on collision, overtaking and one of the noticeable attributes of solitons is that it conserves the shape and size still after collision. After head-on collision, if pre (post)-collision part of soliton moves in front of the initial trajectory then phase shift is called as negative (positive) phase shift. The nonlinear waves exchange some energy between each other to preserve their shapes and sizes during head-on collision. The present work focuses on the study of head-on collision between nonlinear waves propagating in opposite directions in a magnetized spin quantum plasma having inertial ions and degenerate electrons with spin-up and spin-down states [2]. The separated spin evolution quantum hydrodynamic model is considered and the extended Poincaré-Lighthill-Kuo (PLK) method is adopted to derive two Korteweg-de Vries (KdV) equations. Further, the Hirota bilinear method is employed to determine the multi-solitons solutions of two KdV equations i.e., for single-soliton, double-soliton and triple-soliton cases. The analytical expressions of phase shift after head-on collision of nonlinear waves in different cases have also been derived. The combined effects of different physical parameters such as spin density polarisation, magnetic field and other physical parameters on the characteristics of nonlinear waves, time evolution and phase shift due to head-on collision between nonlinear waves have been numerically described.

References:

[1] S.L. Shapiro and S. A. Teukolsy, *"Black Holes, White dwarfs and Neutron Stars – The Physics of Compact Objects",* (Wiley-VCH, Weinhein, 2004).

[2] N. Kaur, R. Kaur and N. S. Saini, "Ion-acoustic cnoidal waves with the density effects of spin-up and spin-down degenerate electrons in dense astrophysical plasma" Z. Naturforsch. **75**(2)a, 103–111 (2020).

AIP-P-11

LARGE SCALE MAGNETIC FIELD GENERATION IN A 3D MHD PLASMA VIA INDUCTION DYNAMO ACTION: A NUMERICAL STUDY

Shishir Biswas‡, Rajaraman Ganesh
Institute for Plasma Research, Bhat, Gandhinagar, Gujarat 382428, HBNI, India.
*‡**E-mail:**shishir.biswas@ipr.res.in, shishirbeafriend@gmail.com*

Generation of large scale magnetic field in cosmos and astrophysical bodies are one of the long standing unsolved problems in astroplasma physics. A possible mechanism behind this is explained via dynamo action i.e. generation of magnetic energy at the cost of kinetic energy [**1**]. Amongst different dynamo models Induction dynamo model [**2**] is one of the celebrated models. In this model a given chaotic plasma flow stretches and folds back the magnetic field lines giving rise to an exponential growth of large scale magnetic field [**Fig.1**] in the limit of low plasma resistivity or large magnetic Reynolds number (R_m). In the present work, we consider a given helical plasma flow, namely the chaotic Arnold-Beltrami-Childress (ABC) flow in the opposite limit of low magnetic Reynolds number R_m. In particular, we numerically investigate a possible correlation between onset of dynamo action as a function of increasing R_m and formation of a 3D magnetic ``Cigar-like" [**Fig.2**] iso-magnetic structures [**3, 4**]. A strong localization of current density structures [**Fig.3**] co-existing with magnetic ``Cigars", possibly due to magnetic reconnection, is also shown. We have performed the above said studies using an in-house developed, multi-node, multi-card GPU based 3D MagnetoHydroDynamic solver (GMHD3D). Details of this study will be presented along with possible future directions.

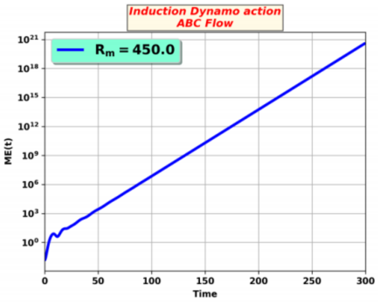

Fig.1: Growth of Magnetic Energy

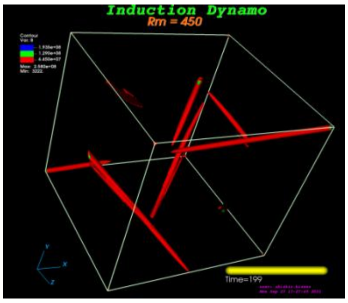

Fig.2: Cigar Formation

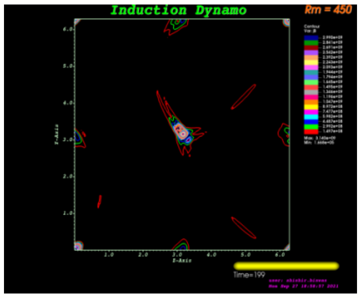

Fig.3: Localized currentdensity (Y-Z plane)

References:

[1] E. N. Parker. Hydromagnetic dynamo models. The Astrophysical Journal, 122:293, 1955.

[2] J. M. Finn and E. Ott. Chaotic flows and magnetic dynamos, Physical review letters, 60(9):760, 1988.

[3] D. Galloway & U. Frisch, Dynamo action in a family of fows with chaotic stream lines, Geophysical & Astrophysical Fluid Dynamics, 36:1, 53-83, 1986

[4] S. B. F. Dorch, On the Structure of the Magnetic Field in a Kinematic ABC Flow Dynamo, Phys. Scr. 61 717, 2000

AIP-P-12

EVOLUTION OF EMIC WAVE SUBPACKETS WITHIN ONE WAVELENGTH: A MULTIPOINT THEMIS OBSERVATIONS

Biswajit Ojha[1], Yoshiharu Omura[2], Satyavir Singh[1], and Gurbax Lakhina[1]
[1] *Indian Institute of Geomagnetism (IIG), Navi Mumbai, India*
[2] *Research Institute of Sustainable Humanosphere (RISH), Kyoto University, Japan*

Electromagnetic Ion Cyclotron (EMIC) rising tone emissions are important in understanding the nonlinear wave evolution and magnetospheric dynamics. These emissions often appear as a series of repetitive structures (known as subpackets) with increasing frequencies, known as rising tones. These rising tone emissions are believed to be generated near the geomagnetic equator by the anisotropic distribution of energetic ions (T_perp/T_par>1). Previous simulations and theory investigated the movement of the source regions of these rising tone emissions along the magnetic field lines; but, direct observational evidence was missing. Our findings provide a case study where these emissions are observed simultaneously by NASA's three THEMIS probes (THEMIS A, D, and E) in the outer magnetosphere during the time interval 14:20 UT to 14:30 UT on 09 September 2010. These left-handed polarized waves have wave normal angles less than 30°. THEMIS A was closest to the equator and was in a higher L-shell than THEMIS E and D. The smallest radial separation is ~2000 km between

THEMIS E and D spacecraft. This configuration of THEMIS probes allows us to explore the evolution of rising tone subpackets. These emissions are self-sustaining after the primary linear growth of the triggering wave at lower frequencies. Hilbert Huang Transformation (HHT) is applied to show the variations of the instantaneous frequency and the observed wave amplitude. The direction of energy flow is determined from the analysis of the Poynting flux. There is a rapid nonlinear growth of the EMIC subpackets within one wavelength. Adopting a multipoint observation technique, we show there are scattered source regions with an extent greater than the EMIC wavelength, and the subpacket structure changes nonlinearly within one wave period. These observations are matched very well with the existing nonlinear wave growth theory. Observed ion energies and pitch angle spectra of the ion fluxes are consistent with the energy associated with the Landau and cyclotron resonance conditions. This analysis provides pivotal information about the dynamical evolution of the fine structures of rising emissions and gives an idea about the 3D extent of subpackets.

AIP-P-13

STUDY OF ION ACOUSTIC WAVE WITH KAPPA DISTRIBUTION FUNCTION FOR BOTH ION AND ELECTRON AND ITS RELEVANCE TO MAGNETOSPHERE

N.Tandon, G. Ahirvaar, R. K. Chhajalani
Vikram University, Ujjain (M.P.)-456010,India
E-mail: tandon.neeti2019@gmail.com

The low frequency ion acoustic waves, analogous to sound waves, are generated due to the interaction of solar wind, and magnetosphere of the planet. The ion acoustic mode in magnetosphere is derived, in collision less, unmagnetised plasma, in which vibrations are transmitted through charge, not by collision. It is assumed that ions and electrons both are distributed according to the Kappa function. Equations for the assumed character of both species are linearized. The perturbed equations are obtained by neglecting second order perturbed quantities. From the perturbed equations, the dispersion relation for the ion acoustic wave, using Kappa function, is derived [1,2,3]. The dispersion relation and group velocity is compared, with usual ion acoustic dispersion relation and group velocity then effects of various variables of kappa distribution function on the ion acoustic mode are discussed.

Keywords: Ion acoustic mode, Kappa distribution function, Magnetosphere.

References:

[1] https://doi.org/10.1063/1.1688330 S. Jaheer, Murtaza G., H.A. Shah, Phys. Plasmas, 11, 2246, (2004).

[2] https://doi.org/10.1063/1.3143036 N.S. Saini, I. Kourakis, and M.A. Hellberg, Phys. Plasmas, 16, 062903, (2009).

[3] https://doi.org/10.1063/1.3322895 S. Sultana, I. Kourakis, N.S. Saini, M.A. Hellberg, Phys. Plasmas, 17, 032310 (2010).

AIP-P-14

EXOTIC PLASMAS OF THE NEUTRON STAR ATMOSPHERE: WHY ARE THEY INTERESTING

Anoop Singh[1,2], Shishir P. Deshpande[1,2], Mrityunjay Kundu[1,2]
[1]*Institute for Plasma Research, Bhat, Gandhinagar, Gujarat 382428, India*
[2]*Homi Bhabha National Institute, Training School Complex, Anushaktinagar, Mumbai 400094, India*
E-mail: anoop.singh@ipr.res.in

Neutron stars (NS) are remnants of supernova explosions with a mass approximately equal to the sun compacted to a radius of about 10 km. Amongst the many that are known (about 2000), a special class of NS called accretion-powered pulsars (AXP) have been observed to emit sudden bursts of X-ray radiation, thought to be due to nuclear fusion reactions in a rather thin (~ 100 cm) hydrogen atmosphere. The incredible gravity (g ~ 10^{11} and the magnetic field B ~ 10^{12} G) and particle densities of the order 10^{30} cm^{-3}make thissystem complex and rich with plasma phenomena.

In this paper, we summarize the state of understanding of the observed phenomena and an overview of the physical models that have been proposed. We also present preliminary results on the plasma waves in such systems.

References:

[1] Hansen, C. J., & Van Horn, H. M. (1975). STEADY-STATE NUCLEAR FUSION IN ACCRETING NEUTRON-STAR ENVELOPES. The Astrophysical Journal, 195 (February 1), 735-741.

[2] Lipunov, V. M. (1989). SCIENCE FOR EVERYONE. IN THE WORLD OF BINARY STARS. MIR.

[3] Galloway, D. K., &Keek, L. (2017). Thermonuclear X-ray bursts. 1-57.

[4] Woosley, S. E., &Taam, R. E. (1976). Gamma-ray bursts from thermonuclear explosions on neutron stars. Nature Publishing Group. Nature, 263.

[5] Kulsrud, R. M., &Sunyaev, R. (2020). Anomalous diffusion across a tera-Gauss magnetic field in accreting neutron stars.Journal of Plasma Physics, 86(6).

[6] Lipunov, V. M. (1992). Astrophysics of Neutron Stars. Springer Berlin Heidelberg, 1992.

AIP-P-15

QUASIPERIODIC INERTIAL ALFVÉN SOLITARY WAVES IN MULTICOMPONENT PLASMA

Geetika Slathia, N. S. Saini
Guru Nanak Dev University, Amritsar
E-mail: gslathia93@gmail.com

Over the last many years, there has been a great deal of interest in studying the various kinds of nonlinear solitary structures in different plasma environments such as laboratory experiments, space, and astrophysical environments. When an electron-ion plasma consists of additional charged particles, such as two species of electrons (hot-cold), two species of ions (positive-negative), or positrons etc., it is referred to as multicomponent plasma. The characteristics of wave propagation in multicomponent plasma is entirely different. It can also be induced in the laboratory by the positron injection into the electron ion system, ultra-intense laser matter interaction and by the mechanism of relativistic heavy-ion collisions. It also occurs in many astrophysical environments like the inner region of accretion disks, solar flares, magnetosphere of neutron stars, in the vicinity of black holes, in active galactic cores etc. The Alfvén waves are pure magnetohydrodynamics (MHD) waves and propagate in a plasma when ion inertial force is balance by the magnetic pressure gradient force. Alfvén waves are the low frequency non-dispersive waves which are formed when ions oscillate in an oscillating magnetic field. The existence of these nonlinear structures has also been confirmed by various laboratory experiments and space observations. Among the variety of nonlinear solitary structures, kinetic Alfvén waves (KAWs) and inertial Alfvén waves (IAWs) are one of the modes that has been studied to understand the formation of coherent nonlinear soliton structures in multicomponent plasmas (e.g., in planetary rings, cometary tails, and magnetosphere of Jupiter). Inertial Alfvén waves (IAWs) are also a class of dispersive Alfvén waves which are formed when the perpendicular scale length is approximately equal to the electron inertial. In the case of IAWs, the plasma beta lies in the range β me/mi 1. The nonlinear Korteweg-de Vries (KdV) equation describing the evolution of IAWs is derived by using the standard reductive perturbation method and low-amplitude KdV and dressed solitons are obtained. The quasiperiodicity and chaos are also investigated numerically in the presence external periodic force in the multicomponent plasma. The influence of different plasma parameters on the dynamical evolution of the IAWs has been observed. The findings of present investigation may be helpful to provide a new insight to understand the evolution of IAW and in the formation of various nonlinear structures in different space plasma regions.

AIP-P-16

ROLE GRAVITY WAVE INDUCED SEED PERTURBATIONS ON EQUATORIAL SPREAD F DAY TO DAY VARIABILITY UNDER THE INFLUENCE OF POST SUNSET ELECTRODYNAMICAL AND NEUTRAL WIND FORCINGS: A QUANTITATIVE ASSESSMENT

Sruthi T V, Manju G
Space Physics Laboratory, Vikram Sarabhai Space Centre, Thiruvananthapuram,695022
E-mail: sruthitv10@gmail.com

The present study investigates the role of gravity wave induced seed perturbations in the day to day variability of ESF, under the influence of the post sunset background conditions modulated by prevailing electrodynamics and neutral wind. Ionospheric foF2 data over geomagnetic equatorial station Trivandrum (8.5ºN, 77º E) corresponding to vernal equinoctial period encompassing high, low and moderate solar activity years, are used for the study. Meridional wind data for low and moderate solar activity years is obtained from ESA's sun synchronous satellite GOCE (Gravity field and steady-state Ocean Circulation Explorer) for the selected longitude bin close to Trivandrum location in the post sunset hours. Because of the non-availability of satellite data for high solar year, meridional wind was derived (Krishna Murthy et al., 1990) using ionosonde h'F (Base height of ionosphere at 2.5 MHz) data from Trivandrum (TVM- 8.5ºN, 77º E) and Sriharikota (SHAR -13.7º N, 80.2º E). The gravity wave induced TIDs in the post sunset ionosphere are extracted using wavelet analysis technique applied on the temporal variations of foF2. Ionospheric base height (h'F) at 1900hr is also scaled for same days which are used as a proxy for electrodynamical contribution. This particular study is carried out for geomagnetically quiet days (AP<=18) of ve season which is the most favoured season for ESF occurrence over Indian longitudes. By considering thermospheric wind and electric field effects in association with gravity wave seed, an exponential threshold curve is generated which could clearly demarcate ESF and NSF (Non spread F) days. Previous studies have addressed ESF variability in electrodynamical domain (wherein the layer height is above a threshold level). The present study, for first time succeeds in demarcating ESF and NSF days by incorporating effects of electric field, neutral wind and gravity waves seed perturbations simultaneously. The details of the analysis will be presented and discussed.

PAPERS FOR BUTI YOUNG SCIENTIST AWARD

BUTI-01

Fluid simulation of ion acoustic solitary waves in a relativistic pulsar wind

Kuldeep Singh,[1,2] Amar Kakad,[3] Bharati Kakad,[3] and N. S. Saini[1]

[1] *Department of Physics, Guru Nanak Dev University, Amritsar, India-143005*
[2] *Department of Mathematics, Khalifa University of Science and Technology, Abu Dhabi, UAE*
[3] *Indian Institute of Geomagnetism, New Panvel, Navi Mumbai, India-410218*

ABSTRACT

We have studied the evolution of ion acoustic solitary waves (IASWs) in pulsar wind. The pulsar wind is modelled by considering a weakly relativistic unmagnetized collisionless plasma comprised of relativistic ions and superthermal electrons and positrons. Through fluid simulations, we have demonstrated that the localized ion density perturbations generated in the polar wind plasma can evolve the relativistic IASW pulses. It is found that the concentration of positrons, relativistic factor, superthermality of electrons, and positrons have a significant influence on the dynamical evolution of IASW pulses. Our results may provide insight to understand the evolution of IASW pulses and their role in astrophysical plasmas, especially in the relativistic pulsar winds with supernova outflow which is responsible for the production of superthermal particles and relativistic ions.

Keywords: Fluid simulations —solitary waves — superthermal distribution — relativistic pulsar wind

1. INTRODUCTION

Numerous theoretical and experimental corroborations have elucidated the formation of different kinds of nonlinear ion acoustic solitary waves (IASWs) in various space and astrophysical plasma environments (Bharuthram & Shukla 1986; Cairns et al. 1996; Shukla & Mamun 2002; Gill et al. 2003; Kakad et al. 2016). These nonlinear solitary wave excitations are evolved due to the equipoise between dispersion and nonlinearity in the given plasma system. Many plasma physicists have well described the dynamics of small and arbitrary amplitude solitary waves by employing the reductive perturbation theory (Washimi & Taniuti 1966) and Sagdeev theory (Sagdeev 1966), respectively. In last few decades, the researchers have explored a great variety of low frequency IASWs in electron-positron-ion (e-p-i) plasmas having different thermal/non-thermal velocity distributions (Tajima & Taniuti 1990; Shukla & Stenflo 1993). It is discerned that there are abundance of electrons and positrons in accretion disks (Shukla et al. 1984; Popal et al. 1995), pulsar magnetosphere (Goldreich & Julian 1969), solar atmosphere (Tandberg-Hansen & Emshie 1988), and active galactic nuclei (Miller & Witta 1987). The admixture electron-positron (e-p) plasmas with fraction of ions has been confirmed by Advanced Satellite for Cosmology and Astrophysics (ASCA) in various astrophysical regions (Michel 1982; Kotani et al. 1996). Moreover, the positron can be produced by exploding the positronium atom in Tokamak e-i plasma (Surko et al. 1986; Tinkle 1994; Greaves & Surko 1995). Surko & Murphy (1990) described that annihilation time of positron in the plasma is more than one second. Therefore, variety of low frequency ion acoustic (IA) waves are generated in e-p-i plasmas which otherwise cannot exist in e-p plasmas. The impact of positron density in plasma can considerably alter the dynamics of solitary waves. Hence, the investigation of e-p-i plasmas become more essential to study the characteristic features of space/astrophysical and laboratory plasmas. Numerous investigations have been reported to study the different kinds of nonlinear structures in e-p-i plasmas in the frame work of Maxwellian/non-Maxwellian velocity distribution of charged particles (Chatterjee & Ghosh 2011; Saini et al. 2013; Ghosh & Banerjee 2016; Singh et al. 2017; Goswami et al. 2018; Sarma et al. 2018; Halder et al. 2019; Haque 2020).

Corresponding author: Kuldeep Singh
singh.kdeep07@gmail.com

Various spacecraft measurements have shown that the superthermal particle distributions which are effectively modelled by the kappa distribution are frequently observed in the solar wind (Formisano 1973; Livadiotis 2018), Jupiter (Leubner 1982), and Saturn's plasma environments (Armstrong et al. 1983; Masters et al. 2016). These superthermal distributions have significant impact on the characteristics of nonlinear waves generated in these plasma environments. These ubiquitous population of superthermal charged particles have mean velocity larger than mean thermal velocity. Vasyliunas (1968) modelled the solar data obtained from OGO 1 and OGO 2 spacecrafts and characterized the superthermality of particles by the parameter κ (spectral index). The one-dimensional κ-distribution function to model the superthermal plasma can be as (Hellberg et al. 2009; Summers & Thorne. 1991),

$$F^{\kappa}(v_{\jmath}) = \frac{n_{\jmath 0}}{\sqrt{\pi\kappa v_{\kappa}^{2}}}\frac{\Gamma(\kappa)}{\Gamma(\kappa-\frac{1}{2})}\left(1+\frac{v_{\jmath}^{2}}{\kappa v_{\kappa}^{2}}\right)^{-\kappa} \tag{1}$$

where $v_{\kappa} = \sqrt{\left(\frac{\kappa-3/2}{\kappa}\right)\left(\frac{2k_B T_{\jmath}}{m_{\jmath}}\right)}$ is the characteristic speed, $T_{\jmath}$ is the temperature of species and k_B is the Boltzmann constant. The κ index describes slope of the tail of superthermal distribution. In the limit $\kappa \to \infty$, the distribution function approaches the Maxwellian distribution. A large number of investigations for the study of different kinds of nonlinear structures in the frame work of superthermal distribution have been done in different space plasma environments (Saini et al. 2009; Baluku et al. 2010; Sultana et al. 2012; Bains et al. 2014; Saini et al. 2015; Lotekar et al. 2016, 2017; Singh et al. 2018; Singh & Saini 2019).

The relativistic effects become influential as the streaming velocity of particles is in the order of the speed of light. The weak relativistic effects come into picture as the energy of ions/electrons is in the range of MeV, for more specific description of plasma. Such kind of relativistic plasmas are abundant in space/astrophysical environments (Ikezi et al. 1970; Arons 1979; Grabbe 1989; Coroniti 2017). The high velocity streaming ions having energy range from 0.1 to 100 MeV are usually found in the various astrophysical/space regions. As we consider the energy of ion depends on its kinetic energy, the ions get relativistic velocity. Thus, where the ion streaming speed is $V_d = 0.1c$, one can consider the relativistic ions for the study of IASWs in plasma. The relativistic ions are crucial for the study of IASWs propagating in various astrophysical plasma environments (Nejoh 1992). Earlier studies revealed that superthermally distributed pair of electrons and positrons are created by relativistic pulsar wind comprised of relativistic ions (Becker 1986). It is also evident that plasma waves are much stronger to accelerate ions with relativistic speed only if $M\vartheta \gg 1$, where mass ratio $M(= m_e/m_i)$ and dimensionless parameter $\vartheta = eE/m_e\omega c$. In relativistic pulsar wind, the value of $\vartheta = 10^{11}$ (Gunn & Ostriker 1971; Chian 1982). The primary goal of our present investigation is in the pulsar wind plasma, where superthermal electron-positron pair is created by relativistic streaming ions. The superthermal electrons and positrons are created because of stochastic heating as the relativistic pulsar wind runs into the interaction with the supernova outburst of the pulsar magnetosphere (Arons 2009; Blasi & Amato 2011; Shah & Saeed 2011; Coroniti 2017). Lazar et al. (2010) explained that only weakly relativistic effects are considered if the thermal parameter $\mu(= mc^2/K_BT_i)$ is greater than unity (i.e., $\mu > 1$). A plasma with weakly relativistic temperature is predominantly populated by low energetic ions. In most of the astrophysical environments (e.g. pulsar wind and gamma-ray burst), for ions, $K_BT_i \sim 1keV$ and $\mu \sim 50-100$. Since ions are much heavier, it would probably be realistic to resume only to the weakly relativistic effects (Piran 2004). This plasma model is well justified by numerous investigations (Shah & Saeed 2011; Arons 2009; Saini & Singh 2016). Therefore, this exquisite example is well founded to explore the nonlinear ion acoustic waves in the pulsar wind having weakly relativistic ions and superthermal electrons-positrons pair. Many researchers illustrated the characteristics of nonlinear ion acoustic (IA) waves in a relativistic plasma environments (Pakzad 2011; Saeed et al. 2010; Gill et al. 2009; Sarma et al. 2018).

In the recent past, Saini & Singh (2016) investigated the interaction of solitary waves in a relativistic superthermal multicomponent plasma having superthermal electrons and positrons with small dust impurity. However, all the primary findings of these theoretical plasma models are taken by employing perturbative or non-perturbative methods with different assumptions to obtain the analytical solution that represents the IA wave structure. These techniques are not competent to provide the generation mechanisms of the nonlinear solitary waves. To tackle these limitations, computer simulation technique is the supportive tool to understand the evolution of the nonlinear solitary waves. Kakad et al. (2013, 2014, 2016) employed the fluid simulations to describe the dynamics of IASWs in a nonrelativistic electron-ion fluid plasma. Using initial Gaussian-type density perturbations under the short and long wavelength regimes, their simulations have successfully validated with the nonlinear fluid theory. Later, Lotekar et al. (2019) developed an efficient poisson solver by adopting the successive over relaxation method in numerical simulation of plasma composed of kappa distributed electrons (Lotekar et al. 2016, 2017). In the present study, we use the similar schemes and techniques in the development of the relativistic fluid code to model IASWs in pulsar wind plasma.

The objective of the present study is to investigate the evolution of IASWs and explore the effect of superthermality and density of positrons on their evolution in pulsar wind. To the best of our knowledge, no fluid simulation of the generation of IASWs in a weakly relativistic plasma composed of relativistic inertial ion fluid, superthermal electrons and positrons have been reported so far. The manuscript is structured as follows. The fluid equations and numerical methods employed in this simulation have been illustrated in Section 2. In Section 3, the simulation results are described. The comparison of characteristics of IASWs in relativistic and non-relativistic plasma is given in Section 4. The results are concluded in Section 5.

2. PLASMA MODEL

We assume that the pulsar relativistic wind encounters a head-on collision with the ejecta of supernova explosion surrounding the pulsar, producing superthermal electrons and positrons due to the stochastic heating process (Arons 2009; Blasi & Amato 2011; Shah & Saeed 2011; Coroniti 2017). We perform the simulation for such a region by considering an unmagnetized plasma comprising of superthermal electrons as well as positrons, and relativistic ion fluid to examine the evolution of IASWs. The quasi-neutrality is yielded as $n_{e0} = n_{i0} + n_{p0}$, where n_{j0} for $(j = i, e, p)$ are unperturbed density for plasma species, respectively. In the present plasma model, pressure and relativistic factor of ions are taken into consideration. The characteristic features of nonlinear relativistic IA waves are governed by basic set of fluid equations as follows:

$$\frac{\partial n_i}{\partial t} + \frac{\partial (n_i u_i)}{\partial x} = 0, \tag{2}$$

$$\frac{\partial (\gamma u_i)}{\partial t} + u_i \frac{\partial (\gamma u_i)}{\partial x} + \frac{q_i}{m_i}\frac{\partial \phi}{\partial x} + \frac{1}{m_i n_i}\frac{\partial P_i}{\partial x} = 0, \tag{3}$$

$$\frac{\partial P_i}{\partial t} + u_i \frac{\partial P_i}{\partial x} + \nu P_i \frac{\partial (\gamma u_i)}{\partial x} = 0, \tag{4}$$

$$\epsilon_0 \frac{\partial^2 \phi}{\partial x^2} = -e(n_i - n_e + n_p), \tag{5}$$

where n_i and u_i are the density and velocity of the ions in the x-direction, respectively. ϕ is the electrostatic potential, and q_i (m_i) is the charge (mass) of the ions. In Equation (4), i.e., the equation of state, we have assumed ions to be adiabatic with with adiabatic index $\nu = 3$. The relativistic factor $\gamma = (1 - \beta^2)^{-1/2}$, where $\beta = \frac{V_d}{c}$ and c is speed of light. From the kappa distribution function, the expressions of superthermal electron and positron densities are written as

$$n_e = n_{e0}\left(1 + \frac{q_e \phi}{(\kappa_e - \frac{3}{2})k_B T_e}\right)^{-\kappa_e + \frac{1}{2}}, \tag{6}$$

and

$$n_p = n_{p0}\left(1 + \frac{q_p \phi}{(\kappa_p - \frac{3}{2})k_B T_p}\right)^{-\kappa_p + \frac{1}{2}}, \tag{7}$$

In the equation above, $T_{e(p)}$ is the temperature of the electrons(positrons) and q_e=$-e$ and q_p=$+e$ are the basic electronic charges on electron and positron, respectively.

In this fluid simulation, we compute the numerical solution of Equations (2)-(7) into a discrete system (equidistance in space and time) and every plasma quantity is also computed on these grid points. The spatial derivatives in the above Equations (2)-(4) are computed using the 4^{th} order central finite difference scheme (Kakad et al. 2014, 2016; Lotekar et al. 2016, 2017, 2019) which is given by,

$$\frac{\partial \mathfrak{F}_\ell}{\partial x} = \frac{\mathfrak{F}_{\ell-2} - \mathfrak{F}_{\ell+2} + 8(\mathfrak{F}_{\ell+1} - \mathfrak{F}_{\ell-1})}{12\Delta x} + O(\Delta x^4). \tag{8}$$

Here, $\mathfrak{F}_\ell$ denotes the any plasma quantity at ℓ grid points. This method is accurate up to the 4^{th} power of Δx. In the time leap-frog method (accuracy is Δt^2) is employed to carry out the time integration of Equations (2)-(4). The high frequency numerical noise arises due to the discretization of space and time in solving Equations (2)-(4). Thus, fourth order compensating filter is used to eliminate these numerical errors (Kakad et al. 2014; Lotekar et al. 2019):

$$\mathfrak{F}_\ell^\star = \frac{10\mathfrak{F}_\ell + 4(\mathfrak{F}_{\ell+1} + \mathfrak{F}_{\ell-1}) - (\mathfrak{F}_{\ell+2} + \mathfrak{F}_{\ell-2})}{16} \tag{9}$$

Here, $\mathfrak{F}_\ell^\star$ represents the filtered quantity at grid points (ℓ). We have developed a fluid simulation code with periodic boundary conditions. In the simulation Δt and Δx are considered in such a way that the Courant-Friedrichs-Lewy(CFL) condition (i.e., $c\frac{\Delta t}{\Delta x} \leq 1$) is always fulfilled for the convergence of the finite difference scheme. For all simulation runs, $u_i = V_d$ at $t = 0$ and no electric field (i.e., $\phi = 0$). The background densities of electron, positron and ion are $n_{i0} + n_{p0} = n_{e0}$. The Gaussian type initial density perturbation (IDP) is used in the equilibrium ion density to perturb the plasma as (Lotekar et al. 2019)

$$n_i = n_{i0} + \Delta n \exp\left[-\left(\frac{x - x_c}{l_0}\right)^2\right] \tag{10}$$

where, Δn and l_0 denote the amplitude and width of the IDP, n_{i0} is the equilibrium density of relativistic ions. x_c is the centre point of the simulation system.

The algorithm of this relativistic fluid code is as follows: initially Gaussian perturbation in the equilibrium density of relativistic ions is given by Equation (10). The initial values of the plasma variables (n_i, u_i and P_i) are used to compute the variables in the next time step by using Equations (2)-(4). One has to evaluate the superthermal electron and positron densities because there are no time dependent equations for them that can be used to upgrade their numerical values in every time steps. The superthermal electrons and positrons density equations (Equations (6)-(7)) are function of the superthermal indices (κ_e and κ_p) and electrostatic potential (ϕ). First we have discretized the Poisson Equation (5) using second order central finite difference scheme, and then applied the successive-over-relaxation (SOR) method as described in Lotekar et al. (2019) to get the values of potential at j^{th} grid as follows

$$\bar{\phi}_j^{R+1} = \zeta\phi_j^{R+1} + [1-\zeta]\phi_j^R, \tag{11}$$

where the discretized expression of ϕ_j^{R+1} is obtained as:

$$\begin{aligned}\phi_j^{R+1} = \frac{1}{2}\Bigg[\Delta x^2 \Bigg[n_i - n_{e0}\left(1 + \frac{q_e\phi^R}{(\kappa_e - \frac{3}{2})k_BT_e}\right)^{-\kappa_e+\frac{1}{2}} \\ + n_{p0}\left(1 + \frac{q_p\phi^R}{(\kappa_p - \frac{3}{2})k_BT_p}\right)^{-\kappa_p+\frac{1}{2}}\Bigg]_j + \phi_{j+1}^R + \phi_{j-1}^{R+1}\Bigg].\end{aligned} \tag{12}$$

Here, j and R are the grid point and iteration number, and ζ is a relaxation parameter of SOR method. After performing the test for various values of ζ, we found that the code gives best performance for ζ=0.9. Therefore, we have taken $\zeta = 0.9$ for all the simulation runs. The approximate value of the solution is improved to $\bar{\phi}_j^{R+1}$ is upgraded by using the weighted mean of iterations of previous (ϕ_j^R) and current values of potential (ϕ_j^{R+1}). The termination criteria to stop the iteration process in the simulation is given as:

$$\max|\phi^R - \phi^{R+1}| < \tau \tag{13}$$

To achieve the better numerical stability, we have used the tolerance $\tau = 10^{-10}$ for all simulations runs. Initially, the value of electrostatic potential at previous time step is a guess which is substituted in Equation (5), and then solved for the electrostatic potential. After every iteration, the new value of ϕ will be considered as new guess, and the procedure will be repeated until the termination criteria as mentioned in Equation (13) is achieved. The charge separation arise due to the superthermal distribution of electron and positron (i.e., the left-hand side of the Equation (5) is non-zero). This charge separation yields the evolution of a finite ϕ at every time step.

3. SIMULATION RESULTS

We demonstrate the results from the one-dimensional relativistic fluid simulations of pulsar wind plasma by considering the periodic boundary conditions. In each simulation run, we consider the grid spacing $\Delta x = 0.5$, time interval

$\Delta t = 0.003$, width of the IDP $l_0 = 20$, and amplitude of IDP $\Delta n = 0.2$. $m_i/m_e = 100$, $m_e/m_p = 1$, $T_e/T_i = 10$ and $T_e/T_p = 1$. The values of plasma frequencies in the system are $\omega_{pi} = 0.094$, $\omega_{pe} = 1.0$ and $\omega_{pp} = 0.0316$ and the corresponding Debye lengths are $\lambda_{Di} = 1.05$, $\lambda_{De} = 3.16$ and $\lambda_{Dp} = 10$, respectively. Here, $n_{i0} + n_{p0} = n_{e0} = n_0 = 1$. In this paper the parameter density is in units of $[n_0]$, time is in units of $[\omega_{pe}^{-1}]$, electrostatic potential is in units of $[m_i v_{thi}^2/e]$, and velocity is in units of $[\omega_{pe}\lambda_D]$. Here, Debye length, $\lambda_D = \sqrt{\epsilon_0 k_B T_i/n_0 e^2}$. The details of different input parameters used in all simulations runs are given in Table 1. We consider an unmagnetized plasma composed of relativistic streaming ions, superthermal electrons and positrons, the IDPs are used to perturb the background density of relativistic ions, which yields the charge separation that drives IASWs. Here, we illustrate the evolution of relativistically drifting IASW structures for simulation Run-1A (iii).

3.1. *Evolution of stable relativistic IASWs*

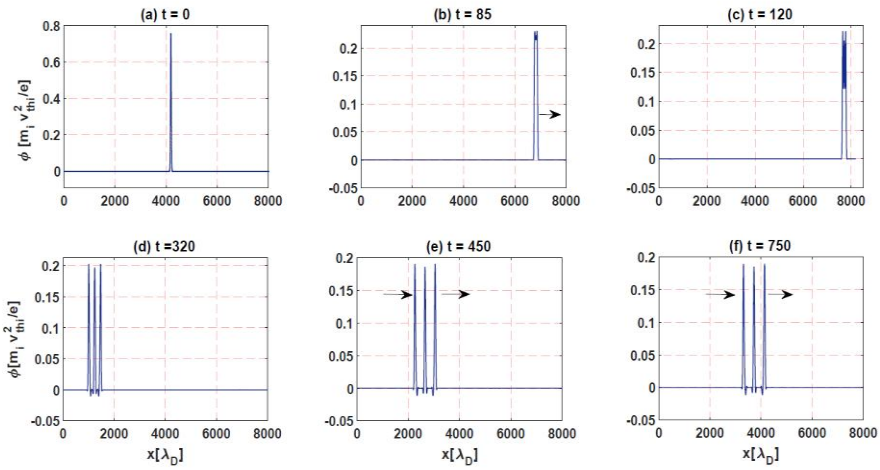

Figure 1. (Color online) Figure shows the evolution of the relativistic ion acoustic solitary waves in superthermal relativistic plasma for Run-1A (iii). (a) Formation of finite electrostatic potential pulse at first time step. (b)-(c) Splitting of electrostatic potential pulse into two IA solitary waves which are moving towards the right-side of simulation boundary (d) Formation of two IA solitary wave pulses. (e)-(f) Two stable IA solitary waves are propagating toward the right-side of the boundary with different speed. The parameters used in this run are given in Table 1

Figure 1 shows the evolution of the relativistic IA solitary waves, when the short wavelength IDP is introduced in the background relativistic ion density. The amplitude of the IDP used in the simulation runs is 20% of the equilibrium density. At equilibrium, the electrostatic potential is zero due to quasi-neutrality. As the electrons and positrons obey the superthermal distributions, the initially applied perturbation in the equilibrium ion density yields the finite electrostatic potential in next time step during simulation. Figure 1(a) describes this potential pulse at the first time step. It is noticed that the amplitude of the potential pulse is decreased with time. This drop in the potential stops after some time, and the pulse starts splitting from its top while drifting towards the right-side of the x-axis as depicted in Figure 1(b)-(c). This further evolved into two identical relativistic IA solitary wave pulses along with the one smaller pulse (compare to other two pulses) at the center as shown in Figure 1(d). The smaller wave pulse between the two identical solitary pulses is evolved due to the presence of pressure gradient in the equation of ions. This pulse may disappears if we unplug the ion pressure/thermal effects from the fluid model equations (not shown here). Further, Figure 1(e) illustrates that the two identical solitary wave pulses propagate with the different speeds towards right-side of the boundary. These pulses are recognised as relativistic ion acoustic solitary wave pulses. The amplitude of the relativistic IASW pulses slowly reduces, and small amplitude IA oscillations are formed at the edge of both pulses. The amplitude of the IA oscillations is much smaller than the amplitudes of the relativistic IA solitary wave pulses. The IA oscillations along with the IA wave pulses are shown in Figure 1(e). After this stage, the IA wave pulses move with the constant amplitudes and speeds. These stable pulses are shown in Figure 1(f), which we termed as the relativistic IA solitons.

3.2. *Spatio-temporal evolution of stable relativistic IASWs*

We have explored the effect of the positron concentration and the particle distributions on the evolution of IASW pulses through the spatial and temporal evolution of their associated electrostatic potential in the simulation, which is illustrated, respectively in Figures 2 and 3. The IASW pulses propagating away from the center of the simulation system towards the right-side boundary, due to the drift velocity (V_d). As the IASW pulses cross the right-side boundary then it reappear from the left-side boundary due to the periodic boundary conditions considered in the simulation. One can see from Figures 2 and 3 that the initially excited pulse evolved into the two identical IASW pulses and one smaller pulse between them. These two identical pulses get detached from pulse at the center due to the difference in their phase speeds. After a long time, both IASW pulses move stably by preserving their shape and size in the system, which is the main characteristic feature of the solitons in the plasma system.

3.2.1. *Influence of positron concentration*

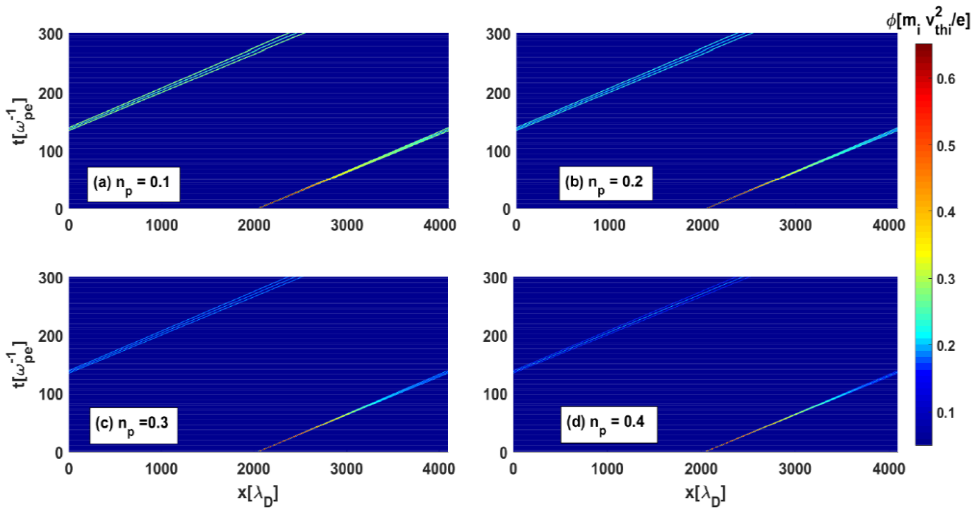

Figure 2. Spatio-temporal evaluation of electrostatic potential for different values of positrons density (n_p) from Run-1 A(i-iv).

The difference in the spatio-temporal characteristics of the electrostatic potential is clearly seen in Figures 2(a)-(d) for the different values of positron density (n_p). By comparing the Figures 2(a) and 2(d), it seen that the increase in the concentration of positrons results in the lower amplitudes of relativistic IASW pulses. It is noticed that the phase velocity of the IASW pulses decrease with increase in the concentration of positrons. Hence, more the number of positrons in the plasma means slow moving IASW pulses are generated.

3.2.2. *Influence of Superthermal distribution*

Figures 3(a)-3(d) show the spatio-temporal characteristics of the electrostatic potential in the course of the evolution of IASW pulses for the different values of superthermal indices of electron and positron distributions (κ_e and κ_p). It is observed that the phase speeds and amplitudes of IASW pulses in case of lower values of the κ index are smaller as compared with higher κ index. This is because the lower (higher) kappa index corresponds to the presence of considerably higher (lower) superthermal population. This indicates that the system with more number of superthermal electrons and positrons has smaller most probable thermal speed. Hence, for the superthermal electrons/positrons (i.e., lower κ_e and κ_p) the wave phase speed is lesser than the Maxwellian case (higher κ_e and κ_p) by comparing Figure 3(a) and 3(d). Furthermore, it is seen that the impact of superthermality of positrons is more significant than the superthermality of electrons by comparing Figure 3(b) and 3(c).

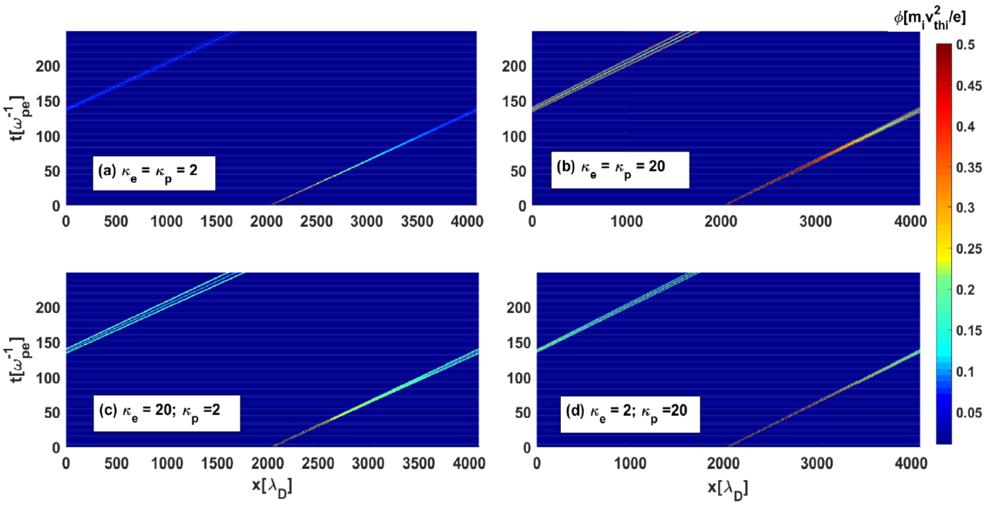

Figure 3. Spatio-temporal evaluation of electrostatic potential for different values of superthermal indices of electrons and positrons (κ_e and κ_p). The Panel (a) plotted from Run-2A (i), Panel (b) from Run-4A, Panel (c) from Run-2A (iv), and Panel (d) from Run-3A (iv). The plasma parameters of these runs are given in Table 1.

3.3. *Dispersion characteristics of relativistic IASWs*

The free energy given initially in the form of IDP to the system is transferred to the different wave modes. The dispersion characteristics are useful in recognising the different waves evolved in the plasma. The dispersion diagrams are obtained by employing the fast Fourier transformation of the electrostatic potential over space and time and compared them with the linear dispersion of the IASWs. The linear dispersion relation of IASWs in relativistic superthermal plasma is theoretically given by (Saini & Singh 2016)

$$\frac{\omega}{k} = V_d \pm \left\{ \frac{1}{m_i \gamma} \left(\frac{n_{i0} T_e T_p}{n_{e0} T_p (\frac{\kappa_e - 0.5}{\kappa_e - 1.5}) + n_{p0} T_e (\frac{\kappa_p - 0.5}{\kappa_p - 1.5})} + 3T_i \right) \right\}^{\frac{1}{2}} \tag{14}$$

3.3.1. *Influence of concentration of positrons*

Figures 4(a)-(d) depict the dispersion diagram of relativistic IASWs under the influence of positron density. In these figures, we can see that the energy given in form of the IDP is transferred to the ion acoustic modes. From the dispersion curve one can obtained the phase speed of IASW pulse (ω/k). This figure shows that the rise in the positrons density lowers the phase speed of IASW pulses. Furthermore, we plotted the linear dispersion equation (Equation 14) for the parameters considered in each panel. It is seen that the the dispersion relation obtained from the four different simulation runs is exactly matches with the linear dispersion relation (Equation 14) shown by white dashed curve.

3.3.2. *Influence of superthermal distribution*

Figures 5(a)-(d) illustrate the dispersion diagram of relativistic IASWs for different κ index of the superthermal distribution of electrons and positrons. From the dispersion plots of these four simulation runs: Run-2A (i), Run-4A, Run-2A (iv), and Run-3A (iv), it is observed that the increase in the kappa indices results in the higher speed of the stable IASW pulses. These observations of IASWs are consistent with the observations from the spatio-temporal evolution plots. It is noticed that the power distributed among the k (wave number) range is more for nearly Maxwellian case (κ_e and $\kappa_p = 20$) than the superthermal (κ_e and $\kappa_p = 20$). Figures 5(c)-(d) show that the spectra of smaller κ_p has less power than the spectra of larger κ_p. It is observed that the dispersion curves obtained from the simulations are exactly matches with the linear dispersion curves obtained from the theory, that are shown with the dashed curves. This confirms that the ion density perturbations in the polar wind can excite the stable IASW pulses.

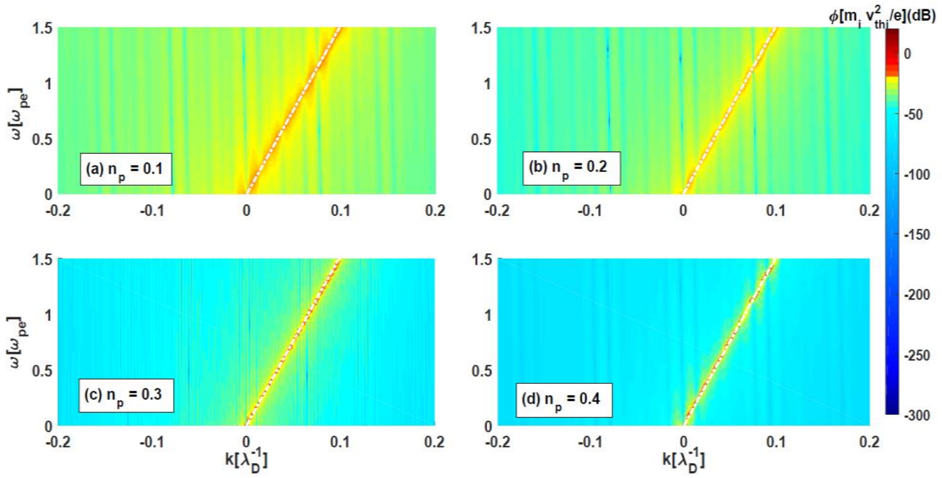

Figure 4. $\omega - k$ diagram for different values of positron density (n_p) from Run-1A (i-iv). The white dashed lines are plotted from the theoretical linear dispersion of IA waves in each case.

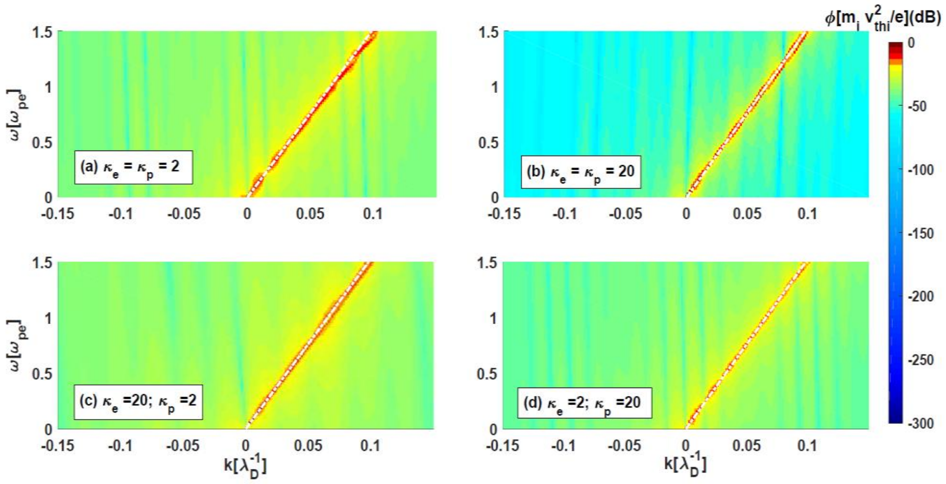

Figure 5. $\omega - k$ diagram for different values of superthermal indices of electrons and positrons (κ_e and κ_p). The white dashed lines are plotted from the theoretical linear dispersion of IA waves in each case. The Panel (a) plotted from Run-2A (i), Panel (b) from Run-4A, Panel (c) from Run-2A (iv), and Panel (d) from Run-3A (iv). The plasma parameters of these runs are given in Table 1.

4. CHARACTERISTICS OF IASWS IN RELATIVISTIC AND NON-RELATIVISTIC PLASMA

In this investigation, the peak amplitude and phase speed is calculated in the stable region. The stable region is the time domain where the generated solitary waves will not change their shape and size. In the stability region, the IASW pulses propagate with constant amplitudes and speeds, therefore, it is convenient to study their characteristics in different simulation runs.

4.1. *Influence of positron concentration*

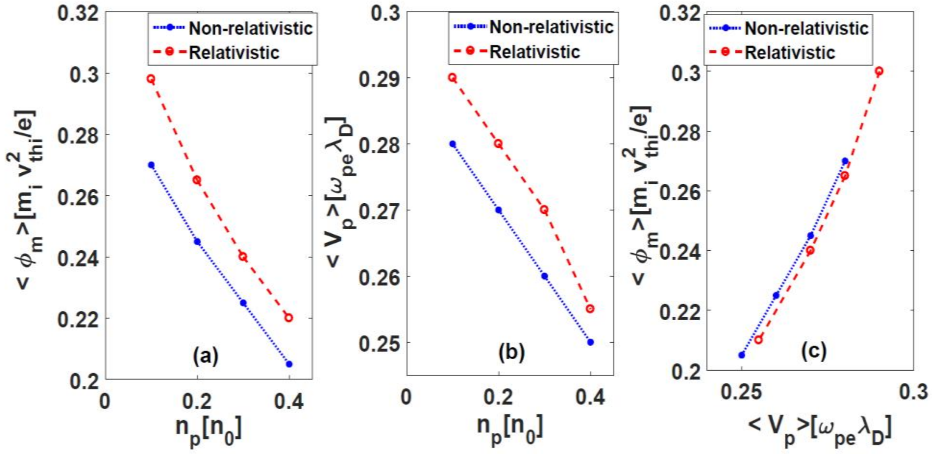

Figure 6. The variation of (a) average peak amplitude $<\phi_m>$ of IASWs (b) average phase velocity ($<V_p>$) of IASWs for different values of positrons density (n_p)(c) variation of average peak amplitude ($<\phi_m>$) vs average phase velocity ($<V_p>$) of IASWs for fixed values of $\kappa_e = 3$ and $\kappa_p = 4$. The parameters of the relativistic [Run-1A (i-iv)](see Figure 2) and non-relativistic [Run-1B (i-iv)] runs are given in Table 1.

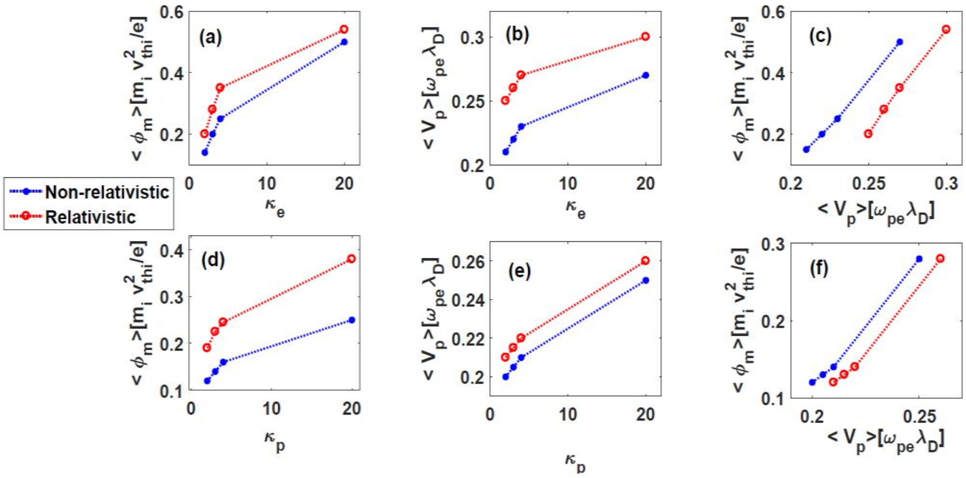

Figure 7. The variation of average peak amplitude $<\phi_m>$ and average phase velocity ($<V_p>$) of IASWs for different values of κ_e (panels-a and b) and κ_p (panels-d and e). The variation of average peak amplitude ($<\phi_m>$) vs average phase velocity ($<V_p>$) of IASWs for the respective case is shown in panel (c) and (f) (see Figure 3). Other parameters used in the simulation are given in Table 1. The upper panels are plotted from the datasets of simulation Run-2A (i-iv) and Run-2B (i-iv), whereas the bottom panels are from Run-3A (i-iv) and Run-3B (i-iv). The parameters used in these runs are given in Table 1.

We have performed the simulations for relativistic ($\beta = V_d/c = 0.1$) and non-relativistic ($\beta = V_d/c = 0$) case separately, for different positron concentrations. Figures 6(a) and (b) respectively depict the variation of peak amplitude and phase speed of relativistic (red curve) and non-relativistic (blue curve) IASW pulses for different values of n_p. It is noticed that rise in the density of positrons reduces the peak amplitude and phase velocity of both relativistic and non-relativistic IASW pulses. The increase in positron concentration (i.e., depopulation of ions) reduces the driving force provided by ion inertia, consequently, the IASW pulses amplitude decreases (see Figure 2). It is observed that both peak amplitudes and velocities of IASW pulses are larger for relativistic case than the nonrelativistic case. This is because an increase in relativistic factor (i.e., β) increases the nonlinearity, and enhances the amplitude of IASW pulses. Figure 6(c) shows the variation of peak amplitude with peak speed for both relativistic and non-relativistic cases. Figure 6(c) confirms the KdV-like behaviour of IASWs which means small amplitude solitary waves have lowest order of nonlinearity and dispersion. Such kinds of solitary wave pulses are governed by the well known KdV equation which is used to study the breaking of soliton into multi-solitons moving with different phase velocities and interaction of solitons without changing its shape and size (Saini & Singh 2016). Figure 6(c) illustrates the KdV-like behaviour of IASW pulses in both relativistic and non-relativistic plasmas.

4.2. *Influence of superthermal distribution*

In this section, the simulations for relativistic and non-relativistic case are performed separately, for different kappa index of electrons and positrons. Figures 7(a), (b), (d) and (e) depict the variation of peak amplitude and phase speed of relativistic (red curve) and non-relativistic (blue curve) IASW pulses for different values of κ_e and κ_p. It is found that both amplitude and speed of IASW pulses is escalated with increase in both κ_e and κ_p (i.e., decrease in superthermality of electrons and positrons) for both relativistic and non-relativistic cases. Physically, the increase in κ_e and κ_p increases the nonlinearity as a result the amplitude of IASW pulses increases (see Figure 3). The increase in κ_e and κ_p can also be interpreted as increase in the electrons/positrons pressure, due to which the restoring force increases, and ultimately the speed of the IASW pulses enhances. It is observed that both peak amplitudes and phase velocities are higher for relativistic case that the non-relativistic. Figures 7(c) and (f) show the variation of average peak ($<\phi_m>$) and average peak velocities ($<V_p>$) for relativistic and non-relativistic case, respectively. These figures explain the KdV-like behaviour of IASWs in given plasma system. Furthermore, it is seen that both amplitudes and speeds of the IASW pulses are higher in the case of varying electron density (n_e) as compared to the case of varying positron density (n_p). This shows that the nonthermality of electrons play dominant role in producing the large amplitude faster IASW pulses as compared to the nonthermality of the positrons.

5. CONCLUSIONS

In this paper, we have presented the evolution and propagation of the IASWs in a relativistic pulsar wind plasma composed of weakly relativistic ions and superthermal electrons as well as positrons. Our simulation shows that the time span required for the formation of stable IASW pulses is lesser for the higher values of κ index (i.e., small superthermality effect) and concentration of positrons (n_p). This suggests that the IASWs are generated much faster in superthermal and the positron populated pulsar wind plasma. It is observed that the IASW pulses become stable and their characteristics features like maximum amplitude, and speed (V_p) are constant after some time span, which we named as the stable region. We have obtained the characteristics of the stable relativistic IASW pulses in this region. The dispersion characteristics of IASW pulses obtained from the simulations are compared with the dispersion characteristics obtained from the fluid theory, which is consistent with our simulation results for both relativistic and non-relativistic cases. The peak amplitude and phase speed of the IASW pulses are much higher in relativistic case than non-relativistic case. The peak amplitude and phase speed of the IASW pulses increases with the superthermal index, whereas, the positron concentration reduces the peak amplitude and the phase speed of the IASW pulses. In this study, we have considered the initial density perturbation with amplitude Δn and width l_0 for all simulation runs. However, one can use perturbations with different amplitudes and widths to generate IASW pulses in the simulation. It is expected that the different amplitude and width of perturbations will generate IASW pulses with different characteristics. This particular aspect is not discussed in our paper as we focus on the effect of plasma parameters on the evolution of IASW pulses in pulsar wind plasma. Our simulations conclude that the plasma parameters including relativistic factor play very pivotal role for the evolution of IASW pulses and have an influence on the phase velocity and amplitude of IASW pulses in pulsar wind plasma.

In pulsar wind, the ejection of relativistic streaming ions can create localized high-density regions accompanied by the localized electric field structures (electric potentials), which propagates with acoustic speed. It is known that the wave potentials associated with the localized perturbations can trap the charged particles with energies less than the electric potential energy, and get transported along with the wave (Kakad et al. 2013). In such a case, the charged particles confined by the electric potential accompanied by the solitary wave get energy by the repetition of reflections that lead to the acceleration of charged particles (Ishihara et al. 2018). Such a scenario of the particle acceleration by ion acoustic solitary waves in plasma is discussed by Ishihara et al. (2018). Our study shows that the ion acoustic

Run	$\beta = \frac{V_d}{c}$	n_p	κ_e	κ_p
1	A 0.1 B 0	i 0.1 ii 0.2 iii 0.3 iv 0.4	3	4
2	A 0.1 B 0	0.3	i 2 ii 3 iii 4 iv 20	2
3	A 0.1 B 0	0.3	2	i 2 ii 3 iii 4 iv 20
4	A 0.1 B 0	0.3	20	20

Table 1. Input parameters used in the 26 simulation runs for the different combination of β, n_p, κ_e and κ_p. For all these simulation runs, we assume $\Delta x = 0.5$, $\Delta t = 0.003$, $l_0 = 20$, $\Delta n = 0.2$, $m_i/m_e = 100$, $m_e/m_p = 1$, to investigate the evolution of IASWs in a relativistic plasma system.

solitary waves can be evolved in pulsar wind plasma. Thus, proposed one of the possibilities of the particle transport and particle accelerations through the ion acoustic solitary waves. In this way, the results of our investigation may shed the light on particle acceleration and energy transportation by nonlinear IASWs in astrophysical plasmas, especially when relativistic pulsar winds interacts with supernova outburst surrounding the pulsar (Arons 2009; Blasi & Amato 2011; Shah & Saeed 2011; Coroniti 2017).

ACKNOWLEDGEMENTS

KS thanks the Plasma Science Society of India (PSSI) for providing the fellowship for collaborative research. KS is also grateful to Professor D. S. Ramesh, Director, Indian Institute of Geomagnetism (IIG) for the encouragement and support during his visit to IIG. The model computations were performed on the High Performance Computing System at IIG. This work is accepted for publication in Monthly Notices of the Royal Astronomical Society Journal 2021.

REFERENCES

Armstrong, T. P., Paonessa, M. T., Bell II, E. V., & Krimigis, S. M. 1983, J. Geophys. Res., 88, 8893

Arons, J. 1979, Space Sci. Rev., 24, 417

Arons, J. 2009, Astrophys. Space. Sci. Lib., 357, 373

Bains, A. S., Li, B., & Xia, L. D. 2014, Phys. Plasmas, 21, 032123

Baluku, T. K., Hellberg, M. A., Kourakis, I., & Saini, N. S. 2010, Phys. Plasmas, 17, 053702

Becker, U. 1986, J. Phys. B, 19, 1347

Bharuthram, R., & Shukla, P. K. 1986, Phy. fluids, 20, 3214

Blasi, P., & Amato, E. 2011, Astrophys. Space Sci. Proc., 2, 623

Cairns, R. A., Mamun, A. A., Bingham, R., & Shukla, P. K. 1996, Phys. Scr., 63, 80

Chatterjee, P., & Ghosh, U. N. 2011, Eur. Phys. J. D., 64, 413

Chian, A. C. L. 1982, Plasma Phys., 24, 19
Coroniti, F. V. 2017, Astrophys. J., 850, 184
Formisano, V., Moreno, G., & Palmiotto, F. 1973, J. Geophys. Res., 86, 8157
Ghosh, B., & Banerjee, S. 2016, Turkish J. Phys. , 40, 1-11
Gill, T. S., Kaur, H., & Saini, N. S. 2003, Phys. Plasmas, 10, 3927
Gill, T. S., Bains, A. S., & Saini, N. S. 2009, Can. J. Phys., 87, 861
Goldreich, P., & Julian, W. H. 1969, Astrophys. J., 157, 869
Goswami, J., Chandra, S., & Ghosh B. 2018, Laser and Particle Beams, 36, 136
Grabbe, C. J. 1989, Geophys.Rev., 94, 17299
Greaves, R. G., & Surko, C. M. 1995, Phys. Rev. Lett., 75, 3846
Gunn J. E., & Ostriker, J. P. 1971, Astrophys. J., 165, 523
Halder, P., Mukta, K. N., & Mamun, A. A. 2019, Int. J. Cosmol. Astron. Astrophys., 1(3), 81
Halder, Q. 2020, Results in Phys., 18, 103287
Hellberg, M. A., Mace, R. L., Baluku, T. K., Kourakis, I., & Saini, N. S. 2009, Phys. Plasmas, 16, 094701
Ikezi, H., Taylor, R., & Baker, D. 1970, Phys. Rev. Lett., 25, 11
Ishihara, H., Matsuno, K., Takahashi, M., & Teramae, S., 2018, Phys. Rev. D, 98, 123010
Kakad, A., Omura, Y., & Kakad, B. 2013, Phys. Plasms, 20, 062103
Kakad, B., Kakad, A., & Omura, Y. 2014, J. Geophys. Res.: Space Phys., 119, 5589-5599
Kakad, A., Kakad, B., Anekallu, C., Lakhina, G., Omura, Y., & Fazakerley, A. 2016, J. Geophys. Res.: Space Phys., 121, 4452 Doi: https://doi.org/10.1002/2016JA022365
Kakad, A., Lotekar, A., & Kakad, B. 2016, Phys. Plasmas, 23, 110702
Kotani, T., Kawai, N., Matsuoka, M. & Brinkmann, W. 1996, Publ. Astron. Soc. Jpn. 48, 619
Lazar, M., Stockem, A. & Schlickeiser R. 2010, The Open Plasma Physics J. 3, 138
Leubner, M. P. 1982, J. Geophys. Res., 87, 6335
Livadiotis, G., Desai, M. I. & Wilson III, L. B. 2018, Astrophys. J., 853(2), 142
Lotekar, A., Kakad, A., & Kakad, B. 2016, Phys. Plasmas, 23, 102108
Lotekar, A., Kakad, A., & Kakad, B. 2017, Phys. Plasmas, 24, 102127
Lotekar, A., Kakad, A., & Kakad, B. 2019, Communications in Nonlinear Science and Numerical Simulation, 68, 125
Masters, A., Sulaiman, A. H., Sergis, N., Stawarz, L., Fujimoto, M., Coates, A. J., & Dougherty, M. K. 2016, Astrophys. J., 826, 48
Mendis, D. A., & Rosenberg, M. 1994, Annu. Rev. Astron. Astrophys., 32, 419
Michel, F. C. 1982, Rev. Mod. Phys., 54, 1
Miller, H. R., & Witta, P. J. 1987, Active Galactic Nuclei, Springer, 202
Nejoh, Y. 1992, Phys. Fluid B, 4, 2830
Pakzad, H. R. 2011, Astrophys. Space. Sci., 334, 337
Popal, S. I., Vladimirov, S. V., & Shukla, P. K. 1995, Phys. Plasmas, 2, 716
Piran T. 2004, Rev. Mod. Phys. 76, 1143-210
Saeed, R., Shah, A., & Noaman-ul-Haq, M. 2010, Phys. Plasmas, 10, 3927
Sagdeev, R. Z. 1966, Rev. Plasma Phys. (Consultants Bureau, New york), 4, 23
Saini, N. S., Kourakis, I., & Hellberg, M. A. 2009, Phys. Plasmas, 16, 062903
Saini, N. S., Chahal, B. S., & Bains, A. S. 2013, Astrophys. Sapce Sci, 347, 129
Saini, N. S., Singh, M., & Bains, A. S. 2015 Phys. Plasmas, 22, 113702
Saini, N. S., & Singh, K. 2016, Phys. Plasmas, 23, 103701
Sarma, R., Misra, A. P., & Adhikary, N. C. 2018, Chinese Physics B, 27(10), 105207
Shah, A., & Saeed, R. 2011, Plasma Phys. Controlled Fusion, 53, 095006
Shukla, P. K., Yu, M. M., & Tsintsadze, N. L. 1984, Phys. Fluids, 27, 327
Shukla, P. K., & Stenflo, L. 1993, Astrophy. Space. Sci, 209, 323
Shukla, P. K., & Mamun, A. A. 2002 *Introduction to Dusty Plasma Physics*, Institute of Physics, Bristol
Singh, K., Kaur, N., & Saini, N. S. 2017, Phys. Plasmas, 24, 063703
Singh, K., Sethi, P., & Saini, N. S. 2018, Phys. Plasmas, 25, 033705
Singh, K., & Saini, N. S. 2019, Phys. Plasmas, 26, 113702
Sultana, S., Sarri, G., & Kourakis, I. 2012, Phys. Plasmas, 19, 012310
Summers, D. & Thorne, R. M. 1991, Phys. Fluids B: Plasma Phys., 3, 1835
Surko, C. M., Lemvethal, M., Crane, W. S., Passner, A., Wyocki, F. J., Murphy, T. J., Strachan, J.,& Rowan, W. L. 1986, Rev. Sci. Instrum., 57, 1862
Surko, C. M., & Murphy, T. J. 1990, Phys. Fluids B, 2, 1372
Tajima, T., & Taniuti, T. 1990, Phys. Rev. A, 42, 3587
Tandberg-Hansen, E., & Emshie, A. G.1988, *The Physics of Solar Flares*, Cambridge Univ. Press, Cambridge, p.124
Tinkle, M. D., Greaves, R. G., Surko, C. M., Spencer, R. L., & Mason, G. W. 1994, Phys. Rev. Lett., 72, 352
Vasyliunas, V. M. 1968, J. Geophys. Res., 73, 2839, doi:10.1029/ JA073i009p02839
Washimi, H. & Taniuti, T. 1966, Phys. Rev. Lett., 17, 996

BUTI-02

Dynamics of electrostatic waves in a dense relativistic pair plasma

Ridip Sarma

Department of Mathematics, School of Fundamental and Applied Sciences, Assam Don Bosco University, Tapesia, Sonapur-782402, Assam, India.
e-mail: srmridip@gmail.com

The propagation of three-dimensional (3-D) electrostatic solitary and shock waves with weakly relativistic and ultra-relativistic degenerate electrons and positrons is investigated in a dense magnetized plasma. For this purpose, a 3-D Zakharov-Kuznetsov-Burgers (Z-K-B) equation is derived from the pair of ion continuity and momentum equation with bulk viscosity among ion fluids, and degenerate electrons and positrons. The effect of mass of pair of ions, positron concentration, magnetic field strength and the Fermi temperature of weakly relativistic and ultra-relativistic degenerate electrons and positrons are studied in the present work. The Burgers term in our system is responsible for shock structures in pair ion plasmas. Analytical prediction and numerical analysis enable us to know that the wave yields solitary profile in absence of collisions and exhibits both oscillatory and monotonic depending on collisions between pair of ions and balanced status of dissipation and dispersion. Moreover, it is exhibited that the chaotic dynamics occur when the perturbed Z-K-B equation is perturbed by external force, and we use power spectrum, phase projection, and Lyapunov exponents to observe both weak and developed chaos. For illustration purposes, we have considered the astrophysical parameters in a white dwarf.

Keywords: Electrostatic wave; Strongly coupled; Degenerate; Dense plasma; Chaos

I. INTRODUCTION

In the past, remarkable number of researches have focused on the study of matter under extreme conditions [1-6] because of its applications in compact astrophysical objects (like interior of white dwarfs, neutron stars, etc). Compact objects like white dwarfs (whose interior part is like a dense solid, with an ion lattice surrounded by degenerate electrons, and neutron stars, whose interior portion resembles a mixture of interacting nucleons and electrons along with possibly other elementary particles and condensates) support themselves against collapse by cold, degenerate fermion pressure.White dwarfs are extremely interesting objects and at extremely high densities, the degeneracy occurs through the combined effects of Pauli's exclusion principle (fermions) and Heisenberg's uncertainty principle and it depends on number densities of the constituent particles. These extreme conditions/ densities cannot be computed by inter-terrestrial laboratories and these conditions need to be calculated theoretically, and the findings be confirmed by observations of a laboratory. Just after the big bang, temperatures in mega-electron volt prevailed upto one second, during which electron-positron plasmas were among the main constituents of the universe along with some amount of ions [7, 8]. The density and temperature in the core of compact stars like white dwarfs becomes very high and due to gravitational collapse or electromagnetic field, the constituents in the interior may be accelerated to high energy, which collide with each other to produce electrons and positrons in white dwarfs [7,9,10,11]. There are presently 26 white dwarfs which are known to have magnetic fields in the range of 10^6 to 10^9 G [12]. Table 1 gives an idea about the physical quantities of a typical white dwarf [13].

Table 1: Parameters of a typical white dwarf

Object	Mass ($M_\oplus$)	Radius (km)	Mean density (gm cm^{-3})	Mean pressure (dyne cm^{-2})	GM/Rc^2
White Dwarf	$\leq$1.4	~5× 10^3	~10^7	~10^{24}	~10^{-4}

$M_\oplus \equiv 1.989\times10^{33}$gm=One solar mass.
Inside the core of these dense plasmas (typically at high densities ~10^{-34} cm^{-3} and temperature ~10^{7}K)[10, 11, 14, 15, 16], forms a regular ion lattice structure and electrons (positrons) are relativistically degenerate due to less inertia [17,18] in comparison to ions which remains non degenerate due to their heavier mass in a dense electron-positron-ion plasma (e-p-i) plasma. The outer mantle part of white dwarfs constitutes weakly relativistic degenerate electrons (positrons) at densities ~ 10^{26} cm^{-3} together with strongly coupled ions. Correspondingly at high densities, the electrons (positrons) remain weakly relativistic, when the Fermi energy is less than their rest mass energy. The equation of state for weakly relativistic and ultra-relativistic degenerate electrons (positrons) have been formulated by Chandrashekhar [3,4] as P ~ $n_e^{\frac{5}{3}}$ (weakly relativistic) preventing the white dwarf from collapsing under its own gravity and P ~ $n_e^{\frac{4}{3}}$ (ultra-relativistic), where the white dwarf collapses under self gravitational effect into a denser astrophysical object known as neutron star. This shows that the degenerate pressure in dense plasmas is dependent only on number densities, irrespective of temperature [19]. Mahmood *et al.*[20] studied electrostatic waves in a dense unmagnetized plasma with strongly coupled ions and degenerate electrons. Zeba et al. [21] have shown the propagation of nonlinear ion acoustic waves in a dense unmagnetisede-p-i plasmas with ultra-relativistic degenerate electrons and positrons. But the presence of a high magnetic field plays an important role in the characteristics of waves in compact stars. Also, Shukla et al. [22] have investigated the property of localized ion modes in a one-dimensional strongly coupled relativistically degenerate plasma. Therefore, from all these observations above it is found relevant to investigate the influence of strongly coupled pair of ions and magnetic field in the propagation of multidimensional relativistic (both weakly and ultra) degeneracy pressure of electrons and positrons, like representatives of white dwarfs.
The study of shock wave profiles in plasmas have received wide interest both in experimental [23] as well as theoretical [24] investigation, playing important role in astrophysical scenarios like supernova explosions [25], generation of strong fields in the bow shock region [26], and nonlinear dynamics of the solar wind [27]. Anderson *et al.* [28] exhibited the formation of shocks in Q machine experiments. Investigations on electrostatic nonlinear waves, like solitons and shocks in dense plasmas have attracted more attention due to their significance in space as well as laboratory due to the existence of both dissipative and dispersive properties. We exhibited dissipative and dispersive features in our model with the help of Three dimensional ZakharovKuznetsov Burgers equation in a dense magnetized degenerate plasma. The disipative Burgers equation arises due to the inclusion of ion kinematic viscosity among the plasma constituents. If the dissipation is weak at the characteristic dynamic time scales in the system, it can lead to the formation of solitons. Some theoretical developments have justified that strong correlations of ions modify the dispersive characteristics of collective modes as well as the features of nonlinear localized structures like solitary structures or shock structures in strongly coupled degenerate dense plasmas [22,29].
In the past few years, attention has been devoted to chaotic states from the view point of turbulence in nonlinear dispersive waves and statistics of solitons in the non-equilibrium systems [30,31]. Period doubling and Quasi-period doubling sequences are different routes to

the chaos by virtue of external perturbations [32] and the external perturbations exist in many physical situations [33,34]. Chaotic behaviours are quite common among various astrophysical objects [35] and chaotic attractors are searched by analyzing observational data [36,37], numerical data of hydro-dynamical models [38] and also in white dwarfs where amplitudes show variation and complex, non-stationary power spectra [39,40]. The variation in white dwarfs is studied by considering nonlinear effects [41] and period doubling scenario [42]. Divergence of trajectories responsible for the long term unpredictability in stellar medium can be measured by Lyapunov exponents [43] which are probably the most useful indicator of chaotic dynamics. To the best of our knowledge, most of the earlier studies considered the propagation of ion acoustic solitons in an unmagnetised e-p-i plasma only. Therefore, the goal of the present work is to take into consideration pair of ions to interpret low frequency ion acoustic structures (solitons and shocks) as well as ion kinematic viscosity in a dense (white dwarf) magneto-plasma constituting degenerate electrons and degenerate positrons with weakly relativistic and ultra-relativistic effect. Interestingly, the dispersion term in our Three dimensional Zakharov-Kuznetsov Burgers equation arises due to inertia of negative ions, that we have considered. Further, the ion-ion collision in our system gives rise to the dissipation character, i.e the Burgers term exhibiting both oscillatory and monotonic shock profile. Now, since we are studying energy transport both in ultra-relativistic and weakly-relativistic regime, so an extra energy in the form of electromagnetic waves will be produced. This motivated us to include study of different route to chaotic oscillation in our investigation as well.

II. ANALYSIS

a. GOVERNING EQUATIONS:

We have considered the nonlinear propagation of electrostatic waves in a dense magnetized e-p-i plasma. The environment in our model considered is a white dwarf and the external magnetic field $B_0 = B_0\hat{x}$ is assumed to be directed along the $\hat{x}$-axis. We have taken components like inertial multicharged strongly coupled pair of ions and inertialessrelativisticallydegenerate electrons and positrons with weak interparticle interaction. Since the density of ions is very high, so in the case of ions, viscosity effect will come into consideration. The last two terms of both positive and negative ions are known as bulk viscosity. The basic set of generalized hydrodynamic model equations arewritten as follows:

$$\frac{\partial n_i}{\partial t} + (n_i \nabla . v_i) = 0 \tag{1}$$

$$(1+\tau_m \frac{d}{dt})[(\frac{\partial}{\partial t} + v_i.\nabla)v_i + \frac{z_i e}{m_i}\nabla\Phi + \frac{\gamma_i K_B T_{if}}{m_i n_i}\nabla n_i - \frac{z_i e}{m_i}(v_i \times B)] - \frac{\eta}{\rho_i}\frac{\partial^2 v_i}{\partial x^2} - \frac{(\xi + \frac{\eta}{3})}{\rho_i}\nabla(\nabla.v_i) = 0 \tag{2}$$

$$\frac{\partial n_n}{\partial t} + (n_n \nabla . v_n) = 0 \tag{3}$$

$$(1+\tau_m \frac{d}{dt})[(\frac{\partial}{\partial t} + v_n.\nabla)v_n - \frac{z_n e}{m_n}\nabla\Phi + \frac{\gamma_n K_B T_{nf}}{m_n n_n}\nabla n_n + \frac{z_n e}{m_n}(v_n \times B)] - \frac{\eta}{\rho_n}\frac{\partial^2 v_n}{\partial x^2} - \frac{(\xi + \frac{\eta}{3})}{\rho_n}\nabla(\nabla.v_n) = 0 \tag{4}$$

where $\gamma_s, s = i,n$ stands for adiabatic index for positive and negative ions respectively, ρ_s is the mass density for pair of ions and $T_{sf} = T_* + \mu_s T_s$ is the effective pair of ion temperature in which T_* appears due to electrostatic interactions between strongly coupled ions.

Also, $\frac{d}{dt} = (\frac{\partial}{\partial t} + (v_{i,n}).\nabla)$ is the convective derivative for positive and negative ions respectively.

Also, $\nabla \equiv \left(\frac{\partial}{\partial x}, \frac{\partial}{\partial y}, \frac{\partial}{\partial z}\right)$.

The dynamical equations for inertialess degenerate electrons and positrons are as follows:

$$\nabla\Phi = \frac{1}{en_e}\frac{\partial P_{Fe}}{\partial x} \tag{5}$$

$$\nabla\Phi = \frac{1}{en_p}\frac{\partial P_{Fp}}{\partial x} \tag{6}$$

Also, the Poisson's equation is written as

$$\nabla^2\Phi = 4\Pi e(n_e + Z_n n_n - Z_i n_i - Z_p n_p) \tag{7}$$

Here, P_{Fe} and P_{Fp} are the Fermi pressure of degenerate electrons and positrons in nonrelativistic and ultra-relativistic case. In the present model, electrons and positrons gyrate around the magnetic field, but due to their lesser mass as compared to ions,electrons and positrons are more tightly bound to magnetic field lines having high magnetic field strength. Therefore, the three-dimensional motion of pair of ions with degenerate electron and positron is a valid assumption.

Here, n_j, v_j and m_j, respectively denote the number density (with equilibrium value n_{j0}), velocity, and mass of different species (j=e,p,n,i stands for electrons, positrons, negative ions, positive ions respectively), $Z_i$and $Z_p$are the ion and positron charge numbers, e is the charge. In equilibrium, the charge neutrality condition gives $n_{e0} = Z_i n_{i0} + Z_p n_{p0}$. In Eqs. (2) and (4), τ_m is the visco-elastic relaxation time given by [44,45]

$$\tau_m = \frac{\varsigma + 4\eta/3}{n_{s0}k_B T_s}[1 - \gamma_s\mu_s + \frac{4}{15}u(\Gamma_s)]^{-1} \tag{8}$$

Here T_s (s=i,n) is the temperature for positive and negative ion respectively, k_B is the Boltzmann constant, and ($\varsigma + 4\eta/3$) is the coefficient of the effective ion viscosity, where ς and η respectively stands for bulk and shear viscosity. Furthermore, γ_s is the adiabatic index and $u(\Gamma_s)$ is a measure of excess internal energy of pair of ions respectively. Here Γ_s is the ion coupling parameter and for different values of Γ_s of the order of one or larger, correlation effect becomes important and the plasma is then referred as strongly coupled. The expression for $u(\Gamma_s)$ can be written as [46,47]

$$u(\Gamma_s) = \begin{cases} 5 - \frac{\sqrt{3}}{2}\Gamma_s^{3/2}, where(\Gamma_s < 1) \\ -0.90\Gamma_s + 0.95\Gamma_s^{1/4} + 0.18\Gamma_s^{-1/4} - 0.80, where(1 \le \Gamma_s \le 160) \\ 1.5 - 0.90\Gamma_s + 2980\Gamma_s^{-2}, where(160 < \Gamma_s \le 300) \\ 1.5 - 0.90\Gamma_s + 9.6\Gamma_s^{-1} + 840\Gamma_s^{-2} + 1.1\times10^5\Gamma_s^{-3}, where(300 < \Gamma_s \le 2000) \end{cases} \tag{9}$$

The compressibility parameter μ_s appearing in Eq. (8) is given as

$$\mu_s = 1 + \frac{1}{3}u(\Gamma_s) + \frac{\Gamma_s}{9}\frac{\partial u(\Gamma_s)}{\partial\Gamma_s} \tag{10}$$

The parameter for a particle of species j in degenerate state can be defined as

$$\chi_j = \frac{T_{Fj}}{T_j} = \frac{1}{2}(3\Pi^2)^{2/3}(n_j\lambda_{Bj}^3)^{2/3} \tag{11}$$

Here, T_{Fj} is the Fermi temperature, $E_{Fj} = k_B T_{Fj} = \hbar^2(3\Pi^2)^{2/3}/3\Pi^2$ is the Fermi energy and $\lambda_{Bj} = \hbar/\sqrt{k_B T_j m_j}$ is the thermal de Broglie wave-length. Therefore, depending on the thermal energy $k_B T_j$, particles are said to be degenerate if the number density n_j exceeds the quantum concentration $n_{qj} \equiv (2m_j k_B T_j / \hbar^2)^{3/2} / 3\Pi^2$. Typically, we have $n_{e,p} \geq 10^{27}$ cm^{-3} for astrophysical dense plasmas. So, $\chi_{e,p} > 1$ for $T_{e,p} \leq 10^7 K$. So, when electrons and positrons form a degenerate system andpair of ions are classical, the conditions $\chi_{e,p} > 1$ and $\chi_{i,n} < 1$ must be satisfied.

b. **DEGENERATE EQUATION OF STATE**

The energy distribution is governed by the exclusion principle i.e the Fermi energy, which has a pressure associated with it. The equation of state for relativistically degenerate electrons and positrons is given by

$$P_u = \frac{\Pi m_u^4 c^5}{3h^3}[z(2z^2-3)(1+z^2)^{1/2} + 3\sinh^{-1}(z)], (u = e, p) \tag{12}$$

where $p_u = (3h^3 n_u / 8\Pi)^{1/3}$ is the momentum of electrons on the Fermi surface, $h(=2\Pi\hbar)$ is the Planck's constant and $z = \frac{p_u}{m_u c}$ is the nondimensional parameter. Thus, in the weakly relativistic limit $(z << 1)$ and ultrarelativistic limit $(z >> 1)$ the pressure equation (12) can be written in two different forms

$$P_u = \begin{Bmatrix} \frac{1}{5}\frac{\hbar^2}{m_u}(3\Pi^2)^{2/3} n_u^{5/3} = \frac{2}{5} E_{Fu} n_u, for(z << 1) \\ \frac{\hbar c}{4}(3\Pi^2)^{1/3} n_u^{4/3}, for(z >> 1) \end{Bmatrix} \tag{13}$$

These pressures can be combined to write

$$P_u = K_\gamma n_u^\gamma \tag{14}$$

where $K_\gamma = \frac{R_\gamma}{3\gamma}(3\Pi^2 \hbar^3)^{\gamma-1}$ (15)

In equation (15), we have $\gamma = \frac{5}{3} or \frac{4}{3}$. If $\gamma = \frac{5}{3}$ then $R_\gamma = \frac{1}{m_z}$ and if $\gamma = \frac{4}{3}$, then $R_\gamma = c$.

The weakly relativistic pressure equation will no longer be valid when the Fermi energy becomes higher than the rest energy of electrons. In that case we must use the ultra-relativistic equation of state.

Next, we consider the pressure of ions following [48]

$$\nabla P_s = \gamma_s k_B T_{sf} \nabla n_s \tag{16}$$

where $T_{sf} = T_* + \mu_s T_s$ is the effective ion temperature in which T_* is present due to electrostatic interactions between strongly coupled ions given as [49]

$$T_* = \frac{N_{nn}}{12}\Gamma_s T_s (1+\kappa) e^{-\kappa} \tag{17}$$

Here N_{nn} represents the ion structure corresponding to the number of nearest neighbours (e.g., $N_{nn} = 12$ for the fcc and hcp lattices, $N_{nn} = 8$ for the bcc lattice). Typically, for $n_u = 2*10^{26}$ cm^{-3}, $T_u = 40T_s = 10^7 K$ and $Z_s = 8$ (relevant for weakly relativistic regime), we have $\Gamma_s = 202$, $T_* = 2\times10^8$ k, and $\mu_s T_s = -2.4\times10^7$ K. In a similar manner, considering parameters in the ultra-relativistic regime, we find that T_* is always a few orders of magnitude higher than the kinetic temperature of pair of ions.

c. **PARAMETRIC REGIMES FOR WEAKLY RELATIVISTIC AND ULTRA-RELATIVISTIC DEGENERATE ELECTRONS AND POSITRONS**

Our objective is to study the weakly relativistic and ultra-relativistic fully ionized four component plasma in which electrons and positrons are relativistically degenerate with weak interaction and pair of ions composed of pure oxygen O^{16} forming a classical system (non-degenerate) with a strong electrostatic interaction. We consider the application of present study to the white dwarfs developing a deeper insight into the underlying dense plasma physics.

We have considered the magnetic field strength to be 10^8 G, density of electrons and positrons as $10^{26} cm^{-3}$, system thermal temperature as $10^7 K$. The degeneracy condition of electrons and positrons will be valid only when the value of $T_{Fe,Fp}$ is greater than the system thermal temperature T. At the given value of electron density n_{e0} and positron density n_{p0}, say $n_{e0} = n_{p0} = 10^{26} cm^{-3}$, the Fermi temperature of ions, electrons and positrons turn out to be $T_{Fi} = 1.109\times10^5 K$, $T_{Fe} = 1.95\times10^8 K$, and $T_{Fp} = 1.38\times10^8 K$ respectively. Since we can see that the Fermi temperature of ions remain less than the thermal temperature of the system, so ions remain non-degenerate, whereas the electrons and positrons become degenerate. The degeneracy parameter regime corresponding to equation (8) gives us $\chi_e >> 1$ and $\chi_p >> 1$, whereas for ions $\chi_i << 1$. At higher densities, ions are non-ideal and electrons, positrons represent an ideal Fermi gas. Based on the degree of non-ideality of ions, one can consider either a cellular or crystalline structure or an ionic liquid. Therefore, the criterion for ideality or nonideality is defined by the ratio between average potential energy of Coulomb interaction and the mean thermal energy. The coupling parameter of ions is characterized by the relation $\Gamma_s = \frac{e^2}{k_B T d_s}$, where $d_s = \left(\frac{3}{4\Pi n_{s0}}\right)$ is the mean interionic distance. In the case of Oxygen O^{16}, considering the same dense plasma parameters, we have for ions, electrons, and positrons, a set of numerical values of the Coulomb coupling parameter as $\Gamma_j << 1$ $(j=i,n,e,p)$. Therefore, we can assume that the correlation among pair of ions, electrons and positrons in dense plasmas (i.e white dwarf) are ignored and we consider a fluid model for these four different species. The density regimes for weakly relativistic and degenerate (electrons and positrons) is around $10^{26} cm^{-3} < n_{u0} < 10^{29} cm^{-3}$, whereas for ultrarelativistic case, the density regime is well above $10^{30} cm^{-3}$ in the dense plasma [50,51]. Moreover, the viscosity coefficient $C_{vis} \equiv \left(\frac{\rho + \frac{4\eta}{3}}{n_{s0} k_B T_s}\right)$ in equation (8) tends to increase for high coupling parameter Γ_s. Typical values of C_{vis} in our case are roughly ~ 44.

III. NORMALISED SYSTEM AND DERIVATION OF THREE DIMENSIONAL ZAKHAROV-KUZNETSOV-BURGERS EQUATION AND ZAKHAROV-KUZNETSOV EQUATION

We normalize the physical quantities by representing them in terms of new variables $N_j = \frac{n_j}{n_{j0}}$, $V_s = \frac{v_s}{V_T} = (U,V,W)$, $T = t\omega_{ps}$ and $(X,Y,Z) = \frac{(x,y,z)}{\lambda_D}$, where $\lambda_D = \sqrt{\frac{\gamma_s k_B T_{sf}}{4\Pi n_{s0} Z_s^2 e^2}}$ represents the effective Debye length, $V_T = \sqrt{\frac{\gamma_s k_B T_{sf}}{m_s}}$ represents the effective ion thermal speed, and $\omega_{ps} = \frac{V_T}{\lambda_D}$ represents the ion plasma frequency. We then rewrite the basic equations (1) to (7) in the following dimensionless form:

$$\frac{\partial N_i}{\partial T}+\frac{\partial}{\partial X}(N_iV_{ix})+\frac{\partial}{\partial Y}(N_iV_{iy})+\frac{\partial}{\partial Z}(N_iV_{iz})=0 \tag{18}$$

$$\left(1+\overline{\tau_m}\frac{d}{dT}\right)\left(N_i\frac{dV_{ix}}{dT}+D_\gamma N_i\frac{\partial\Phi}{\partial X}+\frac{\partial N_i}{\partial X}-\Omega N_iV_{ix}\right)-\bar{\eta}\frac{\partial^2V_{ix}}{\partial X^2}-\left(\bar{\zeta}+\frac{\bar{\eta}}{3}\right)\frac{\partial^2V_{ix}}{\partial X^2}=0 \tag{19}$$

$$\left(1+\overline{\tau_m}\frac{d}{dT}\right)\left(N_i\frac{dV_{iy}}{dT}+D_\gamma N_i\frac{\partial\Phi}{\partial Y}+\frac{\partial N_i}{\partial Y}-\Omega N_iV_{iy}\right)-\bar{\eta}\frac{\partial^2V_{iy}}{\partial Y^2}-\left(\bar{\zeta}+\frac{\bar{\eta}}{3}\right)\frac{\partial^2V_{iy}}{\partial Y^2}=0 \tag{20}$$

$$\left(1+\overline{\tau_m}\frac{d}{dT}\right)\left(N_i\frac{dV_{iz}}{dT}+D_\gamma N_i\frac{\partial\Phi}{\partial Z}+\frac{\partial N_i}{\partial Z}-\Omega N_iV_{iz}\right)-\bar{\eta}\frac{\partial^2V_{iz}}{\partial Z^2}-\left(\bar{\zeta}+\frac{\bar{\eta}}{3}\right)\frac{\partial^2V_{iz}}{\partial Z^2}=0 \tag{21}$$

Again,

$$\frac{\partial N_n}{\partial T}+\frac{\partial}{\partial X}(N_nV_{nx})+\frac{\partial}{\partial Y}(N_nV_{ny})+\frac{\partial}{\partial Z}(N_nV_{nz})=0 \tag{22}$$

$$\left(1+\overline{\tau_m}\frac{d}{dT}\right)\left(N_n\frac{dV_{nx}}{dT}-D_\gamma N_n\frac{\partial\Phi}{\partial X}+\frac{\partial N_n}{\partial X}+\Omega N_nV_{nx}\right)-\bar{\eta}\frac{\partial^2V_{nx}}{\partial X^2}-\left(\bar{\zeta}+\frac{\bar{\eta}}{3}\right)\frac{\partial^2V_{nx}}{\partial X^2}=0 \tag{23}$$

$$\left(1+\overline{\tau_m}\frac{d}{dT}\right)\left(N_i\frac{dV_{ny}}{dT}-D_\gamma N_n\frac{\partial\Phi}{\partial Y}+\frac{\partial N_n}{\partial Y}+\Omega N_nV_{ny}\right)-\bar{\eta}\frac{\partial^2V_{ny}}{\partial Y^2}-\left(\bar{\zeta}+\frac{\bar{\eta}}{3}\right)\frac{\partial^2V_{ny}}{\partial Y^2}=0 \tag{24}$$

$$\left(1+\overline{\tau_m}\frac{d}{dT}\right)\left(N_n\frac{dV_{nz}}{dT}-D_\gamma N_n\frac{\partial\Phi}{\partial Z}+\frac{\partial N_n}{\partial Z}+\Omega N_nV_{nz}\right)-\bar{\eta}\frac{\partial^2V_{nz}}{\partial Z^2}-\left(\bar{\zeta}+\frac{\bar{\eta}}{3}\right)\frac{\partial^2V_{nz}}{\partial Z^2}=0 \tag{25}$$

Here, $\overline{\tau_m}=\tau_m\omega_{ps}$, $\left(\bar{\eta},\bar{\varsigma}\right)=(\eta,\varsigma)\omega_{ps}/n_{s0}\gamma_sk_BT_{sf}$, $\Omega=\frac{\omega_{cs}}{\sqrt{4\Pi n_{s0}e^2/m_s}}$, where $\omega_{cs}=\frac{eB_0}{m_sc}$ and the constant D_γ is given for weakly relativistic case as $\gamma=\frac{5}{3}$ and for ultra-relativistic case as $\gamma=\frac{4}{3}$ written as

$$D_\gamma=\begin{Bmatrix}\dfrac{Z_sT_{Fu}/\gamma_sT_{sf}}{\gamma_sT_{sf}}(\gamma=\frac{5}{3})\\[2mm] \dfrac{\beta Z_sm_uc^2}{\gamma_sk_BT_{sf}}(\gamma=\frac{4}{3})\end{Bmatrix} \tag{26}$$

where $\beta=\lambda_c(3\Pi^2n_{e0})^{1/3}$ is the dimensionless parameter with $\lambda_c=\hbar/m_uc$ which represents the reduced Compton wavelength.

Equations (5) and (6) can then be integrated to obtain the expression for electron and positron density respectively as

$$N_e=\left(1+\Phi_\gamma\right)^{\frac{1}{\gamma-1}}\approx1+A_\gamma\Phi_\gamma+B_\gamma\Phi_\gamma^2+C_\gamma\Phi_\gamma^3, \tag{27}$$

and $N_p=\left(1+\Phi_\gamma\right)^{\frac{1}{\gamma-1}}\approx1-A_\gamma\Phi_\gamma+B_\gamma\Phi_\gamma^2-C_\gamma\Phi_\gamma^3$ (28)

where $\Phi_\gamma=\begin{Bmatrix}\dfrac{e\Phi}{k_BT_{Fe}}\left(\gamma=\frac{5}{3}\right)\\[2mm] \dfrac{e\Phi}{\beta m_uc^2}\left(\gamma=\frac{4}{3}\right)\end{Bmatrix}$ (29)

The coeffecients appearing in Eqs. (27) and (28) are as follows

$$A_\gamma=\frac{1}{\gamma-1},\quad B_\gamma=\frac{2-\gamma}{2(\gamma-1)^2},\quad C_\gamma=\frac{(2-\gamma)(3-2\gamma)}{6(\gamma-1)^3} \tag{30}$$

and $\frac{\partial^2\Phi_\gamma}{\partial X^2}+\frac{\partial^2\Phi_\gamma}{\partial Y^2}+\frac{\partial^2\Phi_\gamma}{\partial Z^2}=\frac{\mu_eN_e-N_i+\mu_nN_n-\mu_pN_p}{D_\gamma}$, (31)

where $\mu_p=\frac{n_{p0}}{n_{i0}}$, $\mu_e=\frac{n_{e0}}{n_{i0}}$, $\mu_n=\frac{n_{n0}}{n_{i0}}$

Also, $\frac{d}{dT} \equiv \frac{\partial}{\partial T} + V_{sx}\frac{\partial}{\partial X} + V_{sy}\frac{\partial}{\partial Y} + V_{sz}\frac{\partial}{\partial Z}$

Next, we derive the Zakharov-Kuznetsov equation and Zakharov-Kuznetsov Burgers equation using a reductive perturbation method to study the three dimensional (3-D) propagation of a nonlinear electrostatic wave in a magnetized four component dense plasma (white dwarf) with two extreme conditions of weakly relativistic and ultra-relativistic degenerate electrons and positrons. Then in a coordinate frame moving with speed λ, the space and time variables can be stretched as

$\xi = \varepsilon^{1/2}(X - \lambda T)$, $\eta = \varepsilon^{1/2} Y$, $\varsigma = \xi^{1/2} Z$, $\tau = \xi^{1/2} T$. Also, we suppose $\bar{\eta} = \xi^{1/2}\eta_s$, $\bar{\varsigma} = \xi^{1/2}\varsigma_s$, (32)

where ξ is a small parameter representing the strength of the wave amplitude and the perturbed quantities are expanded in a power series of ξ given below

$$V_{sx} = \varepsilon V_{sx1} + \xi^2 V_{sx2} + \ldots\ldots$$

$$N_s = 1 + \varepsilon N_{s1} + \varepsilon^2 N_{s2} + \ldots\ldots\ldots \tag{33}$$

$$V_{sy} = \varepsilon^{3/2} V_{sy1} + \varepsilon^2 V_{sy2} + \varepsilon^{5/2} V_{sy3} + \ldots\ldots\ldots$$

$$V_{sz} = \varepsilon^{3/2} V_{sz1} + \varepsilon^2 V_{sz2} + \varepsilon^{5/2} V_{sz3} + \ldots\ldots\ldots$$

$$\Phi_\gamma = \varepsilon \Phi_{\gamma 1} + \varepsilon^2 \Phi_{\gamma 2} + \ldots\ldots\ldots$$

Using equations (32) and (33) into equations (18) to (25), (27), (28) and (31), and equating coeffecients of first order of ε, and simplifying, we get the dispersion relation as

$$\lambda^2 = 1 + \frac{(1+\mu_n)D_\gamma}{(\mu_p + \mu_e)A_\gamma}$$

Again equating coeffecients of second order of ε from equations (18) to (25), (27), (28) and (31), we get the desired Zakharov-Kuznetsov Burgers equation

$$\frac{\partial \Phi_{\gamma 1}}{\partial \tau} + A\Phi_{\gamma 1}\frac{\partial \Phi_{\gamma 1}}{\partial \xi} + B\frac{\partial^3 \Phi_{\gamma 1}}{\partial \xi^3} + C\frac{\partial}{\partial \xi}\left[\frac{\partial^2 \Phi_{\gamma 1}}{\partial \eta^2} + \frac{\partial^2 \Phi_{\gamma 1}}{\partial \varsigma^2}\right] - D\nabla^2 \Phi_{\gamma 1} = 0, \tag{34}$$

where $A = \frac{1}{p}$, $B = \frac{q}{p}$, $C = \frac{r}{p}$, $D = \frac{s}{p}$.

Here, $p = \frac{2\lambda\mu_n\left(1+\Omega\overline{\tau_m}\right)}{\left(\lambda^2-1\right)\left\{\lambda^2\left(1+\Omega\overline{\tau_m}\right)-1\right\}} + \frac{2\lambda\left(1-\Omega\overline{\tau_m}\right)}{\left(\lambda^2-1\right)\left\{\lambda^2\left(1-\Omega\overline{\tau_m}\right)-1\right\}}$

$$q = \frac{D_\gamma(3\lambda^2 - \lambda^2\Omega\overline{\tau_m} - 1)}{\left(\lambda^2-1\right)^2\left\{\lambda^2\left(1-\Omega\overline{\tau_m}\right)-1\right\}} - \frac{D_\gamma\mu_n(3\lambda^2 + \lambda^2\Omega\overline{\tau_m} - 1)}{\left(\lambda^2-1\right)^2\left\{\lambda^2\left(1+\Omega\overline{\tau_m}\right)-1\right\}} + \frac{2\left(\mu_e - \mu_p\right)B_\gamma}{D_\gamma}$$

$$r = 1 - \frac{\lambda^4\mu_n\left(1+\Omega\overline{\tau_m}\right)}{\Omega^2\left(\lambda^2-1\right)\left\{\lambda^2\left(1+\Omega\overline{\tau_m}\right)-1\right\}} - \frac{\lambda^4(1-\Omega\overline{\tau_m})}{\Omega^2\left(\lambda^2-1\right)\left\{\lambda^2\left(1-\Omega\overline{\tau_m}\right)-1\right\}}$$

$$s = \frac{\lambda(\varsigma_i + \frac{4\eta_i}{3})}{\left(\lambda^2-1\right)\left\{\lambda^2\left(1-\Omega\overline{\tau_m}\right)-1\right\}} + \frac{\lambda(\varsigma_n + \frac{4\eta_n}{3})}{\left(\lambda^2-1\right)\left\{\lambda^2\left(1+\Omega\overline{\tau_m}\right)-1\right\}}$$

If we consider a limiting case when the dispersion is dominant $(D \to 0)$, then Eq. (34) reduces to the well knownThree dimensional Zakharov-Kuznetsov equation

$$\frac{\partial \Phi_{\gamma 1}}{\partial \tau} + A\Phi_{\gamma 1}\frac{\partial \Phi_{\gamma 1}}{\partial \xi} + B\frac{\partial^3 \Phi_{\gamma 1}}{\partial \xi^3} + C\frac{\partial}{\partial \xi}\left[\frac{\partial^2 \Phi_{\gamma 1}}{\partial \eta^2} + \frac{\partial^2 \Phi_{\gamma 1}}{\partial \varsigma^2}\right] \tag{35}$$

IV. SOLITON, SHOCK-WAVE DYNAMICS & ITS STABILITY, CHAOTIC OSCILLATIONS

(a) SOLITON

It can be seen that the dissipative term appears only in the last term of Eq. (34) and for η_{i}, η_{n}, the dissipative term disappears, yielding the formation of solitary pulses only from Three dimensional Zakharov-KuznetsovEquation (35). However, in our system the dissipation term is present and the particle suffers loss of energy and thus leads to the formation of shock. Thus, we observe that the dissipative coefficient in (34) plays an important role to change the profile of nonlinear structure from soliton to shock and vice versa.

Now, to obtain the solution of eq. (34), we introduce the transformation

$$\chi = l\xi + m\eta + n\zeta - U\tau \,, \tag{36}$$

where l, m and n are the direction cosines between the wave propagation vector k with X, Y and Z axes respectively, U is the velocity of the moving frame. Let $\Phi(\chi) = \Phi_{\gamma 1}(\xi, \eta, \zeta, \tau)$, then eq. (34) takes the form of an ordinary differential equation as follows:

$$-U\frac{d\Phi}{d\chi} + Al\Phi\frac{d\Phi}{d\chi} + lF\frac{d^3\Phi}{d\chi^3} - D\frac{d^2\Phi}{d\chi^2} = 0 \tag{37}$$

where $F = B_{\gamma}l^2 + C_{\gamma}\left(m^2 + n^2\right)$.

Now, Eq. (34) reduces to a well knownZakharov-Kuznetsov equation (35)when the dispersion term vanishes (i.e $D \to 0$), to obtain the solitary wave solution $\Phi = \Phi_0 Sech^2\left(\frac{\chi}{\delta}\right)$,

where the maximum amplitude Φ_0 and the width δ of the solitary waves are given, respectively, by $\Phi_0 = \frac{3U}{Al}$ and $\delta = 2\left(\frac{lF}{U}\right)^{\frac{1}{2}}$

(b) SHOCK WAVE

Next, we will obtain the exact solution of Eq. (34) involving both dissipative and dispersion terms known as the Zakharov-Kuznetsov-Burgers (Z-K-B) equation. Here we use the hyperbolic tangent (Tanh) method [52] for finding the travelling wave solution of the nonlinear evolution equation. Following the method, we introduce a new independent variable $W = \tanh(\rho\chi)$ to (34), to obtain

$$-U\rho\left(1-W^2\right)\frac{d\Phi}{dW} + Al\rho\left(1-W^2\right)\Phi\frac{d\Phi}{dW} + Fl\rho^3(1-W^2)\times\frac{d}{dW}\left\{(1-W^2)\frac{d}{dW}[(1-W^2)\frac{d}{dW}]\right\} - D\rho^2(1-W^2)\frac{d}{dW}[(1-W^2)\frac{d}{dW}] = 0 \tag{38}$$

Let the solution of (38) be a series of the form $\Phi(W) = \sum_{r=0}^{2} a_r W^r$ (39)

Using (39) into (38), we get

$$a_0 = \frac{9}{25}\frac{D^2}{FAl^2}\,,\ a_1 = \mp\frac{6}{25}\frac{D^2}{FAl}\,,\ a_2 = -\frac{3}{25}\frac{D^2}{FAl^2}\,,\ \rho = \pm\frac{D}{10Fl}\,, U = \frac{6D^2}{25Fl} \tag{40}$$

Therefore, (39) can be written as

$$\Phi(\chi) = \frac{3}{25}\frac{D_{\gamma}^2}{FAl^2}\left[2 - 2\tanh\left(\frac{D_{\gamma}}{10Fl}\chi\right) + \sec h^2\left(\frac{D_{\gamma}}{10Fl}\chi\right)\right] \tag{41}$$

(c) STABILITY

To study the stability of a travelling wave solution in our dense magnetized plasma model, we apply the technique as in Reference [53] to the Eq. (37) and obtain two singular points (0,0) and (2(U-D)/A,0). Here, (0,0) represents the equilibrium downstream state and is a saddle point, whereas (2(U-D)/A,0) represents asymptotic behaviour of the solution of the form ~ $\exp(p\chi)$ with p given as

$$p=\frac{C}{2F}[1\pm\sqrt{1-\frac{4B}{C^2}(U-D)}] \tag{42}$$

The singular point $(2(U-D)/A,0)$ is a stable focus or stable node according as $C^2 \lessgtr 4F(U-D)$, wherethe stable focus represents oscillatory nature and stable node represents the monotonic nature of the solution.

(d) CHAOS IN PERTURBED SYSTEM

Chaotic behaviour of the perturbed system are of certain interest from the view point of turbulence in the non-equilibrium systems [54,55]. Different route to the chaos by virtue of external perturbations [56] exist in physical situations described by (i) bifurcation diagram (ii) the Largest Lyapunov Exponent (LPE) (iii) Quasi-periodic motion and Phase Plane plots, etc

Now we will consider the effects of external perturbations on Zakharov-Kuznetsov-Burgers equation i.e eq. (34) as

$$\Phi_{\gamma\tau}+A\Phi_{\gamma}\Phi_{\gamma\xi}+B\Phi_{\gamma\xi\xi\xi}+C(\Phi_{\gamma\varsigma\varsigma\xi}+\Phi_{\gamma\xi\eta\eta})-D\Phi_{\gamma\xi\xi}=g_{\xi}, \tag{43}$$

where g is a periodic function of ξ and represents the external perturbation. Here, D is a damping parameter, g is the forcing term and A, B, C are real parameters. Here, $g=1+\varepsilon g_1+\varepsilon^2 g_2+........$ where $g_k{}'s(k=1,2,3,....)$ real functions and t are a real constant to be determined. Let $\Phi(\xi,\eta,\varsigma,\tau)=\varphi(\alpha)$, then following [57,58], we obtain

$$\varphi_{\alpha\alpha}+l_1\varphi_{\alpha}+l_2\varphi+l_3\varphi^2=g_1\cos(t\alpha), \tag{44}$$

Then, using [59-61], system (44) can be written as the autonomous system of a three dimensional plane

$$X_{\alpha}=Y,\ Y_{\alpha}=-l_1Y-l_2X-l_3X^2+g_1\sin(Z),\ Z_{\alpha}=t \tag{45}$$

The system (45) describes the case in which eq. (34) is perturbed by the external forcing term $g_1\sin(Z)$. In the system (45), $|g_1|$ represents the strength of the external forcing term and $|l_1|$ represents damping coefficient. Here we will analyse the numerical results of system (45) to demonstrate two kinds of chaotic oscillation i.e weak chaos and developed chaos through Quasi-periodic behaviour and Lyapunov exponent process.

iv. PARAMETRIC STUDY AND NUMERICAL ANALYSIS RESULTS & DISCUSSIONS

For degenerate electrons and positrons, the weakly relativistic condition is valid, only if their Fermi energy is much less than the rest mass energy of the species, i.e., $k_BT_{Fu}<<m_uc^2$. The Fermi energies for degenerate electrons and positrons in the considered dense plasma is found to be $k_BT_{Fe}=2.7\times10^{-8}$ erg and $k_BT_{Fp}=1.91\times10^{-8}erg$, respectively, which are much less than their rest mass energies, which comes out to be $m_uc^2=8.12\times10^{-7}erg$. The values of the remaining parameters are $n_{e0}=n_{p0}=10^{28}cm^{-3}$, $B_0=10^9G$, $\omega_{pi}=8.488\times10^{16}s^{-1}$, $\omega_{pe}=5.6308\times10^{18}s^{-1}$, $\omega_{pp}=4.2967\times10^{18}s^{-1}$, respectively. The Fermi lengths for electrons and positrons are $\lambda_{Fe}=2.21\times10^{-9}cm$, $\lambda_{Fp}=1.82\times10^{-9}cm$ respectively and the ion gyro-radius at electron Fermi temperature is $\delta_s=C_s/\Omega_i=1.83\times10^{-5}cm>\lambda_{Fu}$. These values show that our consideration of fluid model in a magnetized dense plasma is valid.

Similarly, degeneracy of electrons and positrons holds in ultra-relativistic case, only if their Fermi energy is much greater than the rest mass energy of the species, i.e., $k_BT_{Fu}>>m_uc^2$. The Fermi energies for degenerate electrons and positrons in the considered dense plasma is found to be $k_B T_{Fe} = 4.613\times10^{-6}$ erg and $k_B T_{Fp} = 3.7996\times10^{-6} erg$, respectively, which are much greater than their rest mass energies, which comes out to be $m_u c^2 = 8.12\times10^{-7} erg$. The values of the remaining parameters are $n_{e0} = n_{p0} = 10^{34} cm^{-3}$, $B_0 = 10^{12} G$, $\omega_{pi} = 8.488\times10^{20} s^{-1}$, $\omega_{pe} = 5.6308\times10^{22} s^{-1}$, $\omega_{pp} = 4.2967\times10^{22} s^{-1}$, respectively. The Fermi lengths for electrons and positrons are $\lambda_{Fe} = 2.21\times10^{-11} cm$, $\lambda_{Fp} = 1.82\times10^{-11} cm$ respectively and the ion gyro-radius at electron Fermi temperature is $\delta_s = C_s/\Omega_i = 1.57\times10^{-9} cm > \lambda_{Fu}$. These values show that our consideration of fluid model in a magnetizedultra-dense plasma is valid.

The collective effects in electron-positron plasmas can be studied if the electron-positron time scale is much longer than the electron-positron plasma effects, which is typically inverse of the plasma frequency. In the present regime, the processes of creation and annihilation of electron-positron pairs become important. Before studying the nonlinear properties of the electron-positron plasma, it is necessary to have a look at the electron-positron pair annihilation time. Based on the theory of Svensson [62] concerning the electron-positron pair equilibria in beam plasma, to neglect the annihilation effect, the following inequality must be satisfied

$$\omega_{pu}^{-1} \ll \tau_{ann}, \qquad (46)$$

whereω_{pu}^{-1} is the inverse of the plasma frequency equal to $\sqrt{\frac{4\pi e^2 n_{u0}}{m}}$ and τ_{ann} is the annihilation time. The annihilation time τ_{ann} in the present model can be expressed by the following relation

$$\tau_{ann} = \frac{4}{3}\frac{1}{n_u \sigma_\tau c}\left(\frac{E_{Th}^2}{\frac{1}{4}+ln(2\aleph E_{Th}+1)}\right) \text{for} E_{Th} \gg 1\,, \qquad (47)$$

where σ_τ($6.65\times10^{-25}\text{cm}^2$) is the electron Thomson cross section, and E_{Th} $\left(\frac{k_B T_j}{m_u c^2}\right)$ the normalised thermal energy. Also, $\aleph = e^{-\aleph_E} \equiv 0.5615$ with $\aleph_E (\approx 0.5772)$ is the Euler's constant.Combining Eqs. (45) and (46) and using $n_{e0} = n_{p0} = n_0$, the pair annihilation condition becomes $\left(\frac{E_{Th}^2}{\frac{1}{4}+ln(2\aleph E_{Th}+1)}\right) \gg 2.6\times10^{-19} n_0^{\frac{1}{2}}$. (48)

For some illustration purpose,we have chosen the number density value for weakly relativistic case as$n_0 = 5\times10^{28} cm^{-3}$, that is typically found in dense plasma (viz. outermost mantle of white dwarf region). On using the number density value into Eq. (48), one can obtain 0.229003 >>2.6×10^{-5}, which indicates that the electron-positron pair annihilation can be ignored in our plasma model equations (1)-(7).

Similarly, if we chose the number density value for ultra-relativistic case as $n_0 = 5\times10^{34} cm^{-3}$, that is typically found in dense plasma (viz. core of massive white dwarf region). On using the number density value into Eq. (48), one can obtain 0.229003 >>2.6×10^{-2}, which again indicates that the electron-positron pair annihilation can be ignored in our plasma model equations (1)-(7).

(a) SOLITARY WAVE PROFILE

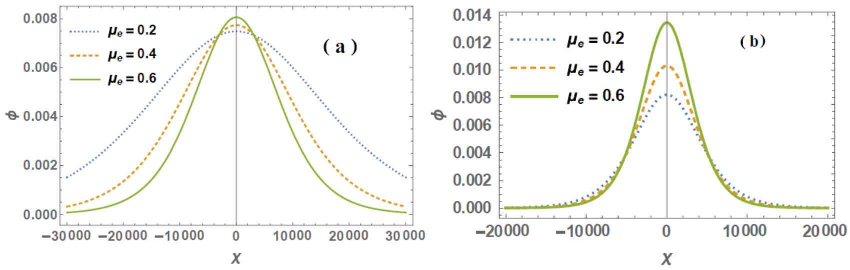

Fig. 1. The Ion Acoustic solitonwaves from Equation (35) are plotted by varying electron concentration $\mu_e = 0.2$ (dotted curve), $\mu_e = 0.4$ (dashed curve) and $\mu_e = 0.6$ (solid curve) at $n_{e0} = 10^{28}$ cm^{-3}, $B_0 = 10^{12}$ G, in (a) weakly relativistic and $n_{e0} = 10^{34}$ in a (b) ultra-relativistic dense magnetized plasma

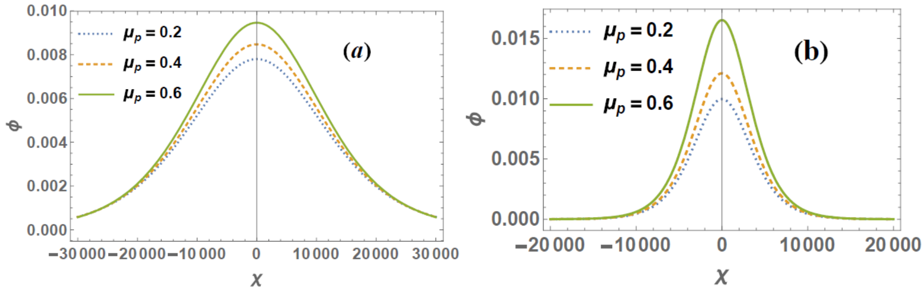

Fig. 2. The Ion Acoustic soliton waves from Equation (35) are plotted by varying positron concentration $\mu_p = 0.2$ (dotted curve), $\mu_p = 0.4$ (dashed curve) and $\mu_p = 0.6$ (solid curve) at $n_{e0} = 10^{28}$ cm^{-3}, $B_0 = 10^{12}$ G, in (a) weakly relativistic and $n_{e0} = 10^{34}$ in a (b) ultra-relativistic dense magnetized plasma.

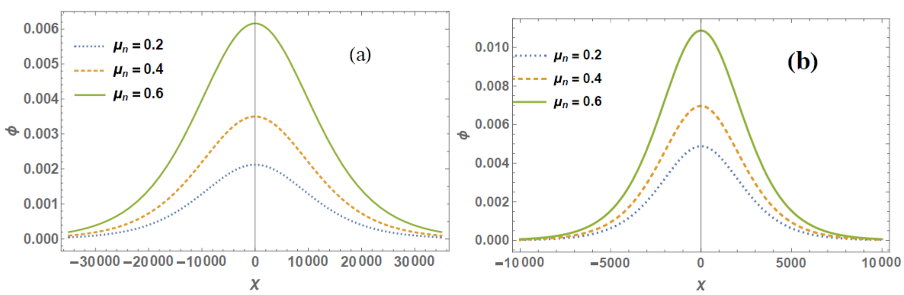

Fig.3. The Ion Acoustic soliton waves from Equation (35) are plotted by varying negative ion concentration $\mu_n = 0.2$ (dotted curve), $\mu_n = 0.4$ (dashed curve) and $\mu_n = 0.6$ (solid curve) at $n_{e0} = 10^{28}$ cm^{-3}, $B_0 = 10^{12}$ G, in (a) weakly relativistic and $n_{e0} = 10^{34}$ in a (b) ultra-relativistic dense magnetized plasma.

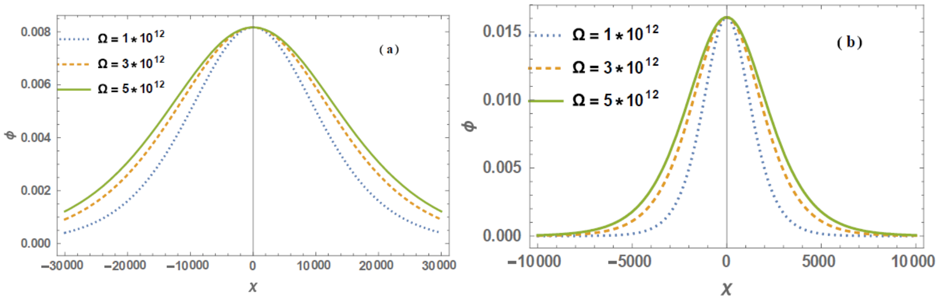

Fig.4. The Ion Acoustic soliton waves from Equation (35) are plotted by varying magnetic field strength $\Omega = 1\times10^{12}$ (dotted curve), $\Omega = 3*10^{12}$ (dashed curve) and $\Omega = 5*10^{12}$ (solid curve) at $n_{e0} = 10^{28}$ cm^{-3}, $\mu_e = 0.5$, $\mu_p = 0.5$, $\mu_n = 0.5$ in (a) weakly relativistic and $n_{e0} = 10^{34}$ in a (b) ultra-relativistic dense magnetized plasma.

(b) SHOCK WAVE PROFILE

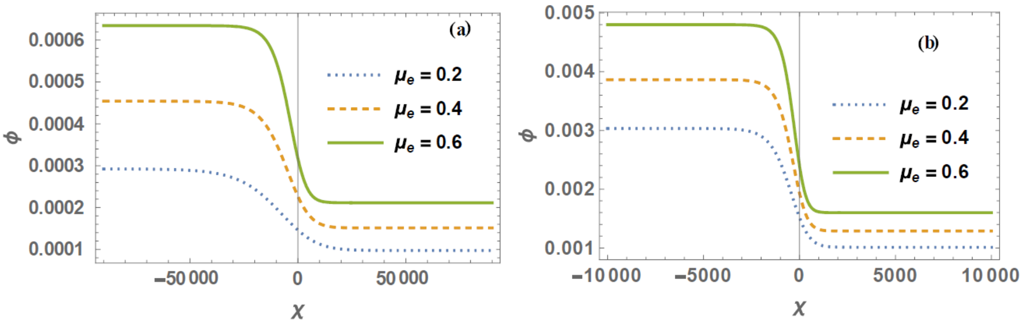

Fig. 5. The Ion Acoustic shock wave from Equation (34) are plotted by varying electron concentration $\mu_e = 0.2$ (dotted curve), $\mu_e = 0.4$ (dashed curve) and $\mu_e = 0.6$ (solid curve) at $n_{e0} = 10^{28}$ cm^{-3}, $B_0 = 10^{12}$ G, in (a) weakly relativistic and $n_{e0} = 10^{34}$ in a (b) ultra-relativistic dense magnetized plasma.

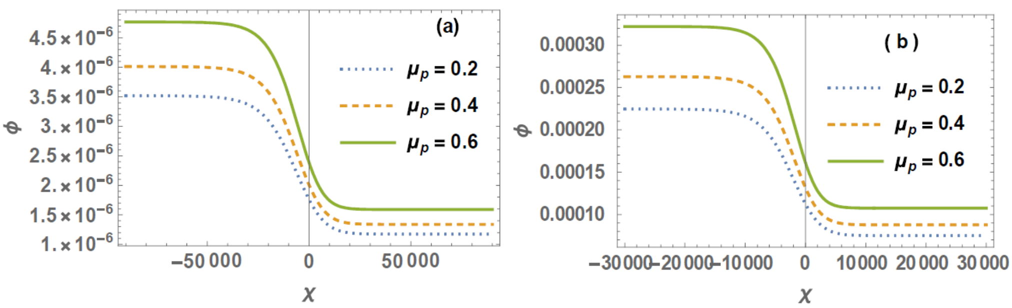

Fig. 6. The Ion Acoustic shock wave from Equation (34) are plotted by varying positron concentration $\mu_p = 0.2$ (dotted curve), $\mu_p = 0.4$ (dashed curve) and $\mu_p = 0.6$ (solid curve) at $n_{e0} = 10^{28}$ cm^{-3}, $B_0 = 10^{12}$ G, in (a) weakly relativistic and $n_{e0} = 10^{34}$ in a (b) ultra-relativistic dense magnetized plasma.

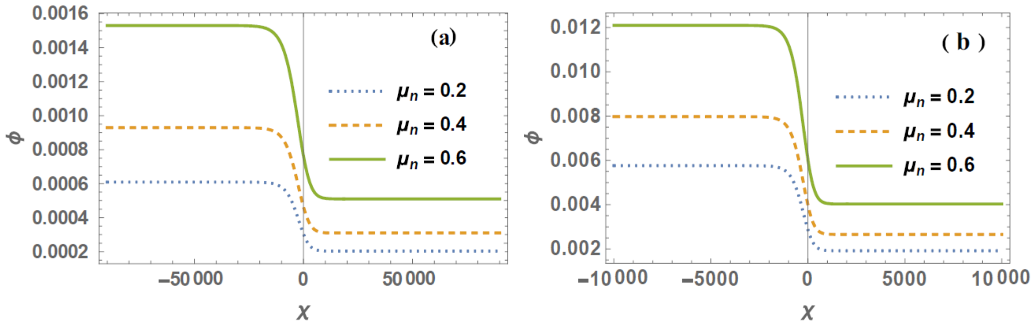

Fig.7. The Ion Acoustic shock wave from Equation (34) are plotted by varying negative ion concentration $\mu_n = 0.2$ (dotted curve), $\mu_n = 0.4$ (dashed curve) and $\mu_n = 0.6$ (solid curve) at $n_{e0} = 10^{28}$ cm^{-3}, $B_0 = 10^{12}$ G, in (a) weakly relativistic and $n_{e0} = 10^{34}$ in a (b) ultra-relativistic dense magnetized plasma.

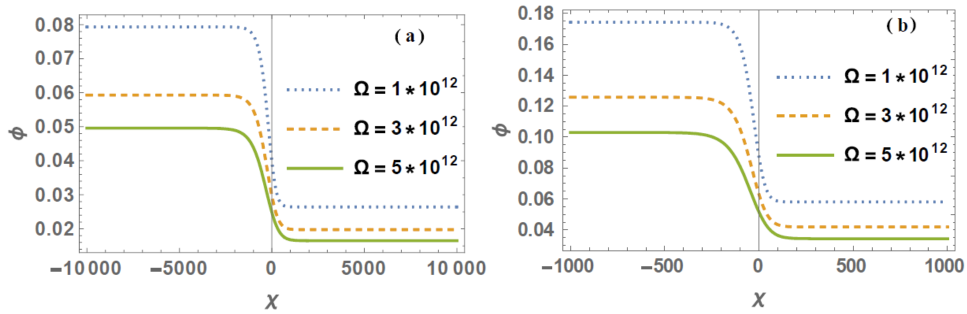

Fig8. The Ion Acoustic shock wave from Equation (34) are plotted by varying magnetic field strength $\Omega = 1*10^{12}$ (dotted curve), $\Omega = 3*10^{12}$ (dashed curve) and $\Omega = 5*10^{12}$ (solid curve) at $n_{e0} = 10^{28}$ cm^{-3}, $\mu_e = 0.5$, $\mu_p = 0.5$, $\mu_n = 0.5$ in (a) weakly relativisticand $n_{e0} = 10^{34}$ cm^{-3} in a (b) ultra-relativistic dense magnetized plasma.

(c) OSCILLATORY AND MONOTONIC NATURE OF ION ACOUSTIC SHOCK WAVE AND ITS STABILITY

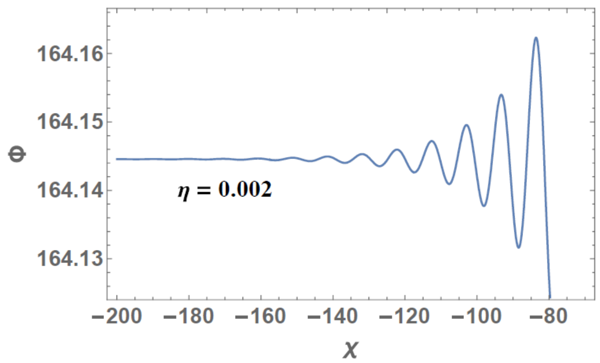

Fig 9(a).Numerical solution of Eq. (34) is plotted against χ to show the profile of transition of Oscillatory to montonicshock wave for $\eta =$ 0.002.

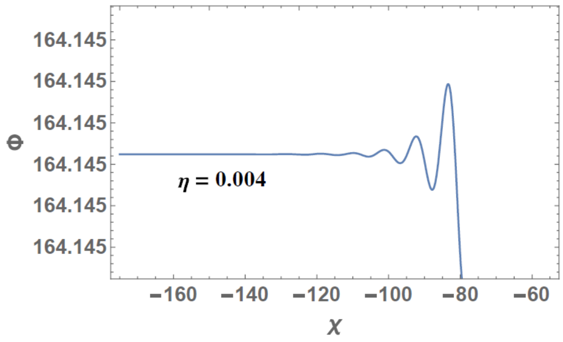

Fig 9(b).Numerical solution of Eq. (34) is plotted against χ to show the profile of transition of Oscillatory to montonicshock wave for $\eta =$ 0.004.

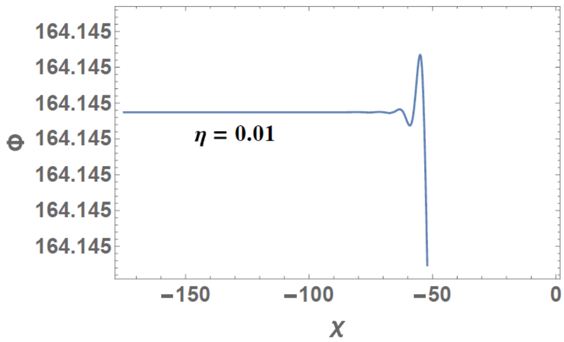

Fig 9(c).Numerical solution of Eq. (34) is plotted against χ to show the profile of transition of Oscillatory to montonicshock wave for $\eta =$ 0.01.

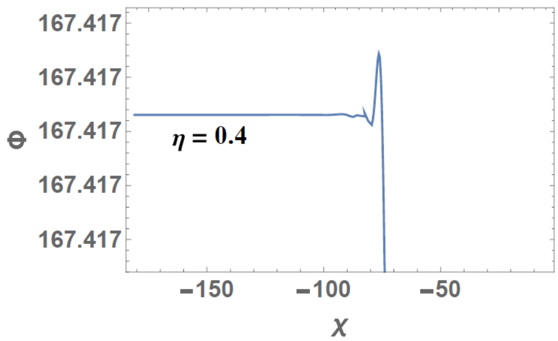

Fig 9(d). Numerical solution of Eq. (34) is plotted against χ to show the profile of transition of Oscillatory to montonic shock wave for $\eta =$ 0.2.

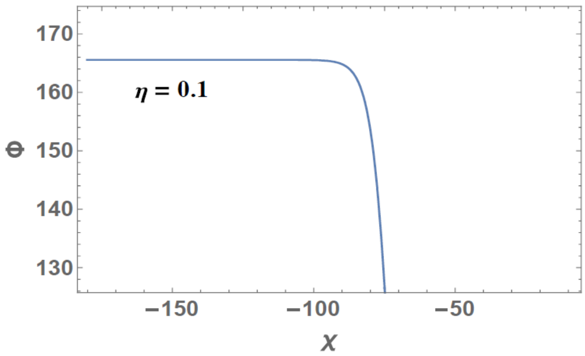

Fig 9(e). Numerical solution of Eq. (34) is plotted against χ to show the profile of transition of Oscillatory to montonic shock wave for $\eta =$ 0.1 .

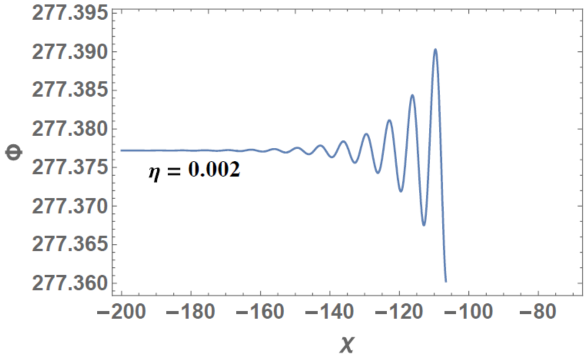

Fig 10(a). Numerical solution of Eq. (37) using condition (41) is plotted against χ to show the profile of transition of Oscillatory to montonic shock wave for $\eta = 0.002$.

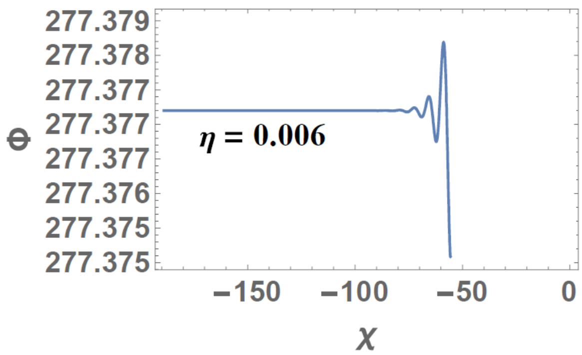

Fig 10(b). Numerical solution of Eq. (37) using condition (41) is plotted against χ to show the profile of transition of Oscillatory to montonic shock wave for $\eta = 0.006$.

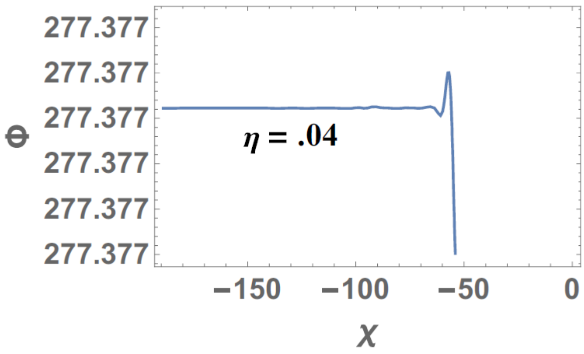

Fig 10(c). Numerical solution of Eq. (37) using condition (41) is plotted against χ to show the profile of transition of Oscillatory to montonic shock wave for $\eta = 0.04$.

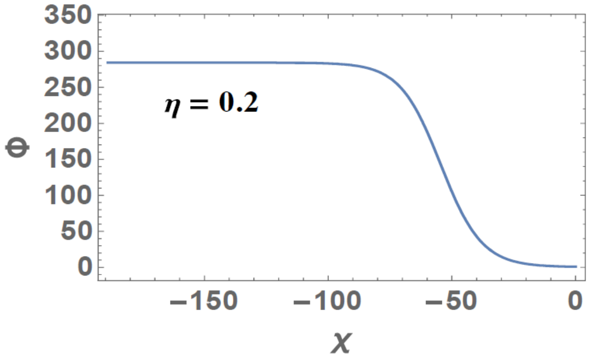

Fig 10(d). Numerical solution of Eq. (37) using condition (41) is plotted against χ to show the profile of transition of Oscillatory to montonic shock wave for $\eta = 0.2$.

(d) PHASE PHASE ANALYSIS AND SPECTRAL ANALYSIS OF CHAOTIC MOTION

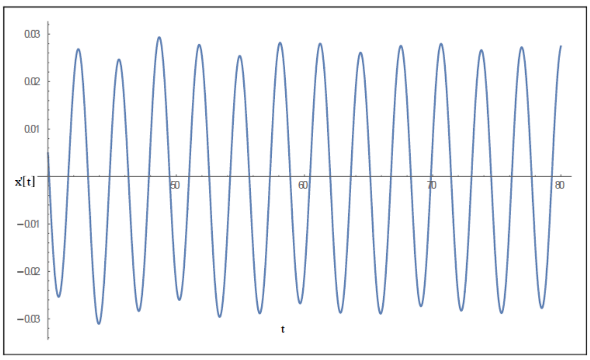

Fig. 11. Evolution of Y of system (45) with l_1=0.2, l_2=0.37, l_3=0.34.

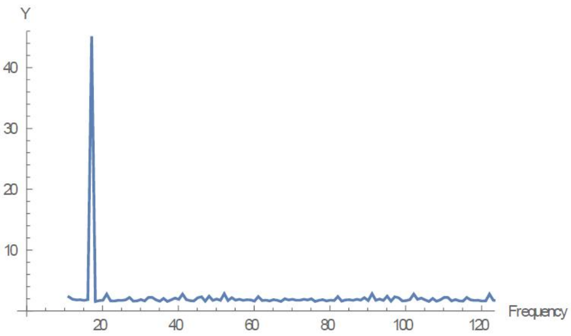

Fig. 12. Power spectra of the solutions in a dense plasma produced by System (45). Parameters are $\tau = 0.54$,(a) $l_1 = 1.5, l_2 = 0.3, l_3 = 0.5$, and $g_1 = 0.04$

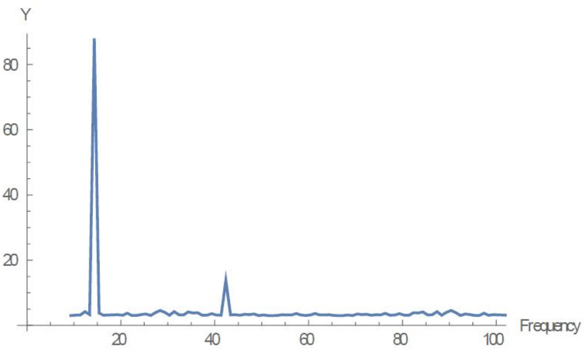

Fig.13(a). Power spectra of the solutions in a dense plasma produced by System (45). Parameters are $\tau = 0.54$, (a) $l_1 = 0.9, l_2 = 0.22, l_3 = 0.35$, and $g_1 = 0.08$

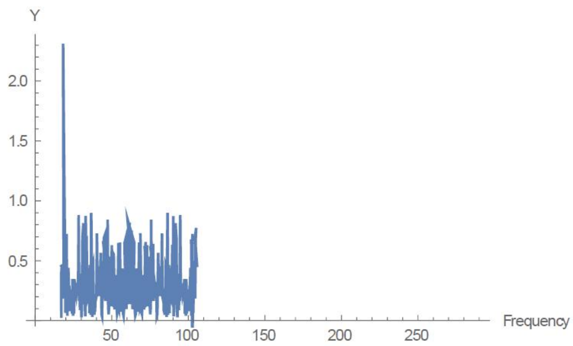

Fig. 13(b).Power spectra of the solutions produced by System (45). Parameters are $\tau = 0.54$, (a) $l_1 = 0.9, l_2 = 0.22, l_3 = 0.35$, and $g_1 = 0.9$

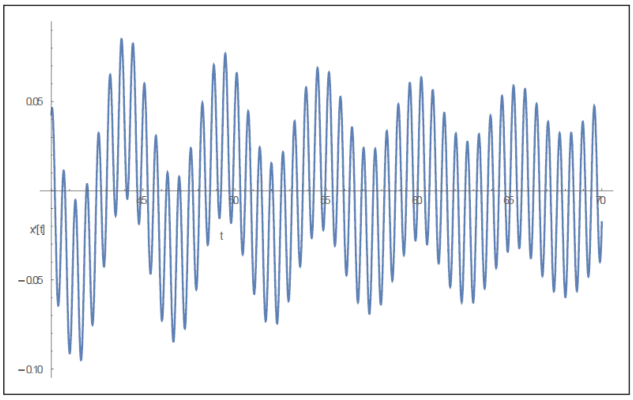

Fig. 14 (a).Quasiperiodicity representation of x'[t] along with time t based on system (45) for the case of Fig. 13(a).

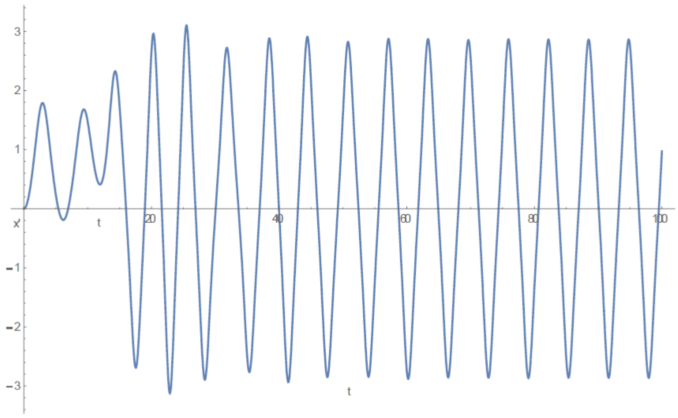

Fig.14 (b).Quasiperiodicity representation of x'[t] along with time t based on system (45) for the case of Fig. 13(b).

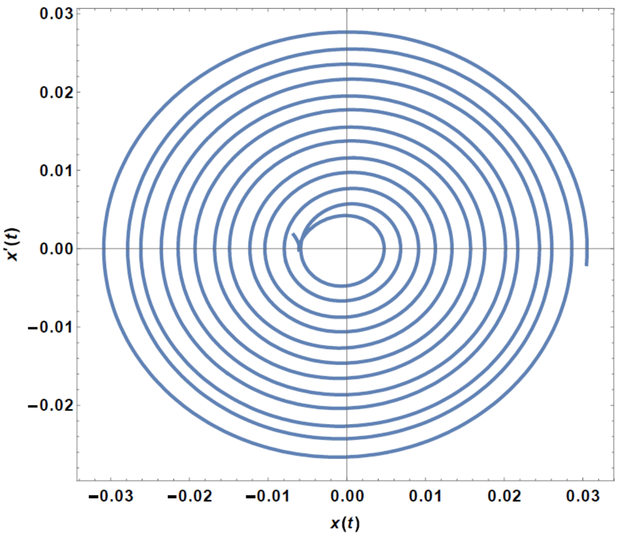

Fig.15. Phase projection of system (45), with respect to time evolution t=10 to t=100.

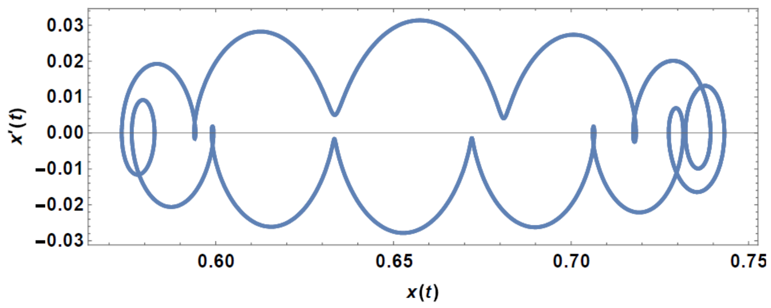

Fig. 16(a). Phase projection of system (45) exhibiting chaotic motion, with respect to time evolution t=0.1 to t=50.

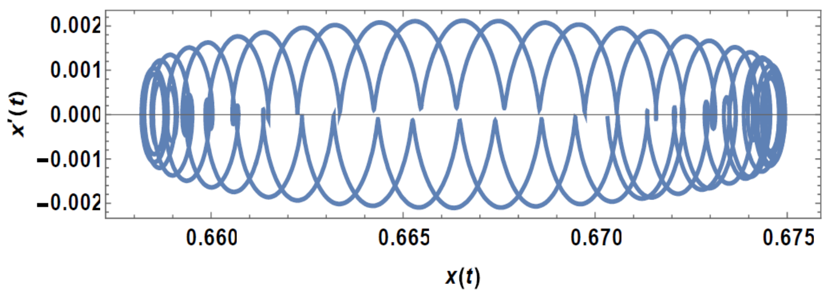

Fig. 16(b). Phase projection of system (45) exhibiting chaotic motion, with respect to time evolution t=0.1 to t=200.

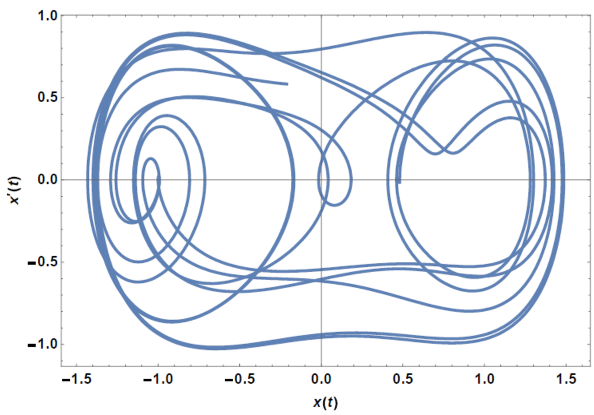

Fig. 17(a). Phase projection of system (45) exhibiting chaotic motion, with respect to time evolution t=1 to t=20.

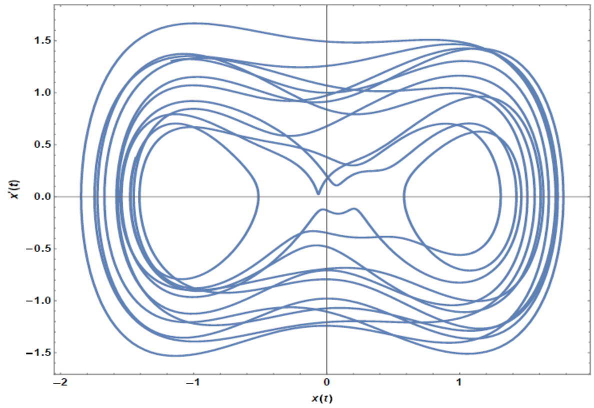

Fig. 17(b). Phase projection of system (45) exhibiting chaotic motion, with respect to time evolution t=1 to t=100.

(e) LYAPUNOV ANALYSIS

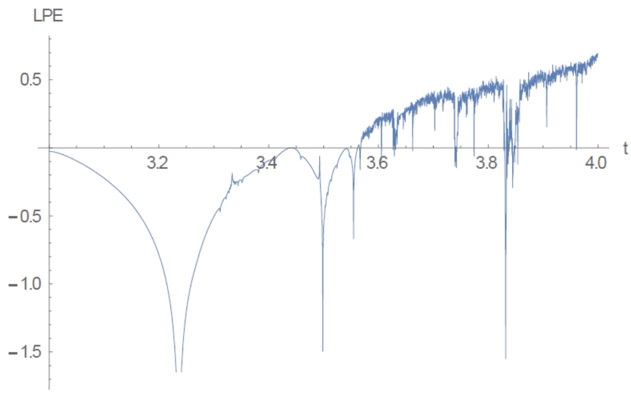

Fig. 18(a).Lyapunov exponents representing weak chaos where $\tau = 0.54$, (a) $l_1 = 1.3, l_2 = 0.3, l_3 = 0.5$, and $g_1 = 0.03$

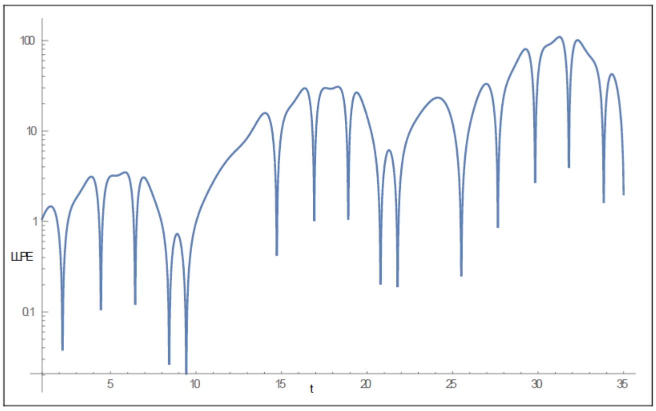

Fig. 18(b). Largest Lyapunov exponents representing developed chaos where $\tau = 0.54$, (a) $l_1 = 1.3, l_2 = 0.3, l_3 = 0.5$, and $g_1 = 0.9$

In this manuscript we investigate the nature of solitary structure, shock like wave structure, oscillatory shock wave profile, and exploring chaotic behaviour for the perturbed (43) through quasi-periodic analysis, phase plane analysis and Lyapunov exponents in a degenerate dense plasma. It is important to understand that solitons exist because of the balance between nonlinearity and dispersion, while the dissipative effect is very weak or negligible whereas one encounters shock wave like profile when the dissipative effect is very weak or negligible whereas one encounters shock wave like profile when the dissipative effect is significant than the dispersion. Thus we have two special cases

Case 1: When the dissipative effect is negligible i.e the frictional force is absent and we put D=0 in Eq. (34). Then from Eq. (34) we get a Three dimensional ZakharovKuznetsov Eq. (35), through which we can plot soliton structure of an Ion acoustic wave with dense astrophysical parameters in a weakly relativistic and ultra-relativistic case.

Case 2:Another case is if $D \neq 0$, then we obtain a three dimensional ZakharovKuznetsov Burgers Eq. (34), through which we get an exact solution (41), which consists of contribution from both dispersive and dissipative effects, which in turn influencing the shape of the wave potential. In this special solution (41), we have covered entire ranges of plasma parameters i.e shock pulse polarity is positive because the amplitude coefficient is independent of the intrinsic plasma parameter values. Similarly we have found that A cannot have negative values or either vanish for all possible parameter values in a weakly relativistic and ultra-relativistic case in a dense plasma.

However solution (41) has some limitations as it is valid in case of special constraints [63]. Interestingly, this constraint feature is such that the shock structure prevails over solitary oscillations. Therefore, we intend to study the stability character of Eq. (37) using asymptotic behaviour of the solution of the form $\sim \exp(p\chi)$ with p given as Eq. (42), through exact numerical simulation. This study will help us to understand the shock wave transition in a dense magnetized plasma better. Further, since the interior core of a dense magnetized plasma in an ultra-relativistic regime possesses very high density and temperature ranges, there is every possibility of existence of high energy density than the surface of dense plasma in a weakly relativistic regime. So, there may be a fast energy transportation from interior to exterior of dense stars leading to some chaotic behaviour. This prompted us to include chaotic motion investigation of the three dimensional ZakharovKuznetsov Burgers equation (34) in a dense magnetized plasma under harmonic excitation in a numerical simulation.

Now, in this section, we plot numerically different cases of non-relativistic and ultra-relativistic degenerate dense electron-positron-ion plasmas that can exist in a white dwarf. The range of density for a plasma to be in the nonrelativistic and degenerate (electrons and positrons) regime is around $10^{26} cm^{-3} < n_{i0} < 10^{29} cm^{-3}$, whereas for a plasma to be in the ultra-relativistic regime, the densities should be well above $10^{30} cm^{-3}$ [50,51].It can be observed in Figs 1, 2 and 3 that with increase of electron, positron and negative ion concentration, the potential rises both in nonrelativistic and ultra-relativistic case. This may be due to the fact that the potential strength increases due to addition of electrons, positrons, and negative ions, which also enhances the total Fermi pressure in ultra dense white dwarfs.In Fig. 4, both for (a) nonrelativistic and (b) ultra-relativistic , it can be seen that with increase of magnetic field strength, there is no effect on the amplitude of the solitary waves, but on the other hand the width of the solitary wave potential gets enhanced. This is due to the fact that due to increase in degenerate electron and degenerate positron population, it reflects more particles and the solitary wave is damped faster using all its energy due to the reflection. Also with a high magnetic field strength the wave becomes less dispersive. This is because of the confinement of plasma species with such high magnetic field strength leads the wave motion to get diverted in a direction which causes the wave to become less dispersive whereas the amplitude doesn’t change. Figs 5, 6 and 7 shows that the shock strength in both nonrelativistic and ultra-relativistic case increases with the increase in electron concentration, positron concentration and negative ion concentration inertial force to derive magnetosonic waves in dense epi plasma. More the positron, electron and negative ion concentration as depicted in Figs. 5, 6 and 7 respectively, the more is the intensity of the energy carried forward by these particles in the form of electrostatic waves through collision. It will excite a low frequency Ion Acoustic wave, thereby increasing Ion Acoustic wave fluctuations and interacting nonlinearly with the resonant plasma wave. When there is a perfect balance between nonlinearity, dispersion and dissipation, Ion acoustic wave potential profile evolves with increasing concentration of positron, electron and negative ions.Fig 8 shows that the shock wave slows down in the plasma under the impact of strong magnetic field strength. Here we observe that the plasma becomes more dispersive when a high magnetic field strength is introduced in the system leading to enhancement of shock structure, width and reduction of amplitude for all three kinds of perturbing shock pulses.

Next, we numerically simulate the nonlinear propagation of Three dimensional ZakharovKuznetsov Burgers equation of the form (38) in the moving frame, investigating various plasma parameters in dense magnetized plasma. We plot the behaviour of shock for different values of damping parameter (η) or viscosity $(\eta = 0.002 \; to \; \eta = 0.1)$ in Figs. 9(a) to 9(e). Here we find that the influence of the damping parameter η varies the behaviour of shock profile, a transition from oscillatory shock to montonic shock front. When is very small, i.e. $\eta = 0.002$ in Fig. 9(a), the shock wave display a train of oscillations at the front of a shock. This is due to the dispersive effect dominating over the dissipative effect. However with the gradual increase of viscosity η as seen in Figs. 9(b) to 9(e), the dissipation effect is in balance with the dispersive parameter, the oscillatory shock wave decreases and completely disappears at a very high $\eta = 0.1$, leaving only the monotonic shock front. Tese observations from our model are worth interesting as the features are interpreted from a three dimensional ZakharovKuznetsov Burgers equation of the form (38), not investigated before. Here the shock wave nature depends on dissipation and dispersion parameters of a damped oscillator in (37). We can infer that for small dissipation, the particle trapped in a potential well will fall to the bottom of the well while oscillating between its walls and an oscillatory wave evolves. Further, for very small dissipating values of the system, the energy of the particle decreases with significant slowness and the few oscillations at the beginning of the wavefront will be close to solitons. It can be observed in our findings that when the value of dissipation parameter is greater than the critical value of the dissipation of the system, the motion displays aperiodic behaviour and monotonic shock profiles are obtained. Now to confirm our predictions for shock wave stability behaviour in a dense magnetized plasma (white dwarf) relativistic regime, we investigate the influence of viscosity parameter (η) . We numerically solve the Eq. (37) analyzing asymptotic behaviour of the solution of the form $\sim \exp(p\chi)$ with p given as Eq. (42) and imposing the boundary conditions $\Phi \to 1, \frac{d\Phi}{d\chi} \to 0$ as $|W| \to 0$. Figs. 10 (a to d) shows a train of oscillations ahead of the system, which decays with increase of damping parameter η and monotonic shock transition takes from oscilattory shock profile. These findings reveal that stability nature of shocks preserves the monotonicity as the dissipation effect is dominant. Now, to analyse physical interpretation of system (43), we exhibit the dynamical chaos or quasiperiodic motion occurring in the plasma system in g, g_1 and l_1. Using numerical interpretation in Fig. 11, we illustrate the evolution of Y in system (45) analyzing the power spectrum of the solutions in system (45). Our simulated prediction in Fig. 11, is consistent with the power spectrum as can be observed in Fig. 12. We can observe in Fig. 11, that a power spectrum is exhibited with a single frequency exhibiting the evolution of Y for system (45). Now to analyse numerically quasiperiodic motion, we use some quantitative techniques such as spectral analysis, phase plane and Lyapunov methods, give rise to two chaotic motions, i.e. weak chaos and developed chaos. Fig 13(a) displays graphical representation of Y of system (45)having two distinct frequencies, where one of the frequency is due to the external perturbation. Now comparing Fig. 13(a) with Fig. 12(a), we can observe that the quasiperiodicoscillation is generated due to the original frequency of system (43) being superimposed with external periodic perturbative perturbation and $|l_1|>>|g_1|$ simultaneously. Such quasiperiodicphenomena which is a small chaotic deviation from the periodic solutions are known as weak chaos [64-67], which is the superimposition of two frequencies. Again, another chaotic behaviour of system (45) can be observed in Fig. 13(b), where the original frequency has been broken and the peak of the frequency observed in Fig. 13(b) is much bigger than the original frequency seen in Fig. 12. These type of oscillations are known as developed chaos where a random sequence of uncorrelated shocks are observed ignoring the driver periods. These observations in Figs. 13(a) and 13(b) is consistent with a quasi-periodic evolution of Y in system (45) during the whole perturbative duration. Figs. 14(a) and 14(b) exhibits the evolution of Y in system (45) during the whole perturbed time. Fig. 14(a) represents the quasiperiodicity of Y for the case of Fig. 13(a) and Fig. 14(b) represents the quasiperiodicity of Y for the case of Fig 13(b). We have a situation in Fig. 13, where a soliton propagating is reflected at the left hand as a plasma wave. It is interesting to note that after a plasma wave is reflected, a small bump develops and yet it doesnot form a real soliton. After the bump dies away, the real soliton starts to appear and evolves fully as time passes. Now to find out that whether the quasi-periodic behaviour described in Figs. 13 and 14 turn into weak chaos and developed chaos with time evolution, we will analyse through phase projections, as represented in subsequent simulatons. For various values of time t, we observe that there exists an exponentially decreasing force like $g(t)=e^{-2t}$, where in Fig. 15 we can see that two parallel power spectra on the (x(t), x'(t)) plane merge into a significant one during the propagation. An interaction between the two power spectra emerging from exponentially decreasing force on the x-t and x'(t)-t planes, it can be observed that the amplitude of two spectras decrease when coupling parameter Γ increases. From Figs. 16 and 17, it can be inferred that different external force strength exhibit various chaotic oscillations giving rise to two chaotic state i.e the weak chaos and the developed chaos. Weak chaos is a small chaotic deviation from the periodic oscillations which is superimposition of original frequency with the external periodic perturbed frequency and $|l_1|>>|g_1|$ should be satisfied. On the other hand developed chaos is another chaotic behaviour of the system (45), which describes the evolution of bigger frequency of random sequence of uncorrelated shocks [68, 69] than the original frequency of the system.The weak chaotic oscillation is displayed in Figs. 16. Fig. 16 (a) states quasiperiodicity from time t=0.1 to 50. Gradually, with time evolution from t=0.1 to 200, the quasiperiodic state displays weak chaotic propagation satisfying the condition $|l_1|>>|g_1|$ in Fig. 16(b). Further, Figs. 17 exhibits developed chaotic behavior of system (28). Starting from time t=1 to t=20 as represented in Fig. 17 (a) and gradually with time evolution t=1 to t=100, the propagation turns into developed chaos and strong chaotic behavior can be expected with the parameters in appropriate ranges satisfying $|l_1|<<|g_1|$ in Fig. 17(b).Lastly, to confirm that the projections in Figs. 11 to 17 represents chaotic oscillations, we will investigate the external perturbating force g_1 and damping factor l_1 through the Lyapunov exponents and the largest Lyapunov exponents as exhibited in Figs. 18(a) and Fig. 18(b). However, as shown in Fig. 18(a), we can observe that the chaos becomes weak i.e the strength of the external perturbations becomes weak when $|l_1|>>|g_1|$. However the chaotic behavior becomes developed only when $|l_1|<<|g_1|$. Our investigation therefore reveals that the Lyapunov exponents and the largest Lyapunov exponents shown in Figs. 18(a) and 18(b) are consistent with Figs. 11 to 17 and it may be concluded that the Eq.(43) generates the chaos representing weak and developed chaotic behaviour.

v. CONCLUSION

Here, we have investigated the propagation of electrostatic waves in a dense magnetized plasma (white dwarf) with weakly relativistic and ultra-relativistic degenerate electrons and positrons.In the present model, the equilibrium of electrons and positrons has been considered to be maintained by two pressure equations according to Chandrasekhar, whereas that of ions is associated with the strong coupling effects. In this system, the dissipative effect is introduced by taking into consideration the kinematic viscosity among the ions fluid. The evolution of this system is investigated deriving the three dimensional Z-K-B equation. By depending on the dissipation of the system, the analytical solution indicating either solitary or shock waves can be investigated and only one of them exist at a time. In the weakly relativistic dense plasma, the amplitude Φ_{wr} has a numerical value of 0.02 stat-volt. We calculate the value of energy density, corresponding to this value, gives us $10^{18} ergcm^{-3}$, which gives a huge value. Similarly if we calculate the the value of the energy density, corresponding to it's amplitude Φ_{wr}, then we find the value as $5.87\times10^{22} ergcm^{-3}$. So, we see that the nonlinear electrostatic structures in an ultra-relativistic regime have more energy density than a weakly relativistic regime. Therefore, when these structures move from an ultra-relativistic regime (interior) to a weakly relativistic regime (surface) of a white dwarf, they liberate extra energy in the form of electro-magnetic waves. Thus, we study numerically the chaotic behaviour of the system using astrophysical parameters in the previous section. Different routes to chaos such as period doubling,quasi-periodic behaviour, etc are investigated by applying phase projection, power spectrum and Lyapunov exponents.

REFERENCES

1. S. Chandrasekhar, Philos. Mag. (suppl.) **11**, 592 (1931).
2. S. Chandrasekhar, Astrophys. J. **74**, 81 (1931).
3. S. Chandrasekhar, Mon. Not. R. Astron. Soc. **95**, 676 (1935).
4. S. Chandrasekhar, An Introduction to the study of stellar structure (Dover, New York, 1939), P 412.
5. S. Chandrasekhar, Phys. Rev. Lett. **12**, 114 (1964).
6. S. Chandrasekhar and R. F. Tooper, Astrophys. J. **139**, 1396 (1964).
7. W. Misner, K. S. Thorne, and J. A. Wheeler, Gravitation (San Francisco, C A: W. H. Freeman Publishers, 1973).
8. G. W. Gibbons, S. W. Hawking, and S. Siklos, The Very Early Universe (Cambridge: Cambridge Univ. Press, 1983).
9. R. J. Manchester, and J. H. Taylor, Pulsars (San Francisco, CA: W.H. Freeman Publishers, 1973).
10. D. Koester, and G. Chanmugam, Reports on Progress in Physics,**53**, 837 (1990).
11. K. Kashiyama, K. Ioka, and N. Kawanaka, Physical Rev. D, **83**, 023002 (2011).
12. G. D. Schmidt, White Dwarfs IAU Coll. No. 114 ed G Wegner (Berlin: Springer-Verlag), p 305, 1989.
13. S. Balberg and S. L. Shapirio, The properties of matter in white dwarf and neutron star.
14. S.L. Shapiro, and S. A. Tukolsky, Black Holes, White Dwarfs and Neutron Stars (New York: Wiley, 1983).
15. J. Dalligault, and M. S. Murillo, Phys. Rev. E, **71**, 036408 (2005).
16. J.Patterson, Astrophys. J. Suppl. 54,443 (1984).
17. H. M. Vanhorn, The Astrophyical Journal**151**,227 (1968)

18. S. Chandrasekhar, Mon. Not. R. Astron. Soc. **95**, 207 (1935).
19. N. M. Vernet, *Basics of the Solar Wind* (Cambridge: Cambridge Univ. Press, 2007).
20. S. Mahmood, A. Mushtaq, Phys. Lett. A **372**, 3467 (2008).
21. J. Zeba, W. M. Moslem, and P. K. Shukla, The Astrophysical Journal, 750,72 (2012).
22. P. K. Shukla, A. A. Mamun, and D. A. Mendis, Phys. Rev. E **84**, 026405 (2011).
23. T. Takeuchi, S. Lizuka, and N. Sato, Phys. Rev. Lett. **80**, 77 (1998).
24. N. J. Zabusky and M. D. Kruskal, Phys. Rev. Lett. **15**, 240 (1965).
25. R. M. Kulsrud, J. P. Ostriker and J. E. Gunn, Phys. Rev. Lett. **28**, 636 (1972).
26. S. D. Bale, M.A. Balikhin, T.S Horbury, V. V. Krasnoselskikh, H. Kucharek, E. Mobius, S. N. Walker, A. Balogh, D. Burgess, B. Lembege, E. A. Lucek, M. Scholer, S. J. Schwartz and M. F. Thomsen, Space Sci. Rev. **118**, 161 (2005).
27. E. Lee, G. K. Parks, M. Wilbr, and N. Lin, Phys. Rev. Lett. **103**, 031101 (2009).
28. H. K, Henderson, N. D'Angelo, P. Michelson, and P. Nielson, Phys. Rev. Lett. **19**,149 (1967).
29. A. A Mamun and P. K. Shukla, Eur. Phys. Letter. **94**, 65002 (2007); 87, 55001, (2009).
30. M. W. Hirsch, S. Smale, and R. L. Denaney, *Differential Equations, Dynamical Systems, and an Introduction to Chaos* (Elsevier, Washington, 2004).
31. K. Nozaki, and N. Bekki, Phys. Rev. Lett. 50, 1226 (1983).
32. D. J. Zheng, W. J. Yeh, and O. G. Symko, Phys. Lett. A, 140, 225 (1989).
33. G. P. Williams, *Chaos Theory Tamed* (Joseph Henry, Washington, 1997).
34. W. Beiglbock, J. P. Eckmann, H. Grosse, M Loss, S. Smirnov, L. Takhtajan and J. Yngvason, *Concepts and Results in Chaotic Dynamics* (Springer, Berlin, 2000).
35. R. Buchter, J. Perdang, E. A. Spiegel, Reidel Dordrecht, p.11. Chaos in Astrophysics (1985).
36. W. Voges, H. Atmanspacher, H. Sceingraber, The Astrophysical Journal, **320**, 794 (1987)
37. I. McHardy, B. Czerny, Nature, **325**, 695 (1987).
38. J. R. Buchler, G. Konacs, Astrophys. J. Lett. **320**, L57 (1987).
39. H. M. Van Horn; Proc. of the 25th Liege International Astrophys. Colloqium, Theoretical Problems in Stellar stability and Oscillations, University of Liege, Liege, Belgium (1984).
40. D. Winget, Proc. on the Workshop Multimodes stellar pulsations, Budapest, Hungary (1988).
41. M. Auvergne, A. Baglin, Proc. Tenth Europ. Reg. IAU Meeting, Prague, Vol. 5 Ed. P. Harmanec, Publ. Astron. Inst. Czechosl. Acad. Sciences No.70.
42. M. J. Goupil, M. Auvergne and A. Barglin, Astron. Astrophys. 196, L13 – L16 (1988).
43. H. D. I Abarbanel, R. Brown, M. B. Kennel, Variation of Lyapunov exponents on a strange attractor, Journal of Nonlinear Science **1**, 175 (1991).
44. R. T. Farouki and S. Hamaguchi, Phys. Rev. E, **47**, 4330 (1993).
45. P. K. Shukla, and B. Eliasson, Reviews of Modern Physics, **83**, 835 (2011).
46. R. T. Farouki, and S. Hamaguchi, Phys. Rev. E, **47**, 4330 (1993).
47. W. L. Slattery, G. D. Doolen, and H. E. Dewitt, Phys. Rev. A, **21**, 2087 (1980).
48. P. K. Shukla, A. A. Mamun, and D. A. Mendis, Phys. Rev. E, **84**, 026405 (2011).
49. G. Gozadivos, A. V. Ivlev, and J. P. Boeuf, New J. Phys. **5**, 32 (2003).
50. A. Rasheed, N. L. Tsintsadze, and G. Murtaza, Comm. Theoretical Phys., **18**, 112701 (2011).
51. R. Sabry, W. M. Moslem, and P. K. Shukla, CoThP, **19**, 122903 (2012).
52. M. W. Hirsch, S. Smale, and R. L. Devaney, Differential Equations, Dynamical Systems, and an Introductionto Chaos (Elsevier, Washington, 2004).
53. K. Nozaki, and N. Bekki, Phys. Rev. Lett. **50**, 1226 (1983).
54. R. Roychoudhury, G. C. Das and J. Sarma, Phys. Plasmas **6**, 2721 (1999).
55. M. Belic, N. Petrovic, W. P. Zhong, R. H. Xie, and G. Chen, Phys. Rev. let. **101**, 123904 (2008).
56. D.J. Zheng, W.J Jeh, and O. G. Symko, Phys. Lett. **A 140**, 225 (1989).
57. J. Yu, W. J. Zhang, and X. M. Gao, Chaos, Solitons Fractals **33**, 1307(2007); H. J. Cao, J. M. Seoane, and A. F. Sanju_an, ibid. **34**, 197 (2007).

58. E. Infeld and G. Rolands, *Nonlinear Waves, Soliton and Chaos* (Cambridge University, Cambridge, 1990).
59. R. Scharf and A. R. Bishop, Phys. Rev. **A 46**, 3164 (1992); J. K. Yang and D. J. Kaup, SIAM J. Appl. Math. **3**, 967 (2000); K. S. Sreelatha and K. B. Joseph, Chaos, Solitons Fractals **9**, 1865 (1998).
60. H. T. Moon, Phys. Rev. Lett. **64**, 412 (1990); M. Higuchi and K.Fukushima, Chaos, Solitons Fractals **9**, 845 (1998).
61. K. B. Blyuss, Rep. Math. Phys. **46**, 47 (2000).
62. M. A. Malkov, Physica D **95**, 62 (1996).
63. T. V. Laptyeva, J. D. Bodyfelt, D. O. Krimer, and S. Flach, Europhys. Lett. **91**, 30001 (2010).
64. R. Svensson, *Astrophys. J.* **258**, 335 (1982).
65. B. Sahu and R. Roychoudhury, Czech J. Phys., **53**, 517 (2003).
66. M. Mulansky, K. Ahnert, A. Pikovsky, and D. L. Shepelyansky, J. Stat.Phys. **145**, 1256 (2011).
67. D. M. Basko, Ann. Phys. **326**, 1577 (2011).
68. N. M. Ryskin and V. N. Titov, Tech. Phys. **48**, 1170 (2003).
69. C. C. Lalescu, C. Meneveau, and G. L. Eyink, Phys. Rev. Lett. **110**,084102 (2013).

BUTI-03

First Order Phase Transition and Crystal-Fluid Coexistence in a Complex Plasma System

M. G. Hariprasad, P.Bandyopadhyay, G. Arora, A Saravanan, Swarnima Singh and A. Sen

Institute for Plasma Research, HBNI, Gandhinagar-382428

hari.prasad@ipr.res.in

Abstract

The first order crystal-fluid phase transition and the non-equilibrium crystal-fluid coexistence of charged dust particles in a DC glow discharge Argon plasma in DPEx devices is investigated. After forming a stable crystalline structure at a particular discharge voltage, it is observed that the crystal melts instantaneously with a negligible reduction of neutral gas pressure after a threshold value. The structural and thermodynamical analysis essentially indicate that the nature of the melting process is a first-order phase transition. In extended experiments conducted in a large crystal, surprisingly instead of complete melting, the system shows a crystal-fluid coexistence at a neutral pressure below a critical value. The central region remains in the fluid state approximately 30 times hotter than the surrounding crystal and exhibits the necessary condition for a non-equilibrium phase coexistence. In brief, this experimental study opens up opportunities to investigate a number of fundamental problems in interdisciplinary science with kinetic level information.

Introduction

A dusty plasma system consisting of electrons, ions, neutral atoms/molecules and charged micron-sized particles. The diversity in space and time scales of these constituent particles make the dynamics of dusty plasma very complex, and henceforth the dusty plasma is also known as “complex plasma”. The complex plasma drawn immense attention and considered as a potential model system to investigate interdisciplinary problems after the invention of complex plasma crystal by Lin *et al.* and Thomas *et al.* in 1994 [1, 2]. An important characteristic parameter of a complex plasma is the Coulomb parameter (Γ), defined as the ratio of the dust electrostatic potential energy to its thermal energy. When Γ exceeds a critical value, the system transforms to a crystalline state. For the situation Γ less than one, the complex plasma posses a gaseous state, and for an intermediate value of Γ, the medium behaves like a liquid [3, 2, 1]. The formation of an ordered arrangement among the dust particles with characteristic features of a crystalline structure arises because of the strong correlations between the dust particles as they occupy a large charge on their surface [2, 1]. The ease of observation of the individual dust dynamics coupled with the convenient time scales of the collective dynamics of such systems has spurred plenty of laboratory investigations in interdisciplinary fields [1, 2, 4, 5, 6, 7, 8]. The possibility of the complex plasma crystal as a testbed is explored widely for studying problems associated with heat transport, lattice waves, Mach cones, voids, crystal defects *etc.* [9, 10, 8, 11, 12].

Moreover, a complex plasma also provides an excellent opportunity to study the phase transition scenarios and phase coexistence in complex systems in kinetic level. The phase transition in complex plasma system posesses different scenarios like equilibrium and non-equilibrium phase transitions, first-order and second-order melting, defect induced melting, instability driven melting etc... Eventhogh coexisting phases are observed in complex plasmas a stable self-sustained non-equilibrium coexistence crytsal-fluid structure is not explored till date. Moreover, most of the past studies in complex plasma phase transtions and phase coexistence are carried out in RF discharge plasma only. In this work, we investigate a first-order phase transition and a non-equilibrium crystal-fluid coexistence in a DC glow discharge plasma where the ion-wake induced non-equilibrium nature is much stronger.

Experimental set-up and procedure

The experiments are carried out in versatile tabletop Dusty Plasma Experimental devices, which are described in detail in Ref. [13, 11]. The DPEx device is an inverted Π-shaped Pyrex glass tube with one horizontal and two vertical arms as shown in Fig. 1(a). The horizontal arm acts as the main chamber and is used for performing experiments and for optical diagnostics. The two vertical units serve as auxiliary chambers and are used for venting the system, electrode connections, gas inlets *etc.*. A rotary pump is used to evacuate the vessel, and a mass flow controller is employed for feeding the gas into the chamber in a controlled way. A circular disc acts as an anode, whereas a long tray electrode placed in the main vessel serves as a grounded cathode as presented inFig. 1(b). Melamine Formaldehyde (MF) dust particles are introduced into the chamber by a software-controlled dust dispenser. A green laser line source and a CCD camera serve as the diagnostics tools for recording the dynamics of dust particles. The recorded images are analyzed to investigate dust dynamics for various experiments with the help of IDL-based super Particle Identification Tracking (sPIT) code.

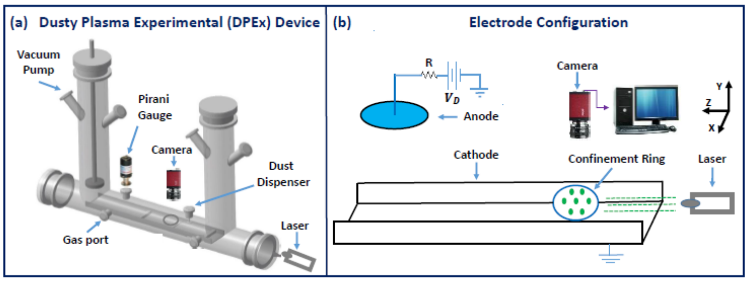

Figure 1: Schematic of the (a) DPEx device (b) electrode configuration.

Initially, a base pressure of 0.1 Pa is achieved in the DPEx device, and a working pressure of 4–12 Pa is maintained by balancing the pumping rate and the gas flow rate. An Argon plasma is created by striking a DC voltage of 300 – 600 V between the asymmetric electrodes. The mono-dispersive dust particles are introduced into the plasma using the dust dispenser after the initiation of the plasma. The dust particles attain a negative charge in the background of Argon plasma due to the higher mobility of electrons compared to that of the ions. The negatively charged dust particles experience gravitational force in the downward direction which is then balance by the cathode sheath electrostatic force and the dust particles levitate at a height from the cathode. A circular ring is placed on the cathode to provide radial confinement to the particles and it also gives the crystal a circular shape. At specific discharge conditions, a two-dimensional finite complex plasma crystal forms and remains stable inside the circular ring over a wide range of discharge conditions.

Results and discussion

First-order Phase Transition: The present set of experiments on the phase transition is carried out at a discharge voltage of 480 V by varying the neutral gas pressure from p = 7.5 Pa to p = 5.5 Pa at intervals of 0.1 − 0.2 Pa. For p = 7.5 − 6.9 Pa, the 2D dust cloud forms an ordered state with hexagonal symmetry as depicted in Fig. 2(a). When the neutral pressure decreases below 6.9 Pa, the crystal disintegrates into a disordered state of a highly random nature as shown in Fig. 2(b). Interestingly, this sudden change happens with a negligible variation in the neutral pressure from 6.9 Pa to 6.7 Pa. The nature of this phase transition is further examined by analyzing the behavior of the system and estimating the statistical parameters by employing diagnostic tools like the pair correlation function, Voronoi diagram, and Langevin dynamics.

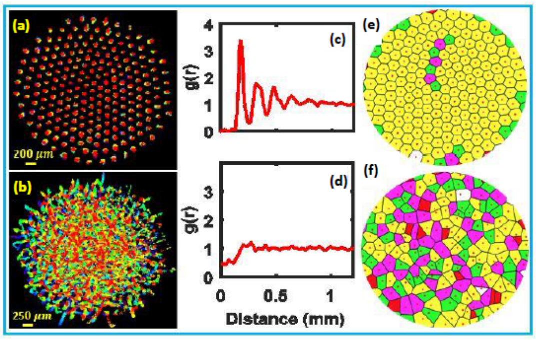

Figure 2: (a), (b) Overlapped position coordinates of dust particles for consecutive 50 frames (p=6.9 Pa and p=6.7 Pa). (c), (d) correlation functions and (e), (f) Voronoi diagrams corresponds to (a) and (b), respectively.

The radial pair correlation function (RPDF) [14], $g(r)$, is used to find the configurational order, which provides useful information on the structural and thermodynamical properties of a system and is useful to identify its phase state. Fig. 2(c) represents the ordered state of Fig. 2(a), in which the pair correlation function exhibits several periodic peaks, which is essentially a signature of a crystalline state. When the neutral gas pressure is slightly reduced to a value of 0.2 Pa to 6.7 Pa from 6.9 Pa, the periodic peaks in the pair correlation function disappear suddenly, which essentially indicating a sharp phase transition to a disordered fluid state as shown in Fig. 2(d).

The Voronoi diagram is employed in addition to the pair correlation function to establish the structural transition which gives the information of the cell structure of a system along with the details of crystal defects. Fig. 2(e) and (f) show the Voronoi diagrams for the pressure values of 6.9 Pa and 6.7 Pa, respectively. The hexagonal structures are marked in yellow and the red, pink, green, *etc.* structures correspond to other polygons. At 6.9 Pa (see Fig. 2(e)), the hexagonal structures spread throughout the Voronoi diagram, which confirms the findings of the pair correlation analysis. At 6.7 Pa (after the sudden structural transition), the Voronoi diagram shows a complete breakdown of hexagonal symmetry in the system, and many five-fold and seven-fold cells are formed throughout the complex plasma structure. It clearly shows the instantaneous transition of the complex plasma system from ordered hexagonal crystal to a completely disordered fluid structure.

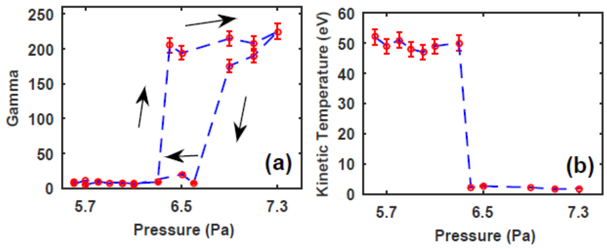

Figure 3: Variations of (a) coupling parameter, (b) dust kinetic temperature

In addition to the structural analysis, we have also experimentally estimated the thermodynamical parameters like screened Coulomb coupling parameter (Γ) and dust temperature using Langevin dynamics. Fig. 3(a) shows the variation of Coulomb coupling parameter (Γ) with the neutral gas pressure. At high neutral gas pressures (beyond $p = 6.9$ Pa), the coupling parameter turns around $\Gamma \sim 200$. It means the system posses a strongly coupled crystalline state [15]. Γ decreases abruptly from ~ 200 to ~ 8 when the neutral gas pressure is reduced from 6.9 Pa to 6.7 Pa, which essentially demonstrates a phase transition of a complex plasma crystal to a complex plasma fluid [15, 16]. It is worth mentioning that the coupling parameter becomes almost twenty-five fold less with a pressure variation of only 0.2 Pa, which is one of the salient features of a first-order phase transition. Our use of the Coulomb coupling parameter for such a purpose is justified as it intrinsically includes the variation in the specific heat capacity, the entropy, and the internal energy as demonstrated in the simulation studies of Vaulina *et al.* [16]. Moreover, sudden rise in dust temperature from 2 eV to 50 eV is observed during the phase transition from the crystal phase to the fluid phase as shown in Fig. 3(b) and the ion wake induced instability is regarded as the triggering mechanism.

Non-equilibrium Phase Coexistence: In the next set of experiments, a large-sized hexagonally ordered complex plasma structure is observed when the neutral gas pressure and discharge voltage are set at 9 Pa and 450 V, respectively. The complex plasma system is observed to be exhibitting various phases with variation in neutral gas pressure. Voronoi diagram is utilized to examine the structural details of various states in this experiment. Fig. 4 depicts the Voronoi diagrams of the complex plasma at different neutral gas pres-

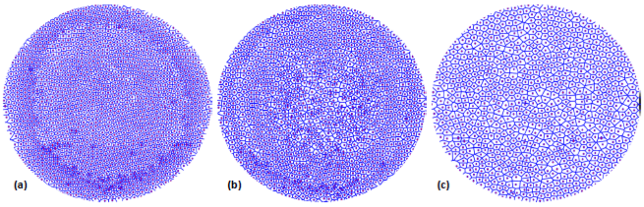

Figure 4: Voronoi diagram corresponds for various neutral gas pressures at (a) 8 Pa (crystalline state) (c) 6.5 Pa (crystal-fluid coexistence state) and (c) 5 Pa (cold fluid state).

sures. Fig. 4(a) presents the Voronoi diagram of the complex plasma system at $\sim$ 8 Pa. The Voronoi diagram points out an ordered structure at higher pressure. The crystal is mostly filled with hexagonal cells at P $\sim$ 8 Pa, as they are the building blocks of a two-dimensional complex plasma. The scenario changes when the neutral gas pressure is reduced further to $\sim$ 6.5 Pa as depicted in Fig. 4(b). Fig. 4(b) shows that the center portion of the complex plasma structure becomes fully disordered and filled with defects, and its periphery contains hexagonal cells. It essentially indicates a crystal-fluid coexistence state at that specific pressure. Even though the structural analysis shows a coexistence of crystal-fluid state in a complex plasma system, more dynamical characterization is needed to establish its equilibrium and non-equilibrium nature. Further reduction in neutral gas pressure to $\sim$ 5 Pa leads to the disappearance of coexisting phases and the system transformed to a fully fluid state as presented in Fig. 4(c). The dust temperature is experimentally determined to examine more about the nature of the phase transition at different pressures. Fig. 5(a) shows the variation of dust temperature with the neutral gas pressure. At higher pressures ($\sim$ 7.5 - 9 Pa) in crystalline state, the dust temperature is measured to be $\sim$ 2-3 eV which does not vary significantly when the neutral gas pressure reduces. However, the temperature suddenly jumps to a value of $\sim$ 10 eV at the neutral gas pressure of $\sim$ 7.2 Pa during the emergence of coexisting phases. The dust temperature keeps on increasing and attains a maximum value of $\sim$ 30 eV till the neutral gas pressure reduces to a value of $\sim$ 6.4 Pa. Surprisingly beyond the value of P $\sim$ 6.4 Pa, the dust temperature decreases with the decrease in the neutral gas pressure and the system turns out to a completely fluid phase. Finally, the system achieves a temperature of $\sim$ 2-3 eV at $\sim$ 5.5 Pa, almost equal to the temperature at higher pressures ($\sim$ 7.5 - 9 Pa).

An important concern on the coexistence structure is the nature of its thermodynamic state. Generally, in equilibrium systems, the temperatures of the two coexisting phases remain the same [17] whereas, in a non-equilibrium coexistence state, the phases can exhibit different temperatures [6]. Fig. 5(b) depicts the spatial temperature profile of the complex plasma in coexisting phase. The '0' location refers to the center of the complex plasma. Fig. 5(b) shows that the dust temperature has a maximum value ($\sim$ 30 eV) in the fluid phase (at center), which then reduces by almost ten folds ($\sim$ 3 eV) in the crystalline phase (at the periphery). This drastic difference of temperatures between the two coexisting phases essentially implies a non-equilibrium nature of the system.

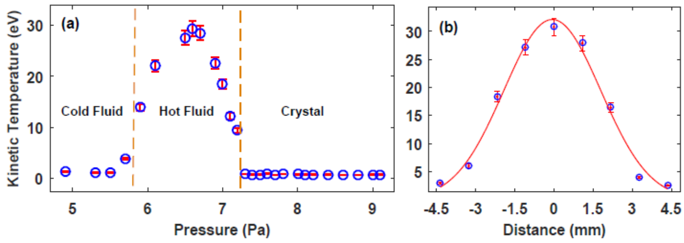

Figure 5: (a) Variation of dust temperature with neutral gas pressure (b) Spatial profile of the dust temperature in crystal-fluid coexisting phase.

Summary and conclusion

Comprehensive experiments have been performed to explore the nature of the phase transition and phase coexistence of a complex plasma system over a range of neutral gas pressures. The complex plasma crystal produced in DC glow discharge melts completely with a negligible reduction of neutral gas pressure after it reaches a threshold value. The nature of the melting process in our experiments is established as a first-order phase transition from the estimation of the structural and thermodynamical analysis. The melting observed in our experiment is a non-equilibrium phenomenon induced by the wakes beneath each dust particle, which forms due to the focusing of streaming ions at a pressure beyond a threshold value. An extended experiment has been performed to examine the coexistence of different phases in a complex plasma. For this set of experiments, a larger-sized complex plasma crystal compared to the previous experiments has been produced over a similar range of discharge conditions. Surprisingly, instead of complete melting, a sudden crystal-fluid coexisting state is observed in the complex plasma when the neutral gas pressure is reduced slowly as in previous experiments. The coexisting phase consists of a hot fluid in the central region surrounded by a cold crystal, in which the temperature of the fluid phase remains 30 times higher than that of the crystal. The mixture of these two states essentially exhibits the necessary condition for a non-equilibrium phase coexistence. Further reduction in neutral gas pressure results in the complete transformation to a cold fluid state from the phase coexisting state. Therefore, we believe such a complex plasma system provides a platform to model several non-equilibrium systems to explore their dynamics at the kinetic level.

Bibliography

[1] H. Thomas, G. E. Morfill, V. Demmel, J. Goree, B. Feuerbacher, and D. Möhlmann. Plasma crystal: Coulomb crystallization in a dusty plasma. *Phys. Rev. Lett.*, 73:652–655, Aug 1994.

[2] J. H. Chu and Lin I. Direct observation of coulomb crystals and liquids in strongly coupled rf dusty plasmas. *Phys. Rev. Lett.*, 72:4009–4012, Jun 1994.

[3] H. Ikezi. *Phys. Fluids*, 29(6):1764–1766, 1986.

[4] Paolo Allegrini, Jack F. Douglas, and Sharon C. Glotzer. Dynamic entropy as a measure of caging and persistent particle motion in supercooled liquids. *Phys. Rev. E*, 60:5714–5724, Nov 1999.

[5] André Schella, Tobias Miksch, André Melzer, Jan Schablinski, Dietmar Block, Alexander Piel, Hauke Thomsen, Patrick Ludwig, and Michael Bonitz. Melting scenarios for three-dimensional dusty plasma clusters. *Phys. Rev. E*, 84:056402, Nov 2011.

[6] Suvendu Mandal, Benno Liebchen, and Hartmut Löwen. Motility-induced temperature difference in coexisting phases. *Phys. Rev. Lett.*, 123:228001, Nov 2019.

[7] A. Melzer, A. Homann, and A. Piel. Experimental investigation of the melting transition of the plasma crystal. *Phys. Rev. E*, 53:2757–2766, Mar 1996.

[8] D. Samsonov, J. Goree, Z. W. Ma, A. Bhattacharjee, H. M. Thomas, and G. E. Morfill. Mach cones in a coulomb lattice and a dusty plasma. *Phys. Rev. Lett.*, 83:3649–3652, Nov 1999.

[9] V Nosenko, S Zhdanov, AV Ivlev, G Morfill, J Goree, and A Piel. Heat transport in a two-dimensional complex (dusty) plasma at melting conditions. *Physical review letters*, 100(2):025003, 2008.

[10] Frank Melandso/. Lattice waves in dust plasma crystals. *Physics of Plasmas*, 3(11):3890–3901, 1996.

[11] Saravanan Arumugam, Pintu Bandyopadhyay, Swarnima Singh, M. G. Hariprasad, Dinesh Rathod, Garima Arora, and Abhijit Sen. Dpex-ii: a new dusty plasma device capable of producing large sized dc coulomb crystals. *Plasma Sources Science and Technology*, 2021.

[12] V. Nosenko, S. K. Zhdanov, A. V. Ivlev, C. A. Knapek, and G. E. Morfill. 2d melting of plasma crystals: Equilibrium and nonequilibrium regimes. *Phys. Rev. Lett.*, 103:015001, Jun 2009.

[13] S Jaiswal, P Bandyopadhyay, and A Sen. Dusty plasma experimental (dpex) device for complex plasma experiments with flow. *Review of Scientific Instruments*, 86(11):113503, 2015.

[14] T. Ott, M. Bonitz, L. G. Stanton, and M. S. Murillo. Coupling strength in coulomb and yukawa one-component plasmas. *Physics of Plasmas*, 21(11):113704, 2014.

[15] Hiroyuki Ikezi. Coulomb solid of small particles in plasmas. *The Physics of fluids*, 29(6):1764–1766, 1986.

[16] O.S. Vaulina and X.G. Koss. Thermodynamics and phase transitions in two-dimensional yukawa systems. *Physics Letters A*, 378(46):3475 – 3479, 2014.

[17] Thomas Speck. Coexistence of active brownian disks: van der waals theory and analytical results. *Phys. Rev. E*, 103:012607, Jan 2021.

BUTI-04

Storage of Excessive Magnetic Free Energy and Photospheric Current Leading to Extreme Eruptive Activity from Solar Active Regions

Prabir Kumar Mitra and Bhuwan Joshi

Udaipur Solar Observatory, Physical Research Laboratory, Badi Road, Udaipur-313001, Rajasthan, India

prabir@prl.res.in

1. Introduction

Solar active regions are identified by groups of dark-spots i.e., sunspots [1] observed on the Solar surface i.e., the Photosphere. Such regions are characterized by the presence of strong magnetic fluxes. With such strong magnetic flux, solar active regions are the most preferred sites for the solar transient phenomena [2] (e.g., solar flares [3]) during which a huge amount of energy (as high as ~10^{32} erg) is released within a short time (few minutes to few hours). During the eruptive flares, plasma and magnetic field are expelled into the interplanetary space from the Sun, interaction of which with the Earth's magnetic field quite frequently causes hazardous effects called 'space weather' [4].

It is globally accepted that the fundamental process causing the sudden release of energy during the transient phenomena is magnetic reconnection, a topological reconfiguration of the magnetic field in a plasma medium [5]. During the process of reconnection, magnetic energy is rapidly converted into plasma heating, bulk motions, and kinetic energy of non-thermal particles. Since, active regions are associated with strong magnetic flux and therefore contain high storage of magnetic field, they are considered to be very important during the studies of solar transient phenomena.

The overall flux content and magnetic complexity of solar active regions vary widely and the total sunspot area on the solar surface also varies with time in a 11 year period cycle [6]. Interestingly, active regions with apparently similar flux content and complexity can have significant difference in the flaring activities. It has remained a mystery still that some active regions profoundly produce large but confined solar flares which are not associated with eruptions [7]. On the other hands, few active regions are historically known to produce frequent eruptive flares.

In this work, we focus on the solar active region NOAA 12673 which was an exceptionally eruptive flare productive active region. With a multi-wavelength observational approach using data from the Atmospheric Imaging Assembly on board the Solar Dynamics Observatory, complemented by rigorous modeling analysis of the solar corona, we aim to understand the specialty of the active region toward its extraordinary flaring activities. In Section 2, we provide a list of the sources of data used in this work and a brief description of the modeling techniques. In Section 3, we provide a brief description of the evolution of the active region through the visible solar surface with an overview of the associated flaring activity. In Section 4, we discuss the evolution of magnetic free energy of the active region, in order to understand the active regions ability of frequently producing large flares. For understanding the triggering locations of the flares, we compute vertical photospheric currents and show their spatial arrangement during different flaring activity periods in Section 5. We discuss and interpret our results in Section 6.

2. Observational Data and methods

For observing the Sun in (E)UV wavelengths, we use high resolution (0."6 pixel^{-1}), 4096×4096 pixel full disk observations from the Atmospheric Imaging Assembly (AIA) [8] on board the Solar Dynamics Observatory (SDO) [9]. For photospheric observation, we use 45 s cadence line of sight (LOS) magnetograms and intensity images observed by Helioseismic and Magnetic Imager (HMI) [10] on board SDO, which takes continuous full disk observation of the solar photosphere with spatial resolution of 0."5 pixel$^{-1.}$ Coronal magnetic field extrapolation was done by employing the optimization based non-linear force free field (NLFFF) and potential magnetic field extrapolation method developed by [11]. In order to compute the degree of squashing factor, we used the code developed by [12]. For visualization of the extrapolated magnetic field, we used the

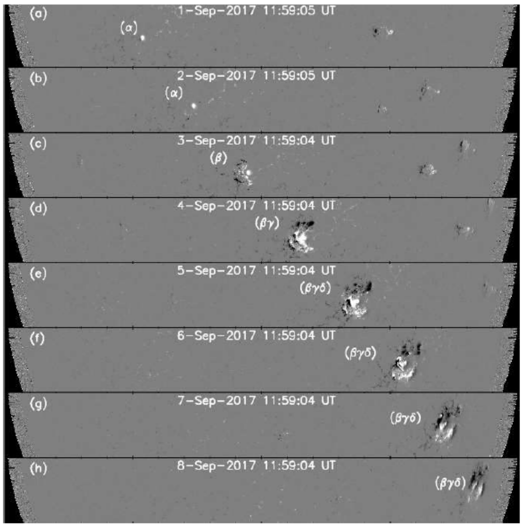

Figure 1. Evolution of the active region NOAA 12673 through its passage on the visible solar hemisphere. The magnetic classifications of the active region is noted in bracket in each panel.

Visualization and Analysis Platform for Ocean, Atmosphere, and Solar Researchers software [13].

3. Evolution of the active region NOAA 12673

The active region NOAA 12673 appeared on the eastern limb of the visible solar disk on 28 September 2017 as a simple unipolar (α-type) active region. It remained relatively unchanged for a few days initially and the quickly evolved subsequently. In Figure 1, we plot the evolution of the active region NOAA 12673 from 1 September 2017 to 8 September 2017. From the figure it becomes clear that between 3 September 2017 and 5 September 2017, it quickly become much complex and turned into the most complex βγδ-type active region on 5 September 2017.

Flaring activity from the active region started on 4 September 2017. In total, the active region NOAA 12673 produced 27 M-class and 4 X-class flares along with numerous C-class flares, which made this active region the most flare productive active region in the solar cycle 24. In Figure 2, we plot the GOES 1-8 Å soft X-ray lightcurves between 4 September 00:00 UT and 7 September 00:00 UT, by the blue curve to show the flaring activities. After this time, the active region moved too close to the western limb of the Sun causing unreliability in the

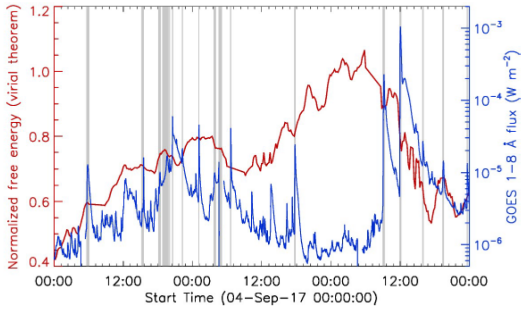

Figure 2. GOES soft X-ray lightcurve in the 1-8 Å channel (blue curve) and the evolution of the normalized magnetic free energy (red curve) between 4-7 September 2017. Durations of all the flares above M-class are highlighted by the gray shaded regions.

measurement of magnetic fields because of the Sun's curvature. From Figure 2, we find that, the overall flaring activity from the active region occurred in two quite distinguishable periods e.g., 4 September ≈00:00 UT – 6 September ≈00:00 UT; and, 6 September ≈00:00 UT – 7 September ≈00:00 UT. Interestingly, the first period was only associated with large M- and C-class flares, whereas, the second period was characterized by two X-class flares, the second of which was the largest flare in the solar cycle 24.

4. Evolution of magnetic free energy

Magnetic free energy is defined as the energy stored in the active region which can be released during the magnetic reconnection activities. Therefore, pre-storage of free magnetic energy can provide crucial information about the flare energetics. In this work, we computed magnetic free energy (E_F) the magnetic virial theorem [14]. According to this theorem, the magnetic energy stored in a coronal force-free magnetic field is given by the surface integral at the photospheric boundary involving the three vector magnetic field components, i.e.

$$E_F = \frac{1}{4\pi}\int_{z=0}(xB_x + yB_y)B_z\,dxdy \; ....(1)$$

where B_x, B_y, and B_z are x-, y-, and z- components of the photospheric magnetic field, respectively.

In Figure 2, we plot the evolution of the magnetic free energy normalized by the corresponding potential magnetic energy by the red curve, as a function of time. From the figure, we find that from the beginning of 4 September 2017, magnetic free energy almost steadily increased till ≈04:00 UT on 5 September 2017 and reached to ≈80% of the potential energy; after which it slowly decreased for ≈6 hrs and reached to a local minima at ≈70% of the potential energy. After this time, the magnetic free energy rapidly increased till the onset of the first X-class flare originated from the active region at ≈09:00 UT on 6 September 2017 and reached to ≈110% of the potential energy. Such high value of free energy suggest storage of excess twisted and sheared magnetic field in the active region which are potential locations for initiation of magnetic reconnection. During the course of these two X-class flares, magnetic free energy decreased drastically, which is expected.

5. Distribution of vertical currents (I_z)

Since magnetic reconnection takes place on a current sheet which allows for diffusion of magnetic field, photospheric regions with high currents are very important toward understanding the triggering mechanisms of solar flares. In order to analyze the effects of current toward the flaring activities, we computed photospheric current density. The vertical component of current density (j_z) on the photosphere can be calculated from horizontal components of magnetic field (B_x and B_y) using the Ampere's law [15]:

$$j_z = \frac{1}{\mu_0}\left(\frac{dB_y}{dx} - \frac{dB_x}{dy}\right) \text{.......(2)}$$

From current density (j_z), we derive current (I_z) by multiplying j_z with the area of one pixel i.e., $\approx 13.14\times10^{10}$ m^2.

In Figure 3, we plot selective I_z maps of the active region NOAA 12673 during the rise phase of the first flaring period (see Figure 2). As we find from Figures 3(b)-(g), regions of strong vertical current of both the directions, gradually accumulated in the active region. A few of such regions are indicated by different colored arrows in these panels. Here, the location indicated by the black arrows in Figures 3(e)-(g) is of particular interest in view of the close proximity of the opposite polarity high-current regions, which are the most preferred locations for the initiation of magnetic reconnection. Indeed, the flares originating during this period were triggered from this location. Another interesting feature in these I_z maps is the elongated location of the negative polarity high current region which is indicated by the brown arrows. Such regions are indicative of the presence of a flux rope.

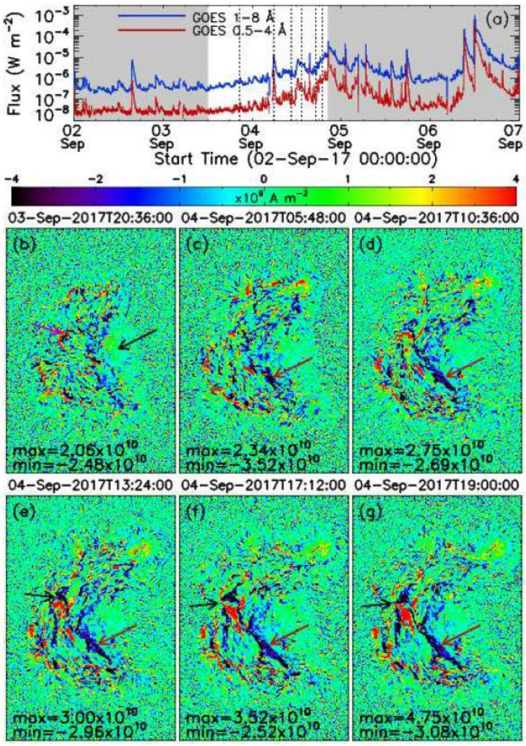

Figure 3. Panel (a): GOES SXR lightcurves showing the flaring activities from the active region NOAA 12673. We select six instances during the evolution of the flares as marked by the vertical lines. In panels (b)-(g), we plot the distribution of vertical component of photospheric current in the active region at those instances. A few regions of strong current of opposite polarities are indicated by arrows of different colors. For better visualization, values of I_z are saturated at $\pm0.4\times10^{10}$ A. Maximum and minimum values of I_z with order of 10^{10} A within the selected fov are indicated in each of these panels.

Observationally, we identified the flux rope as a small filament as observed in the AIA 304 Å channel images (not shown here).

In Figure 4, we plot selective I_z maps of the active region NOAA 12673 during the second phase of flaring activity that included the two X-class flares. We immediately notice the significant deviation of the concentration of the high-current regions from the rising phase of the first flaring period. In Figures 4(b)-(g), we note that the location of the elongated negative polarity current region (indicated by the brown arrows in Figures (c)-(g)) is now characterized by the presence of a positive polarity region in association of the pre-existing negative

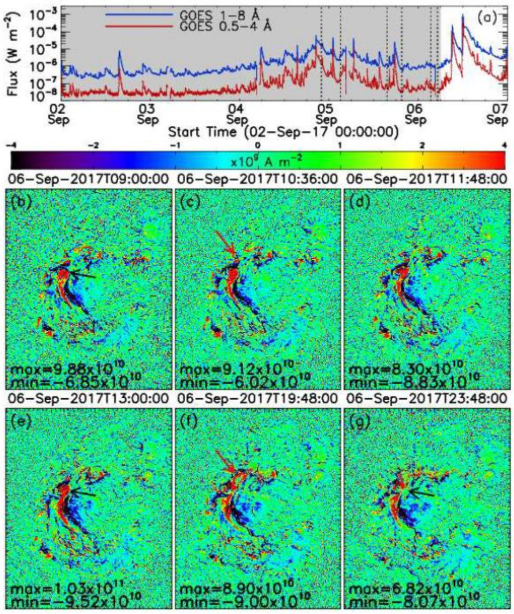

Figure 4. Same as Figure 3 except the I_z maps were plotted at six representative times during the highest flaring activity period of the active region NOAA 12673.

polarity region (indicated by the black arrows in Figures 4(b) and (e)). EUV images of the active region during this phase indicated the presence of a coronal hot channel (not shown here) which is suggestive of an activated flux rope. We further note that exactly at the northern end of the positive polarity region, strong current locations of both polarities were situated in an adjacent/overlapping fashion. Notably, both the X-class flares evolved with the earliest brightening from the northern footpoint of the activated flux rope. Following the two X-class flares, we observed significant decay of the current concentrations of this region, as well as the strength of the currents also reduced.

6. Results and discussion

The active region (AR) NOAA 12673 was highly flare productive. In total, it produced 27 M-class and 4 X-class flares between 4–10 September 2017.

During the highest activity period, the complex AR was characterized by the presence of δ-sunspots, which are identified with a complex distribution of sunspot groups in which the umbrae of positive and negative polarities share a common penumbra [16]. Such complex ARs are known to produce powerful flares (see e.g., [17]). Earlier studies have shown a close relationship between major flare activities and strong magnetic field, especially those with a high gradient and those that are highly sheared across the PIL [18]. The reported eruptive activities in AR 12673, thus, represent the capability of the AR in the rapid generation and storage of huge amount of excess magnetic energy in the corona. In this context, the evolution of normalized free magnetic energy during the flares is noteworthy (Figure 2). Prior to the onset of the X-class flares, the storage of the free energy increased to ≈110% of the potential energy. Although free magnetic energy reduced significantly following the two X-class flares on 6 September 2017, it still contained high storage of free energy (≈50% of the potential energy). Our analysis, therefore, implies that a large amount of free magnetic energy was gradually stored in the AR before the flaring activities which allowed the active region to produce such powerful flares.

An important aspect of this study is to investigate the origin of the pre-flare activities and their spatial relation with the strong photospheric current regions. [19] investigated evolution of photospheric current during two flares of classes M1.0 and M8.7 occurring from two different ARs. Although both ARs were subjected to rapid flux emergence, the two flares differed significantly in the evolution of photospheric longitudinal current. Their analysis revealed that, for the M1.0 flare, the longitudinal electric current density dropped rapidly; while it increased for the case of the M8.7 flare. They concluded rapid emergence of current carrying flux to be responsible for the increasing longitudinal current during the M8.7 flare while their explanation for the decrease of electric current for the M1.0 flare the was dissipation of magnetic free energy in the solar atmosphere. Our analysis suggests that in the triggering location, a few localized regions with high values of vertical component of photospheric electric current with opposite polarities were situated very close to each other (Figure 3-4). This suggests that the initial reconnection most likely occurred from this location. Once the reconnection began, it induced further reconnection events in the nearby stressed magnetic field lines of the region resulting in the enhancement of plasma temperature.

References

[1] Bhatnagar, A. and Livingston, W. 2005, World Scientific Series in Astronomy and Astrophysics
[2] Priest, E. R., & Forbes, T. G. 2002, A&A Rev., 10, 313
[3] Fletcher, L., Dennis, B. R., Hudson, H. S., et al. 2011, SSRv, 159, 19
[4] Poppe, B. B. and Jorden, K. P., 2006, Johnson Books, Boulder, Colorado
[5] Priest, E. R., & Forbes, T. G. 2002, A&ARv, 10, 313
[6] Hathaway, D. H., 2010, LRSP, 7, 1
[7] Sarkar, R. and Srivastava, N., 2018, SoPH, 293, 16
[8] Lemen, J. R., Title, A. M., Akin, D. J., et al. 2012, SoPh, 275, 17
[9] Pesnell, W. D., Thompson, B. J., & Chamberlin, P. C. 2012, SoPh, 275, 3
[10] Schou, J., Scherrer, P. H., Bush, R. I., et al. 2012, SoPh, 275, 229
[11] Wiegelmann, T., Thalmann, J.K., Inhester, B., et al., SoPh. 2012, 281, 37
[12] Liu R. et al., 2016, ApJ, 818, 148
[13] Clyne J., Mininni P., Norton A., Rast M., 2007, New J. Phys., 9, 301
[14] Klimchuk, J. A., Canfield, R. C., Rhoads, J. E., 1992, APJ, 385, 327
[15] Tan, B., Ji, H., Huang, G., Zhou, T., Song, Q., Huang, Y., 2006, SoPH, 239, 137
[16] Künzel, H. 1960, AN, 285, 271
[17] Zirin, H., & Liggett, M. A. 1987, SoPh, 113, 267
[18] Barnes, G., Leka, K. D., Schrijver, C. J., et al. 2016, ApJ, 829, 89
[19] Tan, B., Ji, H., Huang, G., Zhou, T., Song, Q., Huang, Y., 2006, Solar Phys. 239, 137

BUTI-05

2D-3V PIC-MCC based Simulations of Plasma Transport across Magnetic Filter : Instabilities and Double Layer formation

Name of the Doctoral Student : Miral Shah (Email: miral_shah@daiict.ac.in)
Thesis Supervisor : Bhaskar Chaudhury
Group in Computational Science and HPC, DA-IICT, Gandhinagar, India

Collaborators: Mainak Bandyopadhyay and Arun Chakraborty
ITER-India, Institute for Plasma Research, Gandhinagar, India

***Abstract*—In this paper, anomalous plasma transport across the magnetic field in low-temperature plasma devices has been investigated using a PIC-MCC based kinetic model. An in-house hybrid parallel 2D-3V PIC-MCC code has been developed for this investigation. PIC-MCC based code has been validated with ROBIN (RF Operated Beam source in INdia) experimental results, and a good match between simulation and experimental results has been observed. Comprehensive computational investigations reveal the formation of instabilities and double layer under some specific magnetic field and bias voltage conditions. Two types of instabilities with different frequencies (10^5 Hz and 10^6 Hz) has been identified in the magnetic filter region. 10^5 Hz frequency is recognized as $E \times B$ drift instability. For the first time, we report about the possible formation of double-layer in the magnetic filter region of the negative ion source. Ion acceleration is observed in case of double layer formation. Spatio-temporal EDF (Energy Distribution Function) studies show Maxwellian EEDF and non-Maxwellian IEDF in such plasmas.**

I. Introduction

Low-temperature plasmas (LTP) with a magnetic field (magnetic filter) in a low-pressure condition have a wide range of applications such as negative ion source [5], [9], [16], Hall thruster [12], magnetron discharge [15], electron cyclotron resonance source [11], ion-mass separator, linear magnetized machines and end-hall source [14]. Electrons in such plasmas are magnetized, whereas ions are not completely magnetized. The presence of an inhomogeneous magnetic field along with a non-uniform electric field in such applications leads to E×B drifts thereby leading to complex plasma transport [13]. Such a plasma source with a non-thermal equilibrium state, inhomogeneous magnetic and electric field, leads to the asymmetry in the plasma density, temperature, and pressure. The gradients in plasma parameters, different drifts (e.g. ExB drift, grad-B drift, polarization drift, diamagnetic drift etc.) and several collisional processes result in fluctuations or instabilities in the plasma, which can increase the electron cross field mobility that cannot be explained by the physics of classical collisional mobility [4]. Complex plasma transport involving several time and length scales necessitates the need of computationally expensive kinetic simulations, such as Particle-in-Cell Monte Carlo collision (PIC-MCC), to improve the current understanding of anomalous transport in such systems. In this paper, we have used a simple negative ion source geometry with a magnetic filter as a prototype for our investigations, however the complexities and physics issues are similar for all the above mentioned devices of interest.

The LTP (hydrogen) based negative ion source plays an important role in neutral beam injection system - one of the primary means of plasma heating in magnetic fusion [8]. As a first step, we performed 1D-3V PIC-MCC based simulations of such plasmas wherein the ROBIN negative ion source (consisting of an LTP source with a magnetic filter) installed at IPR, Gandhinagar is taken as a testbed problem for the validation of the model [1], [2]. ROBIN has a driver, an expansion chamber, a magnetic filter, and extraction system consisting of 3 different grids (as shown in Fig. (1)). Plasma is generated in the RF driver region and that expands in the expansion chamber before encountering the magnetic filter field. Magnetic filter is localized magnetic field (few tens of gauss) perpendicular to the plasma flow (diffusion flux or transport) and controls the plasma flux flowing from expansion chamber to the extraction system [9]. Although not exactly similar, but we observed a good qualitative match between the simulation and experimental results in terms of plasma density and electron temperature [19]. The quantitative mismatch

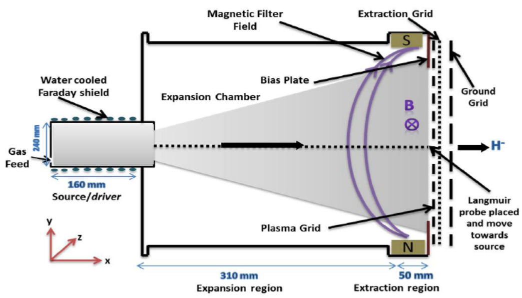

Fig. 1: Schematic of ROBIN (RF-Operated beam source in India) installed at IPR, Gandhinagar, India [1], [2]. H_2 gas is feed inside the *driver* region, plasma forms and expands in the expansion chamber, and a magnetic filter is used to cool the electrons.

between the ROBIN experiment and 1D-simulation results are due to the fact that the effect of drifts and instabilities (present in real experiments) are not captured properly in the 1D model. Our analysis shows that an advanced 2D-3V PIC-MCC model is required for a complete understanding of the physics of plasma transport across the magnetic filter in such large size negative ion sources [19], [17].

II. Computational Model

PIC-MCC is a widely used particle based computational technique to investigate low-temperature plasmas (LTP). It involves solution of Vlasov-Poisson equations, and provides spatial and temporal evolution of the charged-particle velocity distribution functions under the effect of self-consistent electromagnetic (EM) fields and collisions [3], [17]. PIC-MCC method calculates trajectories and velocities of each particle on the Lagrangian grid (mesh-free) and calculates collective behavior such as potential by solving Poisson's equation on Euler grids (as shown in Fig. (2)). The computational cost of PIC-MCC code is decided by grid size, the number of computational particles, dimensions of phase-space, time-step, and total number of iterations [17], [6], [7], [18]. Strict numerical constraints on time-step ($< \omega_p$), grid spacing ($< \lambda_d$), and number of particles per cell (PPC) (> 10) makes computation even more challenging [5], [10]. Considering large size negative ion source geometry, small-time step in the order of few ns, small grid spacing in the order of 10^{-4} m, and high plasma density in the order of 10^{18} m^{-3} makes 2D-3V PIC MCC simulation computationally very expensive for such studies.

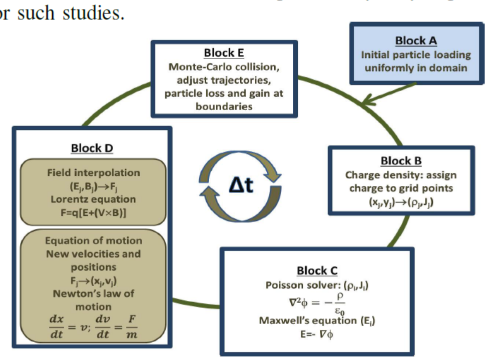

Fig. 2: Flowchart of PIC-MCC model used in this work [17].

III. In-house Parallel 2D-3V PIC-MCC code

We developed an in-house serial 2D-3V PIC-MCC code in C language and validated it with results available in the literature. However, we found that for investigating the physics of negative ion sources (ROBIN), stringent numerical constraints associated with a 2D PIC code makes it computationally prohibitive on CPUs in case of real experimental geometry. On a standard Desktop, it may take several months to simulate such problems. Therefore, we parallelized our 2D-3V PIC-MCC codes for shared as well as distributed memory systems consisting of multi-core as well as many-core architectures. The shared memory code has been parallelized using OpenMP library and we also proposed a hybrid parallel scheme (OpenMP+MPI) which can be used to perform such expensive simulations on a HPC cluster with several nodes [6]. We also implemented a Graphics Processing Unit (GPU) based 2D-3V PIC code using the CUDA C APIs for Kepler architecture [17]. One of the novel contribution towards the PIC-MCC code development has been made in terms of using different particle sorting strategies which significantly improved the memory access time leading to a remarkable enhancement in speedup compared to traditional strategies used for PIC-MCC implementation [6], [17], [18].

IV. Computational characterization of plasma transport across magnetic filter in ROBIN

The parallel 2D-3V PIC-MCC code have been used to simulate ROBIN experiment with real physical dimensions (refer Fig. 1) to understand the plasma transport across magnetic filter. Most of the previous works in this area used a scaled geometry as well as relaxed the stringent numerical criteria for such simulations due to intensive computational requirements, however we performed simulations by satisfying all the strict numerical constraints such as time step, grid spacing and PPC required for kinetic modelling of such LTP experiments [10]. All the results reported in this section and subsequent sections have been obtained using periodic boundary condition, and with two charge species (electrons and ions). For all the 2D simulations (0.52 m in x and 0.1 m in y), we have used 800 and 155 grid points in the x and y direction respectively, 21 particles per cell and a time step of $0.12 \times 10^{-9} s$. More details related to experimental and simulation parameters can be found in Ref. [21]. We found that, simulation becomes stable after tens of microseconds, which is decided by long time-scale phenomena such as ion cyclotron frequency (range of 10^6 Hz). Plasma density and electron temperature profiles from our 2D-3V PIC simulations (Fig. (3)) follow similar trends (qualitative as well as quantitative) as seen in experimental observations.

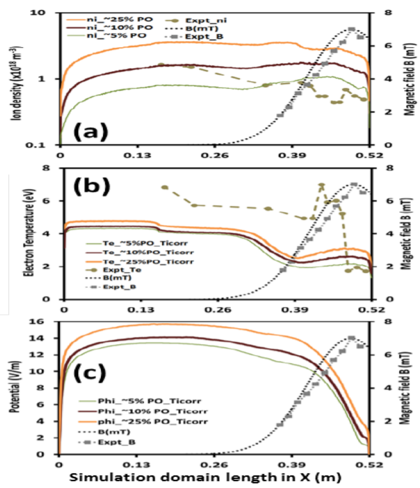

Fig. 3: (a) Plasma (ion) density (m^{-3}) (b) electron temperature (eV) (c) potential (V/m). These results are time (45-50 μs) and space-averaged (11 points around the central Y-axis of the simulation domain) data for 7 mT magnetic field. Olive green color dashed line with circle markers shows ROBIN experimental results. PO is total power given to the system (60 kW). Other solid lines are simulation results for different percentage of power absorption in the system. Black and grey dotted lines shows the simulation and experimental magnetic field in mT (secondary Y-axis).

There are several considerations which need to be taken into account while comparing experimental and simulation results. Firstly, the time window used for measurements of experimental parameters is not accurately known. Secondly, the exact amount of power absorbed in the ROBIN experiment is unknown, however according to experimentalists, only 10 % to 20 % of the given power is absorbed in the ROBIN. Thirdly, our simulation model is 2D, and does not take into account the real 3D geometry, the complex plasma chemistry and the wall effects. Even with these limitations, simulation results show a reasonably good match with the phase-1 ROBIN experimental results particularly with 10 % absorbed power (as shown in Fig. (3)). Particularly the simulations are showing similar important patterns in plasma characteristics as seen in the experiments. Comparison of the simulation and experimental results from ROBIN gives us sufficient confidence to do further case studies for future ROBIN experiments. Several case studies have been performed to understand the role of the magnetic filter profile on plasma transport, which will help in planning future experiments by using the magnetic filter as a switching mechanism to achieve the required density and electron temperature profiles for efficient operation of negative ion source. Our case-studies show that, under ROBIN experimental conditions [1], the lower magnetic field (0.29 m Gaussian width and peak at 94 % of the domain length) gives low electron temperature at the extraction region compared to higher magnetic field values. While comparing different Gaussian widths (7 mT magnetic field magnitude and peak at 94 % of the domain length), the narrow width of the Gaussian magnetic filter reduces more electron temperature than broader width. As the magnetic filter shifts towards the *driver* region, effective trapping results in lower electron temperature compared to filter near the extraction region. From these three different set of case studies, we can conclude that the magnitude, the Gaussian width and the position of the magnetic filter play an important role in obtaining the desired plasma profiles for efficient negative ion production [21].

2D snapshots of plasma density and potential are shown in Fig 4, and we also observe formation of instabilities in the case of 7mT magnetic field. Reasonable match of simulation results with experimental observations provides us the confidence to understand the role of instabilities as well as different diffusion and collisional processes, and subsequently quantifying the plasma transport accurately.

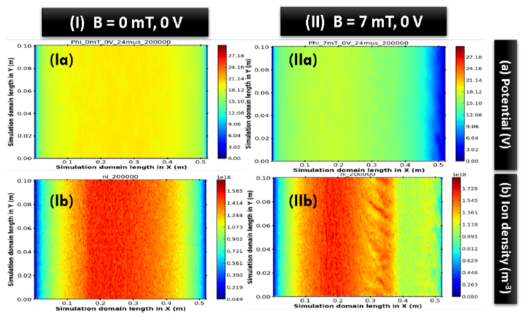

Fig. 4: 2D snapshots of (a) plasma density in m^{-3} and (b) potential in V at 24 μs using 2D-3V PIC-MCC simulations for two different cases. Case-I is without magnetic field 0 mT and case-II is with 7 mT magnetic field. Both cases are with 0 V bias voltage. Figures represent the exact dimension of the simulation domain in the x and y direction.

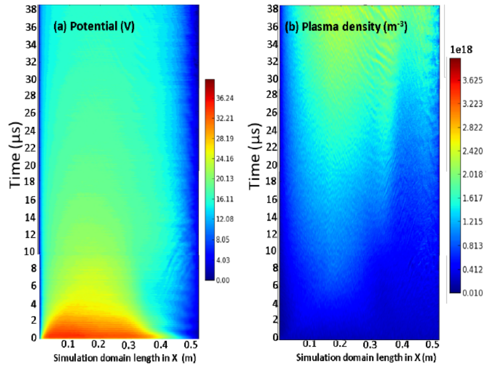

Fig. 5: Temporal evolution of the potential and plasma density in X direction (at middle of the simulation domain Y direction)

V. Role of Instabilities in Plasma Transport across Magnetic Field

Various collision dependent physical phenomena, having different time scales and length scales have been studied using 2D-3V PIC-MCC simulations. We have observed instabilities near the magnetic filter field region as shown in Fig. (4) and its temporal evolution is shown in Fig. (5) [20]. It is also observed that the frequencies of those instabilities are close to some of the electronic and ionic collision frequencies which may create resonant phenomena in the magnetic filter region and influence the cross-field transport, and heating [20]. From our

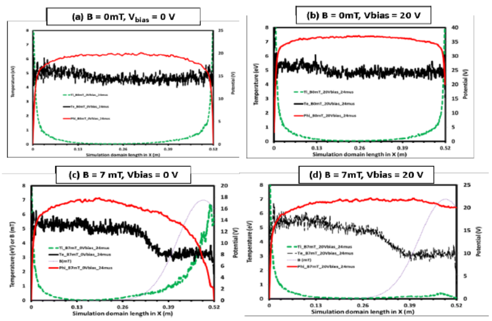

Fig. 6: 1D profile of the plasma parameter taken from center of the simulation domain in Y-direction at 24 µs. Potential in V, electron temperature in eV, and ion temperature in eV shown by red, black, and green solid lines respectively.

investigations, we find that the application of a bias voltage (applied to the extraction boundary) changes the potential profile (shown by red solid line in Fig. (6)) and thereby plays an important role in controlling the ion temperature near the extraction boundary (shown by green solid line in Fig. (6)). In the case of 0 V bias voltage, the ion temperature is very high near the extraction boundary, on the contrary, when a bias voltage close to plasma potential is applied to the plasma grid, there is almost no electric field (no gradient of potential) and so ions are not getting accelerated. The nature of the instabilities also depend on the bias voltage. We are anticipating an ion heating due to instabilities originating in the filter field region.

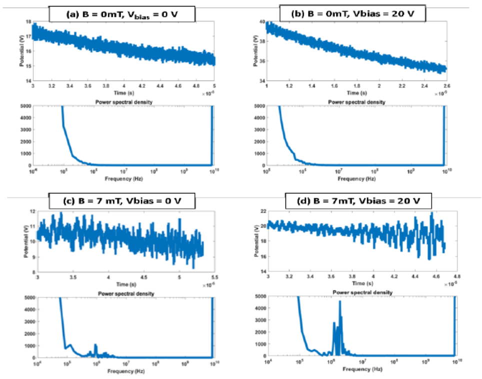

Fig. 7: Top figure in all four cases (a, b, c, d) shows time series of potential at 0.4563 m in X-direction and at 0.05 m in the Y-direction (y-center). FFT analysis of top time series plot is shown on bottom plots for all cases.

2D snapshots clearly shows discrete band structure which corresponds to drifts and instabilities, and the frequencies of the instabilities are identified using Fast Fourier Transform (FFT) analysis (Fig. (7)). The instability corresponding to 10^5 Hz is identified as $E \times B$ drift instability whereas, 10^6 Hz still requires further investigation [20].

VI. Investigation of Double Layers and its Role in Plasma Transport Across Magnetic Field

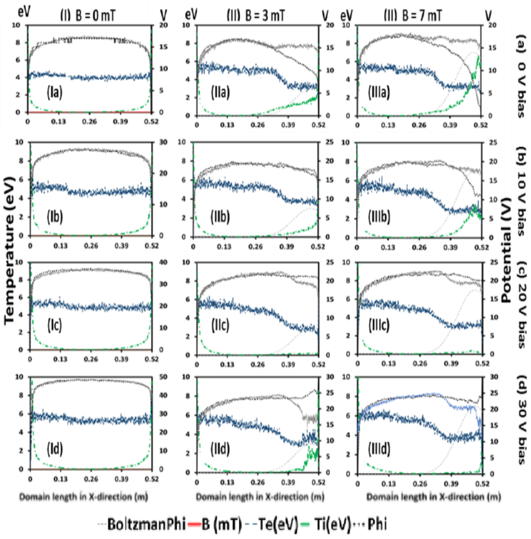

Fig. 8: 1D plasma profiles calculated at the center (Y-direction) of the 2D simulation domain at 24 μs for three different magnetic fields (0, 3 and 7 mT) with four different bias voltages ((a) 0 V, (b) 10 V, (c) 20 V, (d) 30 V). Left and right axes of all plots shows temperature (eV) and potential (V), respectively. Black dotted, green dot dashed, blue dashed, and dark grey dashed lines represent potential, ion temp., electron temp., and potential derived from Boltzmann relation, respectively. Grey dotted line shows magnetic field (mT).

Drifts and instabilities observed in our simulations may lead to double layer (DL) formation which has not been studied yet in the context of negative ion sources. The electrostatic double layer in the plasma is formed due to two parallel layers of opposite and equal charges that create a sharp potential gradient and results in an electric field that accelerates and decelerates charged particles. This motivated us to perform detailed analysis with three different magnetic field values (0 mT, 3 mT, and 7 mT) and four different bias voltages (0 V, 10 V, 20 V, and 30 V) as shown in Fig. (8). Plasma profiles (such as potential, electron and ion temperature, and ion velocities) are studied to understand the formation of DL and its effect on plasma transport. Ion acceleration is found near both source and extraction boundaries either due to sheath, instabilities, or DL as shown by green dashed line in Fig. (8). We observe DL formation under specific conditions such as 7 mT and 3 mT filter field with 0 V bias and we also find that the DL is weak as $e\phi/kT_e < 10$ in all the cases. DL is a barrier, which traps ions near extraction boundary having low potential, and traps electrons in the high potential side near the start of the magnetic filter towards source region. Two velocities components (one due to the free ions and the other due to the trapped ions) are visible in our simulations (Fig. (9d and 9e)). We found that DL depends on both the magnetic field and the difference between bias voltage and plasma potential. DL does not occur when the bias voltage is more or equal to the plasma potential. When the bias voltage is greater than plasma potential, electron sheath forms and reflects ions from the extraction boundary.

A detailed investigation of Energy Distribution Functions (EDFs) helps in interpreting the complex physics involved in such LTP problems. EDF measurement is challenging in such LTP experiments due to the presence of a magnetic field [2], however, the PIC-MCC simulations facilitate the study of the evolution of EDF with time. The EEDF (electron energy distribution function) controls the plasma properties and the rates of electron impact reactions that generate reactive species, whereas IEDF (ion EDF) is associated with surface effects. This is why the shape of the EDF is so important, as the rate coefficient for the electron impact processes (excitation, ionization, and dissociation) are determined by the EEDF. We have studied the temporal and spatial evolution of EDFs using our PIC-MCC code. We have observed that EEDF is Maxwellian in nature (Fig. (10a)), but IEDF is non-Maxwellian in nature (Fig. (10b)). Our detailed Spatio-temporal analysis of EDFs revealed that IEDF is more sensitive to changes in the filter field and bias voltage compared to EEDF. All the past studies have focused on understanding electron transport, however, our simulations suggest that to completely understand the physics of plasma transport in such low-temperature sources, ion transport is equally important and needs to be investigated in more detail.

VII. Conclusion

The important contributions of this work such as identification of instabilities, double layer formation and understanding of EDFs in the context of negative ion sources using comprehensive kinetic simulations (2D-3V PIC-MCC) further improves our understanding of physics of plasma transport across magnetic field and this will help in enhancing the efficiency of negative ion generation process in such sources. The results are also relevant for similar kinds of different LTP based

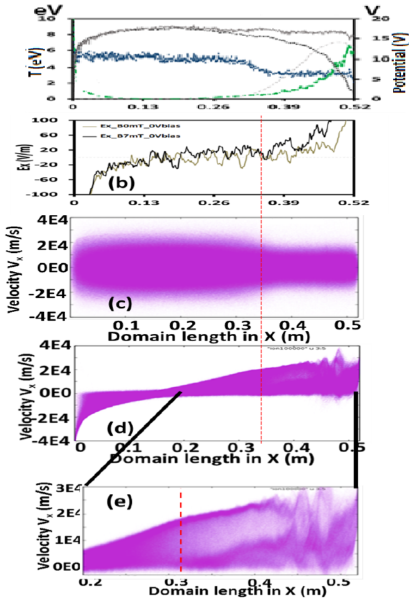

Fig. 9: (a) 1D profiles same as shown in Fig. (8-3a) for 7 mT 0 V bias, (b) Electric field (E_x) in (V/m), where olive green solid line is for B = 0 mT, 0 V bias and black solid line is for B=7 mT, 0 V bias, (c) electron velocity in m/s in case of 7 mT, 0 V bias, (d) ion velocity in m/s in case of 7 mT, 0 V bias, and (e) zoom of ion velocity as shown in (d).

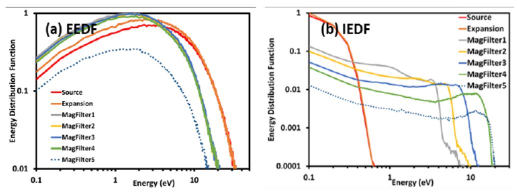

Fig. 10: (a) EEDF and (b) IEDF for B = 7 mT and 0 V bias.

applications involving magnetic field such as Hall thrusters, ECR source, end-hall source and magnetron discharge.

Acknowledgement

The authors acknowledge the DAE-BRNS for the financial assistance to carry out the work (Project Sanction No.39/27/2015-BRNS/34081). Miral Shah would like to thank the DAE, for research fellowship received under the project.

References

[1] G. Bansal, A. Gahlaut, J. Soni, K. Pandya, K. G. Parmar, R. Pandey, M. Vuppugalla, B. Prajapati, A. Patel, H. Mistery, A. Chakraborty, M. Bandyopadhyay, M. J. Singh, A. Phukan, R. K. Yadav, and D. Parmar. Negative ion beam extraction in ROBIN. *Fusion Engineering and Design*, 88(6-8):778–782, 2013.

[2] G. Bansal, K. Pandya, M. Bandyopadhyay, A. Chakraborty, M. J. Singh, J. Soni, A. Gahlaut, and K. G. Parmar. Cesium delivery system for negative ion source at IPR. *AIP Conference Proceedings*, 1390:614–623, 2011.

[3] C. K. Birdsall and L. Fellow. Particle-in-Cell charged-particle simulations, Plus Monte Carlo collision with neutral atom, PIC-MCC. *IEEE Transactions on Plasma Science*, 19(2):65–85, 1991.

[4] J.-P. Boeuf and B. Chaudhury. Rotating instability in low-temperature magnetized plasmas. *Physical review letters*, 111:155005, 10 2013.

[5] J. P. Boeuf, B. Chaudhury, and L. Garrigues. Physics of a magnetic filter for negative ion sources. I. Collisional transport across the filter in an ideal, 1D filter. *Physics of Plasmas*, 19(11), 2012.

[6] B. Chaudhury, M. Shah, U. Parekh, H. Gandhi, P. Desai, K. Shah, A. Phadnis, M. Shah, M. Bandyopadhyay, and A. Chakraborty. Hybrid Parallelization of Particle in Cell Monte Carlo Collision (PIC-MCC) Algorithm for Simulation of Low Temperature Plasmas. In *Communications in Computer and Information Science book series*, pages 32–53. Springer, Singapore, 2018.

[7] J. Claustre, B. Chaudhury, G. Fubiani, M. Paulin, and J. P. Boeuf. Particle-in-cell monte carlo collision model on GPU-application to a low-temperature magnetized plasma. *IEEE Transactions on Plasma Science*, 41(2):391–399, 2013.

[8] U. Fantz. et. al. Low pressure and high power rf sources for negative hydrogen ions for fusion applications (ITER neutral beam injection) (invited). *Review of Scientific Instruments*, 79(2), 2008.

[9] U. Fantz, L. Schiesko, and D. Wünderlich. Plasma expansion across a transverse magnetic field in a negative hydrogen ion source for fusion. *Plasma Sources Science and Technology*, 23(4):044002, 2014.

[10] L. Garrigues, G. Fubiani, and J. P. Boeuf. Appropriate use of the particle-in-cell method in low temperature plasmas: Application to the simulation of negative ion extraction. *Journal of Applied Physics*, 120(21), 2016.

[11] R. Gobin, P. Auvray, M. Bacal, J. Breton, O. Delferrière, F. Harrault, A. A. Ivanov, P. Svarnas, and O. Tuske. Two approaches for H- ion production with 2.45 GHz ion sources. *Nuclear Fusion*, 46(6), 2006.

[12] D. M. Goebel and I. Katz. *Fundamentals of Electric Propulsion: Ion and Hall Thrustes*. Jet Propulsion Laboratory, 2008.

[13] I. Kaganovich. et. al. Physics of E × B discharges relevant to plasma propulsion and similar technologies. *Physics of Plasmas*, 27:120601, 12 2020.

[14] H. R. Kaufman, R. S. Robinson, and R. I. Seddon. End-Hall ion source. *Journal of Vacuum Science & Technology A: Vacuum, Surfaces, and Films*, 5(4):2081–2084, 1987.

[15] D. Lundin, U. Helmersson, S. Kirkpatrick, S. Rohde, and N. Brenning. Anomalous electron transport in high power impulse magnetron sputtering. *Plasma Sources Science and Technology*, 17(2), 2008.

[16] L. Schiesko, P. McNeely, P. Franzen, U. Fantz, and the NNBI Team. Magnetic field dependence of the plasma properties in a negative hydrogen ion source for fusion. *Plasma Physics and Controlled Fusion*, 54(10):105002, 2012.

[17] H. Shah, S. Kamaria, R. Markandeya, M. Shah, and B. Chaudhury. A Novel Implementation of 2D3V Particle-In-Cell (PIC) Algorithm for Kepler GPU Architecture. In *Proceedings of 24th International conference High Performance Computing, Data and Analytics (HIPC 2017)*, pages 1–10, 2017.

[18] K. Shah, A. Phadnis, M. Shah, and B. Chaudhury. Parallelization of the Particle-In-Cell Monte Carlo Collision (PIC-MCC) Algorithm for Plasma Simulation on Intel MIC Xeon Phi Architecture. In *proceedings of nternational Conference for High Performance Computing, Networking, Storage and Analysis (SC17)*. IEEE, 2017.

[19] M. Shah, B. Chaudhury, M. Bandyopadhyay, and A. Chakraborty. 1D-3v PIC-MCC based modelling and simulation of magnetized low temperature plasmas. In *'Proceedings of the Sixth International Conference on Mathematics and Computing*, pages 1–12. Springer International Publishing, 2020.

[20] M. Shah, B. Chaudhury, M. Bandyopadhyay, and A. Chakraborty. The Feasibility of Resonance Induced Instabilities in the Magnetic Filter Region of Low Temperature Plasma Based Negative Ion Sources. *AIP Conference Proceedings*, 2020.

[21] M. Shah, B. Chaudhury, M. Bandyopadhyay, and A. K. Chakraborty. Computational characteristics of plasma transport across magnetic filter in ROBIN using PIC-MCC simulation. *Fusion Engineering and Design*, 151:111402, 2020.

BUTI-06

Experimental verification of cavity modes in a microwave ion source and its influence on the plasma dynamics and the extracted ion beam.

C. Mallick[1,2,a], M. Bandyopadhyay[1,2,a], and R. Kumar[1,2]

[1]Institute for Plasma Research (IPR), Gandhinagar, Gujarat – 382428, India
[2]Homi Bhabha National Institute (HBNI), Anushaktinagar, Mumbai, Maharastra-400094, India

[a)]E-mail: chinmoyju1990@gmail.com;mainak@ipr.res.in

Multiple cavity modes excitation phenomena in an experimental microwave ion source chamber are reported. The frequencies of those cavity modes are close to the operating microwave frequency, 2.45 GHz. Their interactions with each other inside plasma control the microwave (MW) coupling, the plasma dynamics and influence the ion beam quality. The linear superposition of those close frequency cavity modes, recognized as phase modulation generates a new range of plasma oscillations with the same modulation frequency. Newly generated phase-modulated waves are verified from the signatures of experimentally measured frequency emission from the plasma and the hot electron population build-up. The increase of the hot-electron population is caused by the plasma resonance with the modulated waves. Furthermore, few cavity modes are having more power than the threshold value required for nonlinear superposition and causes parametric decay phenomenon (PD).PD is also responsible for generating the ion waves in the over-dense plasma condition and thus causes additional plasma fluctuations of the corresponding frequencies. These above-mentioned phenomena influence the plasma dynamics of the ion source and its ion beam qualities, e.g., emittance and stability. The present work reports the experimental observations of the phase modulation and the parametric decay due to the interaction of multiple cavity modes and emittance growth of the extracted ion beam. The experimental results are supported by analytical calculation and finite element method (FEM) simulation. The influence of above mentioned self-excited plasma oscillations of a microwave ion source on its beam property is never been reported before.

Introduction

A high density and uniform stable plasma are some of the critical parameters in the fields of high current microwave ion sources, microwave plasma chemical vapour diamond deposition, circular wafer processing technologies, surface Plasmon resonance sensors, and antennae applications, *etc*. [1]. The uniform plasma distribution across the plasma column is possible by injecting dual/multiple frequency microwaves and/or modulated microwaves in the plasma cavity. Multiple frequency heating play important role in the microwave discharge ion source (MDIS) by providing a highly intense, single charge-state, low emittance, and stable ion beam for the accelerators operating in large beam loading conditions [2]. The high density production in a microwave plasma is accompanied by the plasma non-uniformity, instabilities and turbulence, *etc*. Plasma non-uniformity and turbulence eventually degrades the ion beam qualities, extracted from the ion source. Ion beam qualities are defined by the beam halo formation and emittance growth. Different instabilities cause transverse emittance growth and unstable beam [2]. These issues are possible to resolve in MDIS by adopting a multiple cavity modes dependent microwave plasma generation [1] in which different cavity modes are excited selectively by altering the ion source chamber cavity geometry. The temporal phase difference between the excited cavity mode produces modulated wave which helps to rotate the plasma and create the uniform plasma column [1]. As a recent evidence of above mentioned multi-mode superposition based solution towards plasma uniformity with devoid of plasma instabilities, two close-frequency heating (TCFH) experiments are performed [3] to damp the kinetic instabilities in microwave plasma alongside producing an intense and higher charge state ion beam.

The superposition interaction (linear and non-linear) of close-frequency cavity modes can generate different low frequency waves. The linear superposition of pairs of cavity modulates the phase of the resultant mode field temporally and hence induces pulsation in the microwave electric field inside the ion source cavity volume. As a result, the generated plasma oscillates with the same modulation frequency. The above-mentioned phase modulation in plasma is experimentally realized by measuring corresponding frequency, emitted from the plasma and also by sensing the energetic electron population build-up inside the overdense plasma. The rise of energetic electron fraction in the plasma is due to the modulated wave resonance and also due to the parametric decay (PD) effect. The parametric decay is a consequence of nonlinear superposition of cavity modes that occur when the microwave power of those cavity modes exceeds certain power threshold. The PD effect generates low frequency ion waves in the plasma. The phase modulation and hot electron generation are supported by a mathematical derivation and also by a microwave plasma simulation carried out by COMSOL Multi-physics software, considering similar experimental configuration and operating conditions [4-5]. An experimental campaign is performed to find out the phase modulated wave and parametrically generated [6] ion type waves. After measurement and data analysis it is verified that the phase modulated wave and ion type waves fall in the range of lower hybrid oscillation and ion acoustic wave range respectively

2. Experimental procedures

The microwave ion source is fed by a 2.45 GHz frequency microwave generated by Sairem made magnetron setup in right hand polarized mode using a microwave launcher. The microwave power is launched from the high magnetic field side of one set of the ring magnets used to create required magnetic field in the ion source volume, as shown in fig.1. The two pairs of ring magnets are used to generate mirror B magnetic field across the chamber. The launcher geometry (four step ridge waveguide and HV break cum vacuum window), and ion source cavity constitutes an integrated assembly that is evacuated by a dry scroll pump and turbo molecular pump assembly. The integrated assembly is connected to a vacuum chamber through the beam extraction system. The extractor unit is consisting of three grids. An Allison emittance scanner is installed in the vacuum vessel on the beam path for extracted beam diagnostics. Throughout the experimental campaign the microwave power is varied from 50 W to 700 W to ionize the injected nitrogen gas in the source chamber that is kept initially at a base pressure 1×10^{-7}mbar.

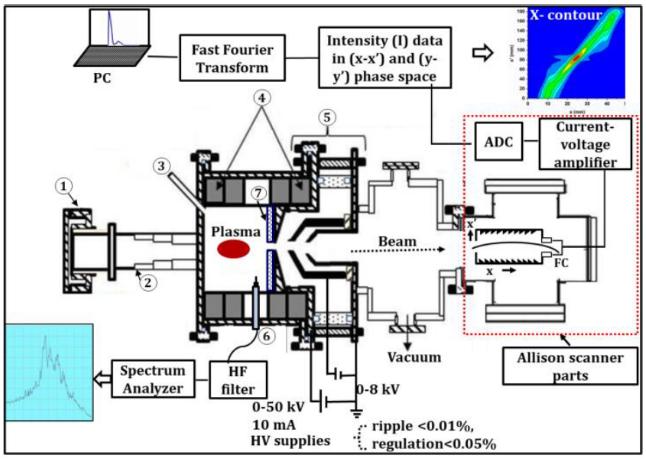

FIG.1: Schematic view of MDIS plasma and its beam emittance diagnostics setup. ① Vacuum window; ② Ridge guide;③ Gas inlet;④ Ring magnets pairs;⑤ ion extraction grids;⑥ RF probe;⑦ Boron nitride (BN) plate.

To study the cavity modes with and without the plasma inside the ion source cavity chamber, frequency emission is detected by an electrostatic probe inserted through a radial port near the beam extraction grid location (also denoted as RF probe). The acquired spectrum is analyzed by a spectrum analyzer and a bandpass filter (make: LORCH MICROWAVE, 9IZ3-2500/A1000-S) combination. Before capturing the cavity modes frequencies, the frequency and power stability characteristics of Sairem made magnetron system is tested to ensure that only a single peak pump frequency, 2.43 GHz is present in the output of the magnetron in a wide power range (50 W to 700 W) with power fluctuations within 2 %. The experiments are performed at operating pressure range from $2 \times 10^{-4} mbar\ to\ 1 \times 10^{-3}\ mbar$. Two single Langmuir probes, separated by 5 mm is inserted through another radial port into the plasma chamber to study the spatially dependent plasma parameters . The floating potential measurement by these two probe tips helps in estimating the wave vectors (k) to classify the ion waves generated by the parametric decay (PD) phenomenon as mentioned before.

To study the influences of the plasma dynamics due to the interactions among different cavity modes, the plasma and ion beam diagnostics are performed in the same operating pressure and power range as mentioned above. For beam diagnostic, the Alisson type emittance scanner heads are spaced apart by ~ 80 cm away from the plasma extraction grid.

An Alisson scanner consists of a front slit, deflecting plates, a rear slit, and a Faraday cup (FC). The slits are moved in stepped fashion across the beam with the help of a stepper motor. Through the slits, beam particles are allowed to fall on the FC under the influence of the electric field created by the deflecting plates. At each step the beamlet section selected by the front slit is stepped across the rear slit and the transmitted current is measured by the Faraday cup. The position of the slit-crossing point and the voltage on the deflecting determines the position and momentum coordinates in the phase space. The beam intensity data in two-dimensional phase space is taken at a fixed voltage (or at a fixed transversal point in the phase plane) applied across the deflecting of the emittance scanner. The scanner heads are operated in such a way that a maximum number of data points are captured of the beam intensity at a particular point in the phase space. For this reason, the vertical and horizontal velocity of the scanner heads are kept at minimum value (10 nm/s). The oscillation frequency present in the beam intensity data is extracted from the fast Fourier transform spectra of the data points.

3. Experimental results

A series of experiments is performed to investigate the cavity modes in the present experimental microwave discharge ion source cavity with and without the plasma conditions. Initially, the frequency emission spectra of the ion source cavity under vacuum condition is captured by the RF probe circuitry to understand the intrinsic cavity modes present in the ion source chamber as mentioned before. The emission spectrum exhibits eight distinct cavity modes with frequency peaks are very close to the operating frequency, 2.45 GHz. The presence of cavity modes is verified by the microwave simulation considering the integrated experimental assembly and its condition using COMSOL Multiphysics electromagnetic module. The simulated microwave field distributions throughout the integrated the microwave ion source chamber confirms the existence of appreciable amplitude of TE_{111} type modal electric fields having the same cavity mode frequencies. A detailed report of the cavity mode frequencies and the distribution of the modal fields under vacuum condition (without the plasma filled cavity) can be found in the reference [4-5].
Once the dominant cavity modes in the vacuum cavity are confirmed, the frequency emission characteristics of the ion source plasma is performed in a wide pressure and power range as mentioned above. The frequency emission data reveals that in plasma condition, there exist mainly three distinct cavity modes with appreciable intensities in any operating conditions. The present paper shows one of the frequency emission spectra in plasma filled cavity in fig. 2 as shown below. The signal is acquired by a RF probe connected to a spectrum analyser, as shown in fig.1. Fig.2 shows the emission spectrum from the plasma at 400 W launched power. It shows the frequency peaks of three distinct cavity modes (i.e., #1, #2 and #3) in presence of plasma. Every peak is spaced apart from each other by a fixed frequency of ~1.3 MHz, which effectively generates a modulation of frequency 1.3MHz due to the interaction among each pairs of the distinct cavity modes.

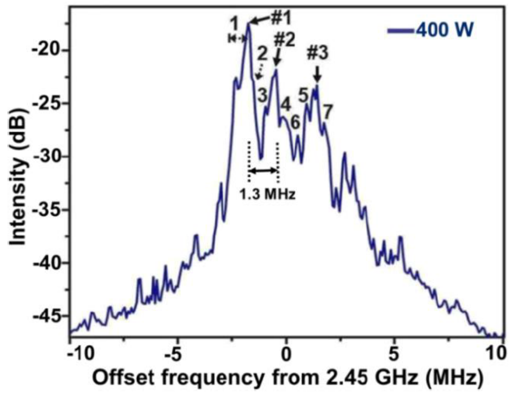

FIG.2: Experimentally observed electromagnetic frequency emission from the plasma with 400W launched power. Sideband peaks are numbered as 1 (555 kHz), 2 (238 kHz), 3 (476 kHz), 4 (317 kHz), 5 (397 kHz), 6 (873 kHz) and 7 (348 kHz).

Additionally, each cavity mode peak is associated with side peaks (named as, 1, 2, 3… *etc.*) with different sideband values ranging from 238 kHz to 873 kHz. These side bands are proved to be originated from the parametric decay phenomenon of each of the three distinct cavity modes. These three cavity modes show sidebands once the microwave power associated with the cavity modes cross the corresponding parametric decay threshold. A detailed description regarding the parametric decay can be found in reference [4].

3.1 Theoretical analysis of phase modulation and parametric decay

(i) Phase modulation:

(a) Mathematical derivation & Microwave plasma simulation

To confirm the phase modulation at 1.3 MHz frequency, an analytical calculation is performed considering extraordinary (*X*) type MW and for a collisionless plasma condition with zero magnetic field gradient along the magnetic field axis in a mirror B field configuration. For two close frequency cavity modes (let say ω_1 and ω_2), it is derived that the linear superposition between them creates a resultant wave with amplitude, $A = B\cos(\omega_{1\,or\,2}t + \psi)]$. Here $\psi = (\omega_{LF}t + \emptyset)/2$; $B = \pm 2\cos\emptyset\cos(\omega_{LF}t - \emptyset)/2$.

Considering the microwave plasma simulation results as an input to the calculation , the following procedures is adopted to estimate the phase modulation frequency analytically. For a MW transverse electric field, the set of Maxwell's equations is simplified to the modified Bessel's differential equations in terms of the axial component of the wave magnetic field,H_z[8]. The solution to this differential equation in the plasma region and the plasma-wall interface region is as follows:

$$H_z = A_1 I_m(Kr);$$

Here $K^2 = (\omega/c)^2(\varepsilon_2^2 - \varepsilon_1^2)\varepsilon_1^{-1}$ and $\kappa^2 = (\omega/c)^2\varepsilon_s$. The terms,$A_i$ (i = 1 and 2), K^{-1}, $J_m(\kappa r)$ and $N_m(\kappa r)$,$\varepsilon_i(i = 1$ and $2)$,ε_s, ω and c are real constants, penetration depth of *X*-mode MW into plasma, Bessel function of 1st kind, Bessel function of 2nd kind, two components of permittivity present in this MW plasma cavity ($\varepsilon_1 = 1 - \Omega_\alpha^2/(\omega^2 - \omega_\alpha^2)$, $\varepsilon_2 = -\Omega_\alpha^2\omega_\alpha/\omega(\omega^2 - \omega_\alpha^2)$) [8] permittivity of sheath, wave frequency, speed of light, respectively. Here, Ω_α and $\omega_\alpha$are the plasma and cyclotron frequencies of plasma particle species α (α = *i* for ion and *e* for electrons). The condition $K^2 > 0$ determines the possible frequency ranges within which the *X*-mode propagates at the interface region of plasma-boundary wall. The solution to this inequality gives two frequency ranges, i.e. low (LF) and high frequency (HF) waves whose ranges are $\omega_{LF} < \omega < |\omega_e|$ and $|\omega_e| < \omega < \omega_1 - |\omega_e|$, respectively. Here $\omega_{LF} = [\Omega_i^{-2} + (\omega_i|\omega_e|)^{-1}]^{-1/2}$ and $\omega_1 = 0.5\omega_e + [\Omega_e^2 + 0.25\,\omega_e^2]^{1/2}$.

Apart from frequency spectra, energetic electron population near the plasma wall interface is a signature of phase modulation. The phase modulated wave can transfer its energy to the electrons if certain conditions are satisfied near the plasma-well interface zone. The wave propagation within the sheath must be satisfied. The plasma parameters, n_i= 5.5× $10^{15} m^{-3}$ and magnetic field $B = 0.23\,T$ near the plasma-wall boundary regions is extracted from the simulation data and used as input to find the wave frequency which can propagate in the sheath., The estimated wave frequency from the above relation is ω_{LF} = ~1.3 MHz and matches well with the observed frequency data in fig.2 The pondermotive force exerted on the electrons by the resultant electric field of the modulated wave of frequency 1.3MHz, where plasma resonance conditions, *i.e.*, $\omega \gg \omega_{pe}$ and $\omega_{pe} = \omega_{LF}$[91-92] are satisfied is given by the following function,

$$f_{avg}(t) = \omega_{LF} * (e^2/2m_e\omega^2)\,\nabla(E^2(r - \omega_{LF}t) \qquad (1)$$

This pondermotive force is calculated by using simulated results in fig.3. Fig.3(b) gives the radial variation of $\nabla(E^2)_r$ within the plasma sheath thickness (fig.3a). The force using above equation is estimated as $6 \times 10^{-16} N$ for some typical parameters, ,$\omega_{LF} = 1.3\ MHz$ and $\nabla(E^2)_r$= 1200V/mm (see fig.3b).

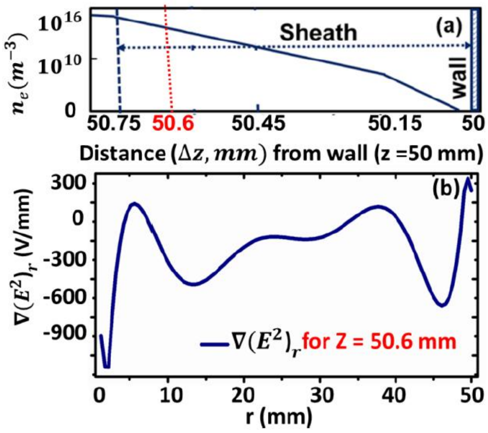

Fig.3: (a) Schematic of plasma sheath near Boron nitride wall (z = 50 mm, see fig.1). (b) Radial gradient ($\nabla(E^2)_r$) of the strongly inhomogeneous electric field within the plasma sheath.

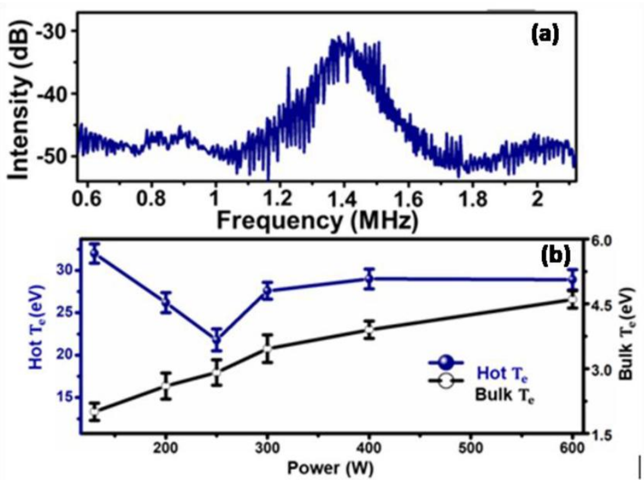

Fig.4.(a) Spectrum acquired by the spectrum analyser of RF circuitry; (b) Variation of bulk and hot electron temperature with different launched power.

(b) Experimental signatures: energetic electron production and frequency emission data

Fig.4(a) represents the phase modulation frequency emission data captured by the RF probe circuitry. Fig 4(b) shows corresponding bulk and hot electron temperature data for different launched power measured by the Langmuir probes. These two figures clearly indicate that after 250W, the hot/ energetic electron temperature has increased due to the increase in high energetic fraction of electron population. Whereas, bulk electron temperature increases monotonically with power.

3.2. Footprints of energetic electrons surface interactions with boron nitride wall

To understand the generation of energetic electrons, after 250W launched power, MW-plasma simulation results are shown in fig. 5(a-b).Figs. 5 (a) and (b) show the simulated 2D plots (r-ϕ variation) of the plasma density and E-field respectively near the plasma-BN plate interface location (see fig.1). Fig. 5(a) shows the formation of discrete density layers. Three distinct but closely-spaced layers of inhomogeneous E-field is shown in Fig. 5 (b) at the same interface location. This inhomogeneous E-field may produce high energy tail of electrons as per the relation, $F_{avg} \propto \nabla(E^2)_{avg}$, discussed in equation 1 and observed in the fig.4(b) plot. Fig. 5(c) shows the experimental footprints of energetic plasma electrons interactions on the BN plate.

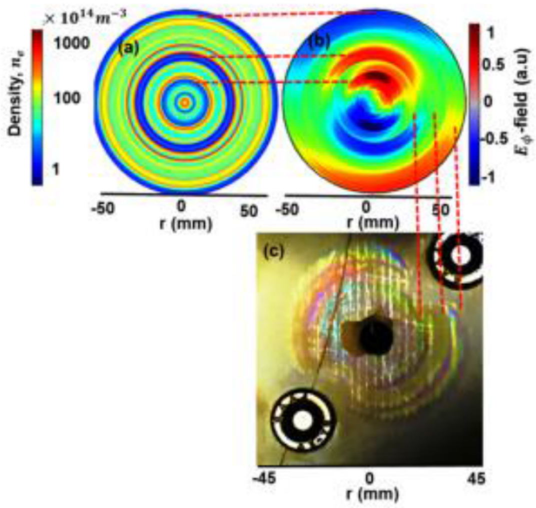

Fig. 5: (a) Simulated plasma density discrete layers along the radial plane within the plasma sheath. Blue colour rings denote minimum density regions; Schematic red dot lines denotes different layers exist in the surface; (b) Surface plot of inhomogeneous electric field; (c) Camera snapshot of inside view of BN plate showing footprints of three layers of plasma exists on the BN plate.

(ii) Parametric decay

The parametric decay of each cavity modes is confirmed from the frequency and k vector selection rules. The sidebands appeared around each cavity modes are classified as ion acoustic waves from the dispersion relation. To satisfy the dispersion equation for ion acoustic wave, the corresponding k-vectors ($k_\perp$ and $k_\parallel$) are estimated from the measured Langmuir probe data. In the present MDIS cavity, IAW appears for $k_\parallel$ values typically in the range from 7 to 22 m^{-1} and $k_\perp$ varies from ~245 to 250 m^{-1}. Putting measured k-vector and Ω_i= 55 kHz (radial position, r = 5 mm and B = 0.05 T) into the dispersion equation given in reference [4-5], the IAW frequency is estimated within the range of measured sideband frequencies.

3.3. Experimental measurements of Ion beam emittance and oscillations

As mentioned above, the ion beam is extracted by applying high voltages on the three grids ion extraction system. The maximum energy of of the extracted ion beam is~ 30keV. It is understood that the plasma uniformity and high density can influence the ion beam qualities. Hence, the emittance measurement in 2D transverse phase space is carried out in the *x-x'* and *y-y'*-planes by monitoring two heads of the emittance scanner. The terms x' and y' are the velocity components in x and y direction and corresponds to the momentum space in those direction. The emittance variation with respect to the increase of power is shown in fig.6(a). Fig. 6(a) shows that the transverse emittance of the beam in *x*-direction and also in *y*-direction is increased with the applied MW power. Below 250 W, it is observed experimentally that the transverse emittance variation in the *x-x'* and *y-y'*-planes is relatively small. The normalized rms value of the emittance is calculated based on the equations given in ref [9]. In the calculation, 95% of the beam fraction is included from the distribution as shown in fig.6(a). The rms-normalized emittance in x-direction,$\varepsilon_x^{rms-norm}$is increased from *0.002π-mm-mrad* to *0.098π-mm-mrad* when MW power is increased from 250W to 400W. Correspondingly the rms-normalized emittance in y-direction is increased from and *0.004π-mm-mrad* to *0.23π-mm-mrad*. It is seen in Fig. 6(a) that the emittance increases nonlinearly with power. To understand the emittance growth, beam oscillation frequency is also recorded by the faraday cup assembly which is an in-built component within the emittance scanners mounted on the beam line, as shown in fig.6(b). Fig. 6(b) shows the beam oscillation frequencies obtained by taking the FFT of the Faraday cup current data during 250W to 700W launched power condition. Fig. 6 (b) clearly shows two frequency peaks (~ 476-873 kHz and ~1.3 MHz) of oscillations in the ion beam in *y* – plane of the beam emittance phase-space. Similar observations are seen in *x*-plane also. The intensity of kHz range oscillations is more than the MHz oscillations and both these range of frequencies oscillations are also observed in plasma as well, discussed before.

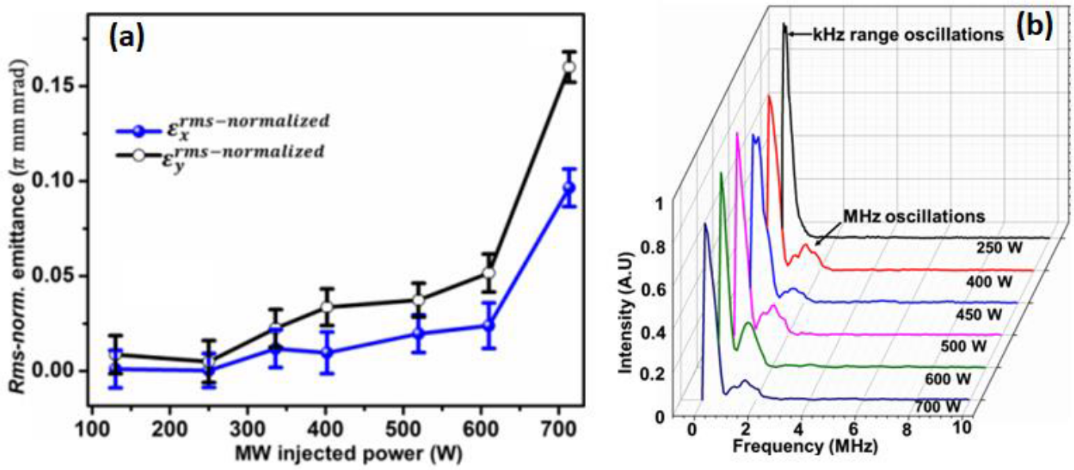

Figure 6 (a) Transverse rms-normalized emittance (*x* and *y*-plane) growth with increase in MW power. (b) Beam oscillations of kHz and MHz range shows different amplitudes at their corresponding frequency range respectively.

4. Summary

To summarize, the transverse ion beam emittance and electromagnetic frequency emission spectra from plasma are measured using the diagnostic instrument Allison scanner at two locations on beamline and a Langmuir probe placed near BN plate) respectively at different input microwave powers in a MW ion source. The emittance increases with launched MW power associated with the oscillations in ~ 476 kHz and ~ 1.3MHz frequency range that falls in the phase modulation and parametrically generated ion acoustic frequencies range.

It is understood that the increase of the beam emittance due to kHz range oscillation is not as significant as the case of 1.3MHz. When the beam oscillations appear, the emittance on both x and y planes increases by 2 to 4 times. It is also demonstrated through experiment and simulation that the linear superposition of cavity modes, the phase modulation, causes inhomogeneous electric field near the plasma boundary and hence the energetic electrons are created in the plasma due to resonance energy transfer from the electric field to the plasma electrons.

References

[1]Hasegawa Y *et al* 2017 *Jpn. J. Appl. Phys.* **56** 046203

[2] Gammino S et al., *Rev. Sci. Instrum.* 2010 **81** 02B313

[3] Naselli E et al., 2019 *Plasma Sources Sci. Technol.***28** 085021

[4] Mallick C., Bandyopadhyay M. and Kumar R., 2019 *Phys. Plasmas***26** 043507

[5] Mallick C., Bandyopadhyay M. and Kumar R., 2018 *Rev. Sci. Instrum.***89** 125112

[6] Castro G. etal2017Plasma Sources Sci. Technol. **26** 055019

[7] R. D'Arcy *et al*., *Nucl. Instrum. Methods Phys. Res. A,* vol. 815, pp. 7-17, 2016.

[8]I. O. Girka, V. M. Kondratenko, and M. Thumm, *J. Plasma Phys.*, vol. 84, p. 905840603, 2018.

[9] A. J. Mendezand Y. Liu, *Rev. Sci. Instrum.,* vol. 81, p. 02B712, 2010.

PLASMA
2021

बिरला प्रौद्योगिकी संस्थान • BIRLA INSTITUTE OF TECHNOLOGY
सा विद्या या विमुक्तये
RANCHI

आज़ादी का अमृत महोत्सव

TECHNOLOGIES FOR
NEW INDIA@75
आजादी का अमृत महोत्सव

Azadi Ka Amrit Mahotsav

PSSI
ESTD.1978